Award Number: W81XWH-08-2-0017

TITLE: Kevlar Vest Protection against Blast Overpressure Brain Injury: Systemic Contributions to Injury Etiology

PRINCIPAL INVESTIGATOR: Joseph B. Long, PhD

CONTRACTING ORGANIZATION: The Geneva Foundation
Tacoma, WA 98402

REPORT DATE: July 2015

TYPE OF REPORT: Final

PREPARED FOR: U.S. Army Medical Research and Materiel Command
Fort Detrick, Maryland 21702-5012

REPORT DOCUMENTATION PAGE

Form Approved
OMB No. 0704-0188

1. REPORT DATE	2. REPORT TYPE	3. DATES COVERED
July 2015	Final	1 May 2008 – 30 July 2015

4. TITLE AND SUBTITLE

Kevlar Vest Protection against Blast Overpressure Brain Injury: Systemic Contributions to Injury Etiology

5a. CONTRACT NUMBER

5b. GRANT NUMBER
W81XWH-08-2-0017

5c. PROGRAM ELEMENT NUMBER

6. AUTHOR(S)

Joseph B. Long, Ph.D.

E-Mail: joseph.b.long.civ@mail.mil

5d. PROJECT NUMBER

5e. TASK NUMBER

5f. WORK UNIT NUMBER

7. PERFORMING ORGANIZATION NAME(S) AND ADDRESS(ES) AND ADDRESS(ES)

The Geneva Foundation
917 Pacific Ave, Suite 600
Tacoma, WA 98402

8. PERFORMING ORGANIZATION REPORT NUMBER

9. SPONSORING / MONITORING AGENCY NAME(S) AND ADDRESS(ES)
U.S. Army Medical Research and Materiel Command
Fort Detrick, Maryland 21702-5012

10. SPONSOR/MONITOR'S ACRONYM(S)

11. SPONSOR/MONITOR'S REPORT NUMBER(S)

12. DISTRIBUTION / AVAILABILITY STATEMENT
Approved for Public Release; Distribution Unlimited

13. SUPPLEMENTARY NOTES

14. ABSTRACT The etiology of blast-induced traumatic brain injury (TBI) is largely undefined. Along with reducing mortality, in preliminary experiments Kevlar vests significantly protected against BOP-induced neuropathological changes in rats. We postulate that: 1) much of the blast-induced fiber degeneration in brain results from pressure surges transmitted through the vasculature that elicit a series of intracranial disruptions, and 2) Kevlar vests are neuroprotective by uncoupling this pressure transmission following exposure to blast. Using a compression driven shock tube, we compare external, systemic (e.g. vascular arterial and venous), and central (e.g. intracranial pressure) BOP-induced pressure changes, and assess the impact of Kevlar vests on these changes. We seek to: 1) determine if measured pressure changes are blast severity-dependent and correspond with outcome measures, and 2)assess the impact of Kevlar vests on measured BOP-induced pressure changes and outcome measures and establish whether a protective vest encasing the thorax ameliorates blast-induced brain injury,pointing to a significant contribution of the effects of blast on the thorax to brain injury. Thesestudies will provide critical insights into the etiology of blast-induced brain injury, and will advance the development of mitigation strategies.

15. SUBJECT TERMS
Traumatic Brain Injury (TBI), blast exposure, blast overpressure

16. SECURITY CLASSIFICATION OF:			17. LIMITATION OF ABSTRACT	18. NUMBER OF PAGES	19a. NAME OF RESPONSIBLE PERSON
a. REPORT	b. ABSTRACT	c. THIS PAGE			USAMRMC
U	U	U	UU	158	19b. TELEPHONE NUMBER *(include area code)*

Standard Form 298 (Rev. 8-98)
Prescribed by ANSI Std. Z39.18

Table of Contents

INTRODUCTION

Body armor has made blast injuries survivable; consequently, we speculate that to a large extent blast-induced head injuries have emerged among troops who without body armor would have simply been killed in action as a result of injury to more vulnerable organs such as the lung. Serendipitously, in a preliminary experiment we noted that along with reducing mortality, lung injury, and cardiovascular disruptions by blast overpressure (BOP), Kevlar vests protected against BOP-induced neuropathological changes in rats. These preliminary findings suggested that a protective vest encasing the thorax might ameliorate blast-induced brain injury, pointing to a significant contribution of the effects of blast on the thorax to brain injury pathophysiology. We hypothesized that much of the blast-induced fiber degeneration in brain results from pressure surges transmitted through the vasculature (venous as well as arterial) that elicit a series of intracranial disruptions, and that Kevlar vests are neuroprotective by uncoupling this pressure transmission following exposure to blast.

BODY

Overview

The project was initiated with an air-driven constant diameter shock tube (fig 2) which was also used to simulate BOP in the pilot work upon which this project was based. As noted above, Kevlar vests somewhat surprisingly protected against BOP-induced neuropathological changes in rats exposed to BOP in this early work, pointing to a potentially significant contribution of the systemic effects of blast to the associated brain injury pathology. This general observation was consistent with speculations by others (Cernak et al., 2001) that blood vessels provide a particularly effective conduit for blast energy transfer to the brain, and that much of the blast-induced neurodegeneration in the brain results from pressure surges transmitted through the vasculature (venous as well as arterial) that elicit a series of intracranial disruptions, including a multiphasic increase in intracranial pressure (ICP). It is noteworthy that a high incidence of traumatic cerebral vasospasm (TCV) has been reported among blast casualties (Armonda et al., 2006), often times unaccompanied by fragment penetration, which is consistent with TCV resulting in part from propagation of the blast wave through the blood vessels and that uncoupling this pressure transmission by vest protection might mitigate TCV and associated brain injury resulting from a blast. As outlined below, we explored this possibility through the specific aims of this project.

It is important to note that over the course of this project, modifications in blast exposure conditions were progressively implemented to greatly improve the fidelity of blast simulation in the cylindrical shock tube. In particular, through consultation with a blast physicist, we learned that our initial use of the shock tube, with rats positioned at its mouth for blast overpressure exposures, was inappropriate and artefactually exposed them to extreme airjetting (and associated blunt trauma) rather than a planar shock wave. With guidance, we developed and utilized a new rat holder that houses pressure gauges and records the ambient flow conditions (static and total pressures) in immediate proximity to the experimental subject. The artefactual biomechanical loading associated with end jet effects was eliminated by using this holder's gauges to map the shock tube and employing shock wave exposures 2.5 feet within the shock tube (fig 1-

2). In addition, when we gained an appreciation of the uncontrolled acceleration and displacement potentially occurring with exposures within the shock tube, we refined our holder to greatly restrict these movements. These gauges provided confirmation of our ability to restrict movement/acceleration and consistently generate better controlled exposures.

As the study progressed, we further learned that cylindrical shock tubes are inherently and universally limited for blast simulation. Most importantly, rather than the sharp peak positive pressures associated with the Friedlander waveform, cylindrical shock tubes typically produce plateau or flat-top waveforms with relatively long durations (6-12 msec) and the dynamic pressure (i.e. blast wind) associated with the constant diameter tube is greatly exaggerated relative to that associated with conventional explosive detonations (fig 17-18). In addition, in the absence of an end wave eliminator, negative phase and recompression waves are artefacts of the rarefaction from the end of the open tube and the secondary shock is moving in the reverse direction (upstream not downstream). Furthermore, without a reflection eliminator, waves reverberate throughout the length of the tube after the passage of the initial shock front (Ritzel et al., 2011). Upon learning of (and in many cases documenting) these limitations, to improve the ecological validity of our blast simulations we acquired a state-of-the-art advanced blast simulator (ABS). With a divergent transition section and an end wave eliminator, this device eliminates the aforementioned artefacts of constant diameter shock tubes and provides a means to produce a controlled high fidelity simulation of blast in the laboratory (figs 16-17). With this device, positive pressure durations can be reduced to 1-2 msec, which may better represent waveforms resulting from IEDs and positional heterogeneity in pressures and flow conditions are eliminated (Ritzel et al., 2011).

With the development of the ABS and the improvements it provided, following its careful characterization we repeated several key experiments using the new ABS to compare and validate results produced in the cylindrical shock tube, particularly since the flow and loading conditions are quite different between the two blast simulation devices and as noted above, changed considerably from those of the initial pilot experiments which gave rise to the study (Long et al, 2009). In particular, during an extended no-cost-extension, we evaluated rats exposed to blast in the ABS and assessed the effects of protective Kevlar vests on their acute pressure responses and associated outcomes. We anticipated that these improvements and comparisons would be informative and important, in particular since poorly designed blast simulations have confounded much of the preclinical biomedical blast literature to date (Needham et al., 2015).

Specific Aims/Milestones:

1. Using a compression-driven shock tube, measure, compare and correlate external (i.e. shock tube), systemic (i.e. vascular arterial and venous), and central (i.e. intracranial pressure) effects of BOP of varied intensities.

After implementing the improvements in blast exposure conditions noted above, we documented that the magnitudes and time courses of pressure responses recorded in different body compartments of anesthetized rats corresponded closely to the ambient pressure conditions associated with blast overpressure. This was true with exposures in both the cylindrical shock tube and the ABS. In particular, it is noteworthy ICP was

essentially superimposable with ambient pressures, revealing that the rat skull provides very little protection against BOP.

2. Determine if measured pressure changes in the experimental subject are blast severity-dependent and correspond with neuropathological and neurobehavioral outcome measures.

In general, with implementation of correct blast simulations the neuropathological and neurobehavioral disruptions caused by BOP were much less striking than initially reported (Long et al, 2008) and were substantially further lessened by the progressive improvements in our blast exposure conditions. In particular, the robust injuries resulting from exposures at the mouth of the shock tube were largely eliminated by proper positioning within the tube, and likely were artefactual as a result of the extreme airjets occurring at the exit. As noted by Needham et al. (2015), widespread ongoing misuse of shock tubes has continued to yield erroneous data that has greatly confounded the preclinical biomedical blast research literature. As described below, use of a state-of-the-art ABS now provides high fidelity blast simulations, and neuropathological and neurobehavioral disruptions have been documented following these exposures and generally resemble those seen with correct exposures in the cylindrical shock tube. In general, fiber degeneration is the most prominent neuropathological feature, and is typically evident in the cerebellum, optic tracts, and internal capsule. Increased exposure pressures produced greater injuries and neurobehavioral disruptions, although the transition to fatal injuries occurred over a narrow range of pressures. Neuropathological and neurobehavioral outcomes were more affected by exposure repetitions than the severities (i.e. peak amplitude) of single exposures. As described below, we developed ambulation across a rotating cylindrical pole as a neurobehavioral test that provides a sensitive means to detect BOP-induced cerebellar and vestibulomotor perturbations. Rats were also evaluated in the Morris water maze (MWM) to evaluate BOP effects on spatial learning and memory.

3. Assess impact of Kevlar vests on measured BOP-induced pressure changes and neurobehavioral and neuroanatomical outcome measures.

Under corrected exposure conditions in both the cylindrical shock tube and the ABS, Kevlar vests did not significantly impact pressure changes or outcome measures using the rotating pole and MWM tests.

4. Assess impact of Kevlar vests on measured BOP-induced pressure changes and acute cerebrovascular measures.

Although under corrected exposure conditions in both the cylindrical shock tube and the ABS Kevlar vests did not significantly impact pressure changes, there were changes in cerebrovascular permeability which will need to be explored further.

KEY RESEARCH ACCOMPLISHMENTS

- Despite our inability over the extended course of this project to generate data that confirmed our initial finding of protective vest effects that could be explained by altered pressure responses, we nevertheless achieved several notable research accomplishments. In particular, as a result of this study, we now have a state-of-the art ABS with which many salient features of the biophysics of BOP can be recreated in the laboratory for biomedical research. The blast flow conditions in the ABS have been carefully and thoroughly evaluated using high speed videography (25,000 frames per sec) in combination with pressure recordings. Using this device, we are now generating data to more comprehensively evaluate systemic contributions to blast injury etiology as part of 2 collaborative project with investigators at the Biotechnology HPC Software Applications Institute (BHSAI) and the New Jersey Institute of Technology. We have also progressively refined ecologically valid models of blast-TBI and concussion in rats and mice that recreate features of human injuries which we anticipate can be used judiciously to investigate bTBI phenomena and identify countermeasures. Moreover, many of the issues afflicting Warfighters exposed to blast, including auditory and vestibular disruption, tinnitus, and visual impairments have been characterized in these rodent models, and are valuable tools for establishing the neurobiological underpinnings of these disorders and for developing effective countermeasures. These research tools can now be applied to evaluate cumulative effects of blast exposures (>2 exposures) which is a highly relevant military medical concern.
- A battery of sensitive neurobehavioral assessments has been carefully developed and refined to distinguish functional disruptions resulting from single or repeated BOP exposures.
- Multiple publications and presentations were prepared which described neurobehavioral, neurochemical, and neuropathological features of blast TBI in rodents. This work established the foundation for additional funded projects, including most recently “Assessment and Treatment of Blast-Induced Auditory and Vestibular Injuries” (Clinical Rehabilitative Medicine Research Program [CRMRP] Neurosensory Research Award), “Elucidation of Inflammation Processes Exacerbating Neuronal Cell Damage to the Retina and Brain Visual Centers, as a Quest for Therapeutic Drug Targets, in a Rat Model of Blast Over Pressure Wave Exposure” ([CRMRP] Vision Research Program - Hypothesis Development Award, and “Central mechanism and treatment of blast-induced auditory and vestibular injuries” (Clinical Rehabilitative Medicine Research Program [CRMRP] Neurosensory Research Award).

REPORTABLE OUTCOMES

Manuscripts and related publications

1. Ahmed, F.A., Kamnaksh, A., Kovesdi, E., Long, J.B., Agoston, D.V. Long-term consequences of single and multiple mild blast exposure on select physiological

parameters and blood-based biomarkers. Electrophoresis. 2013 Aug; 34(15):2229-33.

2. Arun, P., Abu-Taleb, R., Oguntayo, S., Wang, Y., Valiyaveettil, M., Long, J.B., Nambiar, M.P. Acute mitochondrial dysfunction after blast exposure: potential role of mitochondrial glutamate oxaloacetate transaminase. J Neurotrauma. 2013 Oct 1; 30(19):1645-51.

3. Arun, P., Abu-Taleb, R., Valiyaveettil, M., Wang, Y., Long, J.B., Nambiar, M.P. Extracellular cyclophilin A protects against blast-induced neuronal injury. Neurosci Res. 2013 May-Jun; 76(1-2):98-100.

4. Arun. P, Abu-Taleb. R, Oguntayo, S., Wang, Y., Valiyaveettil, M., Long, J.B., Nambiar, M.P. Distinct patterns of expression of traumatic brain injury biomarkers after blast exposure: Role of compromised cell membrane integrity. Neuroscience Letters. 2013 Sept 27; 552: 87-91.

5. Kamnaksh A, Budde MD, Kovesdi E, Long JB, Frank JA, Agoston DV. Diffusion tensor imaging reveals acute subcortical changes after mild blast-induced traumatic brain injury. Sci Rep. 2014 May 2;4:4809. doi: 10.1038/srep04809.

6. Calabrese E, Du F, Garman RH, Johnson GA, Riccio C, Tong LC, Long JB. Diffusion tensor imaging reveals white matter injury in a rat model of repetitive blast-induced traumatic brain injury. J Neurotrauma. 2014 May 15;31(10):938-50. doi: 10.1089/neu.2013.3144. Epub 2014 Mar 27.

7. Kamnaksh A, Kwon SK, Kovesdi E, Ahmed F, Barry ES, Grunberg NE, Long J, Agoston D. Neurobehavioral, cellular, and molecular consequences of single and multiple mild blast exposure. Electrophoresis. 2012 Dec;33(24):3680-92. doi: 10.1002/elps.201200319. Epub 2012 Nov 26.

8. Kovesdi E, Kamnaksh A, Wingo D, Ahmed F, Grunberg NE, Long JB, Kasper CE, Agoston DV. Acute minocycline treatment mitigates the symptoms of mild blast-induced traumatic brain injury. Front Neurol. 2012 Jul 16;3:111. doi: 10.3389/fneur.2012.00111. eCollection 2012.

9. Kamnaksh A, Kovesdi E, Kwon SK, Wingo D, Ahmed F, Grunberg NE, Long J, Agoston DV. Factors affecting blast traumatic brain injury. J Neurotrauma. 2011 Oct;28(10):2145-53. doi: 10.1089/neu.2011.1983.

10. Kovesdi E, Gyorgy AB, Kwon SK, Wingo DL, Kamnaksh A, Long JB, Kasper CE, Agoston DV. The effect of enriched environment on the outcome of traumatic brain injury; a behavioral, proteomics, and histological study. Front Neurosci. 2011 Apr 1;5:42. doi: 10.3389/fnins.2011.00042. eCollection 2011.

11. Kwon SK, Kovesdi E, Gyorgy AB, Wingo D, Kamnaksh A, Walker J, Long JB, Agoston DV. Stress and traumatic brain injury: a behavioral, proteomics, and histological study. Front Neurol. 2011 Mar 7;2:12. doi: 10.3389/fneur.2011.00012. eCollection 2011.

12. Arun P, Oguntayo S, Albert SV, Gist I, Wang Y, Nambiar MP, Long JB. Acute decrease in alkaline phosphatase after brain injury: A potential mechanism for tauopathy. Neurosci Lett. 2015 Nov 16;609:152-8. doi: 10.1016/j.neulet.2015.10.036. Epub 2015 Oct 19.

13. Vogel, EW, Morrison B, Evilsizor MN, Griffiths DR, Thomas TC, Lifshitz, J, Sutton, RL, Long, JB, Ritzel, D, Lings, GSF, Huh, J, Raghupathi, R, McIntosh, TK. Experimental Models of Traumatic Brain Injury: Clinical Relevance and Shortcomings. In: “Cell Therapy for Neurologic Injury”,C. Cox (ed). CRC Press, 2016.

Presented abstracts:

1. Long, J.B. Blast Overpressure in Rats: Recreating a Battlefield Injury in the Laboratory. Presentation at the International State-of-the-Science Meeting on Non-Impact, blastinduced mild traumatic brain injury in Herndon, VA, May 12-14, 2009.

2. Gharavi R.B., Shoge R.O., Long J.B., and Bentley T.B. Characterization of an air-driven shock tube used to recreate battlefield traumatic brain injuries. National Neurotrauma Symposium, June 2010.

3. Riccio C, Bentley T.B., and Long J.B. Blast overpressure injury in rats produces widespread fiber degeneration. National Neurotrauma Symposium, June 2010.

4. Shoge, R.O. Pressure profiles of shock tube exposures. Invited platform presentation at the Advanced Technology Applications for Combat Casualty Care (ATACCC) Meeting, St. Pete’s Beach FL, Aug, 2010.

5. Riccio C., Bentley T.B., and Long J.B. Blast overpressure injury in rats produces widespread fiber degeneration. Poster at the Advanced Technology Applications for Combat Casualty Care (ATACCC) Meeting, St. Pete’s Beach FL, Aug, 2010.

6. Long, J.B. Experimental Evaluation of Blast-induced Traumatic Brain Injury in Rats Using a Cylindrical Shock Tube. Invited speaker at the Third DOD Brain Injury Computational Modeling Expert Panel Meeting, Johns Hopkins University Applied Physics Laboratory, Laurel MD, Dec 2010.

7. Shoge, R.O. Experimental Evaluation of Blast-induced Traumatic Brain Injury in Rats Using a Cylindrical Shock Tube. Invited speaker at the National Capital Region TBI Research Symposium. April 5, 2011.

CONCLUSION

As the result of substantial refinement, under carefully controlled experimental conditions, the biomechanical perturbations of the brain that yield blast-induced mild TBI in injured Warfighters can be recreated with reasonable fidelity to reproduce characteristic sequelae of blast-induced mild TBI. Results to date are generally inconsistent with our initial hypothesis that blast-induced fiber degeneration in brain results from pressure surges transmitted through the vasculature (venous as well as arterial) that elicit a series of intracranial disruptions, and that Kevlar vests are neuroprotective by uncoupling this pressure transmission following exposure to blast. The limited contribution (if any) of this mechanism to blast TBI is now under closer scrutiny in collaborative projects using refined techniques and computational modeling. Despite an inability to generate the hypothesized outcome, the BOP model developed in this study provides an invaluable tool to define underlying neurobiological mechanisms and rationally establish effective guidelines and countermeasures to lessen short-term impairments as well as chronic debilitation (e.g. chronic traumatic encephalopathy).

REFERENCES

1. Cernak I, Wang Z, Jiang J, Bian X, Savic J. Ultrastructural and functional characteristics of blast injury-induced neurotrauma. J Trauma. 2001 Apr;50(4):695-706.
2. Long JB, Bentley TL, Wessner KA, Cerone C, Sweeney S, Bauman RA. Blast overpressure in rats: recreating a battlefield injury in the laboratory. J Neurotrauma. 2009 Jun;26(6):827-40. doi: 10.1089/neu.2008.0748.
3. Needham CE, Ritzel D, Rule GT, Wiri S, Young L.Blast Testing Issues and TBI: Experimental Models That Lead to Wrong Conclusions. Front Neurol. 2015 Apr 8;6:72. doi: 10.3389/fneur.2015.00072. eCollection 2015.
4. Ritzel, D.V., Parks, S.A., Roseveare, J., Rude, G. Sawyer, T., “Experimental Blast Simulation for Injury Studies”, NATO/RTO HFM-207 Symposium, Halifax, Canada, 3-5 Oct 2011.

SUPPORTING DATA

Procedures to optimize controlled shock wave exposures involved development of a gauged holder which tautly suspended the anesthetized rat within the shock tube (fig 1). The total and static pressure gauges incorporated into this holder were used to map the shock tube and the measurements revealed that earlier positioning at the mouth of the shock tube exposed rats to exaggerated flow conditions. In particular, the impulse ratio changed dramatically immediately outside the mouth of the tube, where total pressure impulse increased by factors of 100-fold,

Fig 1.Instrumented rat holder records flow conditions (static and total pressure) during subject exposure & also provided a pressure map of the shock tube

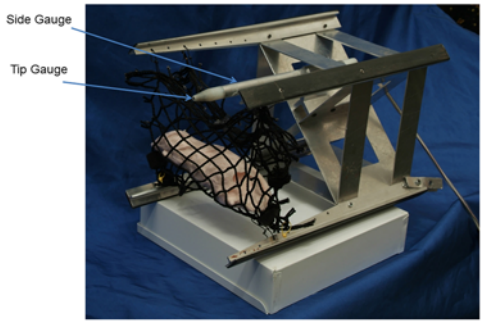

Fig 2. Shock tube pressure recordings.

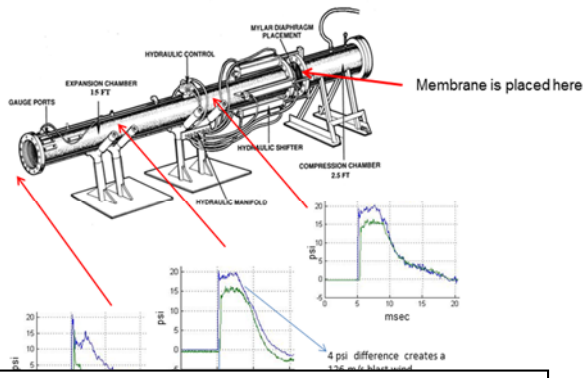

reflecting an even more pronounced potential biomechanical influence of dynamic pressure (i.e. blast wind) in the exit-jet flow. Based upon these measurements, rats were routinely positioned 2.5 ft within the mouth of the shock tube for shock wave exposures.

At this position (12.5 ft from the membrane), we observed that vascular, esophageal, and intracranial pressures tracked closely with ambient pressures (figs 4-7). Shock wave pressure profiles and intracranial, intraesophageal, and intravascular pressures were recorded with anesthetized rats positioned in a transverse prone position 2.5 ft from the mouth of the tube. Rats were tested with and without Kevlar vests. Pressures were recorded using 127 and 254 micron thick

Fig 3.

Overpressure Parameters at Varied Positions within the Blast Tube

254 µ Thick Membrane N=3						
Feet from mouth of tube	Avg Peak Total Pressure (psi)	Avg Peak Static Pressure (psi)	Total Impulse (psi-ms)	Static Impulse (psi-ms)	Total Overpressure Duration (ms)	Static Overpressure Duration (ms)
10	20.87	16.73	118.26	100.48	13.42	13.32
2.5	21.05	16.30	97.92	71.90	8.42	6.70
-0.5	21.17	15.47	65.22	6.88	12.85	1.40

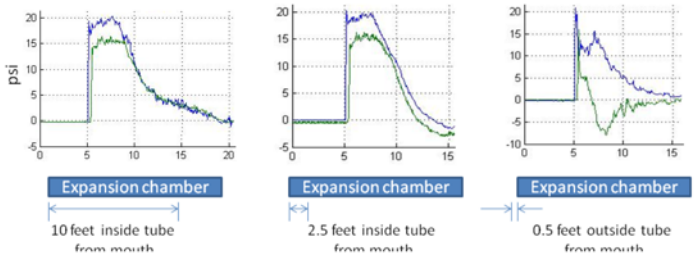

Mylar membranes which typically produced side-on peak pressures of 12 and 20 psi, respectively. Figure 1 shows pressure waveforms generated using a 127 micron thick Mylar membrane and recorded by the pressure sensors inside the tube (side-on and tip piezoresistive gauges) and inside the rat brain (Millar transducers). Each waveform consists of a positive overpressure wave followed by a negative underpressure wave and return to ambient pressure. In this figure, the total (tip) pressure approached 13 psi while the static (side) and intracranial pressure approached 10 psi. The overpressure durations of intracranial and static pressure were quite similar, while the total overpressure measured by the tip gauge had a longer duration. Overall, the induced overpressure profile recorded intracranially and statically in the air surrounding the rat do not vary much in terms of magnitude, impulse, and duration. The total pressure, which is a combination of static and dynamic pressure, had a higher peak pressure and lasted longer than the static and intracranial pressure. Similarly, although experiencing very different loading and injury phenomena, intracranial and intravascular pressures recorded from experimental subjects positioned at the mouth of the tube also closely resembled the external ambient pressures measured at this position (fig 8).

Fig 4.

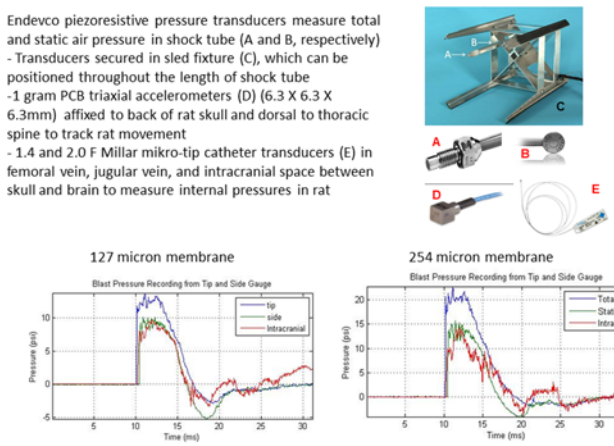

Fig 5. ICP (top), venous (middle), and esophageal (bottom) pressures track closely with ambient static pressures. Representative tracings from 16 recordings

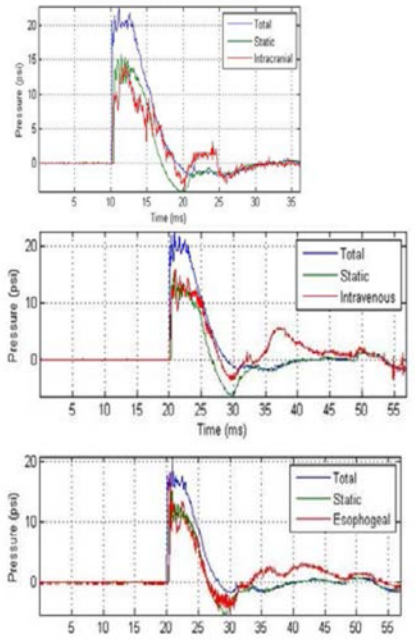

In fact, across all blast pressure exposure conditions, intracranial pressures closely corresponded to external side-on pressure recordings, revealing that the skull provides little protection against elevated pressures in rats. With increased membrane thicknesses,

peak pressures and pressure impulses increased for side-on and tip gauge recordings in the tube, and yielded correspondingly elevated and prolonged intracranial and intravascular pressure responses (fig 7). When outfitted

Fig 6. BOP-induced elevations in ICP increase with greater ambient pressure associated with increased Mylar membrane thickness. Representative tracings from 16 recordings.

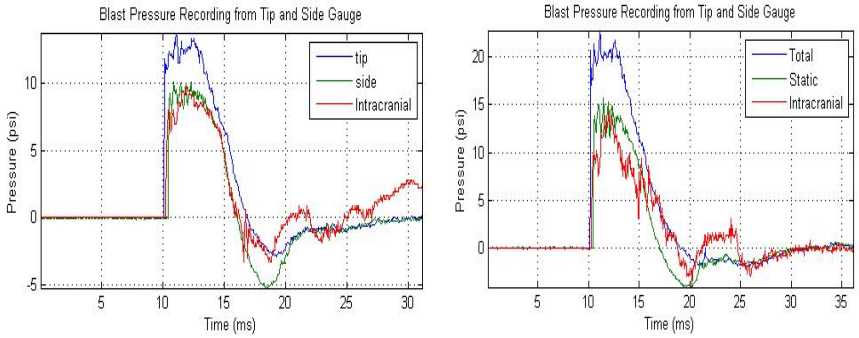

127 micron membrane

254 micron membrane

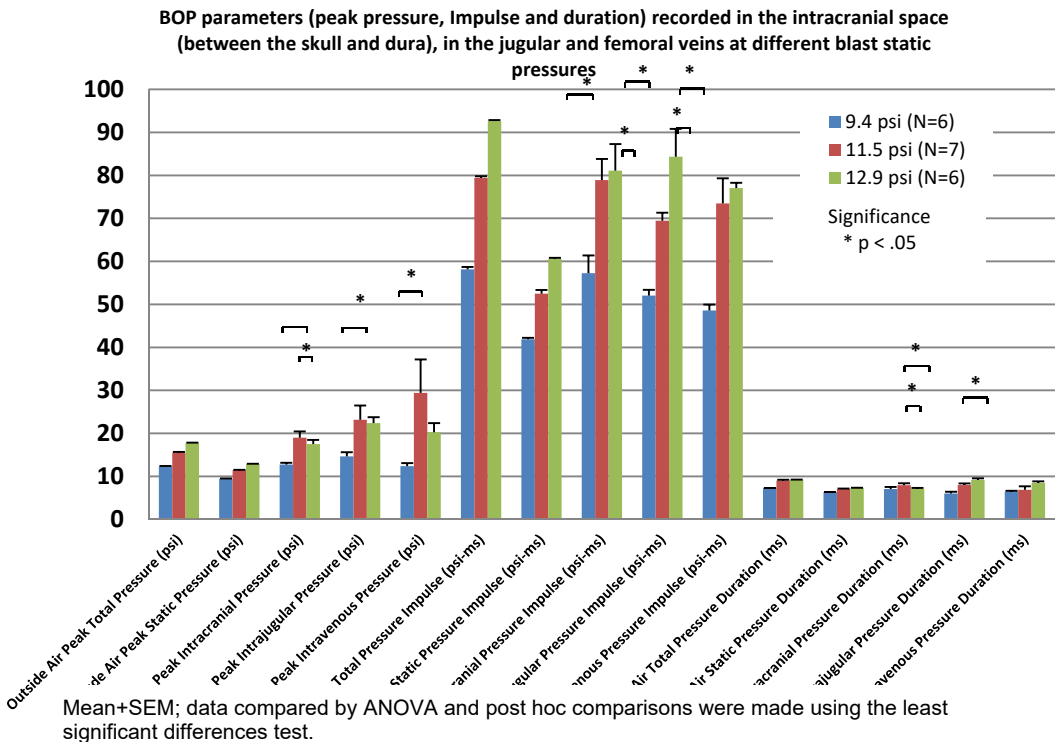

Mean+SEM; data compared by ANOVA and post hoc comparisons were made using the least significant differences test.

with protective Kevlar vests, these pressure responses were unaltered from those measured in rats not wearing vests (fig 8 & 10). Since the initial protective effects were observed at the mouth of the shock tube, we also made comparisons of measurements made at this position and again observed that vests did not alter pressure responses from those made in rats exposed to blast without vests. (fig 9).

Neuropathological and neurobehavioral disruptions of rats exposed to different BOP intensities are presented in fig 11and figs 14-19. In general, the functional impairments

Fig 8. Recordings with rat positioned 2.5 ft from mouth of shock tube

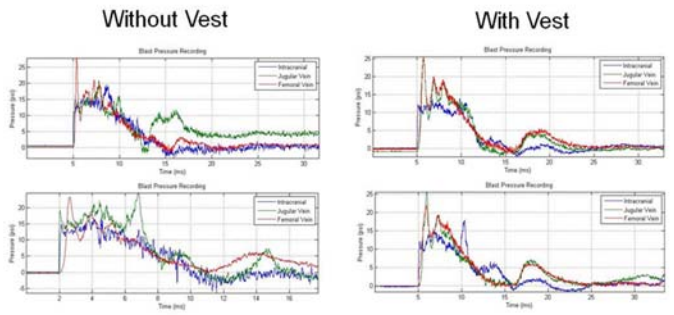

observed using refined BOP exposure conditions in these experiments were much more limited than were seen to result from exposures to comparable pressures at the mouth of the shock tube (Long et al., 2009). The behavioral deficits were typically accompanied by scattered fiber degeneration that characteristically appeared in cerebellum, optic tracts, and the internal and external capsules. In contrast to our earlier findings (Long et al., 2009), these neuropathological features were unaltered by protective vests. Neurobehavioral function was evaluated using ambulation on a rotating pole (fig 12) and spatial navigation in the Morris water maze (MWM). For the rotating pole test, a wooden pole 4 feet in length and 1.5 inches diameter, which could be rotated at different speeds in either clockwise or counterclockwise directions, was suspended

Fig10. Protective vests did not alter rats' pressure responses to BOP

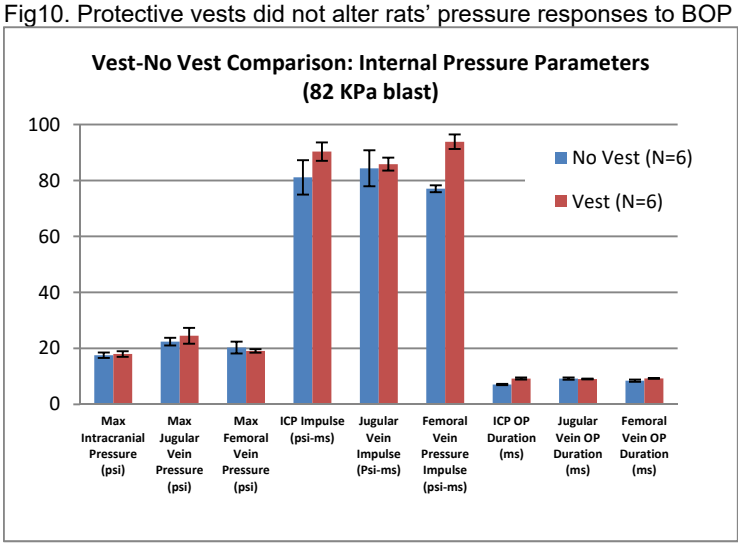

parallel to the floor at a height of approximately 3 feet overlying a foam cushion. Rats were released at one end and trained to traverse the rotating pole to enter a darkened box at its other end. The time from release to entry into the box was recorded with a maximum of 120 seconds allowed to complete each run. When rats failed to traverse the pole, the time and location of the fall was recorded. Runs were scored using a rubric that incorporates balance (1 point for not falling; 0 points for a fall), velocity (distance on the pole covered/time) and distance completed (1 point for a complete run, 0.75 for a fall at the ¾ mark, 0.5 for a fall in the middle and 0 points for a fall at the beginning). On each test day, each rat was given three trials and the two highest scores were averaged as the score for that rat on that day. Longer traverse times and falls from the pole indicate motor deficits. These non-parametric data were examined using the Kruskal-Wallis H statistical test followed by the Mann-Whitney U test if warranted. For Morris water maze testing, rats were release from 4 cardinal compass locations around a 170 cm diameter pool and the time required to locate a hidden platform was recorded, with a maximum allowable time of 120 sec. ANOVA was employed on the MWM data and if significance was achieved, individual differences were distinguished post hoc using the least significant differences test.

Fig 9. Recordings with rat positioned at mouth of shock tube

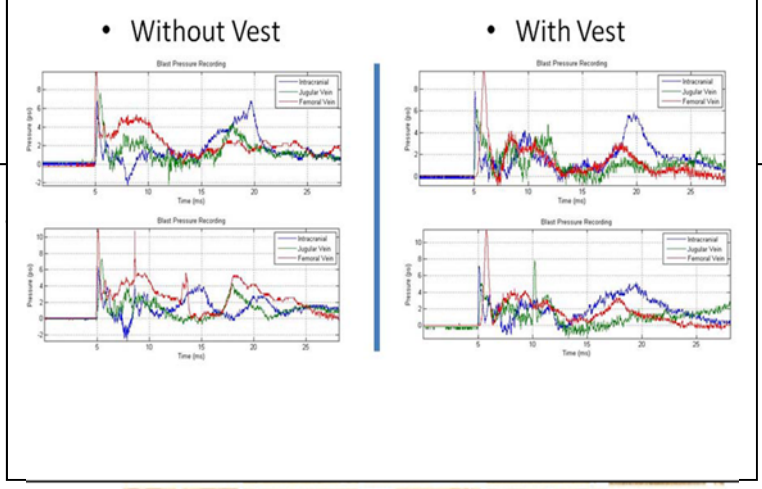

Extravasation of Evans blue dye into the brain was used to quantitate BOP-induced disruption of the blood-brain barrier. These experiments surprisingly revealed appreciable cerebrovascular disruptions at 2 and 5 hr post-BOP that in contrast to other assessments, appeared to be diminished by protective vests (fig 13). -induced BBB disruption is not immediat triggered in response to a systemic media whose release is ameliorated by the prot

Fig 13. Evans blue dye extravasation 2hrs after 12 psi BOP exposure

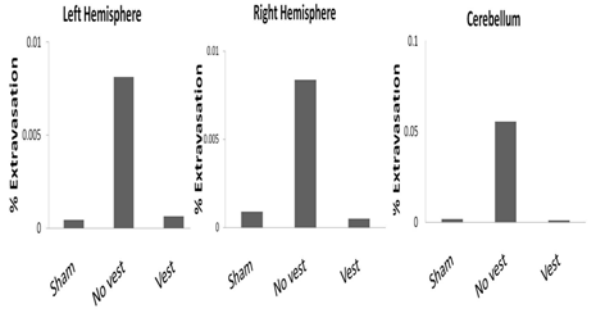

Fig12. Rotating pole test.

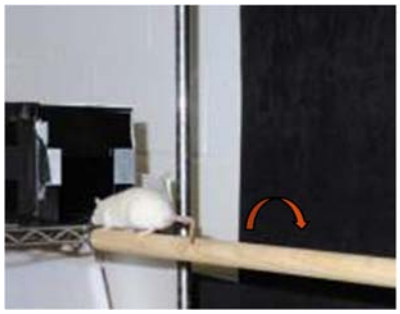

* *

*

n=7, *p<0.05

Fig 14. MWM latencies following 10 psi BOP

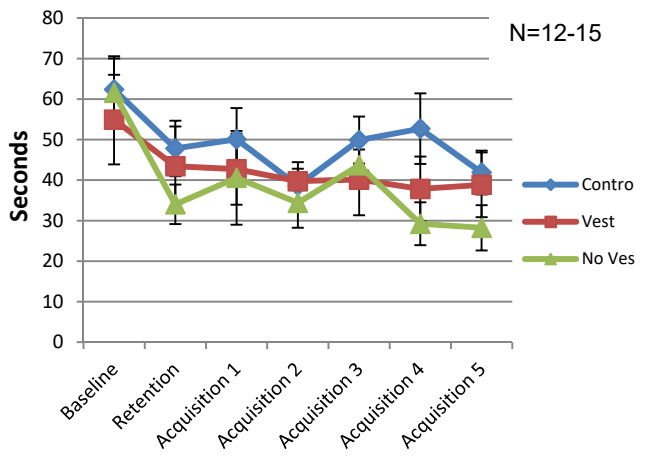

Fig 15. MWM latencies following 12 psi BOP

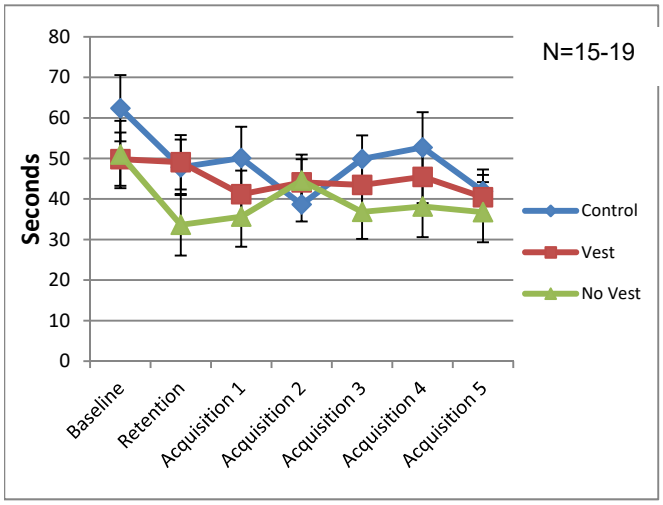

Fig 16. MWM latencies following 13 psi BOP

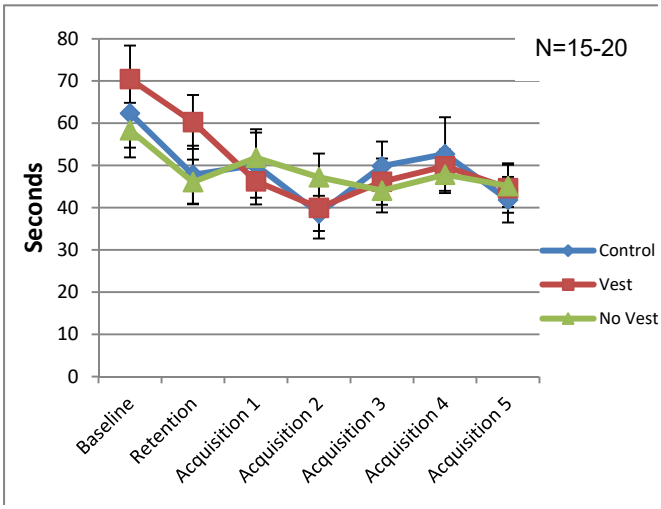

Fig 17. Rotating pole scores following 10 psi BOP

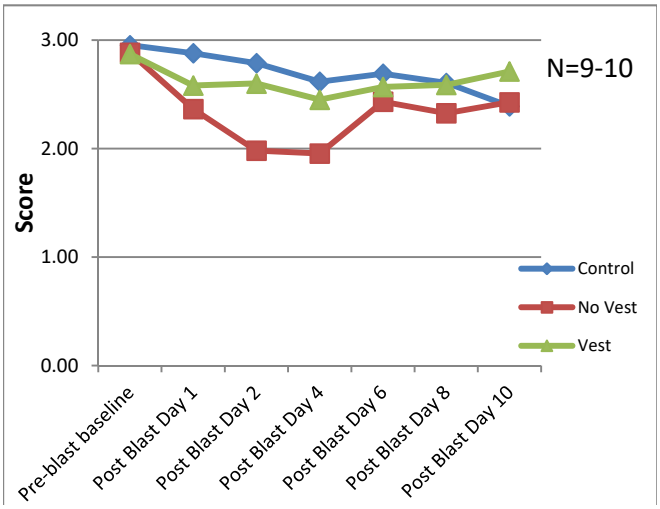

Fig 18. Rotating pole scores following 12 psi BOP

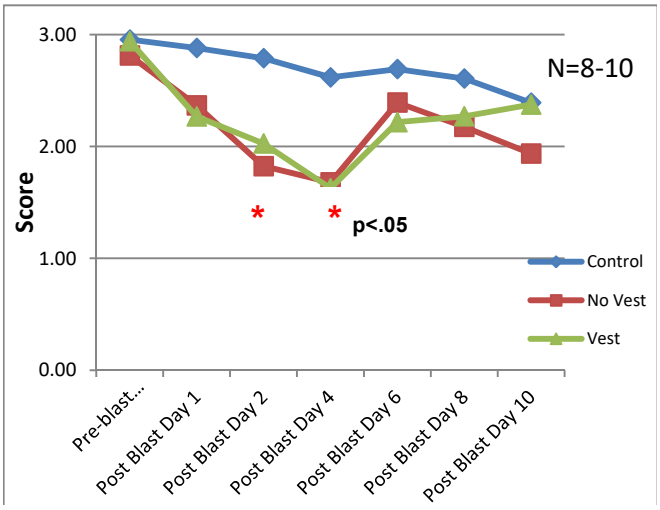

Fig 19. Rotating pole scores following 13 psi BOP

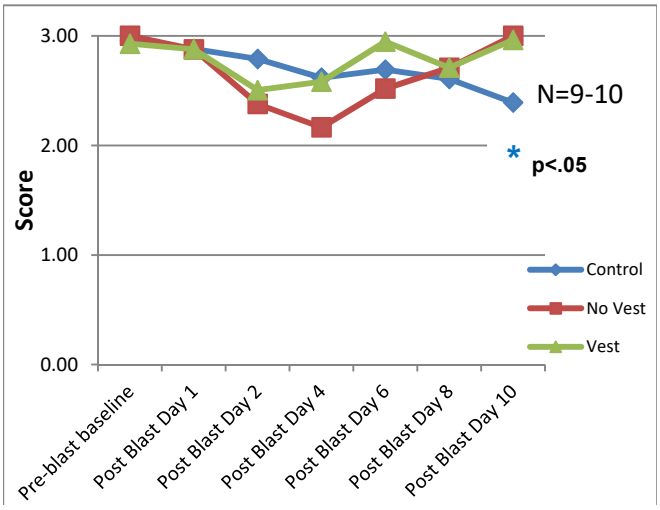

Fig 16. Advanced blast simulator.

Finally, when established and characterized, the ABS (fig 16) was used to repeat several experiments and evaluate pressure responses of anesthetized rats to shock wave exposure and the effects of protective vests on these responses using a higher fidelity blast simulation. For these experiments, rats positioned in longitudinal (fig 17) and transverse orientations relative to shockwave. ICP recordings were made from the lateral ventricle as well as from a probe positioned between the dura and the skull. In both situations (vest and no vest), ICP, femoral, and carotid pressure response tracked closely with ambient pressure conditions and were unaltered by the protective vest figs 20-21). Functional impairments produced by shockwaves in the ABS closely resemble those seen following shockwave exposures in the cylindrical shock tube and are accompanied by similar neuropathological features.

Fig 17. ABS pressure trace

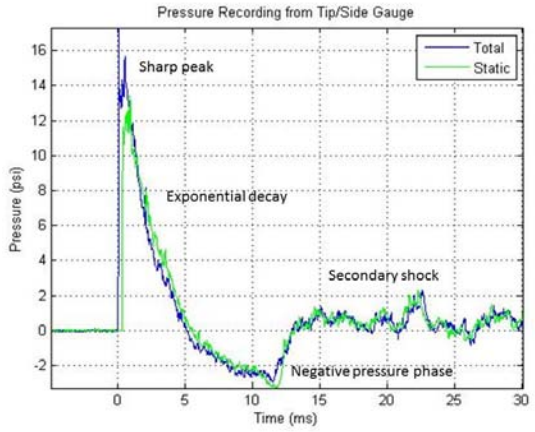

Fig 18. Cylindrical shock tube pressure trace

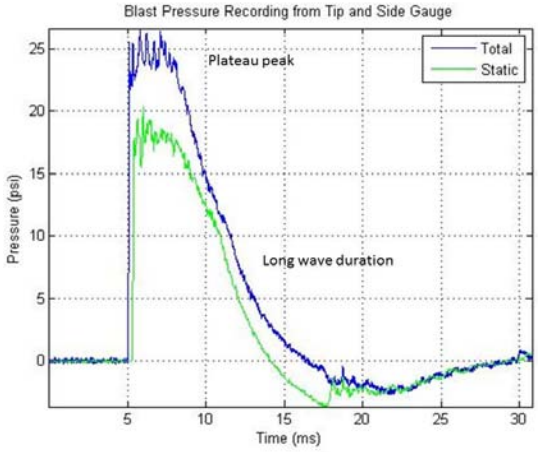

Fig 19.Anesthetized rat longitudinally positioned in the ABS for shock wave exposure

Fig 20. Pressure recordings in ABS without protective vest.

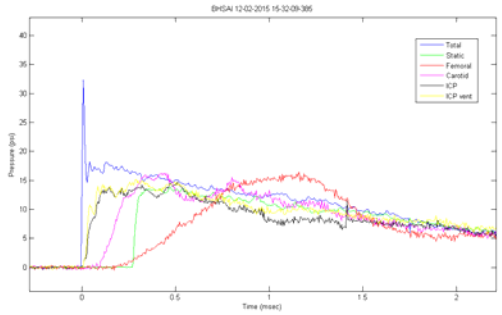

Fig 21. Pressure recordings in ABS with protective vest .

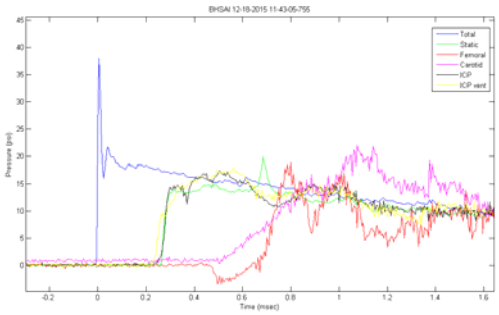

Neuroscience Letters 609 (2015) 152–158

Contents lists available at ScienceDirect

Neuroscience Letters

journal homepage: www.elsevier.com/locate/neulet

Research paper

Acute decrease in alkaline phosphatase after brain injury: A potential mechanism for tauopathy

Peethambaran Arun*, Samuel Oguntayo, Stephen Van Albert, Irene Gist, Ying Wang, Madhusoodana P. Nambiar, Joseph B. Long*

Blast-Induced Neurotrauma Branch, Center for Military Psychiatry and Neuroscience, Walter Reed Army Institute of Research, Silver Spring, MD 20910, USA

HIGHLIGHTS

- Brain injuries due to blast or weight drop decreased the level/activity of TNAP.
- Decreased level/activity of brain TNAP is associated with accumulation of *pTau*.
- Brain injury decreased plasma alkaline phosphatase activity.
- APP accumulation in the brain after injury did not correlate with *pTau* deposition.

ARTICLE INFO

Article history:
Received 18 August 2015
Received in revised form 1 October 2015
Accepted 12 October 2015
Available online 19 October 2015

Key words:
Blast exposure
Head impact/acceleration
Tauopathy
Chronic traumatic encephalopathy
Traumatic brain injury
Tissue non-specific alkaline phosphatase

ABSTRACT

Dephosphorylation of phosphorylated *Tau* (*pTau*) protein, which is essential for the preservation of neuronal microtubule assemblies and for protection against trauma-induced tauopathy and chronic traumatic encephalopathy (CTE), is primarily achieved in brain by tissue non-specific alkaline phosphatase (TNAP). Paired helical filaments (PHFs) and *Tau* isolated from Alzheimer's disease (AD) patients' brains have been shown to form microtubule assemblies with tubulin only after treatment with TNAP or protein phosphatase-2A, 2B and -1, suggesting that *Tau* protein in the PHFs of neurons in AD brain is hyperphosphorylated, which prevents microtubule assembly. Using blast or weight drop models of traumatic brain injury (TBI) in rats, we observed *pTau* accumulation in the brain as early as 6 h post-injury and further accumulation which varied regionally by 24 h post-injury. The *pTau* accumulation was accompanied by reduced TNAP expression and activity in these brain regions and a significantly decreased plasma total alkaline phosphatase activity after the weight drop. These results reveal that both blast- and impact acceleration-induced head injuries cause an acute decrease in the level/activity of TNAP in the brain, which potentially contributes to trauma-induced accumulation of *pTau* and the resultant tauopathy. The regional changes in the level/activity of TNAP or accumulation of *pTau* after these injuries did not correlate with the accumulation of amyloid precursor protein, suggesting that the basic mechanism underlying tauopathy in TBI might be distinct from that associated with AD.

1. Introduction

Advancements in far-forward medical care have greatly increased the survivability of traumatic brain injuries (TBIs), which in recent military conflicts have been primarily attributable to the widespread use of improvised explosive devices and other modern explosive weaponries. In particular, exposure to blast has been described as the major cause of TBI and associated disabilities in the recent wars in Iraq and Afghanistan [20]. Although several biochemical and histopathological changes have been preclinically documented in the central nervous system after blast exposure [7,8,16,19,26,29,33], the potentially complex pathophysiological mechanisms triggering long-term neurobehavioral abnormalities are not well understood, which has hampered the development of effective countermeasures and diagnostic approaches.

Recent studies indicate that chronic traumatic encephalopathy (CTE), a tau protein-linked neurodegenerative disorder which has been observed in several athletes with a history of multiple concussions, shares clinical symptoms and neuropathological features described in victims of blast exposure [10]. In particular, phos-

* Corresponding authors at: 503 Robert Grant Ave, Walter Reed Army Institute of Research, Silver Spring, MD 20910, USA. Fax: +1 301 319 9839.
E-mail addresses: peethambaran.arun.ctr@mail.mil (P. Arun), joseph.b.long.civ@mail.mil (J.B. Long).

http://dx.doi.org/10.1016/j.neulet.2015.10.036
0304-3940/

phorylated *Tau* (*pTau*) protein neuropathology, with perivascular neurofibrillary degeneration, is recognized as a distinct feature of CTE and has been observed postmortem in the brains of blast victims and contact-sport athletes. Brains of mice exposed to blast overpressure in a shock tube also showed neuropathological features of CTE such as phosphorylated tauopathy, myelinated axonopathy, microvasculopathy, neuroinflammation and neurodegeneration, prompting postulation that blast-induced acceleration of the head may play an important role in the development of CTE-like neuropathology [10]. Phosphorylation of *Tau* protein disrupts microtubule assembly in neurons, which can result in tauopathy and the formation of neurofibrillary tangles seen in neurodegenerative disorders such as Alzheimer's disease (AD) [12,15,31]. Dephosphorylation of *pTau* is critical to prevent tauopathy and to restore microtubule assembly for neuroregeneration.

By dephosphorylating *pTau* in neurons, tissue non-specific alkaline phosphatase (TNAP) may play a major role in the etiology of brain disorders involving this neuropathological feature [12,15,31]. Paired helical filaments and *Tau* protein isolated from AD patients' brains were shown to form a microtubule assembly with tubulin *in vitro* only after treatment with alkaline phosphatase or protein phosphatase-2A, -2B and -1, suggesting that *Tau* protein in the paired helical filaments of neurons in AD brain is hyperphosphorylated, which prevents microtubule assembly [12,15,31]. Alkaline phosphatase showed significantly higher activity in dephosphorylating *pTau* compared to the other protein phosphatases studied [31].

A number of studies indicate that accumulation of amyloid precursor protein (APP) and β-amyloid peptides induces the phosphorylation of *Tau,* leading to microtubule disassembly, which is an accepted neuropathological feature of AD [5,11,18,27,28,30,34]. Activation of mitogen-activated protein kinase by accumulated APP has been described as a mechanism yielding the phosphorylation of *Tau* protein [11]. In a hybrid septal cell line, treatment with aggregated β-amyloid peptide resulted in accumulation of *pTau* and paired helical filaments and alkaline phosphatase treatment abolished the effect [18], emphasizing the potentially important role of β-amyloid peptide in triggering and TNAP in preventing *Tau* phosphorylation.

In the present study, we utilized rat models of blast-induced TBI using a shock tube and impact acceleration-induced TBI using weight drop and explored the acute changes in the expression of *pTau* and level/activity of TNAP in different brain regions after these insults. We have also examined whether the alterations in the expression of *pTau* and TNAP are associated with a corresponding acute change in the expression of APP to examine a possible role of accumulated APP in the initiation and development of tauopathy after TBI.

2. Experimental procedures

2.1. Animals and blast injury

All animal experiments were conducted in accordance with the Animal Welfare Act and other federal statutes and regulations relating to animals and experiments involving animals, and adhered to principles stated in the Guide for the Care and Use of Laboratory Animals (NRC Publication 2011 edition) using an Institutional Animal Care and Use Committee approved protocol. Male Sprague Dawley rats, 9–10 weeks old that weighed 300–350 g (Charles River Laboratories, Wilmington, MA) were housed at 20–22 °C (12 h light/dark cycle) with free access to food and water *ad libitum*. A total of 4 animals/group was used for each time point.

2.2. Brain injury by blast exposure

Blast exposure was carried out using a compressed air-driven shock tube as described earlier [6]. Briefly, after 4% isoflurane gas anesthesia in an induction box for 6 min (O_2 flow rate 2 L/min), rats were immediately tautly secured in a transverse prone position in coarse mesh netting 2.5 ft within the mouth of the 15 ft long and 1 ft internal diameter expansion chamber with the right side of the head/body facing the pressure chamber. Rats were exposed to single shockwave (peak static pressure of 19.0 psi (131 kPa) with a 9 ms positive phase duration). Blast overpressure flow conditions were recorded using piezoresistive pressure transducers (Meggit Inc., San Juan Capistrano, CA) mounted in the rat holder which provided measurements of total and side-on pressure waveforms. Sham control animals were included in all individual experiments and were treated in the same fashion without exposure to blast.

2.3. Brain injury by weight drop

As originally described by Marmarou et al. [21], the injury device consisted of a vertically secured 2.5 m long Plexiglas tube with a 19 mm inner diameter. A 0.014 inch Mylar helmet was mounted on the heads of the isoflurane-anesthetized rats to prevent any skull fracture during weight drop. The rats were placed in a prone position on a 12 × 12 × 43 cm foam bed (Type E manufactured by Foam to Size, Inc., Ashland, VA). After placing the rat on the foam bed, the bed was positioned directly under the tube. The rat's head and the cap were adjusted so that the striking plane was horizontal and parallel to the impacting face of the falling weight. The animal's body was held lightly on the form during impact. Brain injury was produced by dropping the cylindrical weight (500 g) from a predetermined height (150 cm). Rebound impact by the weight was prevented by sliding the foam bed and rat away from the tube immediately after impact/acceleration. As noted above, sham controls were anesthetized and handled without being subjected to brain injury.

2.4. Sample collection for analyses

Rats were euthanized 6 and 24 h post-injury and blood plasma and brain samples were collected. Cortex, hippocampus and brainstem were dissected and pooled across hemispheres over ice, immediately frozen and stored at −80 °C along with blood plasma until analyses.

2.5. Measurement of enzyme activity

The activity of TNAP in the brain and activity of total alkaline phosphatase in the blood plasma were determined using a diagnostic kit (Randox Laboratories, Kearneysville, WV) according to the manufacturer's instructions. In this assay, the colorless *p*-nitrophenyl phosphate is hydrolyzed to yellow colored *p*-nitophenol by alkaline phosphatase at alkaline pH in the presence of Magnesium ions. The absorbance of the yellow colored *p*-nitrophenol formed, which will be directly proportional to the activity of alkaline phosphatase, was measured at 400 nm. In the case of brain tissue, 10% homogenates were made in T-PER tissue protein extraction reagent (Pierce Chemical Co., Rockford, IL) containing protease inhibitor cocktail (Sigma–Aldrich, St. Louis, MO) using an ultrasonic homogenizer. The homogenates were centrifuged at 5000 × *g* for 5 min at 4 °C and the supernatants were used for the enzyme assay. Briefly, 5 μl of plasma or brain extract were added to the reaction mixture in the wells of a 96 well assay plate and the increase in optical density at 400 nm was measured every minute up to 5 min using SpectraMax M5 spectrophotometer

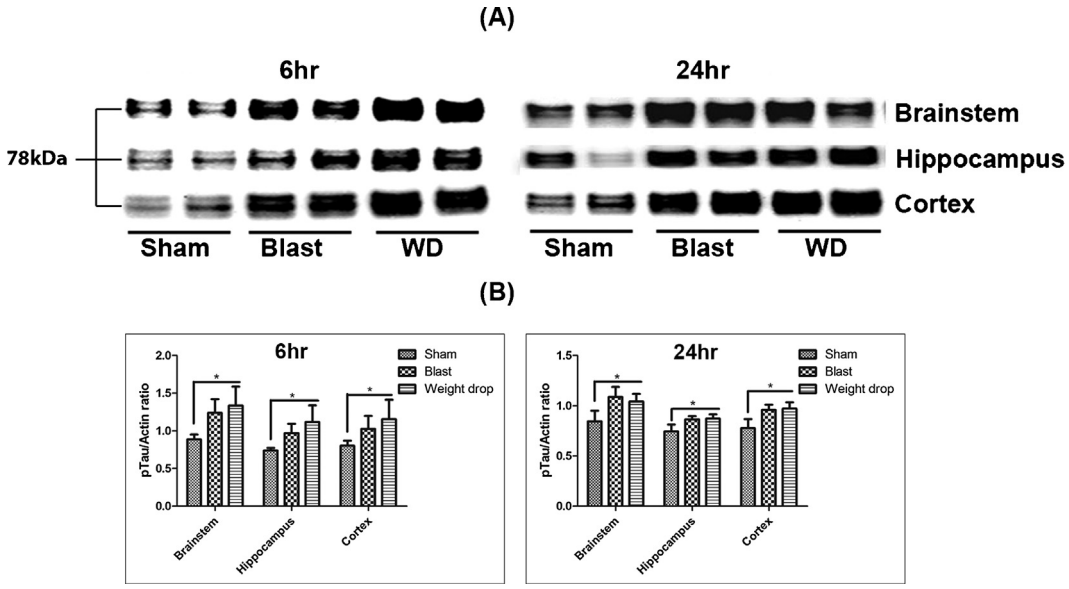

Fig. 1. (A) Western blotting showing the expression of *pTau*, with phosphorylation at serine396, in different brain regions at 6 h and 24 h after blast or weight drop. The antibody detects *Tau* protein only when the serine396 is phosphorylated. Representative figures from two rats out of four in each group are shown. (B) Densitometry analysis showing the ratio of band intensities of *pTau* and β-actin. Values are expressed as mean ± SD. $^{*}p < 0.05$.

(Molecular Devices, Sunnyvale, CA). The increase in optical density per minute was used for determination of enzyme activity.

2.6. Western blot analysis of brain homogenates

Brain homogenates (10% w/v) were prepared in T-PER tissue protein extraction buffer (Pierce Chemical Co., Rockford, IL) containing protease and phosphatase inhibitor cocktails (Sigma–Aldrich, St. Louis, MO) using an ultrasonic homogenizer. The homogenates were centrifuged at 5000 × *g* for 5 min at 4 °C and 2 μL each of supernatants were used for Western blotting. Rabbit polyclonal antibodies, which bind specifically to phosphorylated serine396 (S396) of *Tau* protein, were purchased from Abcam (Cambridge, MA) and used at dilution of 1:5000. Mouse monoclonal antibodies against TNAP and β-actin were obtained from Sigma–Aldrich (St. Louis, MO) and used at a dilution of 1:2000 and 1:40,000, respectively. Secondary antibodies labeled with horse-radish peroxidase (HRP) was purchased from Santa Cruz Biotechnology (Santa Cruz, CA) and used at a dilution of 1:2500. SDS-polyacrylamide gel electrophoresis and Western blotting analysis were carried out as previously described by us earlier [1]. After Western blotting, the protein bands were detected using ECL-Plus Western blot detection reagent (GE Healthcare, Piscataway, NJ) and the chemiluminescence was imaged in an AlphaImage reader (Cell Biosciences, Santa Clara, CA). The band intensity was measured by densitometry using AlphaView software (Cell Biosciences, Santa Clara, CA).

2.7. Statistical analysis

Statistical analysis was carried out by Repeated Measures Analysis of Variance (ANOVA) followed by Tukey's post-hoc test using HSD multiple comparisons (SPSS software, Version 20). Values were expressed as mean ± standard deviation (SD). A *p* value less than 0.05 was considered significant.

3. Results

3.1. Expression of pTau in brain regions after injury

Western blot analyses of extracts from the different brain regions after either blast or weight drop showed significant increases in the expression of *pTau* (S396) at 6 and 24 h post-insult (Fig. 1), with increases ranging from 23 to 34 %. At 6 h, the ratios (mean±SD) of band intensities of *pTau*/actin for sham, blast and weight drop were 0.88 ± 0.06, 1.24 ± 0.17 and 1.34 ± 0.23 respec-

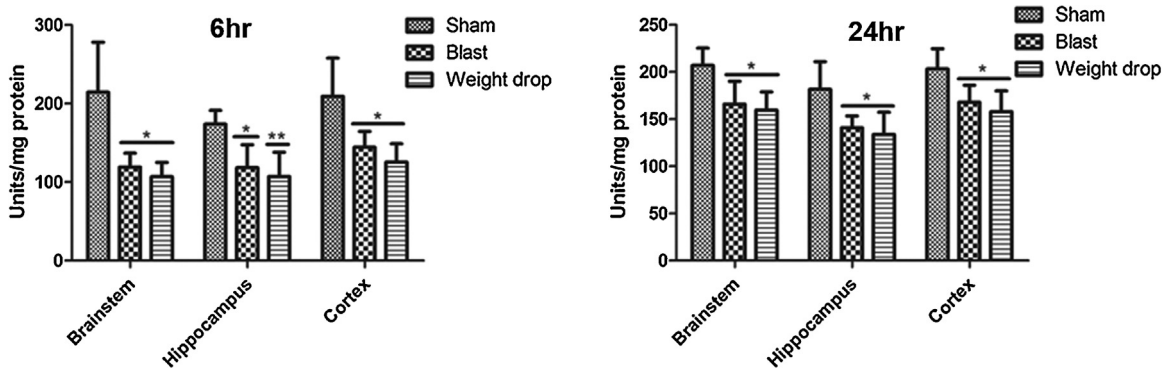

Fig. 2. Activity of TNAP in different brain regions at 6 h and 24 h after blast or weight drop. One unit of enzyme activity is the micromoles of *p*-nitrophenol liberated per minute. Values are expressed as mean ± SD. $n = 4$, $^{*}p < 0.05$, $^{**}p < 0.01$.

tively in the brain stem, 0.74 ± 0.02, 0.97 ± 0.11 and 1.12 ± 0.21 respectively in the hippocampus, and 0.79 ± 0.05, 1.03 ± 0.15 and 1.15 ± 0.02 respectively in the cortex. At 24 h, the ratios for sham, blast and weight drop were 0.84 ± 0.09, 1.09 ± 0.09 and 1.04 ± 0.06, respectively in the brain stem, 0.76 ± 0.05, 0.86 ± 0.02 and 0.87 ± 0.03, respectively in the hippocampus, and 0.78 ± 0.08, 0.96 ± 0.01 and 0.97 ± 0.01, respectively in the cortex. Although the increases resulting from the two different insults were not significantly different at these respective injury severities, the elevated levels of *pTau* in different brain regions of animals exposed to blast overpressure were generally less than those seen in rats subjected to weight drop injury. The levels of *pTau* in different brain regions were similar 24 h after either insult and were significantly greater than measured in the sham controls. We have detected two adjacent bands in the Western blot at the expected position of *pTau*, which could be due to the difference in the number of amino acids phosphorylated or due to other post-translational modifications to *Tau* protein after injury. For densitometry analysis, the intensities of both bands were used.

3.2. Activity of TNAP in brain regions after injury

Fig. 2 shows the activity of TNAP in different brain regions at 6 and 24 h after blast or weight drop induced brain injury. At 6 h, the TNAP activity (units/mg protein) for sham, blast and weight drop were 214.14 ± 62.81, 119.20 ± 16.66 and 106.86 ± 17.29, respectively in the brain stem, 173.84 ± 47.69, 118.31 ± 19.24 and 107.21 ± 22.23, respectively in the hippocampus, 209.07 ± 116.54, 144.29 ± 28.38 and 125.51 ± 30.92 respectively in the cortex. At 24 h, the TNAP activity for sham, blast and weight drop were 206.88 ± 17.48, 166.02 ± 23.17 and 159.58 ± 18.25 respectively in the brain stem, 181.52 ± 28.44, 140.93 ± 11.56 and 133.80 ± 22.52, respectively in the hippocampus, 203.18 ± 20.59, 168.08 ± 16.82 and 158.07 ± 20.80 respectively in the cortex. Both insults significantly decreased the activity of TNAP at both 6 and 24 h post-injury. At 6 h post-injury, blast exposure decreased TNAP activity in brainstem, hippocampus, and cortex by 45%, 32% and 31% respectively, whereas weight drop caused regional decreases of 51%, 39% and 40% respectively. At 24 h, TNAP activity in brainstem, hippocampus and cortex remained decreased by 20%, 23% and 18%, respectively after blast whereas after weight drop, the decreases were 23%, 27% and 23% respectively. Although once again the changes resulting from the two insults were not significantly different, at these respective injury severities, weight drop consistently caused slightly greater decreases in TNAP activity than were seen after blast exposure, which were greater at 6 h than at 24 h post-injury

3.3. Activity of alkaline phosphatase in the plasma

The baseline activities of alkaline phosphatase in the plasma for sham, blast and weight drop groups were 101.45 ± 15.27, 97.61 ± 16.72 and 94.05 ± 10.97, respectively. At 6 h, the activities of alkaline phosphatase in the plasma for sham, blast and weight drop group were 98.43 ± 19.78, 88.56 ± 19.58 and 63.61 ± 3.85 respectively. At 24 h, the activities of alkaline phosphatase in the plasma for sham, blast and weight drop group were 90.48 ± 4.07, 83.08 ± 6.14 and 59.50 ± 5.30, respectively. Total alkaline phosphatase activity in the plasma decreased significantly at 6 and 24 h after weight drop, in contrast to blast exposure, which did not significantly alter activity at either time post-injury (Fig. 3). Weight drop caused 32% and 37% decreases in TNAP activity in the plasma at 6 and 24 h respectively, yielding significantly different measurements than were seen in sham and blast-injured rats at these times.

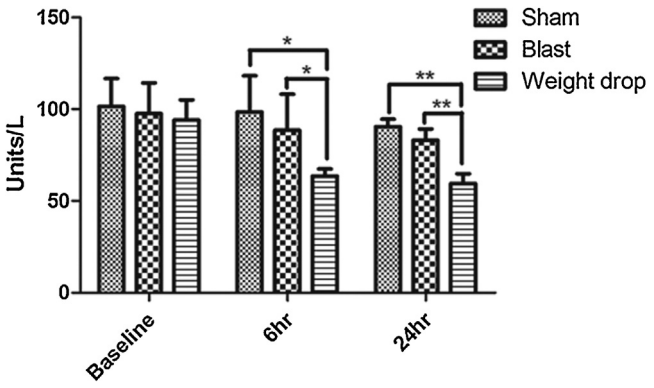

Fig. 3. Activity of alkaline phosphatase in the plasma at different intervals after blast or weight drop. One unit of enzyme activity is the μmoles of *p*-nitrophenol liberated per minute. Baseline—plasma collected before injury. Values are expressed as mean ± SD. $n = 4$, $^{*}p < 0.05$, $^{**}p < 0.01$.

3.4. Expression of TNAP in the brain regions after blast and weight drop

Fig. 4 shows the expression of TNAP in different brain regions at 6 and 24 h post-injury. At 6 h, the ratios (mean ± SD) of band intensities of *TNAP*/actin for sham, blast and weight drop were 0.84 ± 0.06, 0.70 ± 0.04 and 0.64 ± 0.07, respectively in the brain stem, 0.81 ± 0.04, 0.69 ± 0.05 and 0.65 ± 0.06, respectively in the hippocampus, 0.76 ± 0.11, 0.60 ± 0.01 and 0.59 ± 0.03, respectively in the cortex. At 24 h, the ratios for sham, blast and weight drop were 0.80 ± 0.02, 0.72 ± 0.03 and 0.71 ± 0.04, respectively in the brain stem, 0.77 ± 0.05, 0.69 ± 0.02 and 0.69 ± 0.01, respectively in the hippocampus, 0.74 ± 0.01, 0.68 ± 0.03 and 0.67 ± 0.02, respectively in the cortex. Compared to sham controls, both blast and weight drop significantly decreased the expression of TNAP at 6 and 24 h post-injury. The magnitudes of the changes in different brain regions, ranged from 17 to 30 %, were quite comparable after either insult and were generally greater at 6 than at 24 h post-injury.

3.5. Expression of APP in the brain regions after injury

The expression of APP in brain regions at 6 and 24 h after blast or weight drop is shown in Fig. 5. At 6 h, the ratios (mean ± SD) of band intensities of *APP*/actin for sham, blast and weight drop were 0.99 ± 0.10, 1.18 ± 0.27 and 1.09 ± 0.19, respectively in the brain stem, 0.94 ± 0.07, 1.11 ± 0.16 and 1.05 ± 0.18, respectively in the hippocampus, 0.87 ± 0.07, 1.01 ± 0.16 and 0.98 ± 0.16, respectively in the cortex. At 24 h, the ratios for sham, blast and weight drop were 1.02 ± 0.06, 1.51 ± 0.27 and 1.25 ± 0.12, respectively in the brain stem, 0.93 ± 0.02, 1.16 ± 0.12 and 1.00 ± 0.02 respectively in the hippocampus, 0.86 ± 0.03, 1.18 ± 0.02 and 1.00 ± 0.08 respectively in the cortex. The expression of APP in different brain regions was increased significantly after blast and weight drop compared to sham controls. Despite any statistical significance, the increased expression of APP in the brain regions was more after blast exposure compared to weight drop.

4. Discussion

In this study, we report for the first time that brain injury causes an acute decrease in the protein level and activity of TNAP in the brain which is associated with an acute increase in the phosphorylation of *Tau* protein. In view of the previously reported role of this enzyme in the dephosphorylation of *pTau* protein, the acutely diminished level and /activity of TNAP after injury might promote the progressive accumulation of *pTau* as an early event leading to eventual tauopathy. Neither decreased TNAP activity nor increased

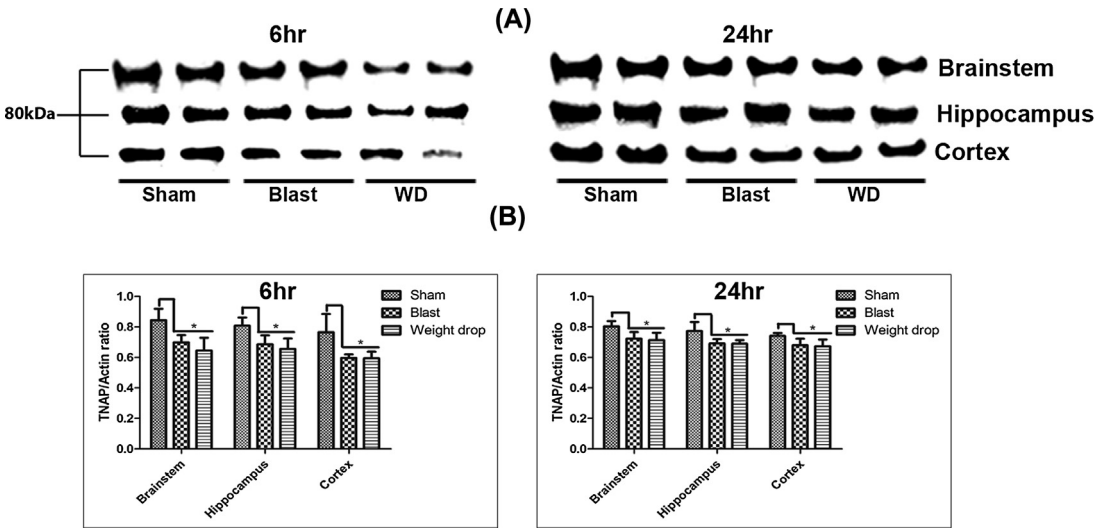

Fig. 4. (A) Western blotting showing the expression of TNAP in different brain regions at 6 h and 24 h after blast or weight drop. Representative figures from two rats out of four in each group are shown. (B) Densitometry analysis showing the ratio of band intensities of TNAP and β-actin. Values are expressed as mean ± SD. $^{*}p < 0.05$.

accumulation of *pTau* in the brain after injury correlated closely with the deposition of APP, suggesting a distinct mechanism of tauopathy after brain injury compared to AD.

There are at least four distinct forms of alkaline phosphatase enzyme present in mammals - intestinal, placental, placental-like and TNAP (present in liver, bone, kidney, brain etc.). TNAP is sequenced in chromosome 1 and sequences for all other isozymes are located in chromosome 2. In the brain, several roles for TNAP have been reported, which include: (1) involvement in the development of the nervous system partly as an ectonucleotidase in neurogenic zones [17], (2) participation in neuronal migration by interaction with collagen [4,22], (3) regulation of the synthesis of neurotransmitters such as γ-aminobutyric acid, dopamine and serotonin [23] and (4) dephosphorylation of *pTau* [12,15,31]. As described in the introduction, TNAP is the principal protein phosphatase enzyme present in the brain that is primarily involved in the dephosphorylation of *pTau*. Although other protein phosphatases such as PP-1, 2A, 2B and 2C can also dephosphorylate *pTau*, TNAP has been shown to have higher activity towards *pTau* than these other phosphatases [31]; hence, a decrease in TNAP level/activity alone can result in significant accumulation of *pTau*. Non-phosphorylated *Tau* protein is essential for microtubule assembly with tubulin and accumulation of *pTau* disrupts this process, resulting in neuronal hypofunction and even neuronal death.

The phosphorylation of *Tau* protein can occur on different amino acids at specific locations of the amino acid sequence. *Tau* protein, phosphorylated at serine396 (S396), is rich in the paired helical filaments which form neurofibrillary tangles observed in the brains of patients with AD [3,13,35]. Our results showed increased phosphorylation of S396 after blast and weight drop-induced brain injuries, pointing to the possibility of formation of neurofibrillary tangles after brain injury. Increased phosphorylation of *Tau* protein at S396 at 24 h after blast exposure has been previously reported [14], supporting our current observation. In addition to S396, increased phosphorylation of several other amino acids in the *Tau* protein was observed in that study which could potentially also contribute to disrupted microtubule assembly after blast exposure. Using head impact-induced single and repetitive mild TBI in *hTau* mice, Ojo et al. showed that repetitive, but not single, mild TBI also induced the phosphorylation of *Tau* at a number of amino acid sites [25]. The phosphorylation of *Tau* protein after single head impact in the

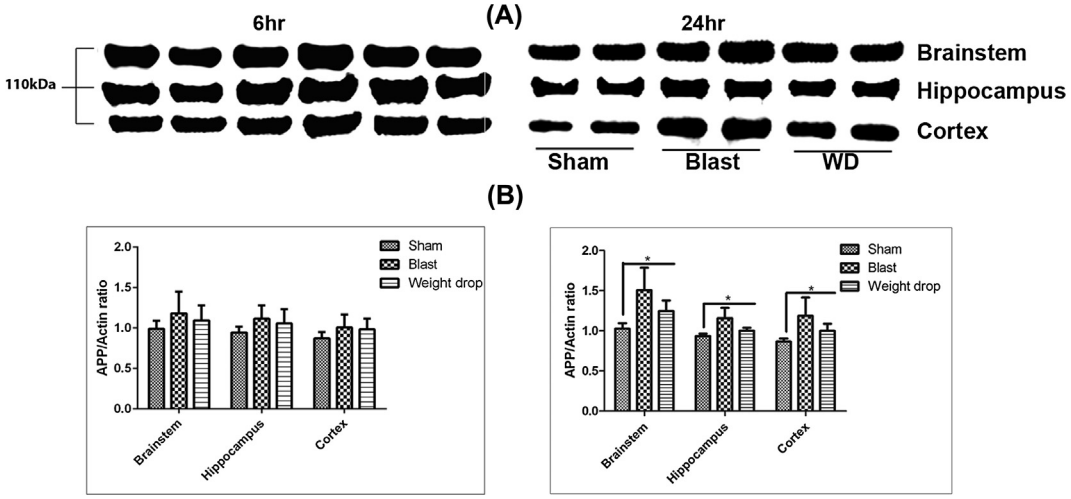

Fig. 5. (A) Western blotting showing the expression of APP in different brain regions at 6 and 24 h after blast or weight drop. Representative figures from two rats out of four in each group are shown. (B) Densitometry analysis showing the ratio of band intensities of APP and β-actin. Values are expressed as mean ± SD. $^{*}p < 0.05$.

current study could simply reflect a more severe insult in these subjects than was produced by a single impact in this earlier work.

In the present study, we have shown that the protein levels and activities of TNAP in the brain decreased significantly after blast exposure or impact-acceleration and were associated with a significant increase in the phosphorylation of *Tau* protein. At these respective injury severities, the decreases in TNAP activity were greater after weight drop than after blast and were concomitantly associated with comparably greater increases in the levels of *pTau,* suggesting that decreased TNAP activity may in part be responsible for the accumulation of *pTau* after these brain insults. If persistent, decreased TNAP activity might promote progressive accumulation of *pTau*, culminating in tauopathy and conditions associated with chronic diseases such as CTE. Long-term studies evaluating the level/activity of TNAP and the accumulation of *pTau* in the brain are warranted to determine their roles in the development of chronic diseases. The decrease in the activity of the enzyme could be due to the decreased level of the protein or due to an inhibition of the enzyme activity. Western blot analyses of extracts from the three brain regions indicate that the TNAP protein level consistently decreased after the brain insults. The decreased protein level of TNAP in the brain regions could be due to decreased synthesis or increased degradation after injury, and further studies using messenger RNA levels are warranted to delineate the underlying mechanism.

The major alkaline phosphatase isozyme present in the blood is TNAP [24], and the decrease in the activity of TNAP in the brain was associated with a significant decrease in the activity of total alkaline phosphatase in the plasma after weight drop but not after blast exposure. Although it is not clear why plasma alkaline phosphatase activity declines after weight drop, this parallel with the brain points to the possibility that the two changes are related and that phosphatase activity in the circulation might be attributed to TNAP enzyme originating in the brain, which is diminished after injury. Unlike weight drop, where injury is localized to the brain, blast is a whole body insult affecting multiple organ systems; consequently, changes in total alkaline phosphatase activity in the circulation after blast may more generally reflect the net outcome of its composite effects on multiple organ systems and not just brain. In particular, since blast exposure disrupts cell membranes in various organs resulting in the release of enzymes and other intracellular components [1,2,32], it is possible that unlike weight drop injury, blast exposure causes the release/leakage of different alkaline phosphatase isozymes into the plasma from peripheral organs such as liver, kidney, intestine, placenta, bone etc., all of which contribute to the alkaline phosphatase activity measured in plasma after blast exposure.

TNAP activity in the plasma has been reported to increase after 7 days post-injury in patients with different brain injury conditions such as post-resuscitation encephalopathy, ruptured cerebral aneurysms, subdural hematoma, cerebral contusion and non-traumatic intracerebral hemorrhage [36]. Although no change in TNAP activity was observed in those patients at early stages of injury, patients who died at early stages of injury had very low or undetectable TNAP activity in their plasma, which is in agreement with our observation of low TNAP activity at acute stages of injury.

In AD, the accumulation of amyloid plaques have been reported to precede and promote tauopathy [11,18,27,28,30,34]. In particular, formation of amyloid β (Aβ) protein has been shown to enhance the phosphorylation of *Tau* protein, resulting in neurofibrillary tangle formation in an APP and *Tau* double transgenic mouse model [28]. The phosphorylation of *Tau* protein has been further proposed to involve the activation of mitogen-activated protein kinase by accumulated APP or Aβ protein [11]. In contrast, previous shock tube studies with rats revealed a divergence in the changes of these proteins in brain after blast exposure. Whereas the expression of APP increased in the brain at 24 h after blast and increased further after 1 week, the levels of Aβ peptides progressively decreased during this time [9], indicating that increased accumulation of Aβ peptides may not trigger the phosphorylation of *Tau* protein after blast exposure. In the present study, comparison of the accumulation of *pTau* (S396) in brain after weight drop and blast injury (Fig. 1) with the expression of APP after these insults (Fig. 5), reveals a similar divergence in these measurements, reinforcing interpretation that accumulated APP may not play a substantial role promoting the phosphorylation of *Tau* protein after blast exposure. Blast or weight drop didn't increase the expression of APP in the brain at 6 h post-injury. At 24 h, both insults significantly increased expression of APP, but the greatest increase in APP was observed after blast exposure (Fig. 5) unlike *pTau*, where the greatest increase was evoked by weight drop (Fig. 1). Although these disparities do not rule out APP promoting phosphorylation of *Tau*, they nevertheless do raise the possibility that the neurobiological mechanisms yielding tauopathy after TBI might be distinct from those of AD.

5. Conclusion

Brain injury after blast exposure or weight drop results in a significant decrease in the expression and activity of TNAP which is associated with a significant increase in the accumulation of *pTau* in different brain regions. In view of the known function of TNAP in dephosphorylating *pTau*, the accumulation of *pTau* after brain injury could be attributed to the decreased TNAP activity/levels in the brain after the injury. The decreased activity of TNAP in the brain after injury was associated with a significantly decreased total alkaline phosphatase activity in the plasma. The accumulation of *pTau* after brain injury did not show a positive correlation with the expression of APP in different brain regions, indicating that the mechanism of tauopathy after brain injury could be distinct from that of AD.

Disclaimer

The contents, opinions and assertions contained herein are private views of the authors and are not to be construed as official or reflecting the views of the Department of the Army or the Department of Defense. The authors report no conflict of interest.

Acknowledgements

Technical help received from Rania Abu-Taleb, Andrea Edwards and Cory Riccio is greatly acknowledged. This work was supported by Congressionally Directed Medical Research Program awards W81XWH-08-2-0018 and W81XWH-11-2-0127 to JBL.

References

[1] P. Arun, R. Abu-Taleb, S. Oguntayo, M. Tanaka, Y. Wang, M. Valiyaveettil, J.B. Long, Y. Zhang, M.P. Nambiar, Distinct patterns of expression of traumatic brain injury biomarkers after blast exposure: role of compromised cell membrane integrity, Neurosci. Lett. 552 (2013) 87–91.
[2] P. Arun, S. Oguntayo, Y. Alamneh, C. Honnold, Y. Wang, M. Valiyaveettil, J.B. Long, M.P. Nambiar, Rapid release of tissue enzymes into blood after blast exposure: potential use as biological dosimeters, PloS one 7 (2012) e33798.
[3] J. Bertrand, V. Plouffe, P. Senechal, N. Leclerc, The pattern of human tau phosphorylation is the result of priming and feedback events in primary hippocampal neurons, Neuroscience 168 (2010) 323–334.
[4] M. Bossi, M.F. Hoylaerts, J.L. Millan, Modifications in a flexible surface loop modulate the isozyme-specific properties of mammalian alkaline phosphatases, J. Biol. Chem. 268 (1993) 25409–25416.
[5] J. Busciglio, A. Lorenzo, J. Yeh, B.A. Yankner, Beta-amyloid fibrils induce tau phosphorylation and loss of microtubule binding, Neuron 14 (1995) 879–888.
[6] E. Calabrese, F. Du, R.H. Garman, G.A. Johnson, C. Riccio, L.C. Tong, J.B. Long, Diffusion tensor imaging reveals white matter injury in a rat model of repetitive blast-induced traumatic brain injury, J. Neurotrauma 31 (2014) 938–950.

[7] I. Cernak, A.C. Merkle, V.E. Koliatsos, J.M. Bilik, Q.T. Luong, T.M. Mahota, L. Xu, N. Slack, D. Windle, F.A. Ahmed, The pathobiology of blast injuries and blast-induced neurotrauma as identified using a new experimental model of injury in mice, Neurobiol. Dis. 41 (2011) 538–551.
[8] I. Cernak, Z. Wang, J. Jiang, X. Bian, J. Savic, Ultrastructural and functional characteristics of blast injury-induced neurotrauma, J. Trauma 50 (2001) 695–706.
[9] R. De Gasperi, M.A. Gama Sosa, S.H. Kim, J.W. Steele, M.C. Shaughness, E. Maudlin-Jeronimo, A.A. Hall, S.T. Dekosky, R.M. McCarron, M.P. Nambiar, S. Gandy, S.T. Ahlers, G.A. Elder, Acute blast injury reduces brain abeta in two rodent species, Front. Neurol. 3 (2012) 177.
[10] L.E. Goldstein, A.M. Fisher, C.A. Tagge, X.L. Zhang, L. Velisek, J.A. Sullivan, C. Upreti, J.M. Kracht, M. Ericsson, M.W. Wojnarowicz, C.J. Goletiani, G.M. Maglakelidze, N. Casey, J.A. Moncaster, O. Minaeva, R.D. Moir, C.J. Nowinski, R.A. Stern, R.C. Cantu, J. Geiling, J.K. Blusztajn, B.L. Wolozin, T. Ikezu, T.D. Stein, A.E. Budson, N.W. Kowall, D. Chargin, A. Sharon, S. Saman, G.F. Hall, W.C. Moss, R.O. Cleveland, R.E. Tanzi, P.K. Stanton, A.C. McKee, Chronic traumatic encephalopathy in blast-exposed military veterans and a blast neurotrauma mouse model, Sci. Transl. Med. 4 (2012) 134ra160.
[11] S.M. Greenberg, E.H. Koo, D.J. Selkoe, W.Q. Qiu, K.S. Kosik, Secreted beta-amyloid precursor protein stimulates mitogen-activated protein kinase and enhances tau phosphorylation, Proc. Natl. Acad. Sci. U. S. A. 91 (1994) 7104–7108.
[12] D.P. Hanger, J.P. Brion, J.M. Gallo, N.J. Cairns, P.J. Luthert, B.H. Anderton, Tau in Alzheimer's disease and Down's syndrome is insoluble and abnormally phosphorylated, Biochem. J. 275 (Pt. 1) (1991) 99–104.
[13] D.P. Hanger, K. Hughes, J.R. Woodgett, J.P. Brion, B.H. Anderton, Glycogen synthase kinase-3 induces Alzheimer's disease-like phosphorylation of tau: generation of paired helical filament epitopes and neuronal localisation of the kinase, Neurosci. Lett. 147 (1992) 58–62.
[14] B.R. Huber, J.S. Meabon, T.J. Martin, P.D. Mourad, R. Bennett, B.C. Kraemer, I. Cernak, E.C. Petrie, M.J. Emery, E.R. Swenson, C. Mayer, E. Mehic, E.R. Peskind, D.G. Cook, Blast exposure causes early and persistent aberrant phospho- and cleaved-tau expression in a murine model of mild blast-induced traumatic brain injury, J. Alzheimers Dis. JAD 37 (2013) 309–323.
[15] K. Iqbal, T. Zaidi, C. Bancher, I. Grundke-Iqbal, Alzheimer paired helical filaments. Restoration of the biological activity by dephosphorylation, FEBS Lett. 349 (1994) 104–108.
[16] J.D. Kocsis, A. Tessler, Pathology of blast-related brain injury, J. Rehabil. Res. Dev. 46 (2009) 667–672.
[17] D. Langer, Y. Ikehara, H. Takebayashi, R. Hawkes, H. Zimmermann, The ectonucleotidases alkaline phosphatase and nucleoside triphosphate diphosphohydrolase 2 are associated with subsets of progenitor cell populations in the mouse embryonic, postnatal and adult neurogenic zones, Neuroscience 150 (2007) 863–879.
[18] W.D. Le, W.J. Xie, R. Kong, S.H. Appel, Beta-amyloid-induced neurotoxicity of a hybrid septal cell line associated with increased tau phosphorylation and expression of beta-amyloid precursor protein, J. Neurochem. 69 (1997) 978–985.
[19] J.B. Long, T.L. Bentley, K.A. Wessner, C. Cerone, S. Sweeney, R.A. Bauman, Blast overpressure in rats: recreating a battlefield injury in the laboratory, J. Neurotrauma 26 (2009) 827–840.
[20] J. Magnuson, F. Leonessa, G.S. Ling, Neuropathology of explosive blast traumatic brain injury, Curr. Neurol. Neurosci. Rep. 12 (2012) 570–579.
[21] A. Marmarou, M.A. Foda, W. van den Brink, J. Campbell, H. Kita, K. Demetriadou, A new model of diffuse brain injury in rats. Part I: pathophysiology and biomechanics, J. Neurosurg. 80 (1994) 291–300.
[22] S. Narisawa, H. Hasegawa, K. Watanabe, J.L. Millan, Stage-specific expression of alkaline phosphatase during neural development in the mouse, Dev. Dyn. Off. Publ. Am. Assoc. Anat. 201 (1994) 227–235.
[23] L. Negyessy, J. Xiao, O. Kantor, G.G. Kovacs, M. Palkovits, T.P. Doczi, L. Renaud, G. Baksa, T. Glasz, M. Ashaber, P. Barone, C. Fonta, Layer-specific activity of tissue non-specific alkaline phosphatase in the human neocortex, Neuroscience 172 (2011) 406–418.
[24] Y. Nishihara, Y. Hayashi, T. Fujii, T. Adachi, T. Stigbrand, K. Hirano, The alkaline phosphatase in human plexus chorioideus, Biochim. Biophys. Acta 1209 (1994) 274–278.
[25] J.O. Ojo, B. Mouzon, M.B. Greenberg, C. Bachmeier, M. Mullan, F. Crawford, Repetitive mild traumatic brain injury augments tau pathology and glial activation in aged hTau mice, J. Neuropathol. Exp. Neurol. 72 (2013) 137–151.
[26] A. Saljo, F. Bao, J. Shi, A. Hamberger, H.A. Hansson, K.G. Haglid, Expression of c-Fos and c-Myc and deposition of beta-APP in neurons in the adult rat brain as a result of exposure to short-lasting impulse noise, J. Neurotrauma 19 (2002) 379–385.
[27] E. Samura, M. Shoji, T. Kawarabayashi, A. Sasaki, E. Matsubara, T. Murakami, X. Wuhua, S. Tamura, M. Ikeda, K. Ishiguro, T.C. Saido, D. Westaway, P. St George Hyslop, Y. Harigaya, K. Abe, Enhanced accumulation of tau in doubly transgenic mice expressing mutant betaAPP and presenilin-1, Brain Res. 1094 (2006) 192–199.
[28] Y. Seino, T. Kawarabayashi, Y. Wakasaya, M. Watanabe, A. Takamura, Y. Yamamoto-Watanabe, T. Kurata, K. Abe, M. Ikeda, D. Westaway, T. Murakami, P.S. Hyslop, E. Matsubara, M. Shoji, Amyloid beta accelerates phosphorylation of tau and neurofibrillary tangle formation in an amyloid precursor protein and tau double-transgenic mouse model, J. Neurosci. Res. 88 (2010) 3547–3554.
[29] S.I. Svetlov, V. Prima, D.R. Kirk, H. Gutierrez, K.C. Curley, R.L. Hayes, K.K. Wang, Morphologic and biochemical characterization of brain injury in a model of controlled blast overpressure exposure, J. Trauma 69 (2010) 795–804.
[30] Y. Tomidokoro, K. Ishiguro, Y. Harigaya, E. Matsubara, M. Ikeda, J.M. Park, K. Yasutake, T. Kawarabayashi, K. Okamoto, M. Shoji, Abeta amyloidosis induces the initial stage of tau accumulation in APP(Sw) mice, Neurosci. Lett. 299 (2001) 169–172.
[31] J.Z. Wang, I. Grundke-Iqbal, K. Iqbal, Restoration of biological activity of Alzheimer abnormally phosphorylated tau by dephosphorylation with protein phosphatase-2A, -2B and -1, Brain Res. Mol. Brain Res. 38 (1996) 200–208.
[32] Y. Wang, P. Arun, Y. Wei, S. Oguntayo, R. Gharavi, M. Valiyaveettil, M.P. Nambiar, J.B. Long, Repeated blast exposures cause brain DNA fragmentation in mice, J. Neurotrauma 31 (2014) 498–504.
[33] Y. Wang, Y. Wei, S. Oguntayo, W. Wilkins, P. Arun, M. Valiyaveettil, J. Song, J.B. Long, M.P. Nambiar, Tightly coupled repetitive blast-induced traumatic brain injury: development and characterization in mice, J. Neurotrauma 28 (2011) 2171–2183.
[34] Z.F. Wang, H.L. Li, X.C. Li, Q. Zhang, Q. Tian, Q. Wang, H. Xu, J.Z. Wang, Effects of endogenous beta-amyloid overproduction on tau phosphorylation in cell culture, J. Neurochem. 98 (2006) 1167–1175.
[35] D. Xia, C. Li, J. Gotz, Pseudophosphorylation of Tau at distinct epitopes or the presence of the P301L mutation targets the microtubule-associated protein Tau to dendritic spines, Biochim. Biophys. Acta 1852 (2015) 913–924.
[36] M. Yamashita, M. Sasaki, K. Mii, M. Tsuzuki, K. Takakura, S. Yoshinoya, A. Ohkubo, Measurement of serum alkaline phosphatase isozyme I in brain-damaged patients, Neurol. Med. Chir. 29 (1989) 995–998.

frontiers in
NEUROLOGY

ORIGINAL RESEARCH ARTICLE
published: 16 July 2012
doi: 10.3389/fneur.2012.00111

Acute minocycline treatment mitigates the symptoms of mild blast-induced traumatic brain injury

Erzsebet Kovesdi[1], Alaa Kamnaksh[2,3], Daniel Wingo[2], Farid Ahmed[2,3], Neil E. Grunberg[3,4], Joseph B. Long[5], Christine E. Kasper[1] and Denes V. Agoston[2]*

[1] *U.S. Department of Veterans Affairs, Veterans Affairs Central Office, Washington, DC, USA*
[2] *Department of Anatomy, Physiology and Genetics, School of Medicine, Uniformed Services University, Bethesda, MD, USA*
[3] *Center for Neuroscience and Regenerative Medicine at the Uniformed Services University, Bethesda, MD, USA*
[4] *Department of Medical and Clinical Psychology, School of Medicine, Uniformed Services University, Bethesda, MD, USA*
[5] *Blast-Induced Neurotrauma Branch, Center for Military Psychiatry and Neuroscience, Walter Reed Army Institute of Research, Silver Spring, MD, USA*

Edited by:
Mårten Risling, Karolinska Institutet, Sweden

Reviewed by:
Mattias Sköld, Uppsala University, Sweden
Candace L. Floyd, University of Alabama at Birmingham, USA

****Correspondence:***
Denes V. Agoston, Department of Anatomy, Physiology and Genetics, School of Medicine, Uniformed Services University, 4301 Jones Bridge Road, Bethesda, MD 20814, USA.
e-mail: vagoston@usuhs.edu

Mild traumatic brain injury (mTBI) represents a significant challenge for the civilian and military health care systems due to its high prevalence and overall complexity. Our earlier works showed evidence of neuroinflammation, a late onset of neurobehavioral changes, and lasting memory impairment in a rat model of mild blast-induced TBI (mbTBI). The aim of our present study was to determine whether acute treatment with the non-steroidal anti-inflammatory drug minocycline (Minocin®) can mitigate the neurobehavioral abnormalities associated with mbTBI, Furthermore, we aimed to assess the effects of the treatment on select inflammatory, vascular, neuronal, and glial markers in sera and in brain regions associated with anxiety and memory (amygdala, prefrontal cortex, ventral, and dorsal hippocampus) following the termination (51 days post-injury) of the experiment. Four hours after a single exposure to mild blast overpressure or sham conditions, we treated animals with a daily dose of minocycline (50 mg/kg) or physiological saline (vehicle) for four consecutive days. At 8 and 45 days post-injury, we tested animals for locomotion, anxiety, and spatial memory. Injured animals exhibited significantly impaired memory and increased anxiety especially at the later testing time point. Conversely, injured and minocycline treated rats' performance was practically identical to control (sham) animals in the open field, elevated plus maze, and Barnes maze. Protein analyses of sera and brain regions showed significantly elevated levels of all of the measured biomarkers (except VEGF) in injured and untreated rats. Importantly, minocycline treatment normalized serum and tissue levels of the majority of the selected inflammatory, vascular, neuronal, and glial markers. In summary, acute minocycline treatment appears to prevent the development of neurobehavioral abnormalities likely through mitigating the molecular pathologies of the injury in an experimental model of mbTBI.

Keywords: TBI, anti-inflammatory, treatment, neurobehavior, proteomics

INTRODUCTION

Traumatic brain injury (TBI) is a prominent health concern worldwide as it is one of the major causes of death and chronic disability (Hyder et al., 2007). The mild form of traumatic brain injury (mTBI) has become an especially significant challenge for the civilian (Thurman et al., 1999) and the military healthcare systems (Hoge et al., 2008; Tanielian and Jaycox, 2008) due to its high prevalence and the absence of serious acute symptoms following injury. Blast-induced mTBI (mbTBI) was the most frequent form of mTBIs sustained during recent military conflicts (Warden, 2006; Terrio et al., 2009). There is currently no objective diagnosis for mbTBI, a minimal understanding of its underlying pathologies, and consequently a lack of specific, evidence based treatments.

Symptoms of blast-induced TBI (bTBI) include increased anxiety as well as memory impairment that may not be detectable for weeks or months after the exposure (Ryan and Warden, 2003; Okie, 2005; Nelson et al., 2009; Terrio et al., 2009; Cernak and Noble-Haeusslein, 2010; Hoffer et al., 2010). The delayed onset of neurobehavioral impairments suggests a lasting secondary injury process involving distinct brain regions (Moser and Moser, 1998). The ventral hippocampus (VHC) along with the prefrontal cortex (PFC) and the amygdala (AD) are involved in mediating anxiety, while the dorsal hippocampus (DHC) is involved in mediating spatial learning and memory (Henke, 1990; Moser and Moser, 1998; Bremner, 2005, 2007). Using a rat model of bTBI, we found that a single mild blast overpressure exposure results in increased anxiety and memory impairment (Kovesdi et al., 2011; Kwon et al., 2011). Importantly, the memory impairment was not detectable within the first week of the exposure; it became significant 2 weeks post-injury and persisted for at least 2 months after (Kovesdi et al., 2011; Kwon et al., 2011).

Our immunohistochemical and proteomics analyses of these animals showed evidence of neuronal and glial cell loss, gliosis, and neuroinflammation at 2 months post-injury. In addition to

an increased presence of microglia in the DHC and the VHC of injured animals as well as increased tissue levels of interleukin-6 (IL-6) and interferon-gamma (IFNγ) in these brain regions. Neuroinflammation can adversely affect neuronal function by directly causing neuronal cell death as well as increasing neuron vulnerability to noxious factors like excitotoxins, which are also elevated after injury (Arvin et al., 1996; Morganti-Kossmann et al., 2002; Cacci et al., 2005; Floyd and Lyeth, 2007; Kochanek et al., 2008; Agoston et al., 2009; Agostinho et al., 2010; Czlonkowska and Kurkowska-Jastrzebska, 2011; Robel et al., 2011). Based on our previous evidence linking neuroinflammation to neurobehavioral abnormalities (Kovesdi et al., 2011), we hypothesized that anti-inflammatory treatment may improve the functional outcome in mbTBI.

To test our hypothesis, we selected the anti-inflammatory drug minocycline for several reasons. Minocycline hydrochloride easily crosses the blood brain barrier (BBB), is well characterized, safe, FDA approved, and has been used experimentally and clinically (Macdonald et al., 1973; Saivin and Houin, 1988). Similar to its tetracycline analogs, the side effects of minocycline treatment are mild and include discoloration of the teeth, gastrointestinal irritability, and candidiasis (Fanning et al., 1977; Gump et al., 1977). In humans, long-term treatment is generally safe and is well tolerated up to 200 mg/day. In animals, the lethal dose of minocycline is very high at 3600 mg/kg (Blum et al., 2004); the "therapeutic" dosage utilized in animal experiments ranges between 10 and 90 mg/kg with an average of 50 mg/kg for daily treatments (e.g., Wells et al., 2003; Stirling et al., 2004; Festoff et al., 2006; Li and McCullough, 2009; Abdel Baki et al., 2010; Lee et al., 2010; Siopi et al., 2011; Wixey et al., 2011; Ng et al., 2012).

Minocycline has been successfully used in various animal models of brain and spinal cord injuries as well as neurodegenerative diseases like Huntington's (Blum et al., 2004), where it was shown to reduce tissue damage and inflammation, and improve neurological outcome (Yrjanheikki et al., 1999; Chen et al., 2000; Kriz et al., 2002; Wu et al., 2002; Wells et al., 2003; Xu et al., 2004; Zemke and Majid, 2004; Festoff et al., 2006; Marchand et al., 2009). Using a rat model of mbTBI, we report that acute treatment with minocycline mitigates the inflammatory response to injury and results in normalized neurobehavior.

MATERIALS AND METHODS

EXPERIMENTAL GROUPS AND HOUSING CONDITIONS

Thirty-two male Sprague Dawley rats (Charles River Laboratories, Wilmington, MA, USA) were used, weighing 245–265 g at the beginning of the experiment. All animals were kept under normal housing conditions (two rats/cage) in a reverse 12–12 h light-dark cycle and provided with food and water *ad libitum* for the entire length of the study. Following baseline behavioral testing (described below), animals were assigned to one of the following experimental groups: (1) sham saline treated (*sham-vehicle*; $n = 8$) and (2) sham minocycline treated (*sham-mino*; $n = 8$), which served as controls for (3) blast injured saline treated (*injured-vehicle*; $n = 8$) and (4) blast injured-minocycline treated (*injured-mino*; $n = 8$), respectively. All animals were handled according to protocol approved by the Institutional Animal Care and Use Committee (IACUC) at the Uniformed Services University (USU).

BEHAVIORAL TESTS

Prior to injury, all rats underwent baseline behavioral assessments for general locomotor activity by the open field (OF) test, and for anxiety by the elevated plus maze (EPM). Rats were also trained for five consecutive days in the Barnes maze (BM) for spatial learning and memory. The baseline test results (data not shown) were used to create the aforementioned experimental groups with no statistical significance among them. Following injury or sham, two behavioral test sessions were conducted starting at 8 and 45 days. The experimental schedule is illustrated in **Figure A1** in Appendix. Within each testing session, the behavioral tests were performed on separate days in the following order: OF (day 1), EPM (day 2), and BM (days 3–7). All behavioral tests were performed during animals' dark cycle.

Open field

Tests were performed using AccuScan's infrared light beams OF system (AccuScan Instruments, Inc.) at baseline and 1, 8, and 45 days post-injury. The OF system is a $16.5 \times 16.5 \times 13$ ($L \times W \times H$) inches clear Plexiglas arena with a perforated lid. The system uses 16×16 grid light beam arrays in the X and Y axes to measure locomotor activity. The system detects beam breaks by the animal and determines the location of the rat within the cage. During the 60 min testing period, horizontal activity (number of beam breaks) and resting time (time spent with inactivity greater than or equal to 1 s) were measured. Data for each animal were recorded and analyzed automatically with Fusion 3.4 software (AccuScan Instruments, Inc.). The horizontal activity and resting time are presented as the average performance of all animals in each experimental group ±standard error of the mean (SEM) at each of the individual time points.

Elevated plus maze

The EPM is an ethologically relevant assessment of anxiety levels in rodents (Carobrez and Bertoglio, 2005; Salzberg et al., 2007; Walf and Frye, 2007). Tests were carried out prior to injury and at 9 and 46 days post-injury as described earlier in details (Kovesdi et al., 2011). Briefly, rats were placed one by one in the center of the maze facing one of the open arms. During the 5 min testing session, each animal was allowed to explore the maze freely while its movement was video-tracked. Time spent in the open and the closed arms (seconds) was recorded for each animal using ANY-maze 4.2 Software (Stoelting Company, Wood Dale, IL, USA). The maze was cleaned with a 30% ethanol solution between each trial. Data are presented as the average time (in seconds) spent in the open vs. the closed arms of the maze in each experimental group ±SEM.

Barnes maze

Barnes maze represents a widely used and less stressful alternative to the Morris water maze for assessing spatial memory in rodents (Barnes, 1979; Maegele et al., 2005; Doll et al., 2009; Harrison et al., 2009). Tests were carried out prior to injury (training session), and at 10 and 47 days post-injury (Test Session I and II,

respectively; Kovesdi et al., 2011). The maze is a circular platform (1.2 m in diameter) that contains 18 evenly spaced holes around the periphery. One of the holes is the entrance to a darkened escape box that is not visible from the surface of the board. The position of the escape chamber relative to the other holes and the testing room remains fixed during all BM trials. On the first day of the training session, each rat was placed in the escape box and covered for 30 s. The escape box was then removed with the animal inside and moved to the center of the maze. The rat was allowed to explore the maze for a few seconds after which it was returned to its home cage. In the second and third trial (only day 1 of the BM training session has three trials), the same rat was placed under a start box in the center of the maze for 30 s. The start box was removed and the rat was allowed to explore freely to find the escape box. Training sessions ended after the animal had entered the escape box or when a pre-determined time (240 s) had elapsed. If the animal had not found the escape box during the given time period, it was placed in the escape box for 1 min at the end of the trial. During the baseline BM session, animals were trained until their daily latency time averaged 10 s. The two post-injury BM test sessions were run for five consecutive days; every rat was tested twice per day as described above. In each trial, the latency to enter the escape box was measured and recorded using ANY-maze 4.2 Software (Stoelting Company, Wood Dale, IL, USA). The escape box and the maze were cleaned with a 30% ethanol solution between each trial and animal. Data are presented as the average latency times of two daily trials per animal per experimental group ±SEM.

MILD BLAST INJURY

On the day of the injury all rats (average weight ∼300 g) were transferred to Walter Reed Army Institute of Research (Silver Spring, MD, USA) as described in detail (Kamnaksh et al., 2011). Sixteen rats were exposed to whole body mbTBI as described earlier (Long et al., 2009; Kovesdi et al., 2011; Kwon et al., 2011). Briefly, rats were anesthetized with 4% Isoflurane for 6 min in an induction chamber (Forane, Baxter Healthcare Corporation, Deerfield, IL, USA), placed in an animal holder within the shock tube in a transverse prone position, and exposed to whole body blast overpressure (20.6 ± 3 psi) while wearing chest protection. The other 16 rats were similarly anesthetized, placed in the shock tube, but were not exposed to blast overpressure (sham). Following blast injury or sham, rats were moved back to their home cages and transported back to the USU animal facility.

PHARMACOLOGICAL TREATMENT

Four hours after injury or sham, rats received a total volume of 0.25 ml/100 g body weight of either physiological saline alone (*vehicle*) or 50 mg/kg of clinical grade minocycline (Minocin®, Triax Pharmaceuticals, Italy) dissolved in saline (*mino*) intraperitoneally (i.p.). Animals received minocycline or saline for four consecutive days at identical times each day. Our minocycline dosage and treatment paradigm was based on previous studies using rodent models of various neurological conditions where minocycline was administered i.p. at an average dose of 50 mg/kg (see **Table A1** in Appendix).

TISSUE COLLECTION AND PROCESSING

At the completion of the last behavioral test session (51 days post-injury or sham), animals were placed inside an induction chamber saturated with Isoflurane and deeply anesthetized until a tail pinch produced no reflex movement. Anesthesia was maintained using a mask/nose cone attached to the anesthetic vaporizer and blood was collected (1.5 ml) from a tail vein; serum was prepared as described earlier (Kwon et al., 2011). For measuring tissue levels of protein markers, rats were decapitated and brains were immediately removed and placed on ice. The amygdala (AD), PFC, VHC, and DHC were dissected, frozen, and stored at −80°C until use as described earlier (Kwon et al., 2011).

Protein measurements

Sample preparation, printing, scanning, and data analysis of serum and brain regions were performed using Reverse Phase Protein Microarray (RPPM) as described earlier (Kovesdi et al., 2011; Kwon et al., 2011). Briefly, frozen brain tissues were pulverized in liquid nitrogen, the powder was transferred into a lysis buffer (Thermo Fisher, Waltham, MA, USA) with protease and phosphatase inhibitors (Thermo Fisher), sonicated, centrifuged, and the supernatants aliquoted and stored at −80°C. Protein concentrations were measured by BCA assay (Thermo Fisher). Blood samples were centrifuged at $10{,}000 \times g$ for 15 min at 4°C; supernatants were aliquoted, flash-frozen, and stored at −80°C.

Tissue samples were diluted in print buffer and then subjected to an 11-point serial 1:2 dilution and transferred into Genetix 384-well plates (X7022, Fisher Scientific, Pittsburg, PA, USA) using a JANUS Varispan Integrator and Expanded Platform Workstation (PerkinElmer, Waltham, MA, USA). Plates were transferred into an Aushon 2470 Arrayer (Aushon Biosystem, Billerica, MA, USA) to be printed on ONCYTE Avid (brain samples) or ONCYTE Nova (serum samples) single-pad nitrocellulose coated glass slides (Grace Bio-Labs, Bend, OR, USA; Gyorgy et al., 2010).

Primary antibodies (**Table A2** in Appendix) were diluted to 10× the optimal Western analysis concentration in antibody incubation buffer as described earlier (Gyorgy et al., 2010). The primary antibody solution was incubated overnight at 4°C with a cover slip. The following day slides were washed and then incubated with an Alexa Fluor® 635 goat anti-mouse (Cat# A-31574), goat anti-rabbit (Cat# A-31576), or rabbit anti-goat IgG (H + L; Cat# A-21086) secondary antibodies from Invitrogen at 1:6000 dilution in antibody incubation buffer for 1 h at room temperature. After washing and drying, fluorescent signals were measured by a Scan Array Express HT microarray scanner (Perkin Elmer, Waltham, MA, USA) using a 633 nm wavelength laser and a 647 nm filter.

Data from the scanned images were imported into a Microsoft Excel-based bioinformatics program developed in-house for analysis (Gyorgy et al., 2010). The linear regression of the log–log data was calculated after the removal of flagged data, which include signal to noise ratios of less than 2, spot intensities in the saturation range or noise range, or high variability between duplicate spots (>10–15%). The total amount of antigen is determined by the y-axis intercept (Y-cept; Gyorgy et al., 2010). Data is reported as the mean Y-cept ±SEM.

Corticosterone assay

Serum corticosterone (CORT) levels were measured with Cayman's Corticosterone EIA Kit according to the manufacturer's instructions (Cayman Chemical, Ann Arbor, MI, USA). Each sample was diluted 1:500 and measured in triplicate (Kwon et al., 2011). Data is reported as the mean concentration (in pg/mg) ±SEM.

STATISTICAL ANALYSIS

All data were analyzed using Graph Pad Instat software (GraphPad Software, Inc., La Jolla, CA, USA). Statistical significance was verified by one-way analysis of variance (ANOVA), followed by Tukey *post hoc* test for multiple comparison. Differences with a p value of <0.05 were considered significant.

RESULTS

BEHAVIORAL TESTS

One day following blast exposure, injured rats showed reduced horizontal activity and slightly increased resting time in the OF compared to sham animals, but the differences were not statistically significant (**Figure 1A**). At 8 days post-injury, the horizontal activity of injured-vehicle animals further decreased. On the other hand, injured-mino rats had a similar horizontal activity to animals in the two sham groups. The horizontal activity of animals in all groups was the lowest at 45 days after injury. Similarly, animals in all experimental groups spent more time resting with injured-vehicle animals spending significantly more time resting than animals in the other three groups (**Figure 1B**).

During the first EPM testing performed 9 days after exposure, injured-vehicle animals spent less time in the open arms and more time in the closed arms of the maze than animals in the other three groups (**Figures 2A,B**). However, the difference at this time point was not statistically significant. At 46 days after injury, the differences in the time spent in the open and closed arms of the maze became significant between injured-vehicle and injured-mino animals. At this later time point, injured-vehicle animals barely spent any time in the open arms of the maze and practically spent all of their time in the closed arms of the maze (**Figures 2A,B**). By contrast, injured-mino animals spent a comparable amount of time to animals in the two other groups did in the open and closed arms of the maze.

In order to assess time-dependent changes in spatial memory, we performed two tests in the BM at two different time points. Test Session I started at 10 days after injury and lasted for 5 days. Injured-vehicle animals performed poorly during the first 2 days of the test (**Figure 3A**). They required approximately twice as much time as animals in the other experimental groups to find the escape

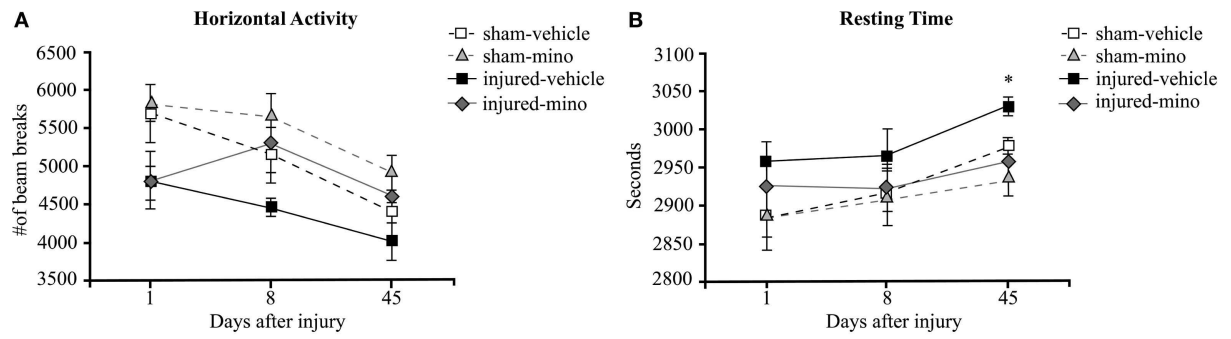

FIGURE 1 | The effect of injury and minocycline treatment on basic locomotor activities at different time points after mbTBI. (A) Horizontal activity (number of beam breaks), and **(B)** Resting time (seconds) were measured in Open field. Data are presented as mean ± SEM. $*p < 0.05$ for injured-vehicle vs. sham-mino rats.

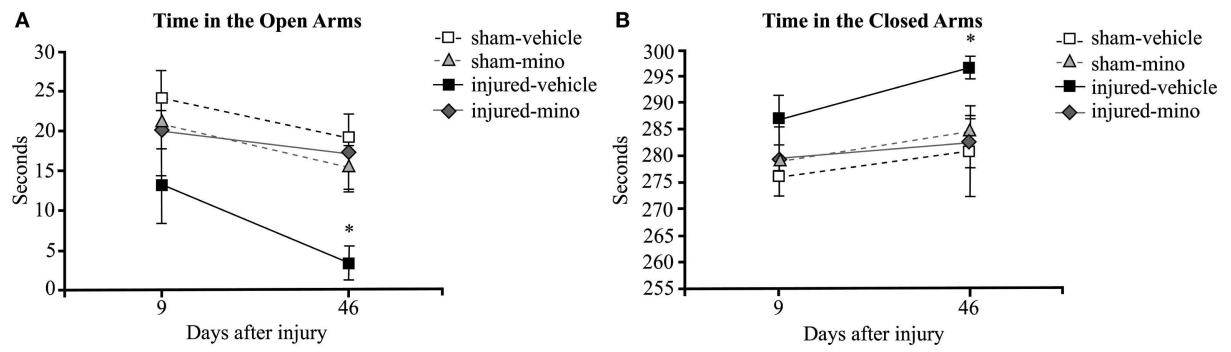

FIGURE 2 | The effect of injury and minocycline treatment on anxiety levels at different time points after mbTBI. (A) Time spent in the open arms (seconds), and **(B)** time spent in the closed arms (seconds) were measured for all animals in the elevated plus maze. Data are presented as mean ± SEM. $*p < 0.05$ for injured-vehicle vs. sham-vehicle rats.

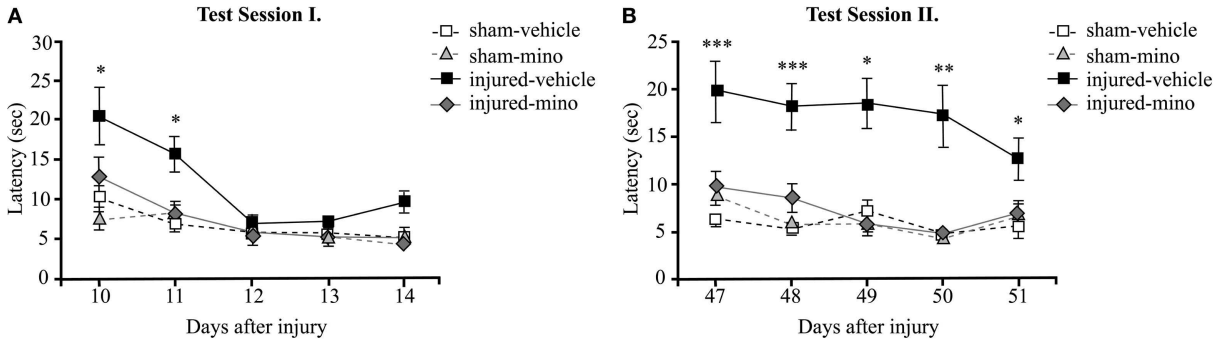

FIGURE 3 | The effect of injury and minocycline treatment on spatial memory at different time points after mbTBI. Latency (seconds) to find and enter the escape box was measured for five consecutive days in the Barnes maze starting at **(A)** 10 days, and **(B)** 47 days after injury or sham. Data are presented as the average of the 2 daily trials per animal in each experimental group ±SEM. $*p < 0.05$, $**p < 0.01$, and $***p < 0.001$ for injured-vehicle vs. sham-vehicle rats.

box. While their performance improved slightly on the second day of testing, injured-vehicle animals still required significantly more time to find the escape box compared to their sham group. On the third day of testing, their performance became roughly similar to animals in the other experimental groups. By contrast, the performance of injured-mino animals was very similar to uninjured (sham) animals; their measured latency times to locate and enter the escape box were almost identical on days 11 through 14. They found the escape box with slightly improved efficiency every day.

During Test Session II (beginning at 47 days post-injury), the performance of injured-vehicle animals was significantly worse than sham-vehicle animals on all five testing days (**Figure 3B**). While their performance slightly improved on each subsequent testing day, injured-vehicle rats still needed significantly more time to find the escape box, even on the last day of testing. Conversely, injured-mino animals performed similar to animals in the two control groups (sham-vehicle and sham-mino). Their performance during Test Session II was similar to that in Test Session I; they required about the same time to find the escape box on each testing day.

PROTEIN ANALYSES

Select protein marker levels were measured in the serum and dissected brain regions of animals in all four experimental groups. Injury without minocycline treatment caused a significant increase in the serum levels of all biomarkers measured (**Figure 4**). Both inflammatory markers, CRP and MCP-1, were significantly elevated in injured-vehicle animals; minocycline treatment resulted in normal or near normal (i.e., sham) sera levels in the injured-mino group. Claudin 5 levels were also elevated following blast injury in the vehicle-treated group, but were reduced to sham levels in injured-mino animals. Similarly, neuronal and glial loss and/or damage markers like NSE, NF-H, Tau, S100β, and GFAP were all significantly elevated in the sera of injured-vehicle animals. Minocycline treatment resulted in a significant reduction in serum levels of all of the markers except for GFAP. Lastly, serum CORT levels were also significantly increased in injured-vehicle rats, but minocycline treatment resulted in significantly lower serum CORT levels in injured-mino animals.

Tissue levels of 13 selected protein biomarkers (**Figure 5**; **Table A3** in Appendix) were determined in the AD, PFC, VHC, and DHC of animals in the various experimental groups. We found significantly elevated levels of all three inflammatory markers (CRP, MCP-1, and TLR9) in the brains of injured-vehicle animals (**Figure 5**). Importantly, minocycline treatment of injured animals resulted in normal or near normal levels of these inflammatory markers; tissue levels of these markers in all four brain regions of injured-mino rats were not statistically different from those of sham-vehicle or sham-mino animals. NSE, S100β, and GFAP similarly showed injury-induced increases in all four brain regions. Minocycline treatment normalized their tissue levels with the exception of GFAP in the PFC, where GFAP levels of injured-vehicle and injured-mino animals were practically the same.

Some of the protein biomarkers that were analyzed showed brain region-dependent increases in response to injury. Of the vascular markers, tissue levels of FLK-1 (**Figure 5**), Claudin 5 and AQP4 (**Table A3** in Appendix) were significantly elevated in the VHC following injury; FLK-1 and AQP4 levels were also elevated in the DHC and the AD, respectively. Similarly, neuronal and glial markers showed brain region-specific increases to injury. For instance, all three markers (NF-H, Tau, and MBP) showed injury-induced increases in the VHC but not in the PFC. Minocycline treatment of injured animals significantly reduced the tissue levels of all of the markers with the exception of Tau, which was not significantly reduced in the AD. Interestingly, VEGF did not show any significant changes in response to injury in any of the analyzed brain regions.

DISCUSSION

Minocycline is an FDA approved, semisynthetic, second-generation tetracycline drug that exhibits anti-inflammatory and/or neuroprotective effects in various experimental models of CNS disorders. These include focal and cerebral ischemia (Yrjanheikki et al., 1998; Xu et al., 2004), TBI (Sanchez Mejia et al., 2001), amyotrophic lateral sclerosis (Zhu et al., 2002), Parkinson's disease (Wu et al., 2002), kainic acid treatment (Heo et al., 2006), Huntington' disease (Chen et al., 2000; Du et al., 2001; Wu et al.,

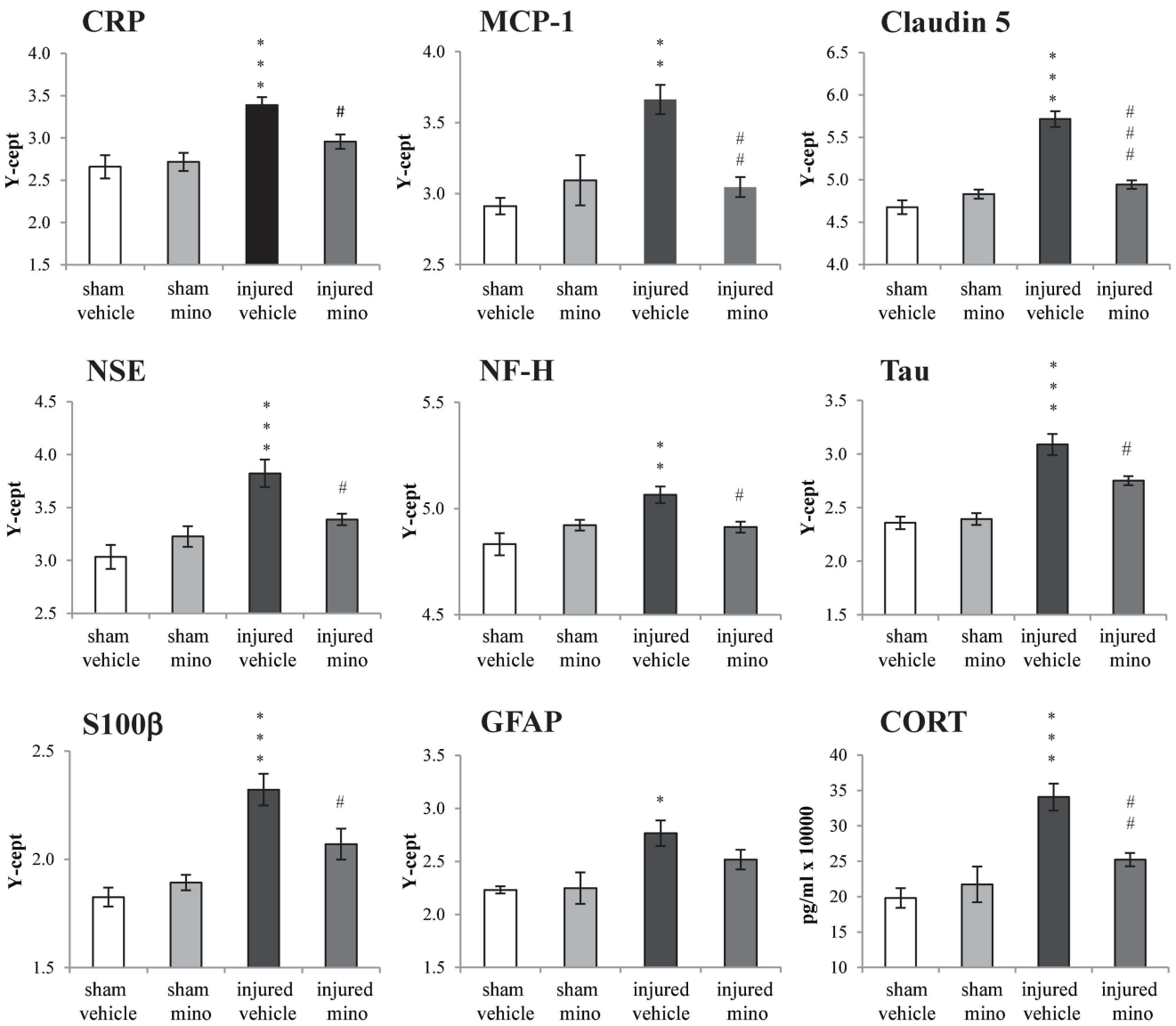

FIGURE 4 | The effect of injury and minocycline treatment on serum levels of selected markers in the different experimental groups. Serum levels of 8 protein markers were assayed by RPPM; CORT levels were assayed by ELISA. Protein values are expressed as *y*-axis intercept (*Y*-cept) and CORT values are expressed as pg/ml. Data are presented as mean ± SEM. $^{*}p < 0.05$, $^{**}p < 0.01$, and $^{***}p < 0.001$ for injured-vehicle vs. sham-vehicle rats. $^{\#}p < 0.05$, $^{\#\#}p < 0.01$, and $^{\#\#\#}p < 0.001$ for injured-vehicle vs. injured-mino rats.

2002; Wang et al., 2003), multiple sclerosis (Brundula et al., 2002; Popovic et al., 2002), Alzheimer's disease (Choi et al., 2007), and spinal cord injury (Wells et al., 2003; Stirling et al., 2004; Festoff et al., 2006; **Table A1** in Appendix). Minocycline's ability to improve outcome in distinct types of CNS disease models may stem from its ability to find multiple targets in different biochemical cascades that play a role in the development of the above-mentioned diseases. Previous studies indicated that minocycline acts as a pleiotropic molecule; it can reduce the release of various chemokines and cytokines (Sanchez Mejia et al., 2001; Bye et al., 2007), lipid mediators of inflammation, matrix metalloproteinases (MMPs), and nitric oxide (NO; Stirling et al., 2005). Minocycline can also inhibit microglia activation (Yrjanheikki et al., 1998, 1999; Tikka and Koistinaho, 2001). The inhibition of microglial inflammatory responses has been reported in various neurodegenerative diseases (Yrjanheikki et al., 1999) including Huntington's (Chen et al., 2000; Popovic et al., 2002; Wu et al., 2002); additional anti-inflammatory actions may be through the impediment of molecules like cyclooxigenase-2 (Patel et al., 1999; Yrjanheikki et al., 1999). Minocycline exerts its neuroprotective effects (Kriz et al., 2002; Wells et al., 2003; Stirling et al., 2004; Zemke and Majid, 2004; Marchand et al., 2009) through the repression of poly (ADP-ribose) polymerase-1 activity (Alano et al., 2006), which plays a central role in caspase-independent apoptosis (Susin et al., 1999; Zhang et al., 2002; Cao et al., 2003; Du et al., 2003), and the suppression of caspase-1 and caspase-3 expression (Chen et al., 2000)

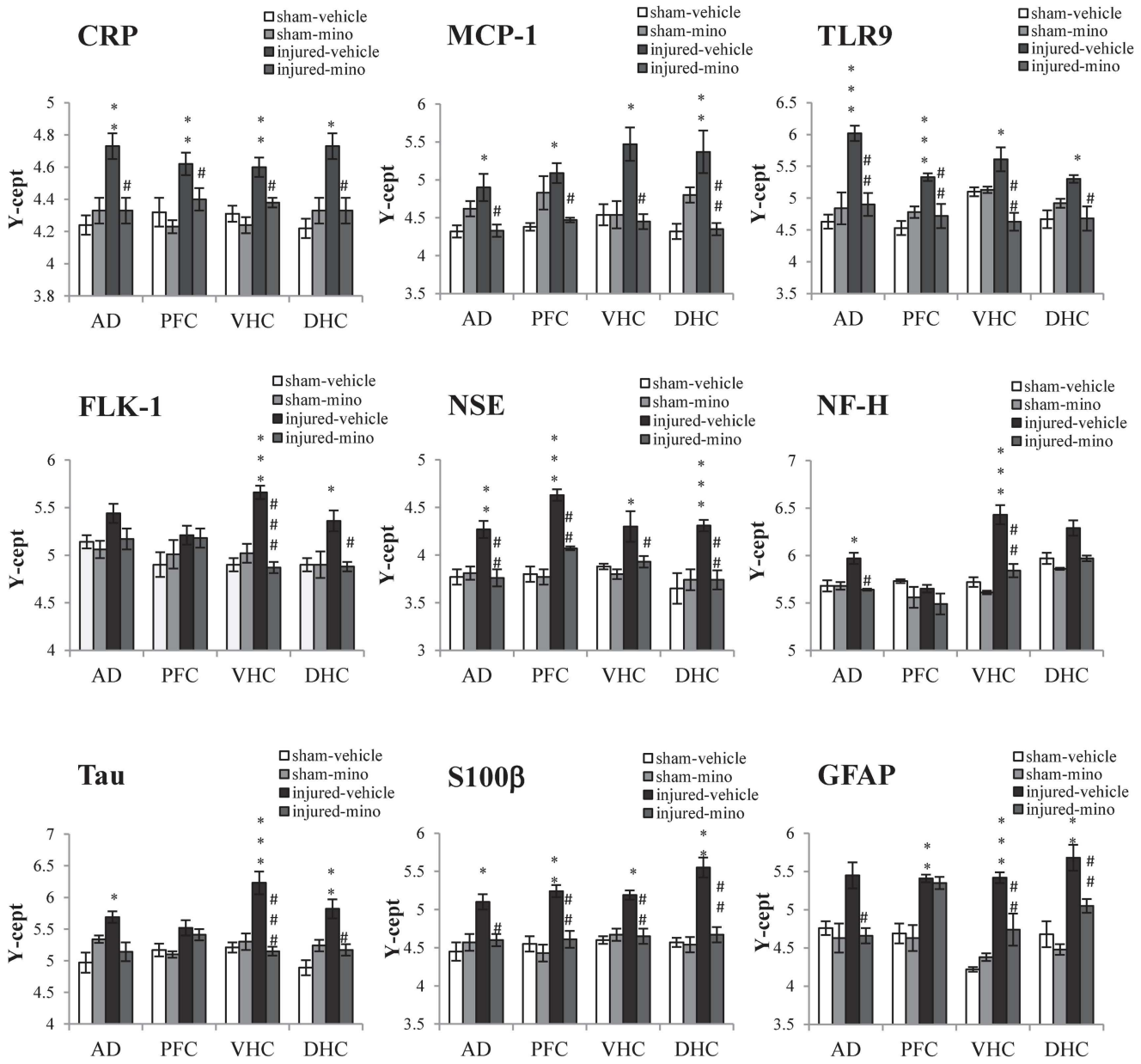

FIGURE 5 | The effect of injury and minocycline treatment on the levels of protein markers in various brain regions in the different experimental groups. Tissue levels of 9 protein markers were measured in the AD, PFC, VHC, and DHC of rats by RPPM. Protein values are expressed as *y*-axis intercept (*Y*-cept) and data are presented as mean ± SEM. $^{*}p < 0.05$, $^{**}p < 0.01$, and $^{***}p < 0.001$ for injured-vehicle vs. sham-vehicle rats. $^{\#}p < 0.05$ and $^{\#\#}p < 0.01$ for injured-vehicle vs. injured-mino rats.

and cytochrome c release from the mitochondria (Zhu et al., 2002). Moreover, minocycline has been shown to sequester excess Ca^{2+} released after injury (Antonenko et al., 2010), and block the injury-induced decrease of soluble alpha amyloid precursor protein in the attenuation of diffuse axonal injury (Siopi et al., 2011). Based on all of these findings, we were compelled to test the effects of minocycline in our rat model of mbTBI.

During our pilot studies we followed a reported treatment schedule of 90 mg/kg of minocycline administered i.p. twice on the first day, 50 mg/kg twice per day for 2 subsequent days, and 50 mg/kg once per day for three additional days (Lee et al., 2003; Teng et al., 2004; Festoff et al., 2006; Yune et al., 2007). However, we found that this treatment caused substantial weight loss likely due to gastrointestinal problems (i.e., diarrhea). Based on these preliminary findings, we decided to modify the treatment paradigm by lowering the dose to 50 mg/kg once per day for four consecutive days. Our conservative treatment schedule caused light and transient diarrhea, and animals recovered and gained weight normally from the third day post-injury until the termination of the experiment on day 51 (data not shown).

Consistent with our previous findings, injured rats had reduced horizontal activity and a somewhat higher resting time than sham animals in the OF 1 day after injury (Kwon et al., 2011). Interestingly, all of the rats, independent of injury and treatment, showed gradually decreasing horizontal activities during the two subsequent OF sessions. There are two plausible explanations for this behavior. Rodents actively explore new areas, but inadvertently become less active on subsequent exposures to the same environment, a process called habituation (Pitkänen et al., 2006). We also observed on numerous occasions in other experiments that the horizontal activity of naïve rats in the OF at baseline is higher than it is 24 h later. We believe that since the OF represents a novel environment for the rats, they actively explore it (Bolivar et al., 2000; Daenen et al., 2001). However, repeated testing may cause the animals to habituate to the OF and in turn spend less time exploring and more time resting. Another possible explanation may be aging, especially during the last OF session, as young rodents have higher motor activity levels than more mature rodents (Sprott and Eleftheriou, 1974; Ingram et al., 1981; Gage et al., 1984; Lamberty and Gower, 1993). The effects of aging have also been observed as decreases in distance traveled in the EPM over time in both, sham and blast injured animals (Kovesdi et al., 2011).

Epidemiological studies have indicated that soldiers frequently develop neurobehavioral abnormalities like increased anxiety and memory impairments in mbTBI (Belanger et al., 2007; Brenner et al., 2009). Anxiety affects rehabilitation, psychosocial adjustment, and cognition in humans (Kersel et al., 2001; Rapoport et al., 2005). The EPM is a simple behavioral assay for evaluating the anxiety responses of rodents (Pellow et al., 1985) and studying the brain sites (limbic regions, hippocampus, amygdala; Silveira et al., 1993; Gonzalez and File, 1997) and the mechanisms underlying anxiolytic behavior (GABA, glutamate, serotonin, hypothalamic–pituitary–adrenal axis neuromodulators; Handley and Mithani, 1984; Pellow et al., 1985; Rodgers et al., 1992; Silva and Brandao, 2000; Korte and De Boer, 2003; Overstreet et al., 2003; Cortese and Phan, 2005). Rodents naturally prefer dark, enclosed spaces, and demonstrate an aversion to open spaces and a fear of heights (Barnett, 1975). Despite these natural inclinations, non-anxious rodents possess exploratory behaviors that cause them to investigate the open arms of the maze while more anxious rats remain in the closed arms of the maze for longer periods of time.

We previously found increased anxiety in our rodent model of mbTBI (Kovesdi et al., 2011). As our current EPM data illustrates, acute minocycline treatment prevented the increase in anxiety following blast overpressure. The time spent in the closed arms of the maze by injured-mino rats was indistinguishable from that of the two sham groups at both testing time points. Conversely, injured-vehicle animals showed signs of increased anxiety early on; they spent less time on the open arms of the maze than animals in the other three experimental groups. While the difference was not statistically significant at this early time point, injured-vehicle animals barely spent any time outside of the closed arms of the maze 46 days after the injury. Even though there is very little information available about the effects of minocycline on anxiety, especially in brain injury, minocycline treatment reduced anxiety in the EPM in models of cardiac arrest/cardiopulmonary resuscitation and fragile X syndrome (Bilousova et al., 2009; Neigh et al., 2009).

Current treatments of increased anxiety are mostly symptomatic (Tenovuo, 2006; Silver et al., 2009), and patients frequently experience side effects from the use of drugs like benzodiazepines (Rickels et al., 1991; Baldwin et al., 2005). Acute minocycline treatment may provide an alternative to the use of these drugs. Interestingly, injured-mino animals also had lower serum CORT levels than injured-vehicle animals at 51 days after the injury. While serum CORT levels have been used as indicators of stress (Dunn et al., 2004), the correlation between serum CORT levels and anxiety is rather complex and likely involve multiple regulatory pathways.

Consistent with available epidemiological data and our previous studies, the memory impairment associated with mbTBI develops over several weeks after the insult (Kovesdi et al., 2011; Kwon et al., 2011). Importantly, the deficit persists for at least 2 months post-injury (Kovesdi et al.). Given that 2 months in the lifespan of a rat roughly translates into several human years (Quinn, 2005), the observed memory impairment mirrors the chronic condition that manifests in humans reasonably well. The BM has been extensively used to study spatial learning and memory in rats (Barnes, 1979), and is considered a less anxiogenic alternative to the Morris water maze since it does not involve swimming (Pompl et al., 1999; Miyakawa et al., 2001; Deacon and Rawlins, 2002; Holmes et al., 2002). BM has been applied to studies of TBI; rodents with hippocampal damage show impaired performance in the maze, supporting the spatial nature of the task (Fox et al., 1998; Paylor et al., 2001; Deacon and Rawlins, 2002; Raber et al., 2004). In BM animals are presumed to learn the location of an escape hole using spatial reference points that are either fixed in relation to the maze (extra-maze cues) or are fixed on the maze itself in relation to the escape hole (proximal cues). It is important to note that during our acclimation and baseline behavioral testing, all animals were exposed to the maze and were trained to "learn" the task of locating and entering the escape box.

Early signs of the memory deficit were detected in the first testing session. Injured-vehicle animals required approximately twice as long to locate the escape box on the first day of testing, while injured-mino animals performed similar to the uninjured shams. On the second day of testing, injured-vehicle rats still needed more time than the other groups. During the last 3 days of testing, injured-vehicle rats relearned and remembered the task, requiring about the same amount of time as the other groups. However, during the second testing session, injured-vehicle rats performed poorly on all five testing days with only minor improvements in their speed from day to day. Conversely, injured-mino rats performed as well as sham animals did throughout. A similar effect was found in a study by Siopi et al. (2011) where acute treatment with minocycline significantly improved recognition memory; the effects lasted for up to 13 weeks in a mouse closed head injury model. There are currently no effective treatments in clinical use for memory impairment. Existing therapies predominantly target symptoms associated with mood disorders (e.g., depression) that can also improve memory performance (Tenovuo, 2006; Silver et al., 2009). Therefore, acute minocycline treatment has the potential to offer a potentially effective alternative.

The observed neurobehavioral impairments implicate the AD, PFC, VHC, and DHC due to their involvement in mediating anxiety and memory (Henke, 1990; Moser and Moser, 1998). In our earlier works we found indications of inflammation, axonal, glial, and neuronal damage in these brain regions (Kovesdi et al., 2011; Kwon et al., 2011). The neuroinflammatory response to various brain insults has been suggested as a potential link between injury and altered behavior, including increased anxiety. As reported earlier, blast can trigger a systemic inflammatory process even when the body is fully protected and only the head is exposed (Cernak et al., 2011). It is crucial to note that the similarities and the dissimilarities between mbTBI and other better-characterized forms of closed head injuries are currently not known with regards to their primary and secondary injury mechanisms. Nevertheless, it has been hypothesized that the different types of TBIs may share pathological components like neuroinflammation, neuronal and glial cell loss, and axonal injuries (Agoston et al., 2009).

In our current study, we found that minocycline treatment normalized significantly elevated sera levels of the inflammatory markers CRP and MCP-1 following exposure to mild blast. CRP and MCP-1 levels are routinely monitored in clinical settings and are used as an indicator of inflammation (Berman et al., 1996; Glabinski et al., 1996; Du Clos, 2000; Lobo et al., 2003). CRP is a component of the acute phase response to injury (Du Clos, 2000) and its expression is stimulated by the release of cytokines (Okamura et al., 1990); elevated CRP serum levels may reflect a combination of systemic as well as neuronal inflammation. Increased levels of MCP-1 are associated with neurological dysfunction after traumatic axonal injury in rats (Rancan et al., 2001), and are detected in the cerebrospinal fluid in diseases related to neuroinflammation such as stroke, meningitis, and multiple sclerosis (Mastroianni et al., 1998; Losy and Zaremba, 2001; Sindern et al., 2001; Chen et al., 2003; Sorensen et al., 2004). MCP-1 has also been suggested to regulate vascular permeability during CNS inflammation (Tekstra et al., 1999;Stamatovic et al., 2003, 2006).

While tissue levels of Claudin 5 did not significantly change except in the VHC, serum levels were significantly increased in injured-vehicle animals. Claudin 5 is a part of the tight junction complex in brain endothelial cells that contribute to the formation of the BBB (Morita et al., 1999; Liebner et al., 2000); increased serum levels suggest that there may be vascular damage in mbTBI that results in the release of Claudin 5 into systemic blood. Importantly, minocycline treatment normalized Claudin 5 sera levels indicating that vascular changes may be secondary to the inflammatory process or that minocycline possesses cytoprotective effects that also extend to endothelial cells.

Elevated serum levels of neuron- and glia-specific proteins have been found clinically as well as experimentally in various forms of TBI (Povlishock and Christman, 1995; Povlishock and Pettus, 1996; Buki and Povlishock, 2006). Increased serum levels of large neuron-specific molecules also point toward a vascular pathology; heightened BBB permeability is required for the release of large proteins like NF-H from the brain parenchyma and into systemic circulation. In a large animal model of blast TBI, the temporal pattern of serum NF-H levels correlated with clinical and pathological outcomes (Gyorgy et al., 2011). In our current study, minocycline treatment significantly reduced sera levels of NSE, NF-H, Tau, and S100β after injury, but not GFAP, an astroglia-specific intermediate filament (Missler et al., 1999) indicative of brain damage.

Consistent with our behavioral and serum data, we found that minocycline treatment prevented or mitigated injury-induced increases of the selected inflammatory markers CRP, MCP-1, and TLR9 in all four brain regions. TLR9 is member of the toll-like receptor family (Aderem and Ulevitch, 2000; Akira et al., 2001; Takeda and Akira, 2005; Mishra et al., 2006; O'Neill, 2006; Casanova et al., 2011) involved in the induction and the regulation of the inflammatory response in TBI (Hua et al., 2007, 2009) as well as other disorders involving neuroinflammation (Prat and Antel, 2005) and ischemic brain damage (Hua et al., 2007, 2009; Doyle et al., 2008; Gao et al., 2009; Marsh et al., 2009).

Of the vascular markers only FLK-1 and AQP4 tissue levels increased in response to the injury; minocycline treatment mitigated the effect of injury on FLK-1 levels but showed no effect on the tissue levels of AQP4. Increases in AQP4 were only detected in the AD and in the VHC while FLK-1 was in the VHC and the DHC. Elevations in AQP4 expression can contribute to the formation as well as the resolution of edema (Kimelberg, 1995; Papadopoulos et al., 2002; Amiry-Moghaddam and Ottersen, 2003; Neal et al., 2007). The pathology of severe bTBI includes the development of rapid and malignant brain edema (Ling et al., 2009; Ling and Ecklund, 2011) probably involving AQP4 (Neal et al., 2007). However, we currently have no information about water imbalance in mbTBI; if present, it is likely limited to the early phase following injury.

FLK-1 is a membrane-bound tyrosine kinase that mediates the effects of VEGF in the CNS (Sondell et al., 2000; Ogunshola et al., 2002; Rosenstein et al., 2003). Activation of FLK-1 stimulates various intracellular signal transduction pathways including the PI3K/Akt pathway that mediates the neuroprotective function of VEGF (Gerber et al., 1998; Wu et al., 2000; Kilic et al., 2006). VEGF/FLK-1 up-regulation following TBI seems to perform an important endogenous cytoprotective mechanism (Skold et al., 2006; Lee and Agoston, 2009). Interestingly, we did not detect changes in the abundance of VEGF in any of the analyzed brain regions following injury. A potential explanation for this negative finding is the relatively late testing time point (51 days post-injury). In a previous study using another model of TBI, we observed significant increases in VEGF tissue levels in the hippocampus (Lee and Agoston, 2009, 2010); the increases were limited to a few days after the injury.

The tissue levels of NSE, NF-H, Tau, S100β, GFAP, and MBP similarly increased in response to the injury, however, increases were brain region-specific. We measured significant injury-induced increases in sera levels of these proteins indicative of neuronal and glial cell losses. Thus, the detected increases in the tissue levels of these proteins are likely compensatory in nature and can be a part of the repair mechanism (Fawcett, 2009). Importantly, in all cases where injury resulted in an increase in the tissue levels of these markers, minocycline treatment mitigated the effect and tissue levels of these markers were restored to levels measured in sham animals.

CONCLUSION

Our study demonstrates that acute minocycline treatment substantially improve the neurobehavioral outcome in a rodent model of mbTBI likely through mitigating the neuroinflammatory response to injury. The strength of our study lies in combining neurobehavioral tests performed at two different time points after injury with determining changes in serum and brain tissue levels of protein biomarkers. The limitations of the current study are the limited types of neurobehavioral and a single terminal time point of proteomics analyses. Based on these promising results, additional neurobehavioral testing shall be performed in future studies along with obtaining blood at several clinically relevant time points for protein assays. Nevertheless, our findings provide a rationale for exploring the viability of using acute minocycline treatment in mbTBI.

ACKNOWLEDGMENTS

We thank the Neurotrauma Team (WRAIR) for their technical help during the blast exposures. This work was supported by Veterans Affairs Grant B5044R.

REFERENCES

Abdel Baki, S. G., Schwab, B., Haber, M., Fenton, A. A., and Bergold, P. J. (2010). Minocycline synergizes with N-acetylcysteine and improves cognition and memory following traumatic brain injury in rats. *PLoS ONE* 5, e12490. doi:10.1371/journal.pone.0012490

Aderem, A., and Ulevitch, R. J. (2000). Toll-like receptors in the induction of the innate immune response. *Nature* 406, 782–787.

Agostinho, P., Cunha, R. A., and Oliveira, C. (2010). Neuroinflammation, oxidative stress and the pathogenesis of Alzheimer's disease. *Curr. Pharm. Des.* 16, 2766–2778.

Agoston, D. V., Gyorgy, A., Eidelman, O., and Pollard, H. B. (2009). Proteomic biomarkers for blast neurotrauma: targeting cerebral edema, inflammation, and neuronal death cascades. *J. Neurotrauma* 26, 901–911.

Akira, S., Takeda, K., and Kaisho, T. (2001). Toll-like receptors: critical proteins linking innate and acquired immunity. *Nat. Immunol.* 2, 675–680.

Alano, C. C., Kauppinen, T. M., Valls, A. V., and Swanson, R. A. (2006). Minocycline inhibits poly(ADP-ribose) polymerase-1 at nanomolar concentrations. *Proc. Natl. Acad. Sci. U.S.A.* 103, 9685–9690.

Amiry-Moghaddam, M., and Ottersen, O. P. (2003). The molecular basis of water transport in the brain. *Nat. Rev. Neurosci.* 4, 991–1001.

Antonenko, Y. N., Rokitskaya, T. I., Cooper, A. J., and Krasnikov, B. F. (2010). Minocycline chelates Ca2+, binds to membranes, and depolarizes mitochondria by formation of Ca2+-dependent ion channels. *J. Bioenerg. Biomembr.* 42, 151–163.

Arvin, B., Neville, L. F., Barone, F. C., and Feuerstein, G. Z. (1996). The role of inflammation and cytokines in brain injury. *Neurosci. Biobehav. Rev.* 20, 445–452.

Baldwin, D. S., Anderson, I. M., Nutt, D. J., Bandelow, B., Bond, A., Davidson, J. R., Den Boer, J. A., Fineberg, N. A., Knapp, M., Scott, J., and Wittchen, H. U. (2005). Evidence-based guidelines for the pharmacological treatment of anxiety disorders: recommendations from the British Association for Psychopharmacology. *J. Psychopharmacol. (Oxford)* 19, 567–596.

Barnes, C. A. (1979). Memory deficits associated with senescence: a neurophysiological and behavioral study in the rat. *J. Comp. Physiol. Psychol.* 93, 74–104.

Barnett, S. (1975). *The Rat – A Study in Behavior*. Chicago: University of Chicago Press.

Belanger, H. G., Vanderploeg, R. D., Curtiss, G., and Warden, D. L. (2007). Recent neuroimaging techniques in mild traumatic brain injury. *J. Neuropsychiatry Clin. Neurosci.* 19, 5–20.

Berman, J. W., Guida, M. P., Warren, J., Amat, J., and Brosnan, C. F. (1996). Localization of monocyte chemoattractant peptide-1 expression in the central nervous system in experimental autoimmune encephalomyelitis and trauma in the rat. *J. Immunol.* 156, 3017–3023.

Bilousova, T. V., Dansie, L., Ngo, M., Aye, J., Charles, J. R., Ethell, D. W., and Ethell, I. M. (2009). Minocycline promotes dendritic spine maturation and improves behavioural performance in the fragile X mouse model. *J. Med. Genet.* 46, 94–102.

Blum, D., Chtarto, A., Tenenbaum, L., Brotchi, J., and Levivier, M. (2004). Clinical potential of minocycline for neurodegenerative disorders. *Neurobiol. Dis.* 17, 359–366.

Bolivar, V. J., Caldarone, B. J., Reilly, A. A., and Flaherty, L. (2000). Habituation of activity in an open field: a survey of inbred strains and F1 hybrids. *Behav. Genet.* 30, 285–293.

Bremner, J. D. (2005). Effects of traumatic stress on brain structure and function: relevance to early responses to trauma. *J. Trauma Dissociation* 6, 51–68.

Bremner, J. D. (2007). Functional neuroimaging in post-traumatic stress disorder. *Expert Rev. Neurother.* 7, 393–405.

Brenner, L. A., Vanderploeg, R. D., and Terrio, H. (2009). Assessment and diagnosis of mild traumatic brain injury, posttraumatic stress disorder, and other polytrauma conditions: burden of adversity hypothesis. *Rehabil. Psychol.* 54, 239–246.

Brundula, V., Rewcastle, N. B., Metz, L. M., Bernard, C. C., and Yong, V. W. (2002). Targeting leukocyte MMPs and transmigration: minocycline as a potential therapy for multiple sclerosis. *Brain* 125, 1297–1308.

Buki, A., and Povlishock, J. T. (2006). All roads lead to disconnection? – Traumatic axonal injury revisited. *Acta Neurochir. (Wien)* 148, 181–193; discussion 193–184.

Bye, N., Habgood, M. D., Callaway, J. K., Malakooti, N., Potter, A., Kossmann, T., and Morganti-Kossmann, M. C. (2007). Transient neuroprotection by minocycline following traumatic brain injury is associated with attenuated microglial activation but no changes in cell apoptosis or neutrophil infiltration. *Exp. Neurol.* 204, 220–233.

Cacci, E., Claasen, J. H., and Kokaia, Z. (2005). Microglia-derived tumor necrosis factor-alpha exaggerates death of newborn hippocampal progenitor cells in vitro. *J. Neurosci. Res.* 80, 789–797.

Cao, G., Clark, R. S., Pei, W., Yin, W., Zhang, F., Sun, F. Y., Graham, S. H., and Chen, J. (2003). Translocation of apoptosis-inducing factor in vulnerable neurons after transient cerebral ischemia and in neuronal cultures after oxygen-glucose deprivation. *J. Cereb. Blood Flow Metab.* 23, 1137–1150.

Carobrez, A. P., and Bertoglio, L. J. (2005). Ethological and temporal analyses of anxiety-like behavior: the elevated plus-maze model 20 years on. *Neurosci. Biobehav. Rev.* 29, 1193–1205.

Casanova, J. L., Abel, L., and Quintana-Murci, L. (2011). Human TLRs and IL-1Rs in host defense: natural insights from evolutionary, epidemiological, and clinical genetics. *Annu. Rev. Immunol.* 29, 447–491.

Cernak, I., Merkle, A. C., Koliatsos, V. E., Bilik, J. M., Luong, Q. T., Mahota, T. M., Xu, L., Slack, N., Windle, D., and Ahmed, F. A. (2011). The pathobiology of blast injuries and blast-induced neurotrauma as identified using a new experimental model of injury in mice. *Neurobiol. Dis.* 41, 538–551.

Cernak, I., and Noble-Haeusslein, L. J. (2010). Traumatic brain injury: an overview of pathobiology with emphasis on military populations. *J. Cereb. Blood Flow Metab.* 30, 255–266.

Chen, M., Ona, V. O., Li, M., Ferrante, R. J., Fink, K. B., Zhu, S., Bian, J., Guo, L., Farrell, L. A., Hersch, S. M., Hobbs, W., Vonsattel, J. P., Cha, J. H., and Friedlander, R. M. (2000). Minocycline inhibits caspase-1 and caspase-3 expression and delays mortality in a transgenic mouse model of Huntington disease. *Nat. Med.* 6, 797–801.

Chen, Y., Hallenbeck, J. M., Ruetzler, C., Bol, D., Thomas, K., Berman, N. E., and Vogel, S. N. (2003). Overexpression of monocyte chemoattractant protein 1 in the brain exacerbates ischemic brain injury and is associated with recruitment of inflammatory cells. *J. Cereb. Blood Flow Metab.* 23, 748–755.

Choi, Y., Kim, H. S., Shin, K. Y., Kim, E. M., Kim, M., Park, C. H., Jeong, Y. H., Yoo, J., Lee, J. P., Chang, K. A., Kim, S., and Suh, Y. H. (2007). Minocycline attenuates neuronal cell death and improves cognitive impairment in Alzheimer's disease models. *Neuropsychopharmacology* 32, 2393–2404.

Cortese, B. M., and Phan, K. L. (2005). The role of glutamate in anxiety and related disorders. *CNS Spectr.* 10, 820–830.

Czlonkowska, A., and Kurkowska-Jastrzebska, I. (2011). Inflammation and gliosis in neurological diseases – clinical implications. *J. Neuroimmunol.* 231, 78–85.

Daenen, E. W., Van Der Heyden, J. A., Kruse, C. G., Wolterink, G., and Van Ree, J. M. (2001). Adaptation and habituation to an open field and responses to various stressful events in animals with neonatal lesions in the amygdala or ventral hippocampus. *Brain Res.* 918, 153–165.

Deacon, R. M., and Rawlins, J. N. (2002). Learning impairments of hippocampal-lesioned mice in a paddling pool. *Behav. Neurosci.* 116, 472–478.

Doll, H., Truebel, H., Kipfmueller, F., Schaefer, U., Neugebauer, E. A., Wirth, S., and Maegele, M. (2009). Pharyngeal selective brain cooling improves neurofunctional and neurocognitive outcome after fluid percussion brain injury in rats. *J. Neurotrauma* 26, 235–242.

Doyle, K. P., Simon, R. P., and Stenzel-Poore, M. P. (2008). Mechanisms of ischemic brain damage. *Neuropharmacology* 55, 310–318.

Du, L., Zhang, X., Han, Y. Y., Burke, N. A., Kochanek, P. M., Watkins, S. C., Graham, S. H., Carcillo, J. A., Szabo, C., and Clark, R. S. (2003). Intra-mitochondrial poly(ADP-ribosylation) contributes to NAD+ depletion and cell death induced by oxidative stress. *J. Biol. Chem.* 278, 18426–18433.

Du, Y., Ma, Z., Lin, S., Dodel, R. C., Gao, F., Bales, K. R., Triarhou, L. C., Chernet, E., Perry, K. W., Nelson, D. L., Luecke, S., Phebus, L. A., Bymaster, F. P., and Paul, S. M. (2001). Minocycline prevents nigrostriatal dopaminergic neurodegeneration in the MPTP model of Parkinson's disease. *Proc. Natl. Acad. Sci. U.S.A.* 98, 14669–14674.

Du Clos, T. W. (2000). Function of C-reactive protein. *Ann. Med.* 32, 274–278.

Dunn, A. J., Swiergiel, A. H., and Palamarchouk, V. (2004). Brain circuits involved in corticotropin-releasing factor-norepinephrine interactions during stress. *Ann. N. Y. Acad. Sci.* 1018, 25–34.

Fanning, W. L., Gump, D. W., and Sofferman, R. A. (1977). Side effects of minocycline: a double-blind study. *Antimicrob. Agents Chemother.* 11, 712–717.

Fawcett, J. (2009). Molecular control of brain plasticity and repair. *Prog. Brain Res.* 175, 501–509.

Festoff, B. W., Ameenuddin, S., Arnold, P. M., Wong, A., Santacruz, K. S., and Citron, B. A. (2006). Minocycline neuroprotects, reduces microgliosis, and inhibits caspase protease expression early after spinal cord injury. *J. Neurochem.* 97, 1314–1326.

Floyd, C. L., and Lyeth, B. G. (2007). Astroglia: important mediators of traumatic brain injury. *Prog. Brain Res.* 161, 61–79.

Fox, G. B., Fan, L., Levasseur, R. A., and Faden, A. I. (1998). Effect of traumatic brain injury on mouse spatial and nonspatial learning in the Barnes circular maze. *J. Neurotrauma* 15, 1037–1046.

Gage, F. H., Dunnett, S. B., and Bjorklund, A. (1984). Spatial learning and motor deficits in aged rats. *Neurobiol. Aging* 5, 43–48.

Gao, Y., Fang, X., Tong, Y., Liu, Y., and Zhang, B. (2009). TLR4-mediated MyD88-dependent signaling pathway is activated by cerebral ischemia-reperfusion in cortex in mice. *Biomed. Pharmacother.* 63, 442–450.

Gerber, H. P., Mcmurtrey, A., Kowalski, J., Yan, M., Keyt, B. A., Dixit, V., and Ferrara, N. (1998). Vascular endothelial growth factor regulates endothelial cell survival through the phosphatidylinositol 3'-kinase/Akt signal transduction pathway. Requirement for Flk-1/KDR activation. *J. Biol. Chem.* 273, 30336–30343.

Glabinski, A. R., Balasingam, V., Tani, M., Kunkel, S. L., Strieter, R. M., Yong, V. W., and Ransohoff, R. M. (1996). Chemokine monocyte chemoattractant protein-1 is expressed by astrocytes after mechanical injury to the brain. *J. Immunol.* 156, 4363–4368.

Gonzalez, L. E., and File, S. E. (1997). A five minute experience in the elevated plus-maze alters the state of the benzodiazepine receptor in the dorsal raphe nucleus. *J. Neurosci.* 17, 1505–1511.

Gump, D. W., Ashikaga, T., Fink, T. J., and Radin, A. M. (1977). Side effects of minocycline: different dosage regimens. *Antimicrob. Agents Chemother.* 12, 642–646.

Gyorgy, A., Ling, G., Wingo, D., Walker, J., Tong, L., Parks, S., Januszkiewicz, A., Baumann, R., and Agoston, D. V. (2011). Time-dependent changes in serum biomarker levels after blast traumatic brain injury. *J. Neurotrauma* 28, 1121–1126.

Gyorgy, A. B., Walker, J., Wingo, D., Eidelman, O., Pollard, H. B., Molnar, A., and Agoston, D. V. (2010). Reverse phase protein microarray technology in traumatic brain injury. *J. Neurosci. Methods* 192, 96–101.

Handley, S. L., and Mithani, S. (1984). Effects of alpha-adrenoceptor agonists and antagonists in a maze-exploration model of "fear"-motivated behaviour. *Naunyn Schmiedebergs Arch. Pharmacol.* 327, 1–5.

Harrison, F. E., Hosseini, A. H., and Mcdonald, M. P. (2009). Endogenous anxiety and stress responses in water maze and Barnes maze spatial memory tasks. *Behav. Brain Res.* 198, 247–251.

Henke, P. G. (1990). Hippocampal pathway to the amygdala and stress ulcer development. *Brain Res. Bull.* 25, 691–695.

Heo, K., Cho, Y. J., Cho, K. J., Kim, H. W., Kim, H. J., Shin, H. Y., Lee, B. I., and Kim, G. W. (2006). Minocycline inhibits caspase-dependent and -independent cell death pathways and is neuroprotective against hippocampal damage after treatment with kainic acid in mice. *Neurosci. Lett.* 398, 195–200.

Hewlett, K. A., and Corbett, D. (2006). Delayed minocycline treatment reduces long-term functional deficits and histological injury in a rodent model of focal ischemia. *Neuroscience* 141, 27–33.

Hoffer, M. E., Balaban, C., Gottshall, K., Balough, B. J., Maddox, M. R., and Penta, J. R. (2010). Blast exposure: vestibular consequences and associated characteristics. *Otol. Neurotol.* 31, 232–236.

Hoge, C. W., Mcgurk, D., Thomas, J. L., Cox, A. L., Engel, C. C., and Castro, C. A. (2008). Mild traumatic brain injury in U.S. Soldiers returning from Iraq. *N. Engl. J. Med.* 358, 453–463.

Holmes, A., Wrenn, C. C., Harris, A. P., Thayer, K. E., and Crawley, J. N. (2002). Behavioral profiles of inbred strains on novel olfactory, spatial and emotional tests for reference memory in mice. *Genes Brain Behav.* 1, 55–69.

Hua, F., Ma, J., Ha, T., Kelley, J. L., Kao, R. L., Schweitzer, J. B., Kalbfleisch, J. H., Williams, D. L., and Li, C. (2009). Differential roles of TLR2 and TLR4 in acute focal cerebral ischemia/reperfusion injury in mice. *Brain Res.* 1262, 100–108.

Hua, F., Ma, J., Ha, T., Xia, Y., Kelley, J., Williams, D. L., Kao, R. L., Browder, I. W., Schweitzer, J. B., Kalbfleisch, J. H., and Li, C. (2007). Activation of Toll-like receptor 4 signaling contributes to hippocampal neuronal death following global cerebral ischemia/reperfusion. *J. Neuroimmunol.* 190, 101–111.

Hyder, A. A., Wunderlich, C. A., Puvanachandra, P., Gururaj, G., and Kobusingye, O. C. (2007). The impact of traumatic brain injuries: a global perspective. *NeuroRehabilitation* 22, 341–353.

Ingram, D. K., London, E. D., and Goodrick, C. L. (1981). Age and neurochemical correlates of radial maze performance in rats. *Neurobiol. Aging* 2, 41–47.

Kamnaksh, A., Kovesdi, E., Kwon, S. K., Wingo, D., Ahmed, F., Grunberg, N. E., Long, J., and Agoston, D. V. (2011). Factors affecting blast traumatic brain injury. *J. Neurotrauma* 28, 2145–2153.

Kersel, D. A., Marsh, N. V., Havill, J. H., and Sleigh, J. W. (2001). Psychosocial functioning during the year following severe traumatic brain injury. *Brain Inj.* 15, 683–696.

Kilic, E., Kilic, U., Wang, Y., Bassetti, C. L., Marti, H. H., and Hermann, D. M. (2006). The phosphatidylinositol-3 kinase/Akt pathway mediates VEGF's neuroprotective activity and induces blood brain barrier permeability after focal cerebral ischemia. *FASEB J.* 20, 1185–1187.

Kimelberg, H. K. (1995). Current concepts of brain edema. Review of laboratory investigations. *J. Neurosurg.* 83, 1051–1059.

Kochanek, P. M., Berger, R. P., Bayir, H., Wagner, A. K., Jenkins, L. W., and Clark, R. S. (2008). Biomarkers of primary and evolving damage in traumatic and ischemic brain injury: diagnosis, prognosis, probing mechanisms, and therapeutic decision making. *Curr. Opin. Crit. Care* 14, 135–141.

Korte, S. M., and De Boer, S. F. (2003). A robust animal model of state anxiety: fear-potentiated behaviour in the elevated plus-maze. *Eur. J. Pharmacol.* 463, 163–175.

Kovesdi, E., Gyorgy, A. B., Kwon, S. K., Wingo, D. L., Kamnaksh, A., Long, J. B., Kasper, C. E., and Agoston, D. V. (2011). The effect of enriched environment on the outcome of traumatic brain injury; a behavioral, proteomics, and histological study. *Front. Neurosci.* 5:42. doi:10.3389/fnins.2011.00042

Kriz, J., Nguyen, M. D., and Julien, J. P. (2002). Minocycline slows disease progression in a mouse model of amyotrophic lateral sclerosis. *Neurobiol. Dis.* 10, 268–278.

Kwon, S. K., Kovesdi, E., Gyorgy, A. B., Wingo, D., Kamnaksh, A., Walker, J., Long, J. B., and Agoston, D. V. (2011). Stress and traumatic brain injury: a behavioral, proteomics, and histological study. *Front. Neurol.* 2:12. doi:10.3389/fneur.2011.00012

Lamberty, Y., and Gower, A. J. (1993). Spatial processing and emotionality in aged NMRI mice: a multivariate analysis. *Physiol. Behav.* 54, 339–343.

Lee, C., and Agoston, D. V. (2009). Inhibition of VEGF receptor 2 increased cell death of dentate hilar neurons after traumatic brain injury. *Exp. Neurol.* 220, 400–403.

Lee, C., and Agoston, D. V. (2010). Vascular endothelial growth factor is involved in mediating increased de novo hippocampal neurogenesis in response to traumatic brain injury. *J. Neurotrauma* 27, 541–553.

Lee, J. H., Tigchelaar, S., Liu, J., Stammers, A. M., Streijger, F., Tetzlaff, W., and Kwon, B. K. (2010). Lack of neuroprotective effects of simvastatin and minocycline in a model of cervical spinal cord injury. *Exp. Neurol.* 225, 219–230.

Lee, S. M., Yune, T. Y., Kim, S. J., Park Do, W., Lee, Y. K., Kim, Y. C., Oh, Y. J., Markelonis, G. J., and Oh, T. H. (2003). Minocycline reduces cell death and improves functional recovery after traumatic spinal cord injury in the rat. *J. Neurotrauma* 20, 1017–1027.

Li, J., and McCullough, L. D. (2009). Sex differences in minocycline-induced neuroprotection after experimental stroke. *J. Cereb. Blood Flow Metab.* 29, 670–674.

Liebner, S., Fischmann, A., Rascher, G., Duffner, F., Grote, E. H., Kalbacher, H., and Wolburg, H. (2000). Claudin-1 and claudin-5 expression and tight junction morphology are altered in blood vessels of human glioblastoma multiforme. *Acta Neuropathol.* 100, 323–331.

Ling, G., Bandak, F., Armonda, R., Grant, G., and Ecklund, J. (2009). Explosive blast neurotrauma. *J. Neurotrauma* 26, 815–825.

Ling, G. S., and Ecklund, J. M. (2011). Traumatic brain injury in modern war. *Curr. Opin. Anaesthesiol.* 24, 124–130.

Lobo, S. M., Lobo, F. R., Bota, D. P., Lopes-Ferreira, F., Soliman, H. M., Melot, C., and Vincent, J. L. (2003). C-reactive protein levels correlate with mortality and organ failure in critically ill patients. *Chest* 123, 2043–2049.

Long, J. B., Bentley, T. L., Wessner, K. A., Cerone, C., Sweeney, S., and Bauman, R. A. (2009). Blast overpressure in rats: recreating a battlefield injury in the laboratory. *J. Neurotrauma* 26, 827–840.

Losy, J., and Zaremba, J. (2001). Monocyte chemoattractant protein-1 is increased in the cerebrospinal fluid of patients with ischemic stroke. *Stroke* 32, 2695–2696.

Macdonald, H., Kelly, R. G., Allen, E. S., Noble, J. F., and Kanegis, L. A. (1973). Pharmacokinetic studies on minocycline in man. *Clin. Pharmacol. Ther.* 14, 852–861.

Maegele, M., Lippert-Gruener, M., Ester-Bode, T., Sauerland, S., Schafer, U., Molcany, M., Lefering, R., Bouillon, B., Neiss, W. F., Angelov, D. N., Klug, N., Mcintosh, T. K., and Neugebauer, E. A. (2005). Reversal of neuromotor and cognitive dysfunction in an enriched environment combined with multimodal early onset stimulation after traumatic brain injury in rats. *J. Neurotrauma* 22, 772–782.

Marchand, F., Tsantoulas, C., Singh, D., Grist, J., Clark, A. K., Bradbury, E. J., and Mcmahon, S. B. (2009). Effects of Etanercept and Minocycline in a rat model of spinal cord injury. *Eur. J. Pain* 13, 673–681.

Marsh, B. J., Williams-Karnesky, R. L., and Stenzel-Poore, M. P. (2009). Toll-like receptor signaling in endogenous neuroprotection and stroke. *Neuroscience* 158, 1007–1020.

Mastroianni, C. M., Lancella, L., Mengoni, F., Lichtner, M., Santopadre, P., D'Agostino, C., Ticca, F., and Vullo, V. (1998). Chemokine profiles in the cerebrospinal fluid (CSF) during the course of pyogenic and tuberculous meningitis. *Clin. Exp. Immunol.* 114, 210–214.

Mishra, B. B., Mishra, P. K., and Teale, J. M. (2006). Expression and distribution of Toll-like receptors in the brain during murine neurocysticercosis. *J. Neuroimmunol.* 181, 46–56.

Missler, U., Wiesmann, M., Wittmann, G., Magerkurth, O., and Hagenstrom, H. (1999). Measurement of glial fibrillary acidic protein in human blood: analytical method and preliminary clinical results. *Clin. Chem.* 45, 138–141.

Miyakawa, T., Yared, E., Pak, J. H., Huang, F. L., Huang, K. P., and Crawley, J. N. (2001). Neurogranin null mutant mice display performance deficits on spatial learning tasks with anxiety related components. *Hippocampus* 11, 763–775.

Morganti-Kossmann, M. C., Rancan, M., Stahel, P. F., and Kossmann, T. (2002). Inflammatory response in acute traumatic brain injury: a double-edged sword. *Curr. Opin. Crit. Care* 8, 101–105.

Morita, K., Sasaki, H., Furuse, M., and Tsukita, S. (1999). Endothelial claudin: claudin-5/TMVCF constitutes tight junction strands in endothelial cells. *J. Cell Biol.* 147, 185–194.

Moser, M. B., and Moser, E. I. (1998). Functional differentiation in the hippocampus. *Hippocampus* 8, 608–619.

Neal, C. J., Lee, E. Y., Gyorgy, A., Ecklund, J. M., Agoston, D. V., and Ling, G. S. (2007). Effect of penetrating brain injury on aquaporin-4 expression using a rat model. *J. Neurotrauma* 24, 1609–1617.

Neigh, G. N., Karelina, K., Glasper, E. R., Bowers, S. L., Zhang, N., Popovich, P. G., and Devries, A. C. (2009). Anxiety after cardiac arrest/cardiopulmonary resuscitation: exacerbated by stress and prevented by minocycline. *Stroke* 40, 3601–3607.

Nelson, L. A., Yoash-Gantz, R. E., Pickett, T. C., and Campbell, T. A. (2009). Relationship between processing speed and executive functioning performance among OEF/OIF veterans: implications for postdeployment rehabilitation. *J. Head Trauma Rehabil.* 24, 32–40.

Ng, S. Y., Semple, B. D., Morganti-Kossmann, M. C., and Bye, N. (2012). Attenuation of microglial activation with minocycline is not associated with changes in neurogenesis after focal traumatic brain injury in adult mice. *J. Neurotrauma* 29, 1410–1425.

Ogunshola, O. O., Antic, A., Donoghue, M. J., Fan, S. Y., Kim, H., Stewart, W. B., Madri, J. A., and Ment, L. R. (2002). Paracrine and autocrine functions of neuronal vascular endothelial growth factor (VEGF) in the central nervous system. *J. Biol. Chem.* 277, 11410–11415.

Okamura, J. M., Miyagi, J. M., Terada, K., and Hokama, Y. (1990). Potential clinical applications of C-reactive protein. *J. Clin. Lab. Anal.* 4, 231–235.

Okie, S. (2005). Traumatic brain injury in the war zone. *N. Engl. J. Med.* 352, 2043–2047.

O'Neill, L. A. (2006). How Toll-like receptors signal: what we know and what we don't know. *Curr. Opin. Immunol.* 18, 3–9.

Overstreet, D. H., Commissaris, R. C., De La Garza, R. II, File, S. E., Knapp, D. J., and Seiden, L. S. (2003). Involvement of 5-HT1A receptors in animal tests of anxiety and depression: evidence from genetic models. *Stress* 6, 101–110.

Papadopoulos, M. C., Krishna, S., and Verkman, A. S. (2002). Aquaporin water channels and brain edema. *Mt. Sinai J. Med.* 69, 242–248.

Patel, R. N., Attur, M. G., Dave, M. N., Patel, I. V., Stuchin, S. A., Abramson, S. B., and Amin, A. R. (1999). A novel mechanism of action of chemically modified tetracyclines: inhibition of COX-2-mediated prostaglandin E2 production. *J. Immunol.* 163, 3459–3467.

Paylor, R., Zhao, Y., Libbey, M., Westphal, H., and Crawley, J. N. (2001). Learning impairments and motor dysfunctions in adult Lhx5-deficient mice displaying hippocampal disorganization. *Physiol. Behav.* 73, 781–792.

Pellow, S., Chopin, P., File, S. E., and Briley, M. (1985). Validation of open:closed arm entries in an elevated plus-maze as a measure of anxiety in the rat. *J. Neurosci. Methods* 14, 149–167.

Pitkänen, A., Schwartzkroin, P. A., and Moshé, S. L. (2006). *Models of Seizures and Epilepsy*. San Diego: Academic Press.

Pompl, P. N., Mullan, M. J., Bjugstad, K., and Arendash, G. W. (1999). Adaptation of the circular platform spatial memory task for mice: use in detecting cognitive impairment in the APP(SW) transgenic mouse model for Alzheimer's disease. *J. Neurosci. Methods* 87, 87–95.

Popovic, N., Schubart, A., Goetz, B. D., Zhang, S. C., Linington, C., and Duncan, I. D. (2002). Inhibition of autoimmune encephalomyelitis by a tetracycline. *Ann. Neurol.* 51, 215–223.

Povlishock, J. T., and Christman, C. W. (1995). The pathobiology of traumatically induced axonal injury in animals and humans: a review of current thoughts. *J. Neurotrauma* 12, 555–564.

Povlishock, J. T., and Pettus, E. H. (1996). Traumatically induced axonal damage: evidence for enduring changes in axolemmal permeability with associated cytoskeletal change. *Acta Neurochir. Suppl.* 66, 81–86.

Prat, A., and Antel, J. (2005). Pathogenesis of multiple sclerosis. *Curr. Opin. Neurol.* 18, 225–230.

Quinn, R. (2005). Comparing rat's to human's age: how old is my rat in people years? *Nutrition* 21, 775–777.

Raber, J., Rola, R., Lefevour, A., Morhardt, D., Curley, J., Mizumatsu, S., Vandenberg, S. R., and Fike, J. R. (2004). Radiation-induced cognitive

impairments are associated with changes in indicators of hippocampal neurogenesis. *Radiat. Res.* 162, 39–47.

Rancan, M., Otto, V. I., Hans, V. H., Gerlach, I., Jork, R., Trentz, O., Kossmann, T., and Morganti-Kossmann, M. C. (2001). Upregulation of ICAM-1 and MCP-1 but not of MIP-2 and sensorimotor deficit in response to traumatic axonal injury in rats. *J. Neurosci. Res.* 63, 438–446.

Rapoport, M. J., Mccullagh, S., Shammi, P., and Feinstein, A. (2005). Cognitive impairment associated with major depression following mild and moderate traumatic brain injury. *J. Neuropsychiatry Clin. Neurosci.* 17, 61–65.

Rickels, K., Case, W. G., Schweizer, E., Garcia-Espana, F., and Fridman, R. (1991). Long-term benzodiazepine users 3 years after participation in a discontinuation program. *Am. J. Psychiatry* 148, 757–761.

Robel, S., Berninger, B., and Gotz, M. (2011). The stem cell potential of glia: lessons from reactive gliosis. *Nat. Rev. Neurosci.* 12, 88–104.

Rodgers, R. J., Lee, C., and Shepherd, J. K. (1992). Effects of diazepam on behavioural and antinociceptive responses to the elevated plus-maze in male mice depend upon treatment regimen and prior maze experience. *Psychopharmacology (Berl.)* 106, 102–110.

Rosenstein, J. M., Mani, N., Khaibullina, A., and Krum, J. M. (2003). Neurotrophic effects of vascular endothelial growth factor on organotypic cortical explants and primary cortical neurons. *J. Neurosci.* 23, 11036–11044.

Ryan, L. M., and Warden, D. L. (2003). Post concussion syndrome. *Int. Rev. Psychiatry* 15, 310–316.

Saivin, S., and Houin, G. (1988). Clinical pharmacokinetics of doxycycline and minocycline. *Clin. Pharmacokinet.* 15, 355–366.

Salzberg, M., Kumar, G., Supit, L., Jones, N. C., Morris, M. J., Rees, S., and O'Brien, T. J. (2007). Early postnatal stress confers enduring vulnerability to limbic epileptogenesis. *Epilepsia* 48, 2079–2085.

Sanchez Mejia, R. O., Ona, V. O., Li, M., and Friedlander, R. M. (2001). Minocycline reduces traumatic brain injury-mediated caspase-1 activation, tissue damage, and neurological dysfunction. *Neurosurgery* 48, 1393–1399; discussion 1399–1401.

Silva, R. C., and Brandao, M. L. (2000). Acute and chronic effects of gepirone and fluoxetine in rats tested in the elevated plus-maze: an ethological analysis. *Pharmacol. Biochem. Behav.* 65, 209–216.

Silveira, M. C., Sandner, G., and Graeff, F. G. (1993). Induction of Fos immunoreactivity in the brain by exposure to the elevated plus-maze. *Behav. Brain Res.* 56, 115–118.

Silver, J. M., Mcallister, T. W., and Arciniegas, D. B. (2009). Depression and cognitive complaints following mild traumatic brain injury. *Am. J. Psychiatry* 166, 653–661.

Sindern, E., Niederkinkhaus, Y., Henschel, M., Ossege, L. M., Patzold, T., and Malin, J. P. (2001). Differential release of beta-chemokines in serum and CSF of patients with relapsing-remitting multiple sclerosis. *Acta Neurol. Scand.* 104, 88–91.

Siopi, E., Cho, A. H., Homsi, S., Croci, N., Plotkine, M., Marchand-Leroux, C., and Jafarian-Tehrani, M. (2011). Minocycline restores sAPPalpha levels and reduces the late histopathological consequences of traumatic brain injury in mice. *J. Neurotrauma* 28, 2135–2143.

Skold, M. K., Risling, M., and Holmin, S. (2006). Inhibition of vascular endothelial growth factor receptor 2 activity in experimental brain contusions aggravates injury outcome and leads to early increased neuronal and glial degeneration. *Eur. J. Neurosci.* 23, 21–34.

Sondell, M., Sundler, F., and Kanje, M. (2000). Vascular endothelial growth factor is a neurotrophic factor which stimulates axonal outgrowth through the flk-1 receptor. *Eur. J. Neurosci.* 12, 4243–4254.

Sorensen, T. L., Ransohoff, R. M., Strieter, R. M., and Sellebjerg, F. (2004). Chemokine CCL2 and chemokine receptor CCR2 in early active multiple sclerosis. *Eur. J. Neurol.* 11, 445–449.

Sprott, R. L., and Eleftheriou, B. E. (1974). Open-field behavior in aging inbred mice. *Gerontologia* 20, 155–162.

Stamatovic, S. M., Dimitrijevic, O. B., Keep, R. F., and Andjelkovic, A. V. (2006). Protein kinase Calpha-RhoA cross-talk in CCL2-induced alterations in brain endothelial permeability. *J. Biol. Chem.* 281, 8379–8388.

Stamatovic, S. M., Keep, R. F., Kunkel, S. L., and Andjelkovic, A. V. (2003). Potential role of MCP-1 in endothelial cell tight junction "opening": signaling via Rho and Rho kinase. *J. Cell Sci.* 116, 4615–4628.

Stirling, D. P., Khodarahmi, K., Liu, J., Mcphail, L. T., Mcbride, C. B., Steeves, J. D., Ramer, M. S., and Tetzlaff, W. (2004). Minocycline treatment reduces delayed oligodendrocyte death, attenuates axonal dieback, and improves functional outcome after spinal cord injury. *J. Neurosci.* 24, 2182–2190.

Stirling, D. P., Koochesfahani, K. M., Steeves, J. D., and Tetzlaff, W. (2005). Minocycline as a neuroprotective agent. *Neuroscientist* 11, 308–322.

Susin, S. A., Lorenzo, H. K., Zamzami, N., Marzo, I., Snow, B. E., Brothers, G. M., Mangion, J., Jacotot, E., Costantini, P., Loeffler, M., Larochette, N., Goodlett, D. R., Aebersold, R., Siderovski, D. P., Penninger, J. M., and Kroemer, G. (1999). Molecular characterization of mitochondrial apoptosis-inducing factor. *Nature* 397, 441–446.

Takeda, K., and Akira, S. (2005). Toll-like receptors in innate immunity. *Int. Immunol.* 17, 1–14.

Tanielian, T., and Jaycox, L. H. (2008). *Invisible Wounds of War: Psychological and Cognitive Injuries, their Consequences, and Services to Assist Recovery*. Santa Monica: RAND Corporation.

Tekstra, J., Beekhuizen, H., Van De Gevel, J. S., Van Benten, I. J., Tuk, C. W., and Beelen, R. H. (1999). Infection of human endothelial cells with *Staphylococcus aureus* induces the production of monocyte chemotactic protein-1 (MCP-1) and monocyte chemotaxis. *Clin. Exp. Immunol.* 117, 489–495.

Teng, Y. D., Choi, H., Onario, R. C., Zhu, S., Desilets, F. C., Lan, S., Woodard, E. J., Snyder, E. Y., Eichler, M. E., and Friedlander, R. M. (2004). Minocycline inhibits contusion-triggered mitochondrial cytochrome c release and mitigates functional deficits after spinal cord injury. *Proc. Natl. Acad. Sci. U.S.A.* 101, 3071–3076.

Tenovuo, O. (2006). Pharmacological enhancement of cognitive and behavioral deficits after traumatic brain injury. *Curr. Opin. Neurol.* 19, 528–533.

Terrio, H., Brenner, L. A., Ivins, B. J., Cho, J. M., Helmick, K., Schwab, K., Scally, K., Bretthauer, R., and Warden, D. (2009). Traumatic brain injury screening: preliminary findings in a US Army Brigade Combat Team. *J. Head Trauma Rehabil.* 24, 14–23.

Thurman, D. J., Alverson, C., Dunn, K. A., Guerrero, J., and Sniezek, J. E. (1999). Traumatic brain injury in the United States: a public health perspective. *J. Head Trauma Rehabil.* 14, 602–615.

Tikka, T. M., and Koistinaho, J. E. (2001). Minocycline provides neuroprotection against N-methyl-D-aspartate neurotoxicity by inhibiting microglia. *J. Immunol.* 166, 7527–7533.

Walf, A. A., and Frye, C. A. (2007). The use of the elevated plus maze as an assay of anxiety-related behavior in rodents. *Nat. Protoc.* 2, 322–328.

Wang, X., Zhu, S., Drozda, M., Zhang, W., Stavrovskaya, I. G., Cattaneo, E., Ferrante, R. J., Kristal, B. S., and Friedlander, R. M. (2003). Minocycline inhibits caspase-independent and -dependent mitochondrial cell death pathways in models of Huntington's disease. *Proc. Natl. Acad. Sci. U.S.A.* 100, 10483–10487.

Warden, D. (2006). Military TBI during the Iraq and Afghanistan wars. *J. Head Trauma Rehabil.* 21, 398–402.

Wells, J. E., Hurlbert, R. J., Fehlings, M. G., and Yong, V. W. (2003). Neuroprotection by minocycline facilitates significant recovery from spinal cord injury in mice. *Brain* 126, 1628–1637.

Wixey, J. A., Reinebrant, H. E., Spencer, S. J., and Buller, K. M. (2011). Efficacy of post-insult minocycline administration to alter long-term hypoxia-ischemia-induced damage to the serotonergic system in the immature rat brain. *Neuroscience* 182, 184–192.

Wu, D. C., Jackson-Lewis, V., Vila, M., Tieu, K., Teismann, P., Vadseth, C., Choi, D. K., Ischiropoulos, H., and Przedborski, S. (2002). Blockade of microglial activation is neuroprotective in the 1-methyl-4-phenyl-1,2,3,6-tetrahydropyridine mouse model of Parkinson disease. *J. Neurosci.* 22, 1763–1771.

Wu, L. W., Mayo, L. D., Dunbar, J. D., Kessler, K. M., Baerwald, M. R., Jaffe, E. A., Wang, D., Warren, R. S., and Donner, D. B. (2000). Utilization of distinct signaling pathways by receptors for vascular endothelial cell growth factor and other mitogens in the induction of endothelial cell proliferation. *J. Biol. Chem.* 275, 5096–5103.

Xu, L., Fagan, S. C., Waller, J. L., Edwards, D., Borlongan, C. V., Zheng, J., Hill, W. D., Feuerstein, G., and Hess, D. C. (2004). Low dose intravenous minocycline is neuroprotective after middle cerebral artery occlusion-reperfusion in rats. *BMC Neurol.* 4, 7. doi:10.1186/1471-2377-4-7

Yrjanheikki, J., Keinanen, R., Pellikka, M., Hokfelt, T., and Koistinaho, J. (1998). Tetracyclines inhibit microglial activation and are neuroprotective in global brain ischemia.

Proc. Natl. Acad. Sci. U.S.A. 95, 15769–15774.

Yrjanheikki, J., Tikka, T., Keinanen, R., Goldsteins, G., Chan, P. H., and Koistinaho, J. (1999). A tetracycline derivative, minocycline, reduces inflammation and protects against focal cerebral ischemia with a wide therapeutic window. *Proc. Natl. Acad. Sci. U.S.A.* 96, 13496–13500.

Yune, T. Y., Lee, J. Y., Jung, G. Y., Kim, S. J., Jiang, M. H., Kim, Y. C., Oh, Y. J., Markelonis, G. J., and Oh, T. H. (2007). Minocycline alleviates death of oligodendrocytes by inhibiting pro-nerve growth factor production in microglia after spinal cord injury. *J. Neurosci.* 27, 7751–7761.

Zemke, D., and Majid, A. (2004). The potential of minocycline for neuroprotection in human neurologic disease. *Clin. Neuropharmacol.* 27, 293–298.

Zhang, X., Chen, J., Graham, S. H., Du, L., Kochanek, P. M., Draviam, R., Guo, F., Nathaniel, P. D., Szabo, C., Watkins, S. C., and Clark, R. S. (2002). Intranuclear localization of apoptosis-inducing factor (AIF) and large scale DNA fragmentation after traumatic brain injury in rats and in neuronal cultures exposed to peroxynitrite. *J. Neurochem.* 82, 181–191.

Zhu, S., Stavrovskaya, I. G., Drozda, M., Kim, B. Y., Ona, V., Li, M., Sarang, S., Liu, A. S., Hartley, D. M., Wu, D. C., Gullans, S., Ferrante, R. J., Przedborski, S., Kristal, B. S., and Friedlander, R. M. (2002). Minocycline inhibits cytochrome c release and delays progression of amyotrophic lateral sclerosis in mice. *Nature* 417, 74–78.

Conflict of Interest Statement: The authors declare that the research was conducted in the absence of any commercial or financial relationships that could be construed as a potential conflict of interest.

Received: 03 January 2012; accepted: 22 June 2012; published online: 16 July 2012.

Citation: Kovesdi E, Kamnaksh A, Wingo D, Ahmed F, Grunberg NE, Long JB, Kasper CE and Agoston DV (2012) Acute minocycline treatment mitigates the symptoms of mild blast-induced traumatic brain injury. Front. Neur. ***3****:111. doi: 10.3389/fneur.2012.00111*

This article was submitted to Frontiers in Neurotrauma, a specialty of Frontiers in Neurology.

APPENDIX

Table A1 | List of animal models of various diseases, dose of minocycline treatment and the observed effects of the treatment.

Animal model of disease	Dose	Effect	Reference
Acute spinal cord injury (mouse)	1 and 24 h (50 mg/kg, i.p.), then 25 mg/kg dose every 24 h for the next 5 days	Improved both hindlimb function and strength after injury and reduced lesion size	Wells et al. (2003)
Amyotrophic lateral sclerosis (mouse)	1 g/kg in a custom made rodent diet	Delayed the onset of motor neuron degeneration, less activation of microglia was detected at early symptomatic stage (46 weeks) and at the end stage of disease in the spinal cord	Kriz et al. (2002)
Cervical spinal cord injury (rat)	1 h (90 mg/kg), then for 3 days after injury	Failed to improve functional and histological recovery.	Lee et al. (2010)
Closed head injury (mouse)	5 min (90 mg/kg, i.p.), and at 3 and 9 h (45 mg/kg) post-TBI	Attenuation of the decrease of post-TBI sAPPα 24 h post-injury. Corpus callosum and striatal atrophy, ventriculomegaly, astrogliosis, and microglial activation reduced 3 months post-injury	Siopi et al. (2011)
Closed head injury (mouse)	30 min (45 mg/kg, i.p.) and every 12 h (22.5 mg/kg, i.p.) for 1 week. Or twice-daily minocycline injections for 2 weeks (6 weeks surviving)	Reduced the activation of microglia/macrophages and improved neurological outcome, but any increase of neurogenesis	Ng et al. (2012)
Controlled contusion spinal cord injury (rat)	Multiple injections (30 mg/kg, i.p.) at 0.5, 1, and 24 h, or a single injection of 90 mg/kg at either 0.5, 1.0, or 24 h after injury	Improved functional recovery, reduced tissue damage, cavity size, apoptosis and activated caspase-3 signal	Festoff et al. (2006)
Controlled cortical impact (rat)	45 mg/kg, i.p. at 1 h, 24 and 48 h after injury	Improved active place avoidance following CCI	Abdel Baki et al. (2010)
Endothelin-1 (ET-1) model of focal ischemia (rat)	45 mg/kg, i.p. at 2 and 12 h following the last injection of ET-1, then 22.5 mg/kg every 12 h (5×)	Improved behavioral outcome. Reduced subcortical and whole hemisphere infarct volume	Hewlett and Corbett (2006)
Focal cerebral ischemia (rat)	45 mg/kg, i.p. twice a day for the first day; 22.5 mg/kg for the subsequent 2 days	Reduced cortical infarction volume, inhibited morphological activation of microglia in the area adjacent to the infarction, induction of IL-1b-converting enzyme, and reduced cyclooxygenase-2 expression and prostaglandin E2 production	Yrjanheikki et al. (1999)
Huntington disease (mouse)	daily 5 mg/kg, i.p.	Inhibited caspase-1 and caspase-3 up-regulation	Chen et al. (2000)
Middle cerebral artery occlusion (MCAO; mice)	45 mg/kg two times in every 12 h starting at 30 min after the onset of MCAO	Neuroprotectant at males, but ineffective at reducing ischemic damage in females	Li and McCullough (2009)
Neonatal hypoxia-ischemia (HI; rat)	2 h after hypoxia (45 mg/kg, i.p.), then every 24 h from P4–P9 (22.5 mg/kg)	Prevention of HI induced changes in SERT, 5-HT and 5-HT positive dorsal raphe neurons. Lasting effect after 6 week of HI	Wixey et al. (2011)
Parkinson disease (mouse)	Daily twice (12 h apart) injections from 1.4 to 45 mg/kg (i.p.) starting 30 min after the first MPTP injection and continuing through four additional days after the last injection of MPTP	Inhibited microglial activation, mitigated both the demise of nigrostriatal dopaminergic neurons and the formation of nitrotyrosine. Prevented the formation of mature interleukin-1β and the activation of NADPH–oxidase and inducible nitric oxide synthase (iNOS)	Wu et al. (2002)
Spinal cord injury (T13 hemisection of the spinal cord; rat)	30 min (40 mg/kg, i.p.) followed twice per day for 2 days post-injury	Reduced the development of pain behaviors at 1 and 2 weeks after SCI, reduced microglial OX-42 expression and decreased the expression of noxious stimulation-induced c-Fos	Marchand et al. (2009)

(Continued)

Table A1 | Continued

Animal model of disease	Dose	Effect	Reference
Spinal cord injury (rat)	Twice a day beginning 30 min after injury (50 mg/kg, i.p.) for 2 days	Reduced apoptotic oligodendrocytes and microglia in proximal and distal segments of the ascending sensory tract. Reduced microglial/macrophage density, attenuated axonal dieback and improved functional outcome	Stirling et al. (2004)
Temporary middle cerebral artery occlusion model (TMCAO; rat)	For 4 h post TMCAO protocol: 3 or 10 mg/kg i.v. at 4, 8, and 12 h; for the 5-h post TMCAO protocol: at 5, 9, and 13 h; and for the 6-h post TMCAO protocol at 6, 10, and 14 h	3 and 10 mg/kg i.v. were effective at reducing infarct size with a 5 hour therapeutic time window after TMCAO. 10 mg/kg extended the window time to ameliorate neurological deficits to 5 h	Xu et al. (2004)

Table A2 | List of antibodies and their respective classifications and dilutions used to measure protein biomarker levels in sera and brain tissues.

Antibody	Vendor	Catalog No.	Dilution in RPPM
INFLAMMATORY			
C-reactive protein (CRP)	Santa Cruz Biotechnology, Inc.	sc-30047	1:20
Monocyte chemoattractant protein (MCP-1)	Santa Cruz Biotechnology, Inc.	sc-1784	1:20
Toll-like receptor 9 (TLR9)	*Santa Cruz Biotechnology, Inc.*	*sc-13218*	*1:20*
VASCULAR			
Claudin 5	Santa Cruz Biotechnology, Inc.	sc-28670	1:20
Vascular endothelial growth factor (VEGF)	*Abcam*	*ab-53465*	*1:50*
VEGF receptor 2 (FLK-1)	*Santa Cruz Biotechnology, Inc.*	*sc-315*	*1:20*
Aquaporin 4 (AQP4)	*Abcam*	*ab-97414*	*1:50*
NEURONAL			
Neuron-specific enolase (NSE)	Abcam	ab-53025	1:20
Neurofilament heavy chain (NF-H)	Sigma Aldrich	N-4142	1:20
Tau protein	Santa Cruz Biotechnology, Inc.	sc-1995P	1:20
GLIAL			
S100 beta protein (S100β)	Abcam	ab-41548	1:20
Glial fibrillary acidic protein (GFAP)	Abcam	ab-7260	1:50
Myelin basic protein (MBP)	*Santa Cruz Biotechnology, Inc.*	*sc-13914*	*1:20*

Biomarkers labeled with italics were only measured in the brain.

Table A3 | The effect of injury and minocycline treatment on tissue levels of the selected protein biomarkers in the different experimental groups.

Markers	Amygdala				Prefrontal cortex				Ventral hippocampus				Dorsal hippocampus			
	Sham vehicle	**Sham-mino**	**Injured-vehicle**	**Injured-mino**	**Sham vehicle**	**Sham-mino**	**Injured-vehicle**	**Injured-mino**	**Sham vehicle**	**Sham-mino**	**Injured-vehicle**	**Injured-mino**	**Sham vehicle**	**Sham-mino**	**Injured-vehicle**	**Injured-mino**
VASCULAR																
Claudin 5	4.49 ± 0.14	4.61 ± 0.09	4.90 ± 0.18	4.81 ± 0.14	4.25 ± 0.16	4.40 ± 0.15	4.63 ± 0.05	4.75 ± 0.08	4.10 ± 0.09	4.38 ± 0.14	*4.78 ± 0.15*	4.59 ± 0.08	4.65 ± 0.12	4.61 ± 0.12	4.64 ± 0.18	4.59 ± 0.06
VEGF	4.97 ± 0.06	5.15 ± 0.07	5.30 ± 0.11	4.97 ± 0.10	5.07 ± 0.05	4.83 ± 0.06	5.12 ± 0.07	4.97 ± 0.12	5.03 ± 0.04	4.90 ± 0.06	5.18 ± 0.07	5.10 ± 0.04	4.99 ± 0.08	5.01 ± 0.08	4.89 ± 0.16	5.00 ± 0.15
AQP4	4.36 ± 0.05	4.44 ± 0.08	*4.78 ± 0.04*	4.53 ± 0.07	4.36 ± 0.12	4.37 ± 0.11	4.58 ± 0.05	4.68 ± 0.13	4.25 ± 0.07	4.30 ± 0.10	*4.80 ± 0.04*	4.49 ± 0.07	4.32 ± 0.09	4.36 ± 0.07	4.41 ± 0.08	4.41 ± 0.12
GLIAL																
MBP	5.63 ± 0.14	5.80 ± 0.06	5.55 ± 0.08	5.64 ± 0.09	5.49 ± 0.06	5.54 ± 0.06	5.64 ± 0.04	5.93 ± 0.15	5.94 ± 0.08	6.00 ± 0.04	*6.37 ± 0.11*	**6.05 ± 0.04**	5.94 ± 0.07	6.04 ± 0.08	*6.51 ± 0.04*	**5.95 ± 0.11**

The levels of seven protein markers were measured by RPPM in the amygdala, prefrontal cortex, ventral hippocampus, and dorsal hippocampus. Measured protein levels are expressed as y-axis intercept (Y-cept) and are presented as mean ± SEM. Values listed in underline italics indicate $p < 0.05$ for injured-vehicle vs. sham-vehicle rats. ***Bold-faced*** *values indicate $p < 0.05$ for injured-vehicle vs.injured-minorats.*

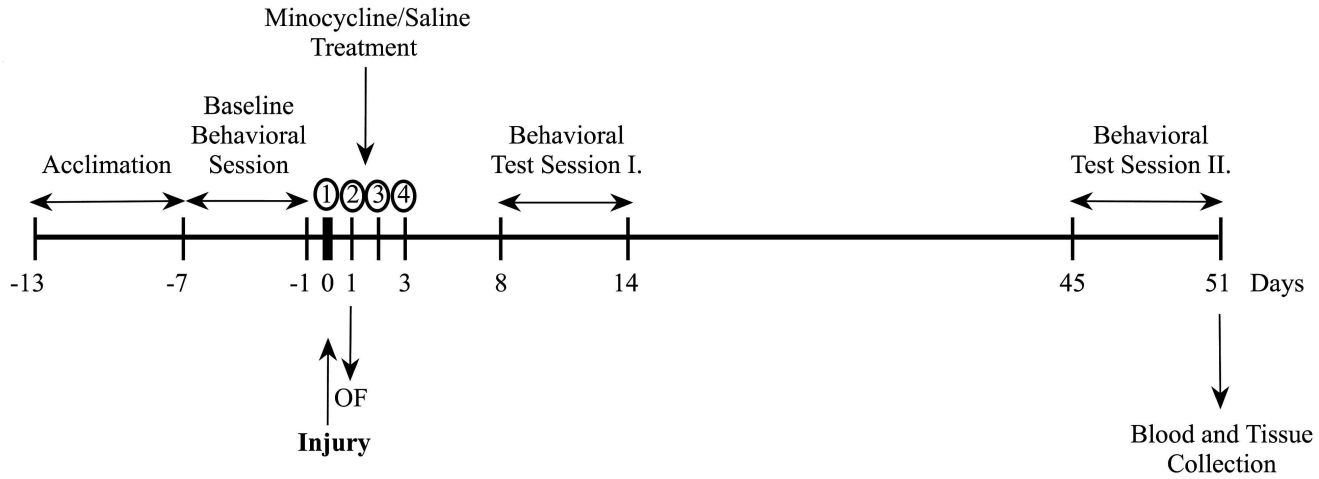

FIGURE A1 | Outline of the experimental schedule. After 1 week of acclimation, baseline behavioral analyses, and injury (or sham), rats were treated intraperitoneally for four consecutive days (marked by circled numbers of 1 through 4) with 50 mg/kg of minocycline or saline starting at 4 hours after injury. Behavioral assessments (Open Field, Elevated Plus Maze, and Barnes Maze) were conducted before injury (Baseline Behavioral Session), and at 1 (open field OF only), 8 (Behavioral Test Session I.), and 45 days (Behavioral Test Session II.) after injury or sham. At the end of the experiment blood and brains were collected, processed, and analyzed using RPPM and ELISA.

JOURNAL OF NEUROTRAUMA 30:1645–1651 (October 1, 2013)

DOI: 10.1089/neu.2012.2834

Acute Mitochondrial Dysfunction after Blast Exposure: Potential Role of Mitochondrial Glutamate Oxaloacetate Transaminase

Peethambaran Arun, Rania Abu-Taleb, Samuel Oguntayo, Ying Wang, Manojkumar Valiyaveettil, Joseph B. Long, and Madhusoodana P. Nambiar

Abstract

Use of improvised explosive devices has significantly increased the incidence of traumatic brain injury (TBI) and associated neuropsychiatric deficits in the recent wars in Iraq and Afghanistan. Acute deleterious effects of single and repeated blast exposure can lead to long-term neurobiological effects and neuropsychiatric deficits. Using *in vitro* and *in vivo* shock tube models of blast-induced TBI, we studied changes in mitochondrial energy metabolism after blast exposure. Single and repeated blast exposures *in vitro* resulted in significant decreases in neuronal adenosine triphosphate (ATP) levels at 6 h post-blast that returned towards normal levels by 24 h. Similar changes in ATP also were observed in the cerebral cortices of mice subjected to single and repeated blast exposures. In neurons, mitochondrial glutamate oxaloacetate transaminase (GOT_2) plays a critical role in metabolism and energy production. Proteomic analysis of brain cortices showed a significant decrease in GOT_2 levels 6 h after repeated blast exposures, which was further confirmed by Western blotting. Western blot analysis of GOT_2 and pyruvate dehydrogenase in the cortex showed direct correlation only between GOT_2 and ATP levels. Activity of GOT_2 in the isolated cortical mitochondria also showed significant decrease at 6 h supporting the results of proteomic and Western blot analyses. Knowing the significant role of GOT_2 in the neuronal mitochondrial energy metabolism, it is quite likely that the down regulation of GOT_2 after blast exposure is playing a significant role in mitochondrial dysfunction after blast exposure.

Key words: adenosine triphosphate; blast exposure; glutamate oxaloacetate transaminase; mini citric acid cycle; mitochondrial dysfunction; pyruvate dehydrogenase; traumatic brain injury

Introduction

Exposure to blast has been reported as the major cause of traumatic brain injury (TBI) and associated disabilities in the recent wars in Iraq and Afghanistan.[1] Significant advances in personnel protection devices and medical care have decreased the mortality of blast victims, but increased the number of surviving casualties with mild, moderate and severe TBI.[2,3] Service members are commonly exposed to single or multiple blasts with different intervals. Preclinical studies in experimental animal models indicate that severity of brain injury increases with number of blast exposures.[3]

Due to the complexity and unique physical forces responsible for blast-induced TBI, it is now widely believed that the TBI resulting from blast exposure is relatively distinct from other closed head or penetrating brain injuries.[4] The primary, secondary, tertiary, and quaternary injury phases of blast exposure are believed to contribute to the multifaceted mechanisms involved in blast TBI. Although several clinical and animal studies have explored the biochemical/histopathological changes and behavioral deficits resulting from blast exposure,[3,5–11] the complex biochemical and molecular mechanisms of blast TBI and how it triggers subsequent secondary pathological processes and long-term neurobehavioral abnormalities are still not well understood. The lack of understanding of the precise mechanisms involved in blast TBI has hampered the development of personal protective gear and specific diagnostic tools for early detection and effective therapies for prevention/treatment.

Acute effects of blast exposure are not well studied because most of the significant pathological changes in the brain manifest during the secondary injury processes, which occur typically by 24 h post-blast exposures. Using an *in vitro* model of

Blast-Induced Neurotrauma Branch, Center for Military Psychiatry and Neuroscience, Walter Reed Army Institute of Research, Silver Spring, Maryland.

blast-induced TBI, we have shown that single and repeated blast exposures lead to transient changes in neuronal cell membrane integrity, which may be a potential mechanism contributing to the secondary injury processes.[12] Transient changes in cell membrane integrity also have been reported in the liver and muscle tissue after single and repeated blast exposures.[13] Acute deleterious effects of any direct or indirect insult on the brain can trigger secondary pathological changes, which lead to chronic neurobehavioral abnormalities. Thus, minimizing or preventing acute changes after brain injury is important to avert chronic neurobehavioral deficits.

In most of the cell types in the body, adenosine triphosphate (ATP) synthesis takes place through utilization of glucose, and mitochondrial pyruvate dehydrogenase (PDH) plays an important role. In the case of brain, amino acids—especially glutamate—also are utilized for the immediate and significant demands for ATP for energy.[14–16] In one study, removal of glucose significantly increased the transamination of glutamate to aspartate in brain synaptosomes and suggested that brain cells utilize glutamate, the most abundant molecule in the brain, for energy production.[15] Mitochondrial glutamate oxaloacetate transaminase (GOT_2) is the enzyme responsible for the transamination of glutamate to aspartate and α-ketoglutarate. Since α-ketoglutarate can directly enter the citric acid cycle to generate ATP, GOT_2 is believed to play major role in ATP production in neurons.[14–16]

In the present study, using the *in vitro* and *in vivo* models of blast-induced TBI, we studied changes in mitochondrial energy metabolism after blast exposure. We first analyzed ATP levels in the neuronal cells in culture and brain cortex after blast exposure to demonstrate mitochondrial energy dysfunction. Decreases in ATP levels were further compared between single and multiple blast exposures to determine its dependency upon the severity of injury. Since GOT_2 plays a central role in neuronal mitochondrial energy metabolism, we investigated its expression in the brain by proteomic analysis. Modulation of GOT_2 was further analyzed by Western-blotting of the brain cortex and enzyme activity analysis in the isolated mitochondria from the cerebral cortex to demonstrate a potential role of GOT_2 in the acute mitochondrial dysfunction after blast exposure.

Methods

Cell culture and blast exposure

SH-SY5Y human neuroblastoma cells, Dulbecco's modified Eagle's medium (DMEM) and fetal bovine serum (FBS) were obtained from American Type Culture Collection (Manassas, VA). One of the major advantageous of SH-SY5Y cells over primary cells and brain slices (derived from animals) is that the effect of blast exposure can be studied in cells of human origin. Cells were grown in DMEM with 10% heat inactivated FBS containing penicillin and streptomycin. The cells incubated at 37°C in a carbon dioxide (CO_2) incubator kept at 5% CO_2 and 95% air in a humidified atmosphere. Cells (4×104 cells/well) were grown on 96 well tissue culture plates 24 h before blast exposure. On the day of blast exposure, the medium was removed from the wells and fresh medium (360 μL) was added to fill the wells. Before blast exposure, the plates were sealed with gas permeable Mylar plate sealers as described previously.[12,17] The plates containing cells were subjected to single and triple blast exposures (21 psi) using shock tube as described earlier.[12,17] Intracellular adenosine triphosphate (ATP) content in the cells was determined at 6 and 24 h post-blast using ATPlite kits (Perkin Elmer, Waltham, MA) as previously described.[17] The ATPlite assay system is based on the production of luminescence caused by the reaction of ATP with added luciferase enzyme and D-luciferin substrate.

Animals and blast exposure

All animal experiments were conducted in accordance with the Animal Welfare Act and other federal statutes and regulations relating to animals and experiments involving animals and adhered to principles stated in the Guide for the Care and Use of Laboratory Animals (National Research Council Publication, 1996 edition). The animal protocol used was approved by Institutional Animal Care and Use Committee, Walter Reed Army Institute of Research. C57BL/6J male mice (8–10 weeks old) that weighed between 21–26 g (Jackson Laboratory, Bar Harbor, ME) were used in this study. Mice were exposed to single and triple blasts using a shock tube as described earlier.[3] Briefly, mice were anesthetized with 4% isofluorane gas (oxygen [O_2] flow rate 1.5 L/min) for 8 min and restrained in the prone position with a net to minimize the movements during blast exposure. Animals were subjected to single or triple blast exposures (21 psi) and brain cortex was dissected after euthanasia at 1, 6, or 24 h post-blast.

ATP determination in the brain cortex

Homogenate (20% w/v) of brain cortex was made in tissue protein extraction buffer (Pierce Chemical Co, Rockford, IL) containing protease and phosphatase inhibitor cocktails (Sigma-Aldrich, St. Louis, MO). The homogenate was centrifuged at 5000 g for 5 min and the ATP content in the supernatant was measured using ATPlite kit as described earlier.[18]

Proteomic analysis

Proteomic analysis of brain cortex was carried out as described by us earlier.[19] Briefly, proteins were isolated from the brain cortex of sham control and repeated blast exposed mice (3 animals/group) at 6 h post-blast using the ToPI-DIGE™ total protein isolation kit (ITSI-Biosciences, Johnstown, PA) and subjected to two-dimensional differential in-gel electrophoresis (2D-DIGE). After 2D-DIGE, the differentially-expressed (> 2-fold change in abundance) protein spots were identified, selectively picked, and subjected to protein digestion followed by LC/MS/MS to identify the peptides. The obtained MS/MS spectra were searched against the National Center for Biotechnology Information non-redundant protein sequence database using the SEQUEST computer algorithm to establish the protein identity.

Western blotting analysis

Polyclonal rabbit antibodies against GOT_2 and pyruvate dehydrogenase (PDH) were obtained from Sigma-Aldrich (St. Louis, MO) and Abcam (Cambridge, MA). Secondary antibody labeled with horse-radish peroxidase (HRP) was purchased from Santa Cruz Biotechnology (Santa Cruz, CA). Mouse monoclonal antibody to β-actin conjugated with HRP (Sigma-Aldrich, St. Louis, MO) was used as a control. Polyacrylamide gel electrophoresis and Western blotting analysis of brain cortex was carried out as described by us previously.[19] Both GOT_2 and PDH antibodies were used at a final dilution of 1:1000. After Western blotting analysis, the protein bands were detected using ECL-Plus Western blot detecting reagent (GE Healthcare, Piscataway, NJ) and the chemiluminescence was measured in an AlphaImage reader (Cell Biosciences, Santa Clara, CA).

Assay of GOT_2 activity in the mitochondrial fraction of brain cortex

Mitochondrial fraction was isolated from the cerebral cortex using Mitochondria Isolation Kit obtained from Thermo Scientific (Rockford, IL) according to the manufacturer's instructions. The

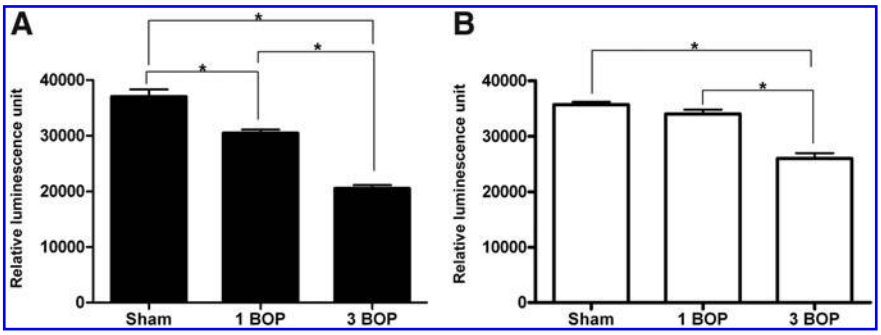

FIG. 1. Changes in adenosine triphosphate levels in SH-SY5Y cells at 6 h **(A)** and 24 h **(B)** after single and repeated blast exposures. Relative luminescence unit represents the total luminescence liberated by the cells in a single well of 96 well plate. Values are expressed as mean ± standard deviation. $*p < 0.05$ ($n = 12$). BOP, blast overpressure exposure.

mitochondrial pellet was suspended in the enzyme assay buffer and disrupted using a sonifier for the enzyme assay. The activity of GOT_2 was measured using the diagnostic kit for measuring GOT, obtained from Randox Laboratories (Kearneysville, WV) according to the manufacturer's instructions. The assay system utilizes the decrease in optical density at 340 nm due to the consumption of NADH during the formation of oxaloacetate and glutamate from aspartic acid and α-ketoglutaric acid catalyzed by GOT.

Statistical analysis

Statistical analysis was carried out by analysis of variance (ANOVA) using SAS software version 9.3 (SAS Institute, Inc., Cary, NC). For single variance, one-way ANOVA followed by *t* test was carried out. For multiple variance, two-way ANOVA followed by Tukey's post-hoc test using HSD multiple comparisons were used. A *p* value of less than 0.05 was considered significant.

Results

Blast exposure leads to acute decrease in neuronal ATP levels

Blast exposure causes a significant decrease in endogenous ATP levels in SH-SY5Y human neuroblastoma cells in a time-dependent manner with the highest decrease at 6 h post-blast, compared with 24 h post-blast (Fig. 1). Neuronal ATP levels were further decreased with multiple blast exposures. After single blast exposure, the ATP level decreased by 17.7% at 6 h, whereas no significant decrease was observed at 24 h post-blast. In the case of triple blast exposures, the ATP levels decreased by 44.6% and 27.7% by 6 h and 24 h, respectively.

ATP levels decreased in the cerebral cortex after blast exposures

Figure 2 shows the changes in ATP levels in the mouse brain cortex at different intervals after single and repeated blast exposures. Similar to the *in vitro* results, blast exposure of mice also resulted in a decrease in brain ATP levels, which varied relative to the time and number of blast exposures. Single blast exposure resulted in a 19.5% decrease in ATP levels at 6 h, whereas triple blasts resulted in a 23.4% decrease as early as 1 h. ATP levels were decreased by 39.7% at 6 h after repeated blast exposures, whereas the decrease was only 11.8% at 24 h post-blast. Thus, compared with by 6 h post-blast, the ATP levels were higher in the brain by 24 h post-blast but still lower than the sham controls which were not exposed to blast.

Proteomic analysis of the cerebral cortex to identify modulation of GOT_2 expression

Proteomic analysis data showed few proteins with >2 fold change in the cerebral cortex at 6 h after triple blast exposures. The proteins which showed >2 fold increase in expression after blast exposure include 14-3-3 protein gamma, calretinin, parvalbumin alpha, 14-3-3 protein zeta/delta, and calpastatin. One of the down-regulated proteins was identified by LC/MS/MS analysis as GOT_2 by matching five peptides. Figure 3 shows the image of the 2D-gel portion showing the expression of GOT_2 in the cortex after repeated blast exposures. GOT_2 expression showed a statistically significant abundance ratio (3.13 ± 0.76) between sham control and blast exposed mice suggesting that blast exposure alters the expression of GOT_2.

Western blotting of GOT_2 and PDH in the cerebral cortex after blast exposure

Western blotting using antibodies specific to GOT_2 showed a significant decrease (47.9%) in the expression of GOT_2 in the

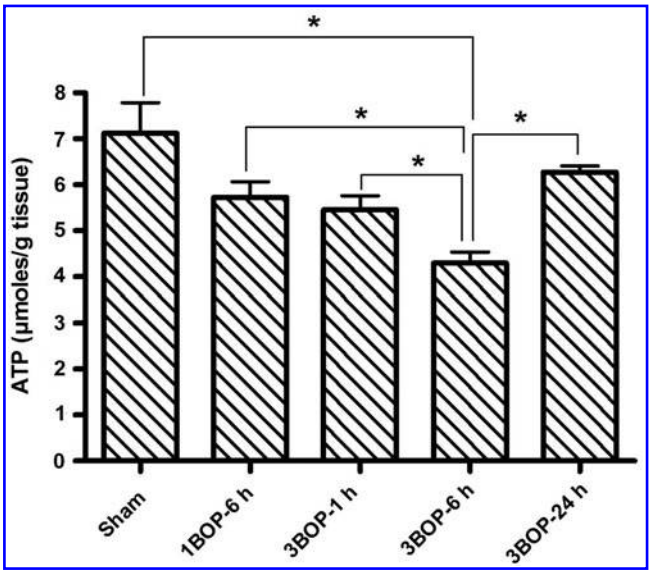

FIG. 2. Changes in adenosine triphosphate levels in cerebral cortex at different intervals after single and repeated blast exposures. Values are expressed as mean ± standard deviation. $*p < 0.05$ ($n = 6$). BOP, blast overpressure exposure.

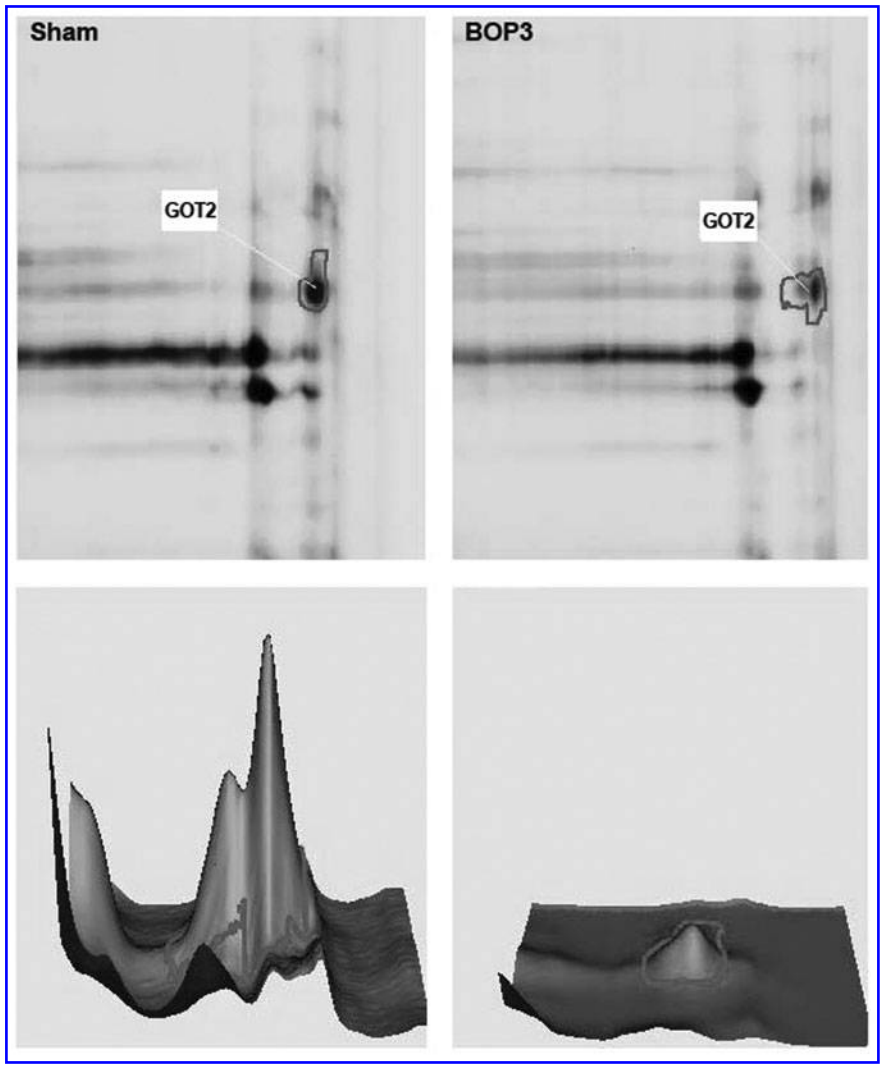

FIG. 3. Representative two-dimensional differential in-gel electrophoresis figure from three different animals in the sham control and blast exposed groups focusing the spot of glutamate oxaloacetate transaminase. Procedures used are detailed in the methods section. The bottom two panels show the sum of pixel intensities within the boundary of each spot in the fluorescent image to demonstrate the level of the protein.

cerebral cortex at 6 h after triple blast exposures, compared with sham controls (Fig. 4A). The ratio of GOT_2 to actin was 0.161 ± 0.025 for sham controls, whereas the ratios were 0.084 ± 0.028 for 6 h ($p = 0.021$) and 0.142 ± 0.036 for 24 h ($p = 0.44$; Fig. 4B). Compared with sham controls, single blast exposure at 6 h and triple blast exposure at 1 h, respectively, showed 20% (ratio of GOT_2 to actin was 0.124 ± 0.016, $p = 0.032$) and 29.9% (ratio of GOT_2 to actin was 0.113 ± 0.032, $p = 0.036$) decreases in the expression of GOT_2 in the cortex. Thus, similar to the reduction in ATP levels, the expression of GOT_2 decreased in the cerebral cortex after blast exposure. The decrease in GOT_2 expression depended upon the number of blast exposures, as well as the time after blast exposure; lowest expression was recorded at 6 h and returned toward normal levels by 24 h post-blast.

Western blotting of PDH with specific antibodies (Fig. 4A, C) showed significant decreases in the cerebral cortex at 6 h post-blast exposure. The decrease in the PDH level does not seem to correlate with ATP levels at 24 h after blast exposure.

Cerebral cortex mitochondrial GOT_2 activity after blast exposure

To determine further that the cerebral cortex mitochondrial GOT_2 activity was indeed decreased after blast exposure, the mitochondrial fraction was isolated from the cerebral cortex to avoid interference from the cytosolic isoform, GOT_1. Disrupted mitochondrial sample was used for measuring GOT_2 activity as described in the methods. The activity of GOT_2 in the mitochondrial fraction showed a 28.8 % decrease at 1 h and a 41.4 % decrease at 6 h after triple blast exposures. No significant changes in mitochondrial GOT_2 activity were observed at 24 h post-blast (Fig. 5).

Discussion

Our results show for the first time in an animal model that blast exposure leads to an acute mitochondrial dysfunction and an associated significant decrease in ATP levels in the brain. After a rapid decrease, the brain ATP levels return toward normal levels at 24 h post-blast exposures. Using the *in vitro* model of blast-induced

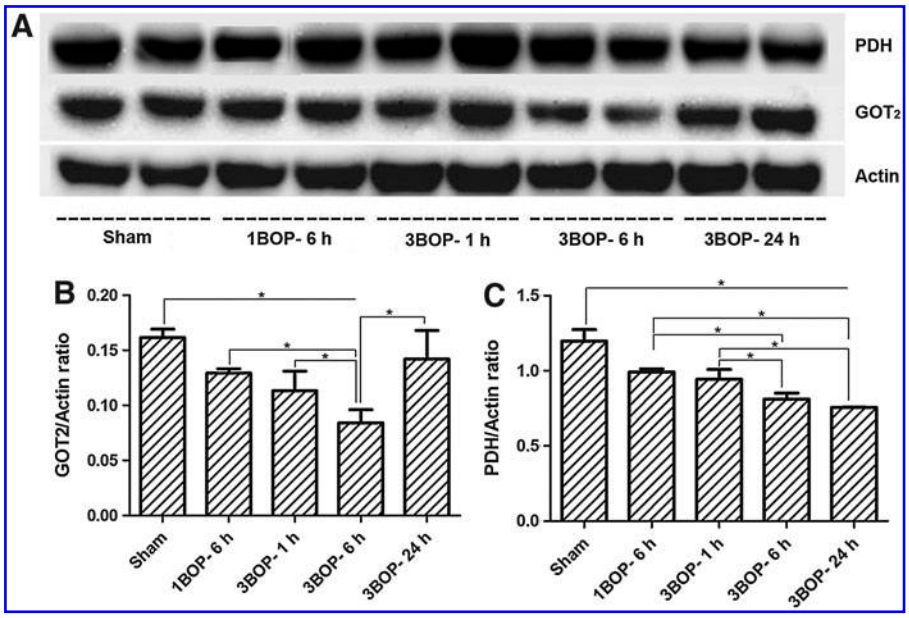

FIG. 4. Western blotting analysis of mice cerebral cortex at different intervals after single and repeated blast exposures. **(A)** Representative figure of the blot obtained from two animals each out of four animals in different groups studied. **(B)** Ratio of the band intensities corresponding to glutamate oxaloacetate transaminase and actin. Values are mean ± standard deviation (*$p < 0.05$, $n = 4$). **(C)** Ratio of the band intensities corresponding to PDH and actin. Values are mean ± standard deviation (*$p < 0.05$, n = 4).

TBI with NG108–15 cells (combination of neuroblastoma and glioblastoma cells), we have shown in a previous study that ATP levels decrease at 24 h after blast exposure.[17] Time points earlier than 24 h were not evaluated in that study. In the current study, we observed that a decrease in ATP levels after blast exposure occurs immediately and was most pronounced at 6 h, compared with at 24 h, indicating severe neuronal mitochondrial dysfunction acutely after blast exposure. The changes in ATP levels after blast exposure were similar *in vitro* and *in vivo*.

Acute mitochondrial dysfunction in the brain has been reported in different animal models of TBI.[18,20–22] Unlike blast-induced TBI, the mitochondrial dysfunction and associated decrease in ATP levels persisted for longer durations in the other forms of TBI. In a controlled cortical impact model of TBI, the ATP levels ipsilateral to the injury were only about 22 % of sham control even after six days post-injury.[18] In that study, the ATP levels measured ipsilaterally may have been associated with significant cell/tissue loss and the cells adjacent to the site of injury might have been undergoing necrosis/apoptosis. In the present study, we have shown that mitochondrial dysfunction and impaired energy production in the brain after blast exposure takes place acutely and the energy levels return toward normal levels by 24 h post-blast. This could be due to the lack of significant tissue loss in the brain after blast exposure. [3] Since delayed neuronal degeneration occurs after blast exposure,[1] it is possible that there could be a secondary phase of mitochondrial dysfunction after blast exposure, which would become evident several days post-exposure.

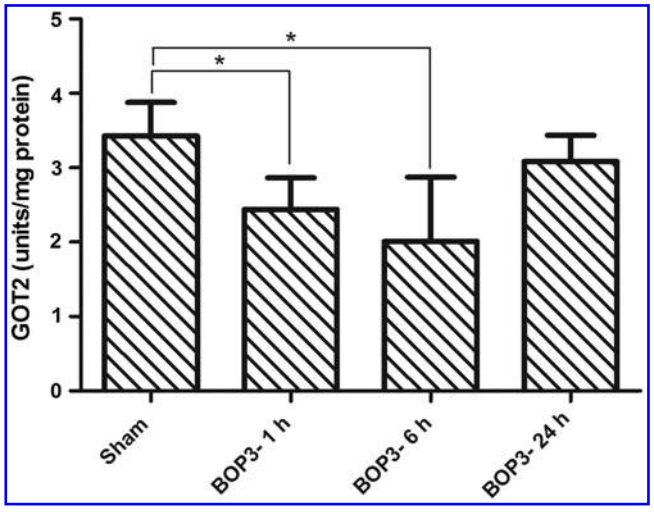

FIG. 5. Activity of glutamate oxaloacetate transaminase in the mitochondrial fraction of mice cerebral cortex at different intervals after repeated blast exposures. Values are mean ± standard deviation (*p < 0.05, $n = 6$).

In the present study, we found a correlation between the decrease in brain ATP levels and the reduced expression/activity of mitochondrial GOT_2. The protein expression and activity of GOT_2 were lowest in the brain at 6 h post-blast and were associated with the maximum decrease in ATP levels. The GOT_2 levels returned to almost normal by 24 h and the ATP level also was significantly restored. These data suggest a potential role of GOT_2 in the acute brain mitochondrial dysfunction associated with blast exposure. Detailed study is required to find out whether the synthesis or degradation of GOT_2 in the brain is affected after blast exposure. Using the same model system, it has been reported that modest levels of neuronal cell death occur immediately after repeated blast exposures, which also could contribute to the decreased tissue levels of ATP and GOT_2 measured after blast exposure.[3] The documented proliferation of astrocytes and microglia in the brain at 24 h after repeated blast exposure[11] can similarly contribute to the apparent recovery of ATP and GOT_2 by 24 h after repeated blast exposures.

A significant role for PDH in mitochondrial dysfunction after TBI has been reported in different brain injury models other than

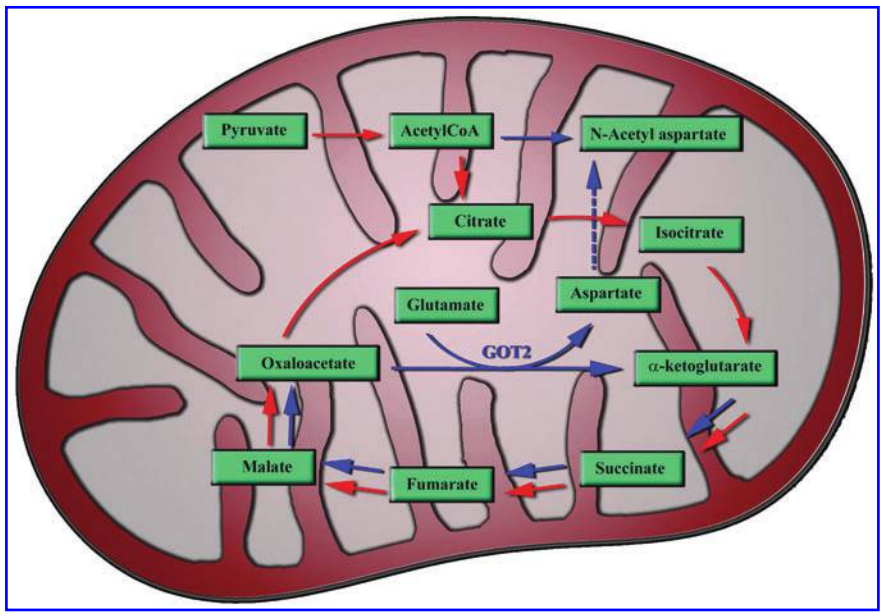

FIG. 6. Schematic representation of the neuronal mitochondria showing the proposed ''mini citric acid cycle'' involving glutamate oxaloacetate transaminase. Red arrow shows the regular citric acid cycle pathway and the blue arrow shows the ''mini citric acid cycle.'' Most of the energy producing steps is in the ''mini citric acid cycle.''

blast TBI.[23,24] Following controlled cortical impact (CCI) in rats, Opii and colleagues showed that PDH activity decreases in the cortex due to oxidative modification of the enzyme.[24] In another CCI study, the level of PDH decreased in the ipsilateral and contralateral sides of the brain at 4 h and decreased further by 24 h post-injury, similar to our present results following blast exposure.[25] Phosphorylation of PDH (p-PDH) has been implicated in the decrease of its activity in the CCI model.[25] After CCI injury, the ratio of p-PDH/PDH decreased at 4 h, increased at 24 h and decreased again at seven days indicating that the activity of PDH will be less at 24 h, compared with at 4 h and at seven days.[25] An imbalance in the activities of PDH kinase and PDH phosphatase in the brain has been implicated in the decreased activity of PDH after CCI.[26] A significant decrease in PDH also was observed in the brain at 72 h following fluid percussion injury, which was the single time point studied.[27] Our results in the blast TBI model also showed decreased expression of PDH, but did not show a direct correlation with the changes in ATP levels.

The potential role of GOT_2 in mitochondrial energy metabolism in the brain has been described earlier.[14,28–30] Figure 6 shows the schematic representation of the role of GOT_2 in brain energy metabolism involving the ''mini citric acid cycle,'' which was proposed by Yudkoff and colleagues in 1994.[16] Using radiolabeled aspartate and glutamine in brain synaptosomal preparations, Yudkoff and colleagues showed that amino acids could provide an alternate source of energy to help maintain ATP levels in the brain through ''mini citric acid cycle''.[16] They also found that in the brain synaptosomes, the fastest reaction that provides metabolite input to the citric acid cycle is that of GOT_2.[16] The ''mini citric acid cycle'' in the brain utilizes glutamine/glutamate for energy production instead of pyruvate, and bypasses a few initial steps in the regular citric acid cycle for faster energy production as required for neuronal activity.[14–16] As shown in the Figure 6, GOT_2 plays a major role in the truncated citric acid cycle. The excess aspartate formed through the ''mini citric acid cycle'' is used for N-acetyl aspartate (NAA) synthesis in the mitochondria,[14] which also explains the high concentrations of glutamate and NAA in the brain, where they are the most abundant molecules. By using GOT_2 to convert glutamate to α-ketogutarate, neurons avoid the formation of toxic ammonia, which is critical in the absence of a urea cycle in the brain.[14,28] Thus, GOT_2 plays a significant role in neuronal energy metabolism and its down regulation after blast exposure might contribute to the decreased ATP levels in the brain. Since low levels of ATP can significantly affect neuronal function, pharmaceutical interventions, which can rapidly restore or provide ATP rapidly to neurons, would potentially be beneficial after blast TBI. In this connection, supplementation to the brain of acetate, which can generate ATP, significantly increased brain ATP levels and improved motor performances in rats subjected TBI using CCI.[18]

Disclaimer

The contents, opinions and assertions contained herein are private views of the authors and are not to be construed as official or reflecting the views of the Department of the Army or the Department of Defense.

Acknowledgments

Support from Mrs. Irene Gist, Blast-induced Neurotrauma Branch, COL, Paul Bliese, Director, Center for Military Psychiatry and Neurosciences at the Walter Reed Army Institute of Research, and Mrs. Patricia Stroy is gratefully acknowledged.

Author Disclosure Statement

No competing financial interests exist

References

1. Magnuson, J., Leonessa, F., and Ling, G.S. (2012). Neuropathology of explosive blast traumatic brain injury. Curr. Neurol. Neurosci. Rep. 12, 570–579.

2. Warden, D. (2006). Military TBI during the Iraq and Afghanistan wars. J. Head Trauma Rehabil. 21, 398–402.
3. Wang, Y., Wei, Y., Oguntayo, S., Wilkins, W., Arun, P., Valiyaveettil, M., Song, J., Long, J., and Nambiar, M.P. (2011). Tightly coupled repetitive blast-induced traumatic brain injury: Development and Characterization in Mice. J. Neurotrauma 28, 2171–2183.
4. Duckworth, J.L., Grimes, J., and Ling G.S. (2013). Pathophysiology of battlefield associated traumatic brain injury. Pathophysiology 20, 23–30.
5. Kocsis, J.D., and Tessler, A. (2009). Pathology of blast-related brain injury. J. Rehabil. Res. Dev. 46, 667–672.
6. Saljo, A., Bao, F., Shi, J., Hamberger, A., Hansson, H.A., and Haglid, K.G. (2002). Expression of c-Fos and c-Myc and deposition of beta-APP in neurons in the adult rat brain as a result of exposure to short-lasting impulse noise. J. Neurotrauma 19,379–385.
7. Cernak, I., Wang, Z., Jiang, J., Bian, X., and Savic, J. (2001). Ultrastructural and functional characteristics of blast injury-induced neurotrauma. J. Trauma 50, 695–706.
8. Cernak, I., Wang, Z., Jiang, J., Bian, X., and Savic, J. (2001). Cognitive deficits following blast injury-induced neurotrauma: possible involvement of nitric oxide. Brain Inj. 15, 593–612.
9. Svetlov, S.I., Prima, V., Kirk, D.R., Gutierrez, H., Curley, K.C., Hayes, R.L., and Wang,. K.K. (2010). Morphologic and biochemical characterization of brain injury in a model of controlled blast overpressure exposure. J. Trauma 69, 795–804
10. Long, J.B., Bentley, T.L., Wessner, K.A., Cerone, C., Sweeney, S., and Bauman, R.A. (2009). Blast overpressure in rats: recreating a battlefield injury in the laboratory. J. Neurotrauma 26, 827–840.
11. Cernak, I., Merkle, A.C., Koliatsos, V.E., Bilik, J.M., Luong, Q.T., Mahota, T.M., Xu, L., Slack, N., Windle, D., and Ahmed, F.A. (2011). The pathobiology of blast injuries and blast-induced neurotrauma as identified using a new experimental model of injury in mice. Neurobiol. Dis. 41:538–551.
12. Arun, P., Abu-Taleb, R., Valiyaveettil, M., Wang, Y., Long, J.B., and Nambiar, M.P. (2012). Transient changes in neuronal cell membrane permeability after blast exposure. Neuroreport 23, 342–346.
13. Arun, P., Oguntayo, S., Alamneh, Y., Honnold, C., Wang, Y., Valiyaveettil, M., Long, J.B., and Nambiar, M.P. (2012). Rapid release of tissue enzymes into blood after blast exposure: potential use as biological dosimeters. PLoS One 7, e33798.
14. Moffett, J.R., Ross, B., Arun, P., Madhavarao, C.N., and Namboodiri, A.M. (2007). N-Acetylaspartate in the CNS: from neurodiagnostics to neurobiology. Prog. Neurobiol. 81, 89–131.
15. Erecinska, M., Zaleska, M.M., Nissim, I., Nelson, D., Dagani, F., and Yudkoff, M. (1988). Glucose and synaptosomal glutamate metabolism: studies with [15N]glutamate. J. Neurochem. 51, 892–902.
16. Yudkoff, M., Nelson, D., Daikhin, Y., and Erecinska, M. (1994). Tricarboxylic acid cycle in rat brain synaptosomes. Fluxes and interactions with aspartate aminotransferase and malate/aspartate shuttle. J. Biol. Chem. 269, 27414–27420.
17. Arun, P., Spadaro, J., John, J., Gharavi, R.B., Bentley, T.B., and Nambiar, M.P. (2011). Studies on blast traumatic brain injury using in-vitro model with shock tube. Neuroreport 22, 379–384.
18. Arun, P., Ariyannur, P.S., Moffett, J.R., Xing, G., Hamilton, K., Grunberg, N.E., Ives, J.A., and Namboodiri, A.M. (2010). Metabolic acetate therapy for the treatment of traumatic brain injury. J. Neurotrauma 27, 293–298.
19. Arun, P., Valiyaveettil., M., Biggemann., L., Alamneh., Y., Wei., Y., Oguntayo., S., Wang., Y., Long., J.B., and Nambiar, M.P. (2012). Modulation of hearing related proteins in the brain and inner ear following repeated blast exposures. Intervent. Med. Appl. Sci. 4, 125–131.
20. Signoretti, S., Marmarou, A., Tavazzi, B., Lazzarino, G., Beaumont, A., and Vagnozzi, R. (2001). N-Acetylaspartate reduction as a measure of injury severity and mitochondrial dysfunction following diffuse traumatic brain injury. J. Neurotrauma 18, 977–991.
21. Lee, S.M., Wong, M.D., Samii, A., and Hovda, D.A. (1999). Evidence for energy failure following irreversible traumatic brain injury. Ann. N. Y. Acad. Sci. 893, 337–340.
22. Tavazzi, B., Signoretti, S., Lazzarino, G., Amorini, A.M., Delfini, R., Cimatti, M., Marmarou, A., and Vagnozzi, R. (2005). Cerebral oxidative stress and depression of energy metabolism correlate with severity of diffuse brain injury in rats. Neurosurgery 56, 582–589.
23. Robertson, C.L., Saraswati, M., and Fiskum, G. (2007). Mitochondrial dysfunction early after traumatic brain injury in immature rats. J. Neurochem. 101, 1248–1257.
24. Opii, W.O., Nukala, V.N., Sultana, R., Pandya, J.D., Day, K.M., Merchant, M.L., Klein, J.B., Sullivan, P.G., and Butterfield, D.A. (2007). Proteomic identification of oxidized mitochondrial proteins following experimental traumatic brain injury. J. Neurotrauma 24, 772–789.
25. Xing, G., Ren, M., Watson, W.D,, O'Neill, J.T., and Verma, A. (2009). Traumatic brain injury-induced expression and phosphorylation of pyruvate dehydrogenase: a mechanism of dysregulated glucose metabolism. Neurosci. Lett. 454, 38–42.
26. Xing, G., Ren, M., O'Neill, J.T., Verma, A., and Watson, W.D. (2012). Controlled cortical impact injury and craniotomy result in divergent alterations of pyruvate metabolizing enzymes in rat brain. Exp. Neurol. 234, 31–38.
27. Sharma, P., Benford, B., Li, ZZ., and Ling, G.S. (2009). Role of pyruvate dehydrogenase complex in traumatic brain injury and Measurement of pyruvate dehydrogenase enzyme by dipstick test. J. Emerg. Trauma Shock 2, 67–72.
28. Madhavarao, C.N., Namboodiri, A.M. (2006). NAA synthesis and functional roles. Adv. Exp. Med. Biol. 576, 49–66.
29. Madhavarao, C.N., Arun, P., Moffett, J.R., Szucs, S., Surendran, S., Matalon, R., Garbern, J., Hristova, D., Johnson, A., Jiang, W., and Namboodiri, M.A. (2005). Defective N-acetylaspartate catabolism reduces brain acetate levels and myelin lipid synthesis in Canavan's disease. Proc. Natl. Acad. Sci. U S A 102, 5221–5226.
30. Madhavarao, C.N., Chinopoulos, C., Chandrasekaran, K., Namboodiri, M.A. (2003). Characterization of the N-acetylaspartate biosynthetic enzyme from rat brain. J. Neurochem. 86, 824–835.

Address correspondence to:
Peethambaran Arun, PhD
Blast-Induced Neurotrauma Branch
Center for Military Psychiatry and Neurosciences
Walter Reed Army Institute of Research
Silver Spring, MD 20910

E-mail: peethambaran.arun.ctr@mail.mil

This article has been cited by:

1. G. Mahmood, Z. Mei, H. Hojjat, E. Pace, S. Kallakuri, J.S. Zhang. 2014. Therapeutic effect of sildenafil on blast-induced tinnitus and auditory impairment. *Neuroscience* **269**, 367-382. [CrossRef]
2. Matthew Boyko, Shaun E. Gruenbaum, Benjamin F. Gruenbaum, Yoram Shapira, Alexander Zlotnik. 2014. Brain to blood glutamate scavenging as a novel therapeutic modality: a review. *Journal of Neural Transmission* . [CrossRef]
3. Ana Paula Oliveira Ferreira, Fernanda Silva Rodrigues, Iuri Domingues Della-Pace, Bibiana Castagna Mota, Sara Marchesan Oliveira, Camila de Campos Velho Gewehr, Franciane Bobinski, Clarissa Vasconcelos de Oliveira, Juliana Sperotto Brum, Mauro Schneider Oliveira, Ana Flavia Furian, Claudio Severo Lombardo de Barros, Juliano Ferreira, Adair Roberto Soares dos Santos, Michele Rechia Fighera, Luiz Fernando Freire Royes. 2013. The effect of NADPH-oxidase inhibitor apocynin on cognitive impairment induced by moderate lateral fluid percussion injury: Role of inflammatory and oxidative brain damage. *Neurochemistry International* . [CrossRef]

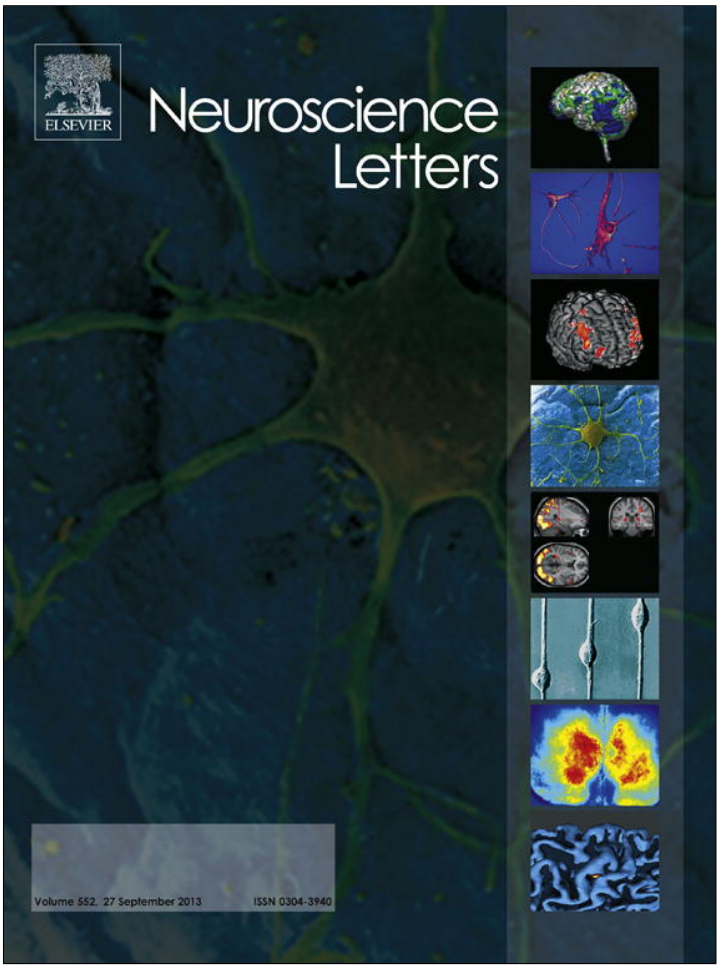

Neuroscience Letters 552 (2013) 87–91

Contents lists available at ScienceDirect

Neuroscience Letters

journal homepage: www.elsevier.com/locate/neulet

Distinct patterns of expression of traumatic brain injury biomarkers after blast exposure: Role of compromised cell membrane integrity

Peethambaran Arun[a,*], Rania Abu-Taleb[a], Samuel Oguntayo[a], Mikiei Tanaka[b], Ying Wang[a], Manojkumar Valiyaveettil[a], Joseph B. Long[a], Yumin Zhang[b], Madhusoodana P. Nambiar[a]

[a] Blast-Induced Neurotrauma Branch, Center for Military Psychiatry and Neurosciences, Walter Reed Army Institute of Research, 503 Robert Grant Avenue, Silver Spring, MD 20910, USA
[b] Department of Anatomy, Physiology and Genetics, Uniformed Services University of the Health Sciences, 4301 Jones Bridge Road, Bethesda, MD 20814, USA

HIGHLIGHTS

- Repeated blast exposures causes acute decrease in GFAP and *Tau* in brain and plasma.
- GFAP and *Tau* levels increases acutely in the liver and spleen after blast exposure.
- No acute changes in GFAP and *Tau* mRNA levels in the liver after blast exposure.
- The acute changes in GFAP and *Tau* suggest blast-induced cell membrane disruption.

ARTICLE INFO

Article history:
Received 29 May 2013
Received in revised form 17 July 2013
Accepted 27 July 2013

Keywords:
Blast exposure
Cell membrane integrity
GFAP
Tau
Polytrauma

ABSTRACT

Glial fibrillary acidic protein (GFAP), a protein enriched in astrocytes, and *Tau*, a protein abundant in neuronal microtubules, are being widely studied as biomarkers of brain injury, and persistent severity-dependent increases in brain and blood have been reported. Studies on the acute changes of these proteins after blast exposure are limited. Using a mouse model of closely-coupled repeated blast exposures, we have evaluated acute changes in the levels of GFAP and total *Tau* by Western blotting. Brain levels of GFAP and *Tau* proteins decreased significantly at 6 h and increased considerably at 24 h after repeated blast exposures. Plasma samples showed a similar initial decrease and later increase over this timeframe. This biphasic pattern points to possible absorption or sequestration of these proteins from plasma immediately after repeated blast exposures. Liver and spleen tissue showed significant increases in the levels of GFAP and *Tau* protein at 6 and 24 h post-blast exposures whereas semi-quantitative RT-PCR analysis of liver showed no significant changes in the levels of GFAP or *Tau* mRNAs. These results suggest that blast exposure causes transient changes in cell membrane integrity in multiple organs leading to abnormal migration of proteins from the tissues to the plasma and *vice versa*. This transient changes in cell membrane permeability and subsequent bidirectional movement of molecules may contribute to the pathophysiology of TBI and polytrauma after blast exposure.

1. Introduction

The incidence of traumatic brain injury (TBI) increased tremendously during the recent wars and exposure to blast from improvised explosive devices has been reported as the major cause of battlefield TBI and associated disabilities in service members [14]. One of the major differences between blast-induced TBI and other closed head or penetrating brain injuries is that blast exposure concomitantly injures other organs of the body, especially air filled organs, resulting in polytrauma. Military personnel are subject to both high intensity single or low intensity repeated blast exposures, and we have previously reported that the severity of brain injury increases with number of blast exposures [27].

Identification of sensitive and specific biomarkers of TBI is potentially useful for the diagnosis of injury and evaluation of the efficacy of therapies. Although no biomarkers unique to blast-induced TBI have been reported in clinical or pre-clinical blast exposure studies to date, several brain proteins that are being

Abbreviations: TBI, traumatic brain injury; GFAP, glial fibrillary acidic protein; BOP, blast overpressure; CSF, cerebrospinal fluid; mRNA, messenger ribonucleic acid; RT-PCR, reverse transcription-polymerase chain reaction.

* Corresponding author. Tel.: +1 301 319 2009; fax: +1 301 319 9839.
E-mail addresses: peethambaran.arun.ctr@mail.mil, peethambaran.arun@us.army.mil (P. Arun).

0304-3940/$ – see front matter © 2013 Elsevier Ireland Ltd. All rights reserved.
http://dx.doi.org/10.1016/j.neulet.2013.07.047

widely evaluated as biomarkers of other forms of brain injury have also been considered as biomarkers of blast TBI. Notably, glial fibrillary acidic protein (GFAP), a protein enriched in astrocytes, and *Tau*, a protein abundant in neuronal microtubules has been monitored after various forms of brain injury including blast-induced TBI [4,7,10,22,24,25].

Changes in blood and cerebrospinal fluid (CSF) levels of GFAP have been widely studied as sensitive biomarkers for the diagnosis TBI in humans [5,9,13,19,21,26,28] and significant up-regulation of GFAP levels in multiple regions of the brain has also been reported at different intervals after blast exposure in animal models of blast-induced TBI [4,7,10,24]. In all these pre-clinical studies, the changes in GFAP were evaluated after 24 h post-exposure. Changes in GFAP levels in the brain or body fluids immediately after single blast exposure have not been well documented. Besides, there are no studies addressing the effects on GFAP levels in the brain or blood after repeated blast exposures.

Apart from GFAP, up-regulation of total and phosphorylated *Tau* proteins have also been shown in the brain, CSF and blood of patients with different forms of TBI, and hence these proteins have been proposed as reliable biomarkers of outcome after TBI [11,15,20,23]. Total and phosphorylated *Tau* proteins in the brain were significantly increased in different animal models of TBI [7,11,22,25]. Limited studies have been carried out to assess the changes in total or phosphorylated *Tau* proteins in the brain or body fluids after blast exposure and there are no such studies after repeated blast exposures. Similar to studies evaluated GFAP levels, the differential expression of *Tau* protein was determined only at 24 h or later in single blast exposure and no studies so far investigated the acute changes in *Tau* proteins after repeated blast exposures.

In the present study, we assessed immediate changes in GFAP and total *Tau* protein in the brains and plasma of mice after closely coupled repeated blast overpressure exposures in a shock tube as described earlier [27]. Western blotting with specific antibodies was used to assess the levels of these potential blast injury biomarkers. Our results after repeated blast exposures showed an initial decrease and later increase in the levels of both GFAP and total *Tau* proteins in the brain and plasma. We further explored the potential mechanism of the contrasting changes in the two biomarkers of TBI after repeated blast exposures.

2. Materials and methods

2.1. Animals and blast exposures

All animal experiments were conducted in accordance with the Animal Welfare Act and other federal statutes and regulations relating to animals and experiments involving animals and adhered to principles stated in the Guide for the Care and Use of Laboratory Animals (NRC Publication 1996 edition). The animal protocol was approved by Institutional Animal Care and Use Committee, Walter Reed Army Institute of Research. C57BL/6J male mice (8–10 weeks old) that weighed between 21 and 26 g (Jackson Laboratory, Bar Harbor, ME) were used in this study. A compressed air-driven shock tube described earlier [12,27] was used for repeated blast exposures. Mice were anesthetized with 4% isoflurane gas (O_2 flow rate 1.5 L/min) for 8 min and restrained in the prone position with a tautly-drawn net to minimize the movements during blast exposure. Animals were subjected to three blast overpressure (BOP) exposures (21 psi) separated by 1 and 30 min as described earlier [28]. Blood plasma, brain, liver and spleen were collected after euthanasia at 6 or 24 h post-blast and frozen immediately. Cerebellum, which showed significant injury after blast exposure in previous studies [27] was dissected out immediately before freezing the brain.

2.2. Western blot analysis of tissue homogenates

Tissue homogenates (20%, w/v) were prepared in tissue protein extraction buffer (Pierce Chemical Co., Rockford, IL) containing protease and phosphatase inhibitor cocktails (Sigma–Aldrich, St. Louis, MO) using an ultrasonic homogenizer. The homogenates were centrifuged at $5000 \times g$ for 5 min at 4 °C and 2 μl each of supernatants were used for Western blotting. Rabbit polyclonal antibodies against GFAP and total *Tau* protein were obtained from Abcam (Cambridge, MA) and Santa Cruz Biotechnologies (Santa Cruz, CA), respectively. GFAP antibody was used at a dilution of 1:40,000 and an antibody to total *Tau* proteins was used at 1:1000 dilution. Secondary antibody labeled with horse-radish peroxidase (HRP) was also purchased from Santa Cruz Biotechnology and used at a dilution of 1:2500. A mouse monoclonal antibody to β-actin conjugated with HRP (Sigma–Aldrich, St. Louis, MO) was used as gel loading control at a dilution of 1:40,000. SDS–polyacrylamide gel electrophoresis and Western blotting analysis of protein extracts from cerebellum, liver and spleen was carried out as described earlier [3]. After Western blotting, the protein bands were detected using ECL-Plus Western blot detection reagent (GE Healthcare, Piscataway, NJ) and the chemiluminescence was imaged in an AlphaImage reader (Cell Biosciences, Santa Clara, CA). The band intensity was measured by densitometry using AlphaView software (Cell Biosciences, Santa Clara, CA).

2.3. Western blotting of GFAP and tau proteins in the plasma

Plasma was purified by removing albumins and globulins using ProteoExtract Albumin/IgG removal kit from EMD-Millipore Corporation (Chicago, IL) according to manufacturer's instructions. Briefly, 850 μl of binding buffer was allowed to pass through the column by gravity-flow. Plasma (35 μl) was diluted 10-fold with binding buffer, allowed to pass through the column and the flow-through was collected. The unbound proteins were also collected by passing 650 μl of binding buffer though the column twice. The collected flow-through fractions were pooled and concentrated using a 3000 MW cut off VIVASPIN 500 centrifugal filters (Sartorius Stedim, Bohemia, NY) according to manufacturer's instructions. Concentrated albumin and globulin free fractions corresponding to 5 μl of original plasma were used for Western blotting as described above.

2.4. Semi-quantitative RT-PCR analysis of liver tissue

Frozen mouse liver tissue was thawed and homogenized by pipetting with 1 ml of TRIzol reagent (Life Technologies, Grand Island, NY). Total RNA was isolated according to manufacturer's protocol. For cDNA synthesis, total RNA (1 μg) was subjected to reverse transcription in a reaction mixture containing dNTPs (0.5 mM), random hexamer primer (0.01 μg/μl), and 40 U of RNase inhibitor (Thermo Scientific, Waltham, MA) and RNasin (Promega Corporation, Madison, WI) for 45 min at 50 °C. Using premix PCR mixture (Thermo Scientific, Waltham, MA), PCR was performed in the presence of 0.33 μM of gene specific primers and 0.5 μl of cDNA in thermal cycler as follows; 95 °C × 1 min, followed by 35 cycles of 95 °C × 30 s, 61 °C × 30 s, 72 °C × 30 s, subsequently 72 °C × 5 min. Primers for GFAP were 5′-CTGGCTGCGTATAGACAGGA-3′ as forward, 5′-GAACTGGATCTCCTCCTCCA-3′ as reverse, and primers for *Tau* were 5′-GTGGAGGCAGTGTGCAAATA-3′ as forward, 5′-GCCAATCTTCGACTGGACTC-3′ as reverse. Aliquots were loaded and electrophoresed in 2% agarose gel. PCR product was visualized with ethidium bromide under UV illuminator and the image was captured using GeneSnap software (Syngene, Frederick, MD). Brain tissue from sham control mice was used as positive control.

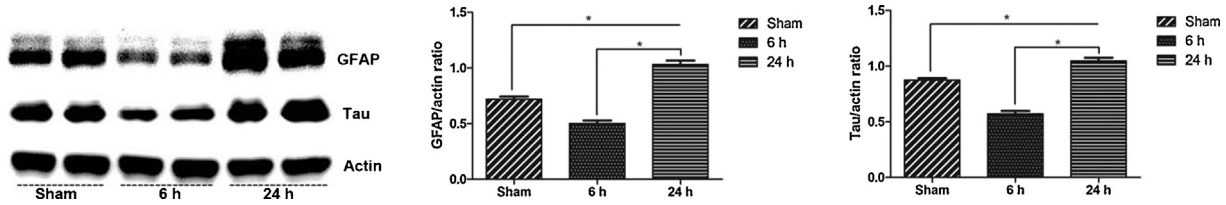

Fig. 1. Western blot analysis of the cerebellum showing the immediate decrease and later increase in the levels of GFAP and *Tau* proteins after repeated blast exposures. Representative blot from two out of four animals in each group is presented. Densitometry analysis was carried out as described in Section 2. $^{*}p < 0.01$ ($n = 4$).

2.5. Statistical analysis

Statistical analysis was carried out by analysis of variance (ANOVA) using SAS software version 9.3. Values were expressed as mean ± standard deviation (SD). A p value less than 0.01 was considered significant.

3. Results

3.1. Changes in GFAP and total Tau protein expression in the brain after blast exposure

Western blot analyses of the cerebellum revealed biphasic time-dependent changes in the expression of both GFAP and total *Tau* proteins after repeated blast exposures (Fig. 1). The levels of these proteins decreased significantly at 6 h and increased appreciably at 24 h after repeated blast exposures. Densitometry analysis indicated that the ratios of GFAP to actin as well as total *Tau* to actin were significantly reduced at 6 h and increased considerably at 24 h after repeated blast exposures.

3.2. Levels of GFAP and total Tau proteins in the plasma after blast exposure

Similar to the brain, biphasic changes in the levels of both GFAP and total *Tau* proteins were recorded in the plasma after repeated blast exposures (Fig. 2). Densitometry of the Western blot showed that plasma levels of GFAP as well as total *Tau* proteins were significantly reduced at 6 h and increased at 24 h after repeated blast exposures.

3.3. Levels of GFAP and total Tau proteins in the liver and spleen after blast exposure

GFAP and total *Tau* proteins were readily detected in the liver and spleen of sham control mice. Densitometry analysis and the ratios of GFAP to actin as well as total *Tau* protein to actin indicated a significant increase in the levels of both GFAP and total *Tau* proteins in the liver and spleen at 6 and 24 h after blast repeated exposures (Fig. 3). Compared to 6 h, the increase in the levels of both GFAP and total *Tau* proteins at 24 h was marginal and was not statistically significant in both tissues.

3.4. Expression of GFAP and Tau mRNA levels in the liver after blast exposure

To investigate whether the increase in GFAP and *Tau* proteins in the liver is due to increased synthesis, RT-PCR of liver tissue mRNA was performed and showed the presence of products with the same base pairs corresponding to GFAP and *Tau* proteins in the brain. Semi-quantitative RT-PCR analysis of liver tissues indicated that the levels of GFAP or *Tau* mRNAs were not increased significantly at 6 or 24 h after repeated blast exposures (Fig. 4).

4. Discussion

Our results showed for the first time that repeated blast exposures caused pronounced biphasic changes in two well-known biomarkers of TBI in the brain and plasma. In the brain and plasma, the levels of GFAP and total *Tau* proteins decreased significantly at 6 h after repeated blast exposures, whereas their levels were increased at 24 h post-blast exposures. The increase in the expression of GFAP at 24 h after blast exposure is in agreement with the previous preclinical studies [4,24]. To our knowledge, no studies have established this acute change in GFAP in the brain or plasma after single or repeated blast exposures. In the case of *Tau* protein, measured changes in total or phosphorylated *Tau* have been restricted to several days after single blast exposure [7,10].

The significant decrease in GFAP and Tau proteins in the brain at 6 h after repeated blast exposures was an unanticipated and somewhat paradoxical result. Since the turnover of GFAP and *Tau* proteins in the brain is very slow [6,16], the acute decrease in GFAP/Tau in the brain after blast exposure can most likely be interpreted as a blast-induced rapid disruption of glial/neuronal cell membranes and protein leakage across a disrupted blood–brain barrier into the circulation. However, Western blotting of plasma showed a similar significant decrease in the levels of both the proteins at 6 h after repeated blast exposures (Fig. 2). Parallel decreases of both putative biomarkers in brain and plasma shortly after blast exposure points to their rapid redistribution or elimination from the blood during this acute timeframe.

Using an *in vitro* model of blast-induced TBI, it has recently been shown that blast exposure causes transient disruption of neuronal cell membrane integrity leading to bidirectional movement of molecules across the cell membrane [1]. Rapid disruption of cell membrane integrity of liver cells and muscle fibers and the

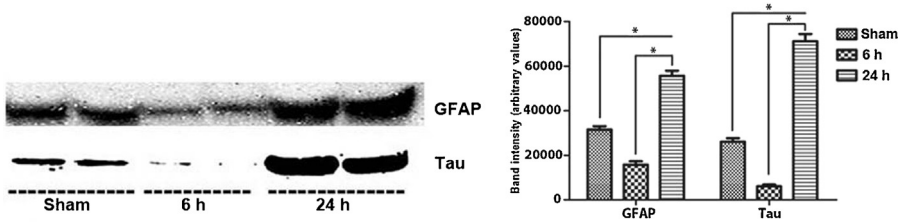

Fig. 2. Western blot analysis of plasma showing the immediate decrease and later increase in the levels of GFAP and *Tau* proteins after repeated blast exposures. Representative blot from two out of four animals in each group is presented. Densitometry analysis was carried out as described in Section 2.$^{*}p < 0.01$ ($n = 4$).

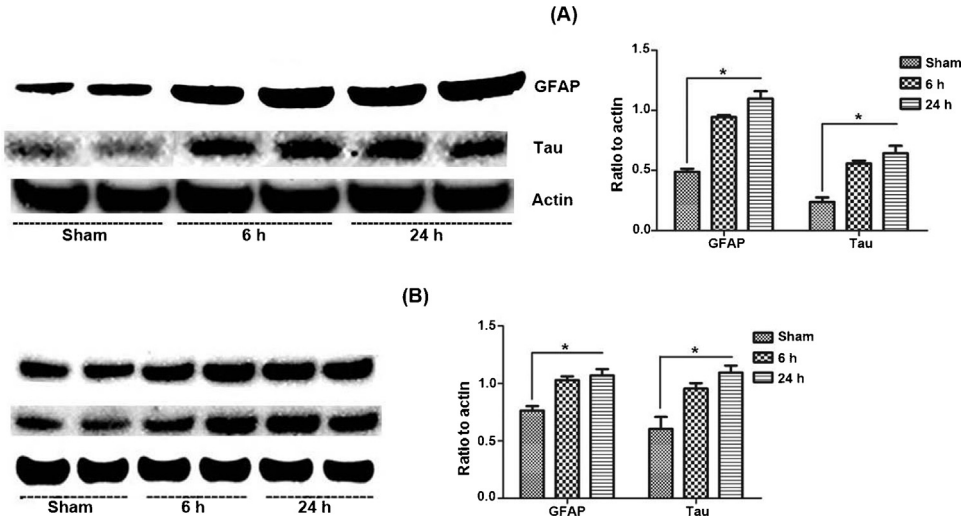

Fig. 3. Western blot analysis of liver (A) and spleen (B) showing the levels of GFAP and *Tau* proteins at 6 and 24 h after repeated blast exposures. Representative blots from two out of four animals in each group for liver and spleen are presented. Densitometry analysis was carried out as described in Section 2.*$p < 0.01$ ($n = 4$).

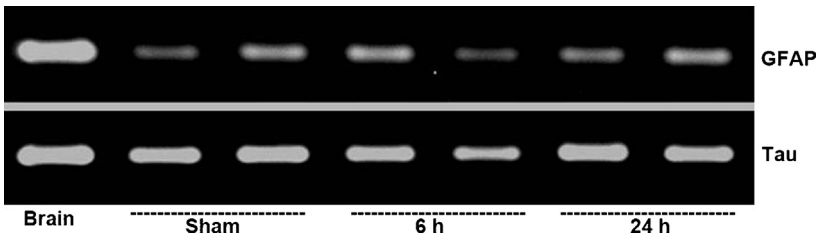

Fig. 4. Semi-quantitative RT-PCR analysis of liver showing the mRNA levels of GFAP and Tau proteins. Total RNA isolated from the brain of a sham control mice was used as positive control. RT-PCR was carried out as described in the methods section. Representative figure from two out of four animals in each group is presented.

subsequent release of organ specific cellular proteins into the circulation after repeated blast exposures have also been reported [2]. Collectively, these data suggest that blast exposure affects the cell membrane integrity of brain and peripheral organs which can lead to widespread bidirectional passage of molecules. The various potential mechanisms of cell membrane disruption after blast exposure have been described in detail by Nakagawa et al. [18].

The parallel decreased levels of GFAP/*Tau* proteins in the brain and plasma at 6 h after repeated blast exposures suggests a possible shift and accumulation of these proteins in peripheral organs. Liver is one of the largest organs of the body and it showed blast overpressure-dependent release of enzyme to circulation, revealing cell membrane disruption [2]. Based upon earlier studies of liver after blast exposure and the expression of GFAP and *Tau* proteins in this organ [2,8,17], we investigated blast-induced changes in the levels of these proteins in the liver. We also examined the spleen, which is a primary component of the reticuloendothelial system where the blood is being processed. Increased levels of GFAP and *Tau* in both the liver and spleen coincided with their simultaneously decreased levels in the brain and plasma at 6 h after repeated blast exposures. To investigate whether their increased levels resulted from locally increased synthesis, we measured the mRNA levels of GFAP and *Tau* proteins in the liver. The semi-quantitative RT-PCR analysis data showed no significant increase in the mRNA levels of GFAP and *Tau* proteins in the liver. These data reinforce the conclusion that these proteins transiently accumulate in these organs following passage from the circulation after repeated blast exposures.

Although GFAP and Tau proteins remained elevated in the liver and spleen after blast exposure, there was no significant difference in the levels at 24 h compared to 6 h, even though the levels of these proteins increased substantially in the plasma at 24 h after the blast exposure. Restoration of vascular, liver, and spleen cell membrane integrity may have prevented further passage of these proteins in these organs. Previous studies using *in vitro* and *in vivo* models of blast-induced TBI indicate that the cell membrane disruption after blast exposure is transient and the restoration of cell membrane integrity take place rapidly [1,2].

A potential pathophysiological consequence of transient disruption of cell membrane integrity after blast exposure is the transport of foreign molecules, including proteins, which can enter various cells of peripheral organs and brain from the blood circulation and may remain intracellularly for longer time leading to chronic pathological changes. Furthermore, the essential molecules rapidly released from the cells due to transient disruption of cell membrane after blast exposure can also affect cellular homeostasis. Thus, the rapid abnormal bidirectional movement of molecules in the brain and peripheral organs immediately after blast exposure may have the possibility to trigger long-term consequences, a potential mechanism contributing to blast-induced polytrauma. These time-dependent bidirectional changes also point to a fundamental issue complicating and potentially limiting the utility of these circulating proteins as acute biomarkers of blast injury.

Disclosure

The contents, opinions and assertions contained herein are private views of the authors and are not to be construed as official or reflecting the views of the Department of the Army or the Department of Defense. The authors report no conflict of interest.

Acknowledgements

Support from Mrs. Irene Gist and COL Paul Bliese are appreciated. We also gratefully acknowledge the technical guidance from Drs. Angela Boutte and Jitendra Dave.

References

[1] P. Arun, R. Abu-Taleb, M. Valiyaveettil, Y. Wang, J.B. Long, M.P. Nambiar, Transient changes in neuronal cell membrane permeability after blast exposure, NeuroReport 23 (2012) 342–346.
[2] P. Arun, S. Oguntayo, Y. Alamneh, C. Honnold, Y. Wang, M. Valiyaveettil, J.B. Long, M.P. Nambiar, Rapid release of tissue enzymes into blood after blast exposure: potential use as biological dosimeters, PLoS ONE 7 (2012) e33798.
[3] P. Arun, M. Valiyaveettil, L. Biggemann, Y. Alamneh, Y. Wei, S. Oguntayo, Y. Wang, J.B. Long, M.P. Nambiar, Modulation of hearing related proteins in the brain and inner ear following repeated blast exposures, Interventional Medicine and Applied Science 4 (2012) 125–131.
[4] I. Cernak, A.C. Merkle, V.E. Koliatsos, J.M. Bilik, Q.T. Luong, T.M. Mahota, L. Xu, N. Slack, D. Windle, F.A. Ahmed, The pathobiology of blast injuries and blast-induced neurotrauma as identified using a new experimental model of injury in mice, Neurobiology of Disease 41 (2011) 538–551.
[5] E. Czeiter, S. Mondello, N. Kovacs, J. Sandor, A. Gabrielli, K. Schmid, F. Tortella, K.K. Wang, R.L. Hayes, P. Barzo, E. Ezer, T. Doczi, A. Buki, Brain injury biomarkers may improve the predictive power of the IMPACT outcome calculator, Journal of Neurotrauma 29 (2012) 1770–1778.
[6] S.J.DeArmond, Y.L. Lee, H.A. Kretzschmar, L.F. Eng, Turnover of glial filaments in mouse spinal cord, Journal of Neurochemistry 47 (1986) 1749–1753.
[7] L.E. Goldstein, A.M. Fisher, C.A. Tagge, X.L. Zhang, L. Velisek, J.A. Sullivan, C. Upreti, J.M. Kracht, M. Ericsson, M.W. Wojnarowicz, C.J. Goletiani, G.M. Maglakelidze, N. Casey, J.A. Moncaster, O. Minaeva, R.D. Moir, C.J. Nowinski, R.A. Stern, R.C. Cantu, J. Geiling, J.K. Blusztajn, B.L. Wolozin, T. Ikezu, T.D. Stein, A.E. Budson, N.W. Kowall, D. Chargin, A. Sharon, S. Saman, G.F. Hall, W.C. Moss, R.O. Cleveland, R.E. Tanzi, P.K. Stanton, A.C. McKee, Chronic traumatic encephalopathy in blast-exposed military veterans and a blast neurotrauma mouse model, Science Translational Medicine 4 (2012) 134ra60.
[8] Y. Gu, F. Oyama, Y. Ihara, Tau is widely expressed in rat tissues, Journal of Neurochemistry 67 (1996) 1235–1244.
[9] M. Honda, R. Tsuruta, T. Kaneko, S. Kasaoka, T. Yagi, M. Todani, M. Fujita, T. Izumi, T. Maekawa, Serum glial fibrillary acidic protein is a highly specific biomarker for traumatic brain injury in humans compared with S-100B and neuron-specific enolase, Journal of Trauma 69 (2010) 104–109.
[10] E. Kovesdi, A.B. Gyorgy, S.K. Kwon, D.L. Wingo, A. Kamnaksh, J.B. Long, C.E. Kasper, D.V. Agoston, The effect of enriched environment on the outcome of traumatic brain injury; a behavioral, proteomics, and histological study, Frontiers in Neuroscience 5 (2011) 42.
[11] P.C. Liliang, C.L. Liang, H.C. Weng, K. Lu, K.W. Wang, H.J. Chen, J.H. Chuang, Tau proteins in serum predict outcome after severe traumatic brain injury, Journal of Surgical Research 160 (2010) 302–307.
[12] J.B. Long, T.L. Bentley, K.A. Wessner, C. Cerone, S. Sweeney, R.A. Bauman, Blast overpressure in rats: recreating a battlefield injury in the laboratory, Journal of Neurotrauma 26 (2009) 827–840.
[13] K.M. Lumpkins, G.V. Bochicchio, K. Keledjian, J.M. Simard, M. McCunn, T. Scalea, Glial fibrillary acidic protein is highly correlated with brain injury, Journal of Trauma 65 (2008) 778–782.
[14] J. Magnuson, F. Leonessa, G.S. Ling, Neuropathology of explosive blast traumatic brain injury, Current Neurology and Neuroscience Reports 12 (2012) 570–579.
[15] N. Marklund, K. Blennow, H. Zetterberg, E. Ronne-Engstrom, P. Enblad, L. Hillered, Monitoring of brain interstitial total tau and beta amyloid proteins by microdialysis in patients with traumatic brain injury, Journal of Neurosurgery 110 (2009) 1227–1237.
[16] J.Morales-Corraliza, M.J. Mazzella, J.D. Berger, N.S. Diaz, J.H. Choi, E. Levy, Y. Matsuoka, E. Planel, P.M. Mathews, In vivo turnover of tau and APP metabolites in the brains of wild-type and Tg2576 mice: greater stability of sAPP in the beta-amyloid depositing mice, PLoS ONE 4 (2009) e7134.
[17] S. Morini, S. Carotti, G. Carpino, A. Franchitto, S.G. Corradini, M. Merli, E. Gaudio, GFAP expression in the liver as an early marker of stellate cells activation, Italian Journal of Anatomy and Embryology 110 (2005) 193–207.
[18] A. Nakagawa, G.T. Manley, A.D. Gean, K. Ohtani, R. Armonda, A. Tsukamoto, H. Yamamoto, K. Takayama, T. Tominaga, Mechanisms of primary blast-induced traumatic brain injury: insights from shock-wave research, Journal of Neurotrauma 28 (2011) 1101–1119.
[19] K. Nylen, M. Ost, L.Z. Csajbok, I. Nilsson, K. Blennow, B. Nellgard, L. Rosengren, Increased serum-GFAP in patients with severe traumatic brain injury is related to outcome, Journal of the Neurological Sciences 240 (2006) 85–91.
[20] M. Ost, K. Nylen, L. Csajbok, A.O. Ohrfelt, M. Tullberg, C. Wikkelso, P. Nellgard, L. Rosengren, K. Blennow, B. Nellgard, Initial CSF total tau correlates with 1-year outcome in patients with traumatic brain injury, Neurology 67 (2006) 1600–1604.
[21] L.E. Pelinka, A. Kroepfl, R. Schmidhammer, M. Krenn, W. Buchinger, H. Redl, A. Raabe, Glial fibrillary acidic protein in serum after traumatic brain injury and multiple trauma, Journal of Trauma 57 (2004) 1006–1012.
[22] E. Rostami, J. Davidsson, K.C. Ng, J. Lu, A. Gyorgy, J. Walker, D. Wingo, S. Plantman, B.M. Bellander, D.V. Agoston, M. Risling, A model for mild traumatic brain injury that induces limited transient memory impairment and increased levels of axon related serum biomarkers, Frontiers in Neurology 3 (2012) 115.
[23] C. Smith, D.I. Graham, L.S. Murray, J.A. Nicoll, Tau immunohistochemistry in acute brain injury, Neuropathology and Applied Neurobiology 29 (2003) 496–502.
[24] S.I. Svetlov, V. Prima, D.R. Kirk, H. Gutierrez, K.C. Curley, R.L. Hayes, K.K. Wang, Morphologic and biochemical characterization of brain injury in a model of controlled blast overpressure exposure, Journal of Trauma 69 (2010) 795–804.
[25] H.T. Tran, L. Sanchez, T.J. Esparza, D.L. Brody, Distinct temporal and anatomical distributions of amyloid-beta and tau abnormalities following controlled cortical impact in transgenic mice, PLoS ONE 6 (2011) e25475.
[26] P.E. Vos, B. Jacobs, T.M. Andriessen, K.J. Lamers, G.F. Borm, T. Beems, M. Edwards, C.F. Rosmalen, J.L. Vissers, GFAP S100B are biomarkers of traumatic brain injury: an observational cohort study, Neurology 75 (2010) 1786–1793.
[27] Wang, Y. Wei, S. Oguntayo, W. Wilkins, P. Arun, M. Valiyaveettil, J. Song, J. Long, M.P. Nambiar, Tightly coupled repetitive blast-induced traumatic brain injury: development and characterization in mice, Journal of Neurotrauma 28 (2011) 2171–2183.
[28] J. Zurek, M. Fedora, The usefulness of S100B, NSE GFAP, NF-H, secretagogin and Hsp70 as a predictive biomarker of outcome in children with traumatic brain injury, Acta Neurochirurgica (Wien) 154 (2012) 93–103.

Neuroscience Research 76 (2013) 98–100

Contents lists available at SciVerse ScienceDirect

Neuroscience Research

journal homepage: www.elsevier.com/locate/neures

Rapid communication

Extracellular cyclophilin A protects against blast-induced neuronal injury☆

Peethambaran Arun*, Rania Abu-Taleb, Manojkumar Valiyaveettil, Ying Wang, Joseph B. Long, Madhusoodana P. Nambiar

Blast-Induced Neurotrauma Branch, Center for Military Psychiatry and Neuroscience, Walter Reed Army Institute of Research, 503 Robert Grant Ave, Silver Spring, MD 20910, USA

ARTICLE INFO

Article history:
Received 19 December 2012
Received in revised form 21 February 2013
Accepted 27 February 2013
Available online 17 March 2013

Keywords:
Traumatic brain injury
blast exposure
cyclophilin A
SH-SY5Y cells
neuroprotection

ABSTRACT

Blast-induced traumatic brain injury (TBI) and subsequent neurobehavioral deficits are major disabilities suffered by the military and civilian population worldwide. Rigorous scientific research is underway to understand the mechanism of blast TBI and thereby develop effective therapies for protection and treatment. By using an *in vitro* shock tube model of blast TBI with SH-SY5Y human neuroblastoma cells, we have demonstrated that blast exposure leads to neurobiological changes in an overpressure and time dependent manner. Paradoxically, repeated blast exposures resulted in less neuronal injury compared to single blast exposure and suggested a potential neuroprotective mechanism involving released cyclophilin A (CPA). In the present study, we demonstrate accumulation of CPA in the culture medium after repeated blast exposures supporting the notion of extracellular CPA mediated neuroprotection. Post-exposure treatment of the cells with purified recombinant CPA caused significant protection against blast-induced neuronal injury. Furthermore, repeated blast exposure was associated with phosphorylation of the proteins ERK1/2 and *Bad* suggesting a potential mechanism of neuroprotection by extracellular CPA and may aid in the development of targeted therapies for protection against blast-induced TBI.

Blast-induced traumatic brain injury (blast TBI) is a principal cause of major disabilities associated with the recent conflicts in Iraq and Afghanistan (Cernak, 2010; Ling et al., 2009; Magnuson et al., 2012; Wang et al., 2011). After more than a decade of rigorous research, still the mechanisms of blast TBI and associated neuropathological and neurobehavioral deficits are not well understood. In addition to understanding the mechanism of injury, identification of endogenous neuroprotective mechanisms against blast TBI is vital for developing therapies and strategies for rehabilitation and recovery.

In vitro models of blast TBI provide a powerful tool to investigate the cellular, biochemical and molecular mechanisms of injury and also to identify putative biomarkers and targeted therapies. Using a compressed air-driven shock tube with neuronal cells, we have developed an *in vitro* model of blast TBI (Arun et al., 2011, 2012). Repeated blast exposures of SH-SY5Y human neuroblastoma cells decreased intracellular levels of cyclophilin A (CPA) (Arun et al., 2011). Unexpectedly, repeated blast exposures also resulted in less neuronal injury than single blast exposure suggesting a possibility that CPA released after blast exposure exerting neuroprotective actions (Arun et al., 2011). In the present study, we have further explored this putative endogenous neuroprotective mechanism against blast injury and tried to validate that extracellular CPA offers neuroprotection against blast exposure.

SH-SY5Y cells, a thrice cloned subline of the neuroblastoma cells SK-N-SH which was isolated from a human brain tumor, was used for this study. Under cell culture conditions, these cells will differentiate into mature neuronal phenotype. The cells were grown in Dulbecco's modified Eagle's medium containing B-27 serum-free supplement and penicillin/streptomycin (Life Technologies, Grand Island, NY). The cells were kept at 37 °C in a CO_2 incubator with 5% CO_2 and 95% air in a humidified atmosphere. Cells (4×10^4 cells/well) were grown on 96 well tissue culture Plates 24 h before blast exposure. On the day of blast exposure, the medium was removed from the wells and 360 μl of fresh medium was added to completely fill the wells. The plates were then sealed with gas permeable Mylar plate seal and the edges of the plates and seal were secured using sterile tapes before blast exposure as described earlier (Arun et al., 2011, 2012).

Culture plates containing the cells were exposed to single or repeated blasts using a compressed air-driven shock tube as described earlier (Arun et al., 2011, 2012). The blast overpressure (21.05 psi) which resulted in significant neurobiological changes in SH-SY5Y cells in our earlier investigations was used for the study

Abbreviations: TBI, Traumatic brain injury; CPA, cyclophilin A; BOP, blast overpressure.

☆ *Disclaimer*: The contents, opinions and assertions contained herein are private views of the authors and are not to be construed as official or reflecting the views of the Department of the Army or the Department of Defense. The authors report no conflict of interest.

* Corresponding author. Tel.: +1 301 319 2009; fax: +1 301 319 9839.
E-mail addresses: peethambaran.arun@amedd.army.mil, arunpdr@gmail.com (P. Arun).

0168-0102/$ – see front matter © 2013 Elsevier Ireland Ltd and the Japan Neuroscience Society. All rights reserved.
http://dx.doi.org/10.1016/j.neures.2013.02.009

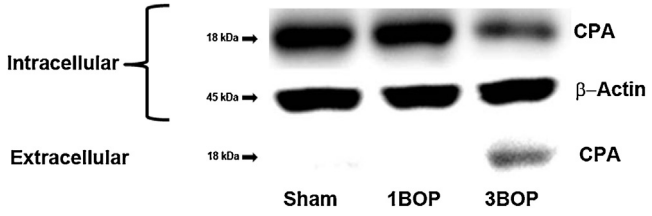

Fig. 1. Western blot analysis using CPA antibodies showing the decreased intracellular level of CPA and its accumulation in the culture medium after repeated blast exposures. 25 μg total protein was used for electrophoresis and Western blotting of the intracellular level of CPA. Volume corresponding to 360 μl culture medium was used for detecting the extracellular level of CPA. A representative figure from three different sets of experiments is shown. BOP – blast overpressure exposure.

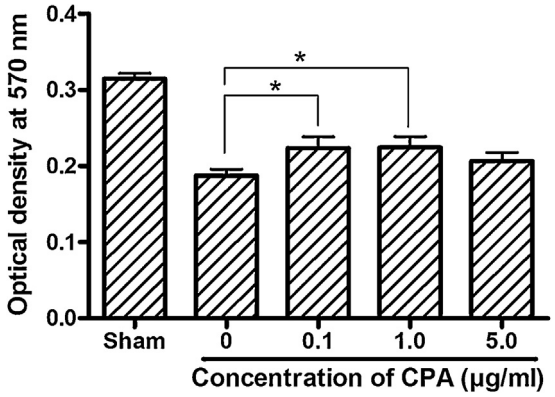

Fig. 2. MTT assay showing cellular injury after single blast exposure and protection by administration of purified recombinant CPA in the culture medium after blast exposure. Cells were exposed to single blast, treated with various doses of CPA after 15 min and MTT assay carried out at 24 h. Values of untreated cells were compared to those of CPA treated groups and expressed as mean ± standard deviation ($n = 12$). Statistical analysis was carried out using analysis of variance followed by Tukey's *post hoc* test. * $p < 0.05$.

(Arun et al., 2011, 2012). For repeated blast exposures, the cells were subjected to three blasts with 2 min intervals between each blast. For sham controls, cells were treated the same way as for blast exposure except that the plates containing the cells were not exposed to blast overpressure.

The SH-SY5Y cells and cell culture medium were collected from different wells of the plates subjected to single or repeated blasts along with sham controls at 24 h post-blast. The medium (9 ml from each group) was concentrated to 100 μl using 3000 MW cut off VIVASPIN 500 centrifugal filters (Sartorius Stedim, Bohemia, NY) according to manufacturer's instructions and 40 μl of the sample was used for polyacrylamide gel electrophoresis followed by Western blotting. The cells were suspended in M-PER mammalian protein extraction reagent (Pierce, Rockford, IL) and the total protein was extracted according to manufacturer's instructions and 25 μg total protein was used for Western blotting. Western blotting was carried out using rabbit polyclonal antibodies to CPA (1:1000 dilution) or mouse monoclonal antibodies to β-actin (1:50,000 dilution) (Sigma–Aldrich, St. Louis, MO), phosphorylated ERK1/2 or phosphorylated *Bad* (1:1000 dilution) (Cell signaling Technology, Danvers, MA).

At 15 min after single blast exposure, the medium was removed and fresh medium containing varying concentrations of purified recombinant CPA (Genway Biotech, San Diego, CA) was added and incubated for 24 h. After 24 h, the neuronal cell viability was assessed using MTT cell viability assay.

At 24 h after blast exposure, the medium was removed from each well and 100 μl fresh medium without CPA was added to conduct the cellular injury test using MTT cell proliferation assay kit (American Type Culture Collection, Manassas, VA, USA). Briefly, 10 μl of MTT reagent was added to each well and incubated in a CO_2 incubator for 2 h. One hundred micro liter detergent reagent was added to the wells and kept overnight at room temperature in dark. The optical density was measured at 570 nm using a SpectraMax M5 spectrophotometer (Molecular Devices, Sunnyvale, CA).

Western blot analysis data showed no significant changes in the level of CPA in SH-SY5Y cells at 24 h after single blast exposure. Also no detectable amount of CPA was found in the cell culture medium at 24 h after single blast exposure. On the other hand, repeated blast exposures resulted in a significant decrease in the level of CPA in SH-SY5Y cells and simultaneously CPA was detected in the culture medium (Fig. 1).

To further investigate the neuroprotective action of extracellular CPA, SH-SY5Y cells were incubated with various doses of CPA after single blast exposure and MTT cell viability assay was performed. The data showed that post-blast exposure treatment with purified recombinant CPA protein significantly protect against cellular injury in a dose-dependent manner (Fig. 2). Optimum protection against blast exposure was obtained at 0.1 μg/ml. At this dose, CPA treatment provided approximately 30% protection against blast-induced cellular injury. Higher concentrations of CPA decreased the degree of protection after blast exposure.

Using the *in vitro* blast TBI model, we have shown earlier that repeated blast exposures results in less cellular injury compared to single blast exposure and suggested the possibility of CPA release after blast exposure and the extracellular CPA playing a role in neuroprotection (Arun et al., 2011). In the present study, using the same model, we demonstrated for the first time that repeated blast exposures of human neuronal cells causes release of CPA. We also demonstrate that extracellular CPA can protect the cells from blast-induced cellular injury and the concentration of extracellular CPA seems to be critical for protection. Higher levels of extracellular CPA were less effective.

Neuroprotection induced by extracellular CPA has been demonstrated in different neuronal injury models. Administration of CPA was found to attenuate disrupted blood-brain barrier permeability and tissue damage in an *ex vivo* stab wound model of brain injury (Redell et al., 2007). The dose of CPA that showed protection in that study was in agreement with the doses used in the present study. Purified recombinant CPA administration to *in vitro* cortical neuronal cell models of ischemia and oxidative stress-induced neuronal injury showed significant neuroprotection supporting our observations (Boulos et al., 2007).

The precise mechanisms of neuroprotection triggered by extracellular CPA are still unresolved. It has been postulated that the neuroprotection induced by CPA involves its binding and signaling through CD147 receptors resulting in extracellular signal–regulated kinase (ERK1/2) activation (Boulos et al., 2007) and induction of anti-apoptotic protein Bcl2 (Seko et al., 2004). The activation of ERK1/2 by phosphorylation can stimulate anti-apoptotic proteins and inhibit pro-apoptotic proteins (Biswas and Greene, 2002; Riccio et al., 1999). In support of this notion, activation of ERK1/2 has been implicated in neuronal survival during excitotoxicity, oxidative injury and hypoxia (Adour et al., 1981; Hetman and Gozdz, 2004; Jin et al., 2002; Singer et al., 1999). To test whether phosphorylation of ERK1/2 occurs after repeated blast exposures due to the release of CPA, we tested phosphorylated ERK1/2 (p-ERK1/2) expression in SH-SY5Y cells at 1 h after repeated blast exposures. Activation of ERK1/2 can induce phosphorylation of the pro-apoptotic protein *Bad* and can inactive it (Jin et al., 2002). Our results indicate that repeated blast exposures result in the up-regulation of p-ERK1/2 and a simultaneous increase in phosphorylated *Bad* (p-*Bad*) suggesting a potential mechanism of neuroprotection (Fig. 3). Detailed studies are warranted to conclude

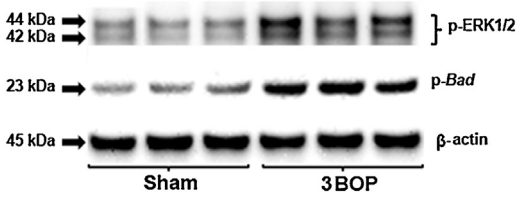

Fig. 3. Western blot analysis showing the expression of phosphorylated forms of ERK1/2 and *Bad* in SH-SY5Y cells at 1 h after repeated blast exposures.

that the extracellular CPA is solely responsible for these effects and also to demonstrate other neuroprotective effects of extracellular CPA.

Acknowledgements

Supports from Mrs. Irene Gist, Blast-induced Neurotrauma Branch and COL. Paul Bliese, Director, Center for Military Psychiatry and Neurosciences at Walter Reed Army Institute of Research are greatly acknowledged.

References

Adour, K.K., Sprague, M.A., Hilsinger Jr., R.L., 1981. Vestibular vertigo. A form of polyneuritis? JAMA 246, 1564–1567.

Arun, P., Spadaro, J., John, J., Gharavi, R.B., Bentley, T.B., Nambiar, M.P., 2011. Studies on blast traumatic brain injury using in-vitro model with shock tube. Neuroreport 22, 379–384.

Arun, P., Abu-Taleb, R., Valiyaveettil, M., Wang, Y., Long, J.B., Nambiar, M.P., 2012. Transient changes in neuronal cell membrane permeability after blast exposure. Neuroreport 23, 342–346.

Biswas, S.C., Greene, L.A., 2002. Nerve growth factor (NGF) down-regulates the Bcl-2 homology 3 (BH3) domain-only protein Bim and suppresses its proapoptotic activity by phosphorylation. J. Biol. Chem. 277, 49511–49516.

Boulos, S., Meloni, B.P., Arthur, P.G., Majda, B., Bojarski, C., Knuckey, N.W., 2007. Evidence that intracellular cyclophilin A and cyclophilin A/CD147 receptor-mediated ERK1/2 signalling can protect neurons against in vitro oxidative and ischemic injury. Neurobiol. Dis. 25, 54–64.

Cernak, I., 2010. The importance of systemic response in the pathobiology of blast-induced neurotrauma. Front. Neurol. 1, 151.

Hetman, M., Gozdz, A., 2004. Role of extracellular signal regulated kinases 1 and 2 in neuronal survival. Eur. J. Biochem. 271, 2050–2055.

Jin, K., Mao, X.O., Zhu, Y., Greenberg, D.A., 2002. MEK and ERK protect hypoxic cortical neurons via phosphorylation of Bad. J. Neurochem. 80, 119–125.

Ling, G., Bandak, F., Armonda, R., Grant, G., Ecklund, J., 2009. Explosive blast neurotrauma. J. Neurotrauma 26, 815–825.

Magnuson, J., Leonessa, F., Ling, G.S., 2012. Neuropathology of explosive blast traumatic brain injury. Curr. Neurol. Neurosci. Rep. 12, 570–579.

Redell, J.B., Zhao, J., Dash, P.K., 2007. Acutely increased cyclophilin a expression after brain injury: a role in blood-brain barrier function and tissue preservation. J. Neurosci. Res. 85, 1980–1988.

Riccio, A., Ahn, S., Davenport, C.M., Blendy, J.A., Ginty, D.D., 1999. Mediation by a CREB family transcription factor of NGF-dependent survival of sympathetic neurons. Science 286, 2358–2361.

Seko, Y., Fujimura, T., Taka, H., Mineki, R., Murayama, K., Nagai, R., 2004. Hypoxia followed by reoxygenation induces secretion of cyclophilin A from cultured rat cardiac myocytes. Biochem. Biophys. Res. Commun. 317, 162–168.

Singer, C.A., Figueroa-Masot, X.A., Batchelor, R.H., Dorsa, D.M., 1999. The mitogen-activated protein kinase pathway mediates estrogen neuroprotection after glutamate toxicity in primary cortical neurons. J. Neurosci. 19, 2455–2463.

Wang, Y., Wei, Y., Oguntayo, S., Wilkins, W., Arun, P., Valiyaveettil, M., Song, J., Long, J., Nambiar, M.P., 2011. Tightly Coupled repetitive blast-induced traumatic brain injury: development and characterization in mice. J. Neurotrauma 28, 2171–2183.

SCIENTIFIC REPORTS

OPEN

SUBJECT AREAS:
WHITE MATTER INJURY
NEURODEGENERATION

Received
29 January 2014

Accepted
27 March 2014

Published
2 May 2014

Correspondence and requests for materials should be addressed to D.V.A. (denes.agoston@usuhs.edu.)

* Current address: Department of Neurosurgery, VA Medical Center-Research 151, Medical College of Wisconsin, 5000 West National Ave., Milwaukee, WI 53295.

Diffusion Tensor Imaging Reveals Acute Subcortical Changes after Mild Blast-Induced Traumatic Brain Injury

Alaa Kamnaksh[1,2], Matthew D. Budde[3]*, Erzsebet Kovesdi[4], Joseph B. Long[5], Joseph A. Frank[3] & Denes V. Agoston[1]

[1]Department of Anatomy, Physiology and Genetics, The Uniformed Services University, 4301 Jones Bridge Road, Bethesda, MD 20814, [2]Center for Neuroscience and Regenerative Medicine, The Uniformed Services University, 4301 Jones Bridge Road, Bethesda, MD 20814, [3]Radiology and Imaging Sciences, National Institute of Biomedical Imaging and Bioengineering, National Institutes of Health, Room B1N256 MSC 1074, 10 Center Drive, Bethesda, MD 20892, [4]US Department of Veterans Affairs, Veterans Affairs Central Office, 810 Vermont Avenue NW, Washington, DC 20420, [5]Blast-Induced Neurotrauma Branch, Center for Military Psychiatry and Neuroscience, Walter Reed Army Institute of Research, 503 Robert Grant Avenue, Silver Spring, MD 20910.

Mild blast-induced traumatic brain injury (mbTBI) poses special diagnostic challenges due to its overlapping symptomatology with other neuropsychiatric conditions and the lack of objective outcome measures. Diffusion tensor imaging (DTI) can potentially provide clinically relevant information toward a differential diagnosis. In this study, we aimed to determine if single and repeated (5 total; administered on consecutive days) mild blast overpressure exposure results in detectable structural changes in the brain, especially in the hippocampus. Fixed rat brains were analyzed by ex vivo DTI at 2 h and 42 days after blast (or sham) exposure(s). An anatomy-based region of interest analysis revealed significant interactions in axial and radial diffusivity in a number of subcortical structures at 2 h only. Differences between single- and multiple-injured rats were largely in the thalamus but not the hippocampus. Our findings demonstrate the value and the limitations of DTI in providing a better understanding of mbTBI pathobiology.

Mild traumatic brain injury (mTBI) continues to be the least understood form of traumatic brain injury (TBI) despite its high incidence and substantial toll on patients and health care systems[1]. In the military, mTBIs are mostly caused by the exposure to low levels of blast from improvised explosive devices resulting in mild blast-induced TBI (mbTBI)[2–4]. The diagnosis of mbTBI currently relies on subjective assessments and self-reports of symptoms such as disorientation, altered states of consciousness, headaches, and emotional and cognitive dysfunction—all of which are involved in post-traumatic stress disorder (PTSD)[5]. Because of the mild and transient nature of symptoms that follow mbTBI, soldiers typically return to duty and are frequently re-exposed to additional mild blasts. Studies have suggested that repeated mbTBI is a risk factor for developing late onset neurodegenerative conditions such as chronic traumatic encephalopathy (CTE)[6].

Objective outcome measures can provide especially valuable, clinically relevant information in a non-/minimally invasive and repeatable manner. Various modalities of magnetic resonance imaging (MRI), including diffusion tensor imaging (DTI), have been utilized in clinical settings following TBI[7–10]. However, only a limited number of clinical studies included readouts at several post-injury time points in Veterans[11–17]. DTI's sensitivity relative to conventional imaging tools has prompted its recent use in experimental mTBI[18–20] with a few rodent blast-induced TBI (bTBI) studies[21–24]. These studies identified a number of brain regions, including the hippocampus and the cerebellum, as being affected in mbTBI[25]. Injury-induced changes in serum, cerebrospinal fluid, and tissue protein biomarker levels have also been extensively investigated in both clinical and experimental TBI[26–28]. Together, imaging and molecular biomarkers would enable the monitoring of pathological processes over time and allow for more direct comparisons between experimental findings and clinical TBI cases.

The full potential and limitations of using imaging and molecular biomarkers in the diagnosis and monitoring of TBIs, especially mTBIs, are currently unknown due to a substantial gap between clinical and experimental findings and their translatability[29]. Furthermore, our understanding of how structural changes relate to cellular, molecular, and functional changes in TBI is very limited. Our previous works using the rodent model of single and repeated mbTBI recapitulated some of the behavioral changes that are observed in human bTBI[30]. Using histo-

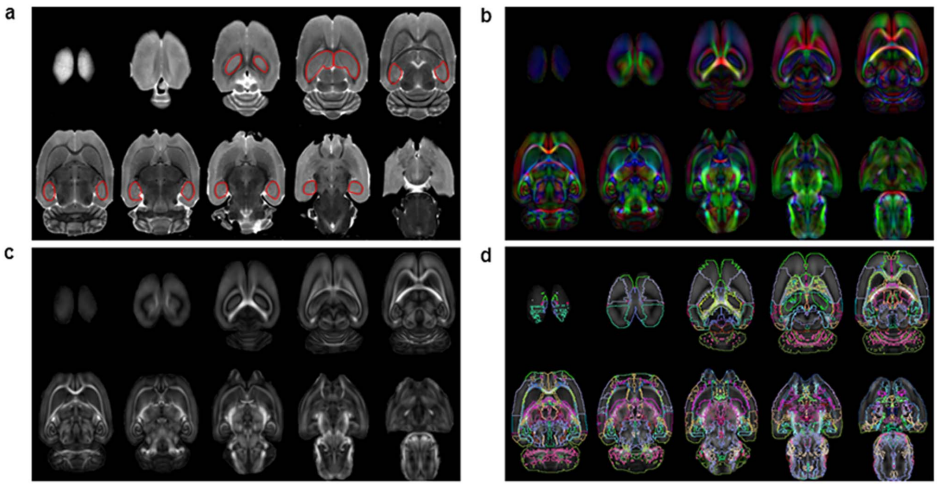

Figure 1 | MRI data analysis. (a) A T2-weighted image from a single subject with the hippocampus manually outlined in red. (b) A mean directionally encoded color image. (c) Map of FA derived from DTI of all spatially registered brains (every second slice is shown). (d) The registered anatomical ROIs derived from the atlas overlaid on the FA map for visualization.

logic and proteomic analyses of functionally relevant brain regions and peripheral blood, we identified several pathologies at different post-injury time points. These include neuronal and glial damage and/or death, axonal damage, metabolic and vascular changes, and inflammation. Additionally, we identified several pathologies that include neuronal and glial damage and/or death, axonal damage, metabolic and vascular changes, and inflammation at different post-injury time points using histologic and proteomic analyses of functionally relevant brain regions and peripheral blood[31–33]. In this preliminary imaging study, we aimed to determine if the same exposure to single and repeated mild blast overpressure that resulted in the abovementioned changes also induced structural changes that are detectable by DTI.

Results

We selected two of our previously tested post-injury termination time points, 2 h and 42 days, for the DTI analyses to mimic early and delayed clinical interventions. A manual region of interest (ROI) analysis was first used to assess hippocampal volume and fractional anisotropy (FA) in the hippocampus as shown in Fig. 1a. No significant differences were identified in hippocampal volume or FA values at either time point (Fig. 2). An anatomically defined ROI analysis was then performed as shown in Fig. 1b–d. In rats terminated ~2 h after blast (or sham) exposure(s), no brain regions had a significant interaction for FA. However, axial diffusivity (AD) and radial diffusivity (RD) had significant interactions in regions of the stria terminalis, thalamic subregions, and the cerebellum. Post hoc analysis revealed that the single-injured (SI) and multiple-injured (MI) groups were significantly different from one another largely in the thalamus and thalamic nuclei. Regions exhibiting significant blast event-related differences (i.e., single vs. repeated blast) are shown in Fig. 3 and Table 1; mean DTI values for these regions are provided in Fig. 4. No brain regions exhibited significant ROI changes in rats terminated 42 days after blast (or sham) exposure(s).

Discussion

Elucidating the role of repeated mbTBI in the development of neurodegenerative conditions is a pressing issue for the military health care system. To that end, a better understanding of mbTBI pathobiology, the period of cerebral vulnerability between insults, and the synergistic effect of repeated injury is critical. In conducting a series of studies comparing single and repeated mild blast injury (5 overpressure exposures administered on consecutive days), we aimed to assess the extent of the damage accumulation in mbTBI (i.e., the

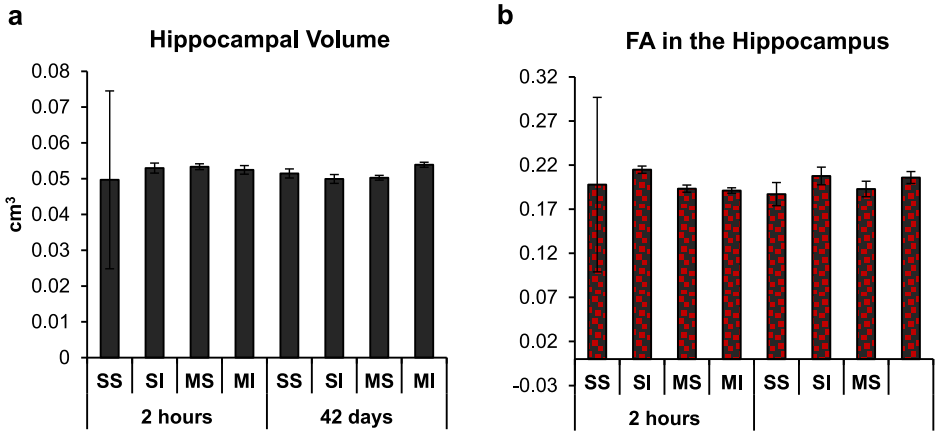

Figure 2 | Volumetric and DTI measures in the hippocampus. (a) Hippocampal volume (cm^3) of sham (SS, single sham; MS, multiple sham) and injured (SI, single-injured; MI, multiple-injured) rats terminated at 2 h and 45 days after blast (or sham) exposure(s). (b) Fractional anisotropy (FA) in the hippocampi of rats at the same time points. Data are presented as the mean ± SEM.

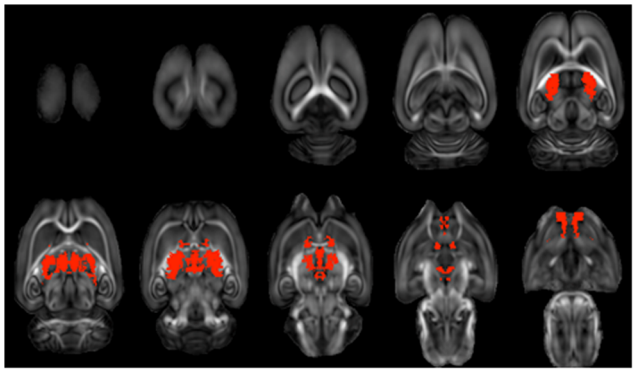

Figure 3 | Brain regions exhibiting significant ROI changes. Regions with a significant Blast x No. of Events interaction were first identified; those with significant differences between single-injured and multiple-injured rats (corrected for multiple comparisons) are shown in red.

cumulative effect of the injury) at different post-injury time points. Of particular interest to us is correlating cellular and molecular level changes with structural and neurocognitive changes toward a definitive diagnosis for mbTBI. The objective of this study was to determine if the exposure to single and repeated mild blast overpressure, which resulted in significant functional, cellular, and molecular changes, also induced structural changes that are detectable by ex vivo DTI.

Based on a number of bTBI studies that implicate the hippocampus in the development of neurobehavioral symptoms, we expected to detect injury-induced structural and/or volumetric changes in this region due to its involvement in TBI[34,35]. We previously found significantly increased numbers of apoptotic, TUNEL-positive cells in the hilus and granular cell layer of the hippocampus as early as 2 h post-injury in both single- and multiple-injured rats[36]. However, we found no significant changes in hippocampal volume or FA in the hippocampus in our current study. This discrepancy may be related to the current spatial resolution of DTI. Another plausible explanation is that even though we found significantly increased rates of cell death in the hippocampus, we also found a substantive gliotic response[30,31,33,37]. Such astroglial hypertrophy can potentially compensate for the loss in volume caused by cell death.

A recent ex vivo DTI rodent study has shown that the microstructure of the hippocampus can be significantly affected in mbTBI[23]. Consistent with impaired cognitive performance, FA values were significantly decreased in select brain regions of blast-exposed rats relative to their sham controls at 4 and 30 days post-injury. The affected brain regions included the hippocampus, thalamus, and brainstem. It is important to note, however, that the blast model and experimental design of our and the Budde et al. study are very different. Nonetheless, hippocampal abnormalities have been found in a number of clinical mbTBI studies using various imaging modalities[12,15,17,38–40].

Since no significant hippocampal changes were detected in our work, an automated, anatomical ROI analysis without a priori assumptions of affected regions was used to examine the brains[23]. Compared to a voxel by voxel approach that includes thousands of independent statistical tests, the whole brain anatomical ROI approach reduces the number of statistical comparisons but avoids tedious manual definition of brain regions[41]. The results of this analysis demonstrated significant changes that are largely confined to midline thalamic structures and the cerebellum. Post hoc analysis revealed that SI and MI rats were significantly different from one another in the thalamus and thalamic nuclei. Previous bTBI studies also found changes in the thalamus using DTI[23] and histological methods[42]. Thalamus-mediated functions account for a significant number of the most frequently reported neurobehavioral symptoms in clinical mbTBI. Among the leading complaints are sleep and emotional disturbances as well as altered sensory sensitivities, both auditory and visual[14].

Cerebellar abnormalities have been found in most human bTBI imaging studies[12,15,16,43] and in a recent rodent bTBI study[24]. These findings illustrate the region-specific vulnerability of the brain to different types of physical insults—an important albeit poorly understood issue in TBI. The cerebellum's susceptibility to injury maybe due to its anatomy; it is located in a relatively small sub-compartment of the skull and the ratio between cerebellar white and grey matters is different from that in the cerebrum. Primary blast injury mainly exerts damage at the interface of biological materials with differing physiochemical properties (e.g., grey and white matter). Indeed, white matter damage—including cerebellar white matter—has been found in virtually all human bTBI imaging studies. Functionally, the cerebellum is involved in certain cognitive and learning functions,

Table 1 | Brain regions exhibiting significant blast event-related effects at 2 h post-injury

	Fractional Anisotropy		Axial Diffusivity				Radial Diffusivity			
	Blast x No. of Events Interaction		Blast x No. of Events Interaction		SI vs. MI *t*-Test		Blast x No. of Events Interaction		SI vs. MI *t*-Test	
Brain Region	*F* value	*p* value[a]	*F* value	*p* value[b]	*t* value	*p* value[b]	*F* value	*p* value[b]	*t* value	*p* value[b]
Stria Terminalis	4.55	0.065	19.28	0.017	6.34	**0.023**	11.91	0.068	4.80	0.099
Posterior Hypothalamic Nucleus	1.25	0.296	13.56	0.043	3.78	0.145	13.57	0.048	4.06	0.189
Islands of Calleja	1.95	0.200	26.50	0.006	−9.89	**0.004**	34.55	0.003	−6.23	**0.042**
Olfactory Tubercle	1.02	0.341	35.79	0.002	−5.28	**0.048**	70.63	0.000	−7.95	**0.010**
Ventral Nucleus of Thalamus	0.98	0.352	29.78	0.004	9.02	**0.007**	20.89	0.014	6.81	**0.026**
Lateral Dorsal Nucleus of Thalamus	3.60	0.094	15.33	0.032	7.01	**0.017**	18.44	0.021	7.28	**0.021**
Lateral Posterior Nucleus of Thalamus	2.06	0.189	15.96	0.026	5.55	**0.040**	18.47	0.018	5.65	0.059
Central Lateral Nucleus of Thalamus	3.09	0.117	20.11	0.014	7.18	**0.014**	24.46	0.009	8.05	**0.005**
Medial Dorsal Thalamus	1.93	0.203	15.71	0.029	7.74	**0.011**	17.07	0.026	7.31	**0.016**
Midline Thalamic Nuclei	7.55	0.025	21.27	0.011	10.00	**0.002**	15.91	0.031	6.72	**0.031**
Thalamus	0.35	0.568	13.29	0.047	4.85	0.065	13.89	0.044	4.77	0.108
Cerebellum	4.24	0.073	17.26	0.022	−3.41	0.212	21.95	0.011	−5.05	0.089

[a]uncorrected.
[b]false discovery rate corrected.
SI, single-injured ($n = 3$); MI, multiple-injured ($n = 3$).
Statistically significant differences between SI and MI rats are indicated in boldface.

hence the detected changes are consistent with clinically observed abnormalities[44,45].

Among the other affected brain structures is the stria terminalis, which serves as a major relay site within the hypothalamic-pituitary-adrenal axis[46]. Similar changes were also found in the olfactory tubercule, including the islands of Calleja. The olfactory tubercule has been shown to play a role in behavioral response as it is interconnected with several brain regions with sensory and arousal/reward functions[47]. In fact, injury to the islands as a result of restricted blood flow has been linked to a number of behavioral and emotional responses such as amnesia and changes in personality—behavioral changes that are not possible to assess in animal models.

A critical limitation toward better understanding human mbTBI is inherent variability as well as the unknown biophysical forces that are experienced during injury. Additionally, most existing DTI studies of veterans have been performed years after the injury. Animal models of mbTBI allow for direct testing of the many effects of blast wave characteristics under carefully controlled conditions[48]. However, we currently have no clear understanding of how human years (physiologically and pathologically speaking) translate into rat months (or weeks). Furthermore, the lack of a consensus regarding a high fidelity experimental bTBI model—as demonstrated by the imaging findings obtained using various blast models—is a major impediment to studying the physical and biological effects of primary blast injury.

Another pressing issue is how DTI findings in mbTBI (or any other neurological disorder) relate to changes detectable by proteomics or histology. We emphasize this point because although rats terminated at 42 days did not exhibit significant ROI changes as measured by DTI, proteomic analyses of plasma at the same time point showed significant and persistent molecular pathologies in SI as well as MI rats[36,49]. These include inflammation, metabolic and vascular changes, neuronal and glial cell damage and/or death, and axonal damage.

A technical limitation of our study is the use of fixed tissues in ex vivo DTI, mainly due to altered diffusivity of water molecules. Nonetheless, previous studies have demonstrated that ex vivo DTI provides valuable structural information that correlates with in vivo changes albeit to a varying extent. This may partially account for the poor correlation between cellular changes obtained by conventional histology and volumetric/DTI measures in the hippocampus. It should be noted that animal in vivo imaging has its own issues with scanning times (and corresponding anesthesia times), image acquisition protocols, and motion artifacts being the major ones.

Despite the increased attention in recent years on blast as a mechanism of mTBI, the subject of how blast waves affect the brain along with diagnosing mbTBI are still a matter of considerable debate. The abovementioned caveats underline the importance of combining objective and clinically relevant outcome measures in experimental TBI to validate and correlate findings, to enable more direct comparisons of pathologies observed in animal and in clinical TBI research, and to enable the development of sensitive and specific diagnostics for mbTBI[29].

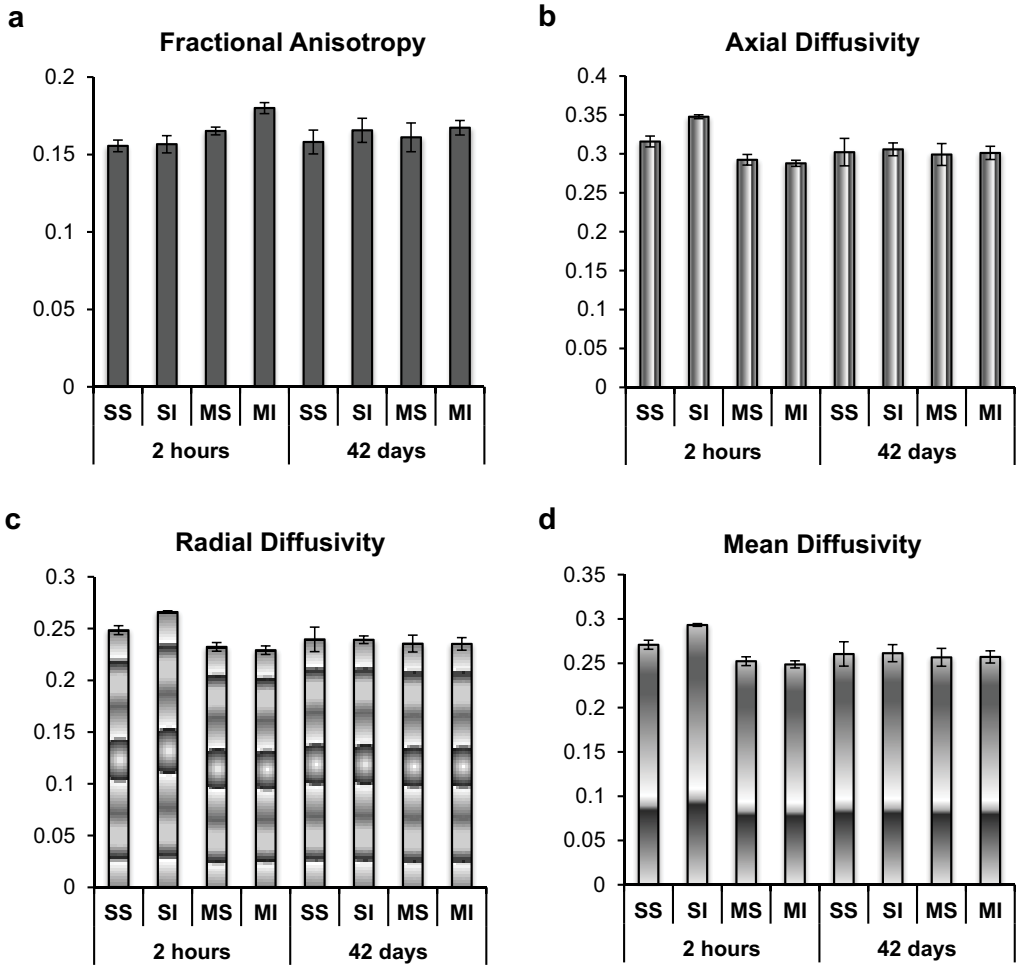

Figure 4 | Mean DTI values at the two time points. Data were extracted from each subject as a single value from the ROIs showing significance in the anatomical ROI analysis. Data are presented as the mean ± SEM for each experimental group (SS, single sham; SI, single-injured; MS, multiple sham; MI, multiple-injured).

Methods

Animals and housing conditions. A total of 60 male Sprague Dawley rats (weight at arrival: 245–265 g) (Charles River Laboratories, Wilmington, MA) were used in the original experiments[36,49]. All animals were housed in standard rat cages with a built-in filter in a reverse 12-h light 12-h dark cycle with food and water ad lib. Animals were handled according to protocol approved by the Institutional Animal Care and Use Committee at the Uniformed Services University (USU; Bethesda, MD).

Experimental groups and manipulations. All animals underwent a 5 day acclimation and handling period and were later assigned to the following groups: naïve, single sham (SS), single-injured (SI), multiple sham (MS), and multiple-injured (MI) as described earlier[36,49]. Rat numbers in the early and late termination groups were: ($N = 30$; naïve = 3, SS = 6, SI = 7, MS = 6, MI = 8) and ($N = 30$; naïve = 3, SS = 6, SI = 7, MS = 6, MI = 8), respectively. Naïve rats were kept in the animal facility at USU without any manipulation for the duration of the studies. SS rats were transported once from USU to Walter Reed Army Institute of Research (Silver Spring, MD) and anesthetized in an induction chamber with a 4% isoflurane (Forane; Baxter Healthcare Corporation, Deerfield, IL) in air mixture delivered at 2 L/min for 6 min. MS rats were similarly transported and anesthetized once per day for 5 consecutive days. SI and MI rats underwent the same procedures as their respective sham controls in addition to receiving a single or multiple (5 total) mild blast exposure(s)[36,49].

Injury conditions. Anesthetized rats in chest protection (weight at injury: 300–330 g) were placed in the shock tube holder in a transverse prone position with the right side facing the direction of the membrane and the incidence of the blast waves. Blast overpressure was generated using a compressed air-driven shock tube yielding a single blast overpressure wave (average peak total pressure: ~137 kPa at the animal level) to produce a mild injury as described in detail[31,37,50]. Following blast (or equivalent time spent anesthetized as a sham), animals were moved to an adjacent bench top for observation and then transported back to the USU animal facility at the conclusion of each injury day.

Preparation of specimens for imaging. A subset of animals from each experiment [(2 h termination: $n = 11$; SS = 2, SI = 3, MS = 3, MI = 3) and (42 day termination: $n = 16$; SS = 4, SI = 4, MS = 4, MI = 4)] was used for MRI/DTI analyses; all other animals were used for proteomics as described earlier[36,49]. Rats were deeply anesthetized with isoflurane inhalant until a tail pinch produced no reflex movement, then transcardially perfused with cold phosphate-buffered saline (PBS) followed by a 4% paraformaldehyde in 1x PBS solution. The brains were removed and post-fixed in the same solution overnight at 4°C and then transferred to a 1x PBS solution containing 0.1% sodium azide until scanning. No hemorrhage or any other signs of macroscopic damage were detected in any of the animals.

Image acquisition. Fixed brains underwent ex vivo DTI within 2 days of perfusion fixation on a Bruker 7 T vertical bore system. Brains were immersed in susceptibility-matching fluid (Fomblin; Solvay Solexis, Inc., West Deptford, NJ) and inserted into a radiofrequency coil 3 cm in diameter. A three-echo diffusion-weighted spin echo sequence was employed (TR = 4 s; TE = 20 ms (first echo; 7.5 ms echo spacing) to acquire diffusion-weighted images (b = 1200 s/mm^2) along 30 directions[51] with diffusion gradient duration (δ) and separation (Δ) of 4 and 10 ms, respectively, along with 5 non diffusion-weighted images[52]. The slice thickness was 0.5 mm with an in-plane resolution of 0.234 mm^2 and a 30 mm^2 field of view (128^2 matrix). The full experiment required 6 h of continuous imaging. DTI data was reconstructed using a linear least squares fit to derive parameter maps of FA, AD, and RD using custom Matlab routines[53].

Data analysis. The analysis of MRI data included volumetric and DTI measures in the hippocampus and an anatomical ROI analysis of DTI data without a priori assumptions of affected regions. Hippocampal volume and FA in the hippocampus were derived from manual segmentation of the hippocampus on T2-weighted and FA maps, respectively, by an operator blinded to animal conditions. For unbiased quantification of DTI measures using anatomically based ROIs, DTI volumes from all subjects were first registered to a common space using an iterative, tensor-based registration routine implemented in DTI-TK[54]. Rigid-body, affine, and diffeomorphic (piecewise affine) methods were used in succession to progressively improve registration accuracy, as this approach has been shown to be superior to other routines[55]. The final image resolution was 120 × 120 × 500 μm^3. Anatomical ROIs were derived from a digital rat brain atlas included as part of the Medical Image Visualization and Analysis Software (MIVA) software package[56]. The regions consisted of 87 subregions of the brain initially derived from the Paxinos Rat brain atlas[57]. A mask of white matter regions derived from the atlas was registered to a mask of white matter regions derived from DTI by thresholding the FA maps at 0.2. An FA value of 0.2 was chosen empirically since it effectively masked the white matter tracts. It should be noted that this threshold value was used for the registration of the ROIs, not for quantification. Registration employed a point-set based registration metric incorporated into Advanced Normalization Tools (ANTS) software package, including elastic warping[58]. The resulting overlap demonstrated high correspondence between the DTI and atlas-based white matter structures (Fig. 1C). The mean FA, AD, and RD within each ROI were derived from each of the registered DTI volumes from each subject for subsequent statistical analysis (Fig. 4).

Statistical analysis. Twenty-seven animals were used for the analyses (2 h termination, $N = 11$; 42 day termination, $N = 16$). A mixed-effect ANOVA was first performed to identify any significant effects of left/right (L/R) asymmetry. Since none of the brain regions exhibited a significant Blast x No. of Events x Side (L/R) interaction, the effect of side was collapsed for all subsequent analyses. For hippocampal volume and FA in the hippocampus, ANOVAs followed by Tukey's HSD test were performed separately at each time point. Subsequently, a one-way ANOVA was performed for each condition across the two time points.

For DTI, a two-way ANOVA was performed to compare the main effects of Blast x No. of Events interaction. Regions that exhibited a significant interaction were subjected to post-hoc analysis using a Student's t-test to compare the SI and MI groups. All statistical tests were corrected for multiple comparisons (87 individual ROIs) by controlling for the false discovery rate[59]. A Spearman correlation analysis was used to identify brain regions significantly correlated to either the number of blast events or the number of sham events. A corrected p value of 0.05 was considered significant for all tests.

1. Laker, S. R. Epidemiology of concussion and mild traumatic brain injury. *PM R* **3**, S354–358; DOI:10.1016/j.pmrj.2011.07.017 (2011).
2. Hendricks, A. M. *et al.* Screening for mild traumatic brain injury in OEF-OIF deployed US military: an empirical assessment of VHA's experience. *Brain. Inj.* **27**, 125–134; DOI:10.3109/02699052.2012.729284 (2013).
3. Vanderploeg, R. D. *et al.* Health outcomes associated with military deployment: mild traumatic brain injury, blast, trauma, and combat associations in the Florida National Guard. *Arch. Phys. Med. Rehabil.* **93**, 1887–1895; DOI:10.1016/j.apmr.2012.05.024 (2012).
4. Xydakis, M. S., Ling, G. S., Mulligan, L. P., Olsen, C. H. & Dorlac, W. C. Epidemiologic aspects of traumatic brain injury in acute combat casualties at a major military medical center: a cohort study. *Ann. Neurol.* **72**, 673–681; DOI:10.1002/ana.23757 (2012).
5. Brenner, L. A., Vanderploeg, R. D. & Terrio, H. Assessment and diagnosis of mild traumatic brain injury, posttraumatic stress disorder, and other polytrauma conditions: burden of adversity hypothesis. *Rehabil. Psychol.* **54**, 239–246; DOI:10.1037/a0016908 (2009).
6. Stern, R. A. *et al.* Long-term consequences of repetitive brain trauma: chronic traumatic encephalopathy. *PM R* **3**, S460–467; DOI:10.1016/j.pmrj.2011.08.008 (2011).
7. Aoki, Y., Inokuchi, R., Gunshin, M., Yahagi, N. & Suwa, H. Diffusion tensor imaging studies of mild traumatic brain injury: a meta-analysis. *J. Neurol. Neurosurg. Psychiatry* **83**, 870–876; DOI:10.1136/jnnp-2012-302742 (2012).
8. Shenton, M. E. *et al.* A review of magnetic resonance imaging and diffusion tensor imaging findings in mild traumatic brain injury. *Brain Imaging Behav.* **6**, 137–192; DOI:10.1007/s11682-012-9156-5 (2012).
9. Voelbel, G. T., Genova, H. M., Chiaravalotti, N. D. & Hoptman, M. J. Diffusion tensor imaging of traumatic brain injury review: implications for neurorehabilitation. *NeuroRehabilitation* **31**, 281–293; DOI:10.3233/nre-2012-0796 (2012).
10. Xiong, K. L., Zhu, Y. S. & Zhang, W. G. Diffusion tensor imaging and magnetic resonance spectroscopy in traumatic brain injury: a review of recent literature. *Brain Imaging Behav.* DOI:10.1007/s11682-013-9288-2 (2014).
11. Benzinger, T. L. *et al.* Blast-related brain injury: imaging for clinical and research applications: report of the 2008 st. Louis workshop. *J. Neurotrauma* **26**, 2127–2144; DOI:10.1089/neu.2009-0885 (2009).
12. Levin, H. S. *et al.* Diffusion tensor imaging of mild to moderate blast-related traumatic brain injury and its sequelae. *J. Neurotrauma* **27**, 683–694; DOI:10.1089/neu.2009.1073 (2010).
13. Mendez, M. F. *et al.* Mild traumatic brain injury from primary blast vs. blunt forces: post-concussion consequences and functional neuroimaging. *NeuroRehabilitation* **32**, 397–407; DOI:10.3233/nre-130861 (2013).
14. Petrie, E. C. *et al.* Neuroimaging, behavioral, and psychological sequelae of repetitive combined blast/impact mild traumatic brain injury in Iraq and Afghanistan war veterans. *J. Neurotrauma* **31**, 425–436; DOI:10.1089/neu.2013.2952 (2014).
15. Matthews, S. C. *et al.* A multimodal imaging study in U.S. veterans of Operations Iraqi and Enduring Freedom with and without major depression after blast-related concussion. *Neuroimage* **54**, S69–75; DOI:10.1016/j.neuroimage.2010.04.269 (2011).
16. Mac Donald, C. *et al.* Cerebellar white matter abnormalities following primary blast injury in US military personnel. *PLoS ONE* **8**, e55823; DOI:10.1371/journal.pone.0055823 (2013).
17. Matthews, S. C., Spadoni, A. D., Lohr, J. B., Strigo, I. A. & Simmons, A. N. Diffusion tensor imaging evidence of white matter disruption associated with loss versus alteration of consciousness in warfighters exposed to combat in Operations Enduring and Iraqi Freedom. *Psychiatry Res.* **204**, 149–154; DOI:10.1016/j.pscychresns.2012.04.018 (2012).
18. Bennett, R. E., Mac Donald, C. L. & Brody, D. L. Diffusion tensor imaging detects axonal injury in a mouse model of repetitive closed-skull traumatic brain injury. *Neurosci. Lett.* **513**, 160–165; DOI:10.1016/j.neulet.2012.02.024 (2012).
19. Albensi, B. C. *et al.* Diffusion and high resolution MRI of traumatic brain injury in rats: time course and correlation with histology. *Exp. Neurol.* **162**, 61–72; DOI:10.1006/exnr.2000.7256 (2000).

20. Cernak, I. *et al.* The pathobiology of moderate diffuse traumatic brain injury as identified using a new experimental model of injury in rats. *Neurobiol. Dis.* **17**, 29–43; DOI:10.1016/j.nbd.2004.05.011 (2004).
21. Henninger, N. *et al.* Differential recovery of behavioral status and brain function assessed with functional magnetic resonance imaging after mild traumatic brain injury in the rat. *Crit. Care Med.* **35**, 2607–2614; DOI:10.1097/01.ccm.0000286395.79654.8d (2007).
22. van de Looij, Y. *et al.* Diffusion tensor imaging of diffuse axonal injury in a rat brain trauma model. *NMR Biomed.* **25**, 93–103; DOI:10.1002/nbm.1721 (2012).
23. Budde, M. D. *et al.* Primary blast traumatic brain injury in the rat: relating diffusion tensor imaging and behavior. *Front. Neurol.* **4**, 154; DOI:10.3389/fneur.2013.00154 (2013).
24. Calabrese, E. *et al.* Diffusion tensor imaging reveals white matter injury in a rat model of repetitive blast-induced traumatic brain injury. *J. Neurotrauma.* DOI:10.1089/neu.2013.3144 (2014).
25. Morey, R. A. *et al.* Effects of chronic mild traumatic brain injury on white matter integrity in Iraq and Afghanistan war veterans. *Hum. Brain Mapp.* **34**, 2986–2999; DOI:10.1002/hbm.22117 (2013).
26. Di Battista, A. P., Rhind, S. G. & Baker, A. J. Application of blood-based biomarkers in human mild traumatic brain injury. *Front. Neurol.* **4**, 44; DOI:10.3389/fneur.2013.00044 (2013).
27. Kobeissy, F. H. *et al.* Neuroproteomics and systems biology-based discovery of protein biomarkers for traumatic brain injury and clinical validation. *Proteomics Clin. Appl.* **2**, 1467–1483; DOI:10.1002/prca.200800011 (2008).
28. Wang, K. K. *et al.* Proteomic identification of biomarkers of traumatic brain injury. *Expert Rev. Proteomics* **2**, 603–614; DOI:10.1586/14789450.2.4.603 (2005).
29. Agoston, D. V., Risling, M. & Bellander, B. M. Bench-to-bedside and bedside back to the bench; coordinating clinical and experimental traumatic brain injury studies. *Front. Neurol.* **3**, 3; DOI:10.3389/fneur.2012.00003 (2012).
30. Kwon, S. K. *et al.* Stress and traumatic brain injury: a behavioral, proteomics, and histological study. *Front. Neurol.* **2**, 12; DOI:10.3389/fneur.2011.00012 (2011).
31. Kamnaksh, A. *et al.* Factors affecting blast traumatic brain injury. *J. Neurotrauma* **28**, 2145–2153; DOI:10.1089/neu.2011.1983 (2011).
32. Kovesdi, E. *et al.* The effect of enriched environment on the outcome of traumatic brain injury; a behavioral, proteomics, and histological study. *Front. Neurosci.* **5**, 42; DOI:10.3389/fnins.2011.00042 (2011).
33. Kovesdi, E. *et al.* Acute minocycline treatment mitigates the symptoms of mild blast-induced traumatic brain injury. *Front. Neurol.* **3**, 111; DOI:10.3389/fneur.2012.00111 (2012).
34. Orrison, W. W. *et al.* Traumatic brain injury: a review and high-field MRI findings in 100 unarmed combatants using a literature-based checklist approach. *J. Neurotrauma* ***26***, 689–701; DOI:10.1089/neu.2008.0636 (2009).
35. Bigler, E. D. Quantitative magnetic resonance imaging in traumatic brain injury. *J. Head Trauma Rehabil.* **16**, 117–134 (2001).
36. Kamnaksh, A. *et al.* Neurobehavioral, cellular, and molecular consequences of single and multiple mild blast exposure. *Electrophoresis* **33**, 3680–3692; DOI:10.1002/elps.201200319 (2012).
37. Ahmed, F. *et al.* Time-dependent changes of protein biomarker levels in the cerebrospinal fluid after blast traumatic brain injury. *Electrophoresis* **33**, 3705–3711; DOI:10.1002/elps.201200299 (2012).
38. Hetherington, H. P. *et al.* MRSI of the medial temporal lobe at 7 T in explosive blast mild traumatic brain injury. *Magn. Reson. Med.* **71**, 1358–1367; DOI:10.1002/mrm.24814 (2014).
39. Masel, B. E. *et al.* Galveston Brain Injury Conference 2010: clinical and experimental aspects of blast injury. *J. Neurotrauma* **29**, 2143–2171; DOI:10.1089/neu.2011.2258 (2012).
40. Scheibel, R. S. *et al.* Altered brain activation in military personnel with one or more traumatic brain injuries following blast. *J. Int. Neuropsychol. Soc.* **18**, 89–100; DOI:10.1017/s1355617711001433 (2012).
41. Lu, H. *et al.* Registering and analyzing rat fMRI data in the stereotaxic framework by exploiting intrinsic anatomical features. *Magn. Reson. Imaging* **28**, 146–152; DOI:10.1016/j.mri.2009.05.019 (2010).
42. Goldstein, L. E. *et al.* Chronic traumatic encephalopathy in blast-exposed military veterans and a blast neurotrauma mouse model. *Sci. Transl. Med.* **4**, 134ra60; DOI:10.1126/scitranslmed.3003716 (2012).
43. Jorge, R. E. *et al.* White matter abnormalities in veterans with mild traumatic brain injury. *Am. J. Psychiatry* **169**, 1284–1291; DOI:10.1176/appi.ajp.2012.12050600 (2012).
44. Stoodley, C. J. The cerebellum and cognition: evidence from functional imaging studies. *Cerebellum* **11**, 352–365; DOI:10.1007/s12311-011-0260-7 (2012).
45. Van Overwalle, F., Baetens, K., Marien, P. & Vandekerckhove, M. Social cognition and the cerebellum: A meta-analysis of over 350 fMRI studies. *Neuroimage* **86**, 554–572; DOI:10.1016/j.neuroimage.2013.09.033 (2014).
46. Crestani, C. C. *et al.* Mechanisms in the bed nucleus of the stria terminalis involved in control of autonomic and neuroendocrine functions: a review. *Curr. Neuropharmacol.* **11**, 141–159; DOI:10.2174/1570159x11311020002 (2013).
47. Rodrigo, J. *et al.* Physiology and pathophysiology of nitric oxide in the nervous system, with special mention of the islands of Calleja and the circunventricular organs. *Histol. Histopathol.* **17**, 973–1003 (2002).
48. Bass, C. R. *et al.* Brain injuries from blast. *Ann. Biomed. Eng.* **40**, 185–202; DOI:10.1007/s10439-011-0424-0 (2012).
49. Ahmed, F. A., Kamnaksh, A., Kovesdi, E., Long, J. B. & Agoston, D. V. Long-term consequences of single and multiple mild blast exposure on select physiological parameters and blood-based biomarkers. *Electrophoresis* **34**, 2229–2233; DOI:10.1002/elps.201300077 (2013).
50. Long, J. B. *et al.* Blast overpressure in rats: recreating a battlefield injury in the laboratory. *J. Neurotrauma* ***26***, 827–840; DOI:10.1089/neu.2008.0748 (2009).
51. Hasan, K. M., Parker, D. L. & Alexander, A. L. Comparison of gradient encoding schemes for diffusion-tensor MRI. *J. Magn. Reson. Imaging* **13**, 769–780 (2001).
52. Budde, M. D. & Frank, J. A. Examining brain microstructure using structure tensor analysis of histological sections. *Neuroimage* **63**, 1–10, DOI:10.1016/j.neuroimage.2012.06.042 (2012).
53. Budde, M. D., Janes, L., Gold, E., Turtzo, L. C. & Frank, J. A. The contribution of gliosis to diffusion tensor anisotropy and tractography following traumatic brain injury: validation in the rat using Fourier analysis of stained tissue sections. *Brain* **134**, 2248–2260; DOI:10.1093/brain/awr161 (2011).
54. Zhang, H., Yushkevich, P. A., Alexander, D. C. & Gee, J. C. Deformable registration of diffusion tensor MR images with explicit orientation optimization. *Med. Image Anal.* **10**, 764–785; DOI:10.1016/j.media.2006.06.004 (2006).
55. Adluru, N. *et al.* A diffusion tensor brain template for rhesus macaques. *Neuroimage* **59**, 306–318; DOI:10.1016/j.neuroimage.2011.07.029 (2012).
56. Ferris, C. F. *et al.* Functional magnetic resonance imaging in awake animals. *Rev. Neurosci.* **22**, 665–674; DOI:10.1515/rns.2011.050 (2011).
57. Paxinos, G. & Watson, C. *The Rat Brain in Stereotactic Coordinates.* (Academic Press, 2007).
58. Avants, B. B. *et al.* A reproducible evaluation of ANTs similarity metric performance in brain image registration. *Neuroimage*, **54**, 2033–2044; DOI:10.1016/j.neuroimage.2010.09.025 (2011).
59. Benjamini, Y., Drai, D., Elmer, G., Kafkafi, N. & Golani, I. Controlling the false discovery rate in behavior genetics research. *Behav. Brain Res.* **125**, 279–284 (2001).

Acknowledgments

We thank the Neurotrauma Team at the Walter Reed Army Institute of Research for their technical help during the exposures, along with Eric Gold and Lindsay Janes for assistance with the MRI experiments. This work was supported by the Center for Neuroscience and Regenerative Medicine grant number G1703F.

Author contributions

A.K. and E.K. carried out animal studies, including the preparation of specimens for imaging. J.L. designed and supervised blast overpressure exposures at Walter Reed. M.B. performed and analyzed MRI/DTI measures under J.F.'s supervision at the NIH. A.K., M.B., and D.A. wrote the main manuscript text; A.K. and M.B. generated and formatted figures 1–4 and table 1. A.K. and D.A. reviewed the manuscript prior to submission.

Additional information

Competing financial interests: The authors declare no competing financial interests.

How to cite this article: Kamnaksh, A. *et al.* Diffusion Tensor Imaging Reveals Acute Subcortical Changes after Mild Blast-Induced Traumatic Brain Injury. *Sci. Rep.* **4**, 4809; DOI:10.1038/srep04809 (2014).

JOURNAL OF NEUROTRAUMA 28:2145–2153 (October 2011)

DOI: 10.1089/neu.2011.1983

Factors Affecting Blast Traumatic Brain Injury

Alaa Kamnaksh,[1,3] Erzsebet Kovesdi,[4] Sook-Kyung Kwon,[1,3] Daniel Wingo,[1] Farid Ahmed,[1,3] Neil E. Grunberg,[2,3] Joseph Long,[5] and Denes V. Agoston[1,3]

Abstract

The overlapping pathologies and functional outcomes of blast-induced TBI (bTBI) and stress-related neurobehavioral disorders like post-traumatic stress disorder (PTSD) are significant military health issues. Soldiers are exposed to multiple stressors with or without suffering bTBI, making diagnosis and treatment as well as experimental modeling of bTBI a challenge. In this study we compared anxiety levels of Naïve rats to ones that were exposed to each of the following conditions daily for 4 consecutive days: C I: transportation alone; C II: transportation and anesthesia; C III: transportation, anesthesia, and blast sounds; Injured: all three variables plus mild blast overpressure. Following behavioral testing we analyzed sera and select brain regions for protein markers and cellular changes. C I, C II, and C III animals exhibited increased anxiety, but serum corticosterone levels were only significantly elevated in C III and Injured rats. C III and Injured animals also had elevated interferon-γ (IFN-γ) and interleukin-6 (IL-6) levels in the amygdala (AD) and ventral hippocampus (VHC). Glial fibrillary acidic protein (GFAP) levels were only significantly elevated in the VHC, prefrontal cortex (PFC), and AD of Injured animals; they showed an apparent increase in ionized calcium-binding adapter molecule (Iba1) and GFAP immunoreactivity, as well as increased numbers of TUNEL-positive cells in the VHC. Our findings demonstrate that experimental conditions, particularly the exposure to blast acoustics, can increase anxiety and trigger specific behavioral and molecular changes without injury. These findings should be taken into consideration when designing bTBI studies, to better understand the role of stressors in the development of post-traumatic symptoms, and to establish a differential diagnosis for PTSD and bTBI.

Key words: behavior; inflammation; traumatic brain injury

Introduction

Psychological stress, traumatic brain injury (TBI), or a combination of the two can result in increased anxiety, memory impairment, and mood disorders (Brenner et al., 2009; Jaffee and Meyer, 2009). Neurobehavioral changes have become a significant health issue in recent military conflicts as soldiers are exposed to various psychological stressors with or without blast-induced TBI (bTBI; Brenner et al., 2009; Van Boven et al., 2009; Vasterling et al., 2009). Exposure to psychological stress alone, in the form of traumatic life-threatening events, can manifest as post-traumatic stress disorder (PTSD; Breslau and Kessler, 2001), which is especially common among soldiers (Keane et al., 2006; Richardson et al., 2010).

Earlier works have shown that bTBI is a specific form of neurotrauma (Cernak et al., 2001a,2001b,2011; Chavko et al., 2011; Pun et al., 2011; Risling et al., 2010). Neurobehavioral changes often result from bTBI and share many PTSD symptoms like altered anxiety levels and memory impairment (Okie, 2005; Ryan and Warden, 2003). Such changes have been frequently observed after survivable bTBI, both moderate and severe. Accumulating evidence shows that even exposure to mild blast overpressure can result in lasting neurobehavioral changes (Elder and Cristian, 2009; Elder et al., 2010; Rosenfeld and Ford, 2010).

Exposure to repeated mild blast overpressure poses special diagnostic challenges since there are typically no visible injuries (Belanger et al., 2007; Brenner et al., 2009), and acute neurobehavioral assessments indicate no significant

[1]Department of Anatomy, Physiology and Genetics [2]Department of Medical and Clinical Psychology, and [3]Center for Neuroscience and Regenerative Medicine at the Uniformed Services University, Bethesda, Maryland.
[4]U.S. Department of Veterans Affairs, Veterans Affairs Central Office, Washington D.C.
[5]Blast-Induced Neurotrauma Branch, Center for Military Psychiatry and Neurotrauma, Walter Reed Army Institute of Research, Silver Spring, Maryland.

impairment. Soldiers return to their duties and many are deployed numerous times. The consequences of repeated exposure to mild explosive blasts are an especially pressing issue for the military healthcare system for several reasons. These include the sheer number of soldiers exposed to repeated blasts, the apparent cumulative effect of the exposures, and the delayed onset of neurobehavioral symptoms (Rosenfeld and Ford, 2010).

Repeated exposure to low levels of blast overpressure can lead to repeated mild bTBI (mbTBI; Elder and Cristian, 2009; Elder et al., 2010; Rosenfeld and Ford, 2010). Repeated mbTBI is currently not very well defined because the observed neurobehavioral abnormalities overlap with those of PTSD (Belanger et al., 2007; Brenner et al., 2009; Vasterling et al., 2009). Importantly, it appears that there is a relationship between the number of exposures to mild explosive blast and the manifestation of neurobehavioral symptoms like anxiety (Rosenfeld and Ford, 2010). Increased anxiety suggests damage to specific neuroanatomical structures, including the ventral hippocampus (VHC), the amygdala (AD), and the prefrontal cortex (PFC), brain structures that are also indicated to be affected in PTSD (Jaffee and Meyer, 2009).

The complexity of battlefield environments combined with potential individual variability makes modeling and identifying the physical and psychological impacts of repeated mbTBI challenging. Earlier works have demonstrated that exposure to high-energy impulse noise alone can trigger distinct cellular and molecular changes (Säljö et al., 2001,2002,2008). Moreover, blast sounds (without direct exposure to high-energy impulse noise) may act as a powerful stressor capable of inducing adverse physiological changes that increase anxiety and alter behavior. This is consistent with soldiers that develop post-traumatic symptoms without sustaining any prior physical injury on the battlefield.

Attempting to mimic field conditions can help us analyze the individual contribution of each environmental factor in the development of neurobehavioral symptoms of repeated mbTBI. In this study, we aimed to control for several experimental variables (i.e., conditions) repeated for 4 consecutive days: Naïve: no experimental manipulation; C I: transportation alone; C II: transportation and anesthesia; C III: transportation, anesthesia, and blast sounds; Injured: all three variables plus exposure to mild levels of blast overpressure (Table 1).

Each of these experimental variables can potentially play a role in the observed behavioral, cellular, and molecular changes. Soldiers are exposed to various stressors, that include transportation (with the potential danger of roadside bomb detonation), heat, and the acoustic cues of blast with or without injury (Jaffee and Meyer, 2009). On the other hand, anesthesia (e.g., by isoflurane) has been shown to be a neuroprotective (Kurz et al., 1997; Xiong et al., 2003), and in turn a confounding factor in studies that include ischemia.

We found that repeated exposure to standard experimental conditions, particularly the acoustic cues of blast, can significantly increase anxiety and trigger cellular and molecular changes, even without injury. These findings suggest that the consequences of multiple blast exposure are influenced by numerous factors; direct exposure to blast overpressure is only one of them. These findings need to be taken into consideration when designing, analyzing, and interpreting bTBI studies for their implications in the overlapping pathologies of psychological stress and blast-induced physical injury.

Methods

Animals and housing conditions

A total of 34 male Sprague-Dawley rats weighing 245–265 g (Charles River Laboratories, Wilmington, MA) were used. The rats were housed 2 per standard rat cage with free access to food and water in a reverse 12-h/12-h light-dark cycle. The animals were handled according to a protocol approved by the Institutional Animal Care and Use Committee (IACUC) at the Uniformed Services University (USU). Behavioral testing was conducted during animals' dark cycle.

Injury and experimental conditions

After 5 days of acclimation and handling, all animals except Naïve rats ($n=6$) were transported daily for 4 consecutive days from USU (Bethesda, MD), to Walter Reed Army Institute of Research (WRAIR, Silver Spring, MD), and exposed to the various experimental conditions (Table 1). For the duration of the study Naïve animals were kept in the animal facility at USU with a constant room temperature of 69°F and 68% humidity; the average sound pressure level (SPL) was measured at 50 ± 10% dB. Normal and peak SPL were measured using a Precision Impulse Integrating Sound Level Meter (Model 1800; Quest Electronics, Oconomowoc, WI). Condition I animals (C I, $n=6$) were transported to WRAIR 2 per cage, but were neither anesthetized nor exposed to the acoustic cues of blast. The rats remained in the vehicle (with food and water *ad libitum*) and were not brought into the facility; the temperature inside the vehicle ranged from 85–92°F, humidity was 54–88%, and SPL was 47–75 dB. Condition II animals (C II, $n=6$) were transported and anesthetized, but not exposed to the acoustics of blast. The rats were placed in an induction chamber and anesthetized for 6 min with 4% isoflurane (Baxter Healthcare Corporation, Deerfield, IL). Following anesthesia, C II rats were removed from the facility prior to any blast exposures and returned to the vehicle; temperature in the holding room was 73°F, humidity was 62%, and SPL was 55 ± 10% dB. Condition III animals (C III, $n=8$) were transported, anesthetized, and exposed to blast sounds. Blast sounds were generated by the blast tube during Injured animals' exposure to mild blast. C III rats were kept in the adjacent holding room for the length of the Injured animals' exposures. Peak SPL during blast overpressure was measured at 95 ± 10% dB. Injured animals ($n=8$; weight ~300 g) were transported, anesthetized, and exposed to blast sounds, as well as blast overpressure using a compression-driven shock tube (Long et al., 2009). Following anesthesia the rats were placed in the shock tube holder in a transverse prone position and exposed to whole-body blast overpressure while wearing chest protection. Blast procedures were conducted as previously described (Kovesdi et al., 2011). The duration of apnea was measured for Injured animals, after which they were returned to their cages. After completion of the blast exposures, all animals were transported back to the USU animal facility.

Behavioral test: Elevated plus maze (EPM)

On the last day of the exposures, basic motor activity and anxiety were measured with an EPM (Kovesdi et al., 2011; Kwon et al., 2011). Briefly, the rats were placed one by one in the center of the maze facing one of the open arms; each

Table 1. Experimental Variables and Animal Groups

Experimental variables				
Group	*Transportation*	*Anesthesia*	*Blast acoustic cues*	*Mild blast TBI*
Naïve ($n=6$)	−	−	−	−
C I ($n=6$)	+	−	−	−
C II ($n=6$)	+	+	−	−
C III ($n=8$)	+	+	+	−
Injured ($n=8$)	+	+	+	+

Transportation			
Duration	*Total distance travelled*	*Temperature*	*Sound pressure level (SPL)*
35 min	6.7 meters	85–92°F	47–75 dB

Anesthesia			
Duration	*Type*	*Concentration*	*Air pressure*
6 min	Isoflurane	4%	~2 psi

Blast acoustic cues			
Normal SPL (in holding room)	*Peak SPL (in holding room)*	*Amount*	*Frequency*
55 ± 10% dB	95 ± 10% dB	8 × daily	6 min apart

Mild blast TBI			
Mylar membrane thickness	*Total pressure*	*Total overpressure duration*	*Apnea*
355.6 μm	19.41 psi	10.60 msec	15 sec

The tabulated values for duration, temperature, SPL, blast pressure, and apnea are 4-day averages. Anesthesia duration and concentration, distance travelled, and frequency are exact. Each group was exposed to a different combination of the described experimental variables. All groups (except Naïve animals) were exposed to their designated conditions daily for 4 consecutive days.

psi, pounds per square inch; TBI, traumatic brain injury; dB, decibel.

animal was allowed to explore freely for 5 min while its movement was video tracked. Total distance travelled (meters) and time spent (seconds) in the center and in each arm was recorded using ANY-maze 4.2 Software (Stoelting Company, Wood Dale, IL).

Tissue collection and processing

One day after behavioral testing, the animals were placed inside an induction chamber saturated with isoflurane and deeply anesthetized. For the reverse phase protein microarray (RPPM) and enzyme-linked immunosorbent assays (ELISA; Naïve = 4, C I = 4, C II = 4, C III = 5, and Injured = 5), the rats were decapitated and the brains were immediately removed and placed in ice. The AD, PFC, and VHC were then dissected, flash frozen in dry ice, and stored at −80°C.

For histology (Naïve = 2, C I = 2, C II = 2, C III = 3, and Injured = 3), the rats were placed under deep isoflurane anesthesia and transcardially perfused with cold phosphate-buffered saline (PBS) followed by 4% paraformaldehyde solution. The fixed brains were then immersed in cold 15% and 30% sucrose in 1 × PBS (consecutively) for cryoprotection. The frozen brains were sectioned coronally at 20 μm thickness using a cryostat (Cryocut 1800; Leica Microsystems, Bannockburn, IL), and sections containing the VHC were kept at −80°C until use.

Protein measures

Preparation of samples. Sample preparation, printing, scanning, and data analysis were performed using RPPM technology as previously described (Gyorgy et al., 2010). Frozen brain sections were immersed in 500 mL T-PER solution with protease and phosphatase inhibitors and sonicated on ice. Serum samples were centrifuged for 15 min at 4°C, and the supernatants were aliquotted and stored at −80°C. Tissue samples were diluted in print buffer to 1 mg/mL, and then diluted in an 11-step dilution in 96-well plates. The samples and dilutions were added to Genetix 384-well plates (X7022; Fisher Scientific, Pittsburgh, PA) using a JANUS Varispan Integrator and Expanded Platform Workstation (PerkinElmer, Waltham, MA), which was programmed to add the samples in a specific pattern for the Aushon Arrayer (Aushon Biosystems, Billerica, MA). The plates were added to the Aushon Arrayer and printed on single nitrocellulose pad slides.

Printing parameters

The Aushon Arrayer was programmed to use 16 pins (4 × 4 pattern). The 384-plate sample configuration and Aushon program were set to print the 12-point dilution in a triplicate 3 × 12 block. Tissue samples were printed two touches per spot, while serum samples were printed with one touch.

Immunochemical detection

Primary antibodies were diluted to 10× the optimal Western blot analysis concentration in antibody incubation buffer. Primary antibodies were diluted to the recommended concentrations: vascular endothelial growth factor (VEGF) 1:100 and glial fibrillary acidic protein (GFAP) 1:5000, and then incubated overnight at 4°C with a cover-slip. On the following day the slides were washed and then incubated with Alexa Fluor® 635 goat anti-mouse (cat. no. A-31574), goat anti-rabbit (cat. no. A-31576), or rabbit anti-goat IgG (cat. no. A-21086) secondary antibodies from Invitrogen (Carlsbad, CA) at 1:6000 dilution in antibody incubation buffer for 1 h at room temperature. After drying, the slides were scanned and data were imported into a bioinformatics program. More information on the primary and secondary antibodies can be found in detail elsewhere (Gyorgy et al., 2010).

Data analysis

Data from the scanned images were imported into a Microsoft Excel-based bioinformatics program developed in house for analysis (Gyorgy et al., 2010). The tool calculates the net intensity of the primary antibody compared to the secondary antibody, and graphs it in a linear logarithmic regression format as previously described (Gyorgy et al., 2010).

Corticosterone (CORT) assay

CORT levels were measured using Cayman's Corticosterone Enzyme Immunoassay (EIA) Kit according to the manufacturer's instructions (Cayman Chemical, Ann Arbor, MI). Each sample was diluted 1:500 and measured in triplicate.

Interleukin-6 (IL-6) and interferon-γ (IFN-γ) assays

IFN-γ and IL-6 levels were measured from brain tissues using the rat interferon-γ ELISA and the rat IL-6 ELISA kits (both from Thermo Fisher, Waltham, MA). The assays were performed according to the manufacturer's instructions.

Histology

Immunohistochemistry. Immunohistochemical stainings were performed as previously described (Kwon et al., 2011). Frozen sections containing the VHC were selected and incubated in mouse anti-GFAP (1:400; Millipore, Temecula, CA) and goat anti-Iba1 (1:1000, ionized calcium-binding adapter molecule; Abcam, Cambridge, MA) overnight at 4°C. After washing with 1×PBS, the sections were incubated with corresponding secondary antibodies (1:100 Alexa Fluor 488 goat anti-mouse IgG and 1:100 Alexa Fluor 488 donkey anti-goat IgG; Invitrogen) for 1 h at room temperature. The sections were washed with 1×PBS and cover-slipped using anti-fading media (Vectashield; Vector Laboratories, Burlingame, CA).

TUNEL assay

The extent of DNA fragmentation was determined using a terminal-deoxy-transferase-mediated dUTP nick-end labeling (TUNEL) *in situ* cell death detection kit, POD (Roche, Indianapolis, IN), according to the manufacturer's instructions and as previously described (Kwon et al., 2011). The TUNEL reaction was performed for 1 h at 37°C; TUNEL-positive cells were visualized by 3,3′-diaminobenzidine (DAB) substrate, and were counted from four sections per animal.

Histological data acquisition

The sections were viewed in an Olympus IX-71 microscope, and images were collected using a SPOT digital camera (Diagnostic Instruments Inc., Sterling Heights, MI), and processed as previously described (Kwon et al., 2011).

Statistical analysis and data comparison

Behavioral and proteomics results were analyzed with analysis of variance (ANOVA) and Tukey *post-hoc* tests. TUNEL histology results were analyzed with a two-tailed Student's *t*-test. Statistical analyses were performed using Graph Pad Instat software (GraphPad Software, San Diego, CA). Data are reported as the average ± standard error of the mean. For each of our numerical measurements, we determined whether the differences among experimental groups were statistically significant ($p < 0.05$ is depicted by one asterisk, $p < 0.01$ by two asterisks, and $p < 0.001$ by three asterisks).

Results

Basic motor function and anxiety

We found that animals in experimental groups C I, C II, and C III travelled somewhat shorter distances than Naïve rats as measured in the EPM. The differences among the three conditions were not statistically significant when compared to Naïve rats or to one another. On the other hand, Injured animals travelled significantly shorter distances than Naïve rats (Fig. 1A).

C I, C II, and C III animals spent significantly less time in the open arms of the maze compared to Naïve rats. The differences between the three experimental conditions were not significant. Injured animals also spent less time in the open arms of the maze compared to Naïve rats, but the difference was not statistically significant (Fig. 1B).

All experimental groups spent more time in the closed arms of the maze than Naïve rats. Injured animals spent the longest time in the closed arms. Due to substantial variations among animals there were no statistically significant differences among any of the experimental groups (Fig. 1C).

We also measured the time the animals spent in the central area of the maze. We saw a trend that somewhat mirrored what we observed in the closed arms; Injured animals spent the least amount of time in the center compared to Naïve or C I rats (Fig. 1D).

Serum corticosterone levels

Serum CORT levels of C I and C II rats were not significantly different from those measured in Naïve rats (Fig. 2). However, C III and Injured animals had significantly increased CORT levels, more than 2× and ~ 2.5× higher than Naïve rats, respectively.

Protein markers in select brain regions

GFAP levels were significantly higher in all measured brain regions of Injured animals only, except for C III animals, which also had significantly elevated GFAP tissue levels in the AD compared to Naïve animals (Fig. 2).

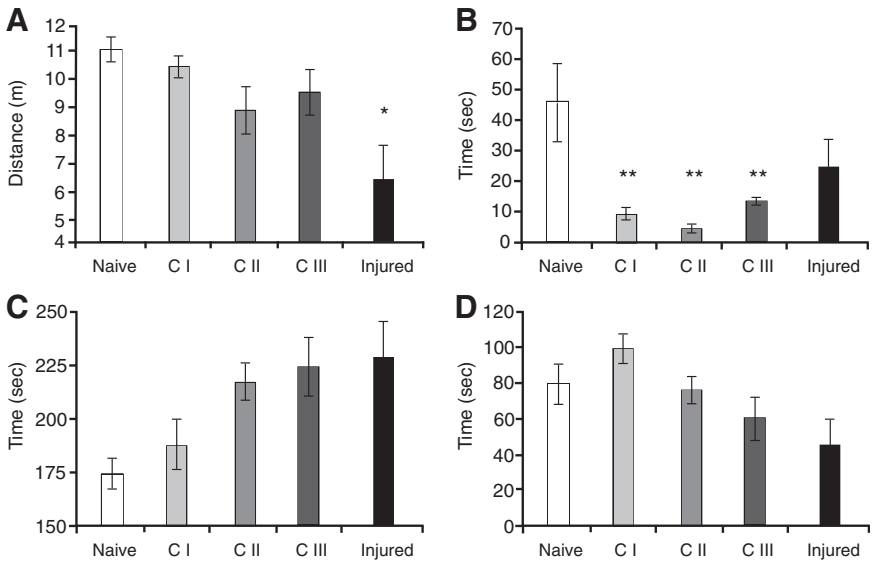

FIG. 1. Anxiety and basic motor function of the animals in the various experimental groups. An elevated plus maze (EPM) was used to measure changes in basic motor function and anxiety levels. (**A**) Total distance travelled (meters). (**B**) Time spent (seconds) in the open arms. (**C**) Time spent (seconds) in the closed arms. (**D**) Time spent (seconds) in the center. Data are presented as mean ± standard error of the mean (*$p < 0.05$ and **$p < 0.01$ compared to Naïve rats).

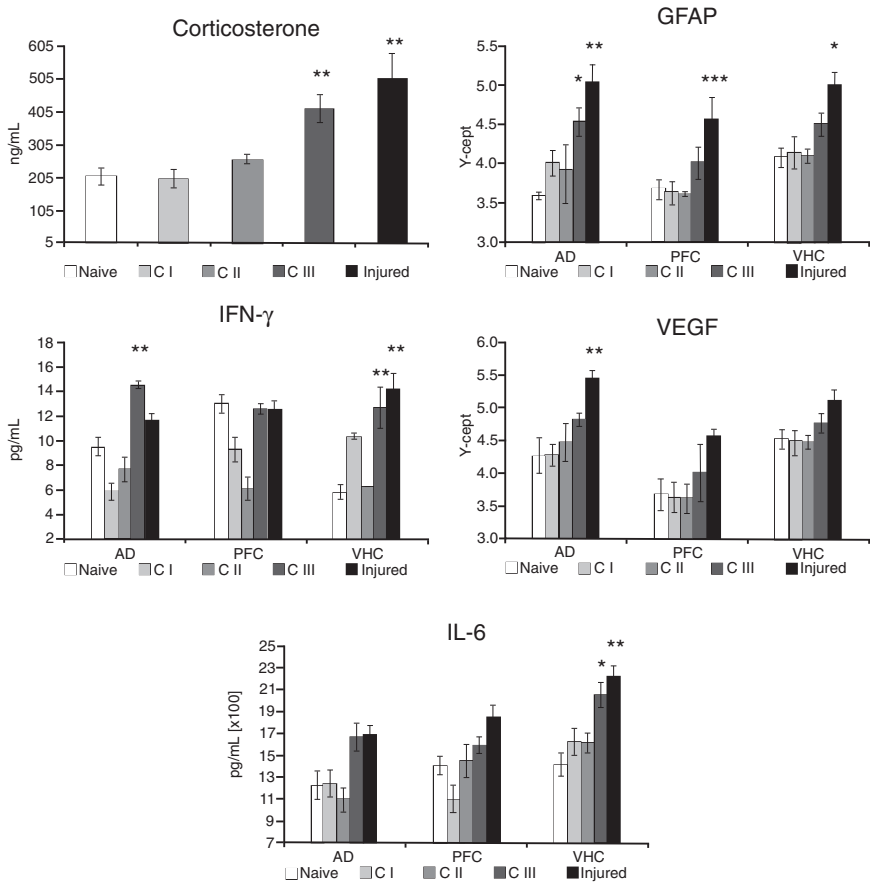

FIG. 2. Protein markers in the AD, the PFC, and the VHC of animals in the various experimental groups. Tissue extracts were prepared from dissected brain regions of Naïve, C I, C II, C III, and Injured rats. Tissue levels of GFAP and VEGF were assayed using RPPM; IL-6, IFN-γ, and corticosterone using ELISA. The Y-axis intercept (Y-cept) and pg or ng/mL indicate measured protein levels (*$p < 0.05$, **$p < 0.01$, and ***$p < 0.001$; data are presented as mean ± standard error of the mean; IFN-γ, interferon-γ; IL-6, interleukin-6; GFAP, glial fibrillary acidic protein; VEGF, vascular endothelial growth factor; AD, amygdala; VHC, ventral hippocampus; PFC, prefrontal cortex; RPPM, reverse phase protein microarray; ELISA, enzyme-linked immunosorbent assay).

We found the highest levels of IFN-γ in the AD and the VHC of Injured and C III animals (Fig. 2); IFN-γ levels in the same brain regions of C I and C II animals were not significantly different from those of Naïve animals. Interestingly, IFN-γ levels in the PFC of C I and C II rats were much lower than the values in the Injured and C III animals.

VEGF showed a similar trend to GFAP levels across all experimental groups, with VEGF values being highest in the brains of Injured animals and lowest in Naïve animals (Fig. 2). VEGF levels were only significantly elevated in the AD of Injured animals.

IL-6 values were significantly higher in the VHC of the Injured and C III groups compared to Naïve animals (Fig. 2). We found that IL-6 levels in the AD and the PFC showed a somewhat similar trend, but the differences in IL-6 tissue levels of C III and Injured rats were not statistically significant.

Cellular changes

We saw elevated Iba1 immunoreactivity in the VHC of Injured rats (Fig. 3A). Of the other experimental groups, only C II animals displayed a slight increase in Iba1 immunoreactivity, but to a lesser degree than in the Injured animals.

The changes we observed using GFAP immunohistochemistry were similar to those measured by proteomics in the VHC. We found an apparent increase in GFAP immunoreactivity in the VHC of Injured animals (Fig. 3B). Interestingly, GFAP expression also appeared to be slightly elevated in the VHC of C III animals.

We assessed changes in the number of TUNEL-positive cells in the hilus and the granular cell layer (GCL) of the VHC. We found that the number of TUNEL-positive cells was increased significantly in the GCL of the VHC of Injured animals only (Fig. 4A). Interestingly, the animals in groups C I and C III had lower numbers of TUNEL-positive cells in the hilus of the VHC.

Discussion

Standard experimental conditions that model select battlefield environments, particularly repeated exposure to the acoustic cues of blast, can significantly increase anxiety and induce cellular and molecular changes, even without injury. However, the observed gliotic response and significant cell death is caused by repeated exposure to mild blast overpressure. These findings support and extend our previous observations about the complexity of factors affecting and/or contributing to the outcome of bTBI (Kwon et al., 2011). At the experimental level, our findings highlight the importance of using appropriate sham groups when designing bTBI studies. We believe that our findings will contribute to a better understanding of the similarities and differences between the pathobiologies associated with environmental stressors and blast-induced physical injury.

Stressors like daily travel, handling, and repeated exposure to the acoustic cues of blast (without injury) significantly increase anxiety. Elevated anxiety may in turn increase vulnerability to and/or worsen the outcome of physical injury (e.g., explosive blast). We have shown earlier that exposing chronically stressed animals to mild blast overpressure prolongs the period of increased anxiety (Kwon et al., 2011). Although the contribution of repeated stress and mild blast exposure to the development of PTSD-like symptoms is currently unknown, repeatedly exposing animals to the acoustic cues of blast can increase serum CORT levels almost as significantly as when combined with blast injury. Abnormal serum CORT levels can alter the inflammatory response (Garcia-Bueno et al., 2008; Miller et al., 2009; Sorrells et al., 2009).

IL-6 and IFN-γ were both significantly elevated in the VHC and the AD of animals repeatedly exposed to the acoustic cues of blast without injury (C III). Repeated exposure to mild blast further increased serum CORT as well as brain IL-6 and IFN-γ levels; these changes corresponded very well with the measured functional outcome (i.e., increased anxiety). In addition to the VHC, the AD is a major neuroanatomical substrate of anxiety (Bannerman et al., 2004; Holscher, 2003). However, the relationship between IL-6 and IFN-γ levels in these brain regions and neurotransmitter systems is not clear at this point (Blalock, 1989; Haddad et al., 2002). Elevated IL-6 levels may contribute to increased cell death due to its neurotoxic effect (Lenzlinger et al., 2001; Stoll et al., 2000).

We found significantly increased numbers of TUNEL-positive cells in the VHC of Injured animals, but not in the VHC of C III animals. This is consistent with our previous finding that blast injury triggers a significant increase in the number of TUNEL-positive cells, while chronic stress has no significant effect (Kwon et al., 2011). In addition to an increase in DNA fragmentation, our histology indicated that the increase in GFAP immunoreactivity is another pathological change specific to injury. Increased GFAP immunoreactivity, combined with a stellar morphology, is a hallmark of practically all TBIs (Eng and Ghirnikar, 1994; Fitch and Silver, 2008).

We previously hypothesized that elevated tissue levels of VEGF are another injury-specific marker (Agoston et al., 2009; Kwon et al., 2011). In this experiment, we only found elevated tissue levels of VEGF in the VHC, PFC, and AD of Injured animals; the rats in all other experimental conditions had tissue levels similar to the VEGF levels measured in Naïve rats. A key factor in increasing VEGF levels is hypoxia; Injured animals sustained a moderate period of apnea, lasting for 15 sec on average. The resulting hypoxia may be responsible for the increase in VEGF levels and the downstream pathological cascade that potentially distinguishes stress from injury associated with apnea. VEGF is a multifunctional molecule (Rosenstein and Krum, 2004) involved in mediating various pathological processes, including increased vascular permeability following TBI (Agoston et al., 2009; Skold et al., 2005).

Increased membrane permeability, early gene induction in certain brain regions, and possible microglia activation have been shown to result from a single exposure to impulse noise at around 200 dB (Säljö et al., 2001,2002,2003). It is important to note that in our experimental set-up, C III and Injured animals were not exposed to such high intensity noises (Table 1); the acoustic cues C III and Injured animals were exposed to likely act as additional stressors rather than direct pressure wave energy experienced as impulse noise (Dancer et al., 1998). As discussed above, we found significantly elevated levels of IL-6 and IFN-γ in the VHC of C III animals. Similarly, serum CORT levels were significantly elevated in the same group of animals. Our findings suggest that repeated exposure to the acoustic cues of blast may serve as an effective stressor that triggers distinct neurobehavioral changes implicated in the development of post-traumatic symptoms, and possibly shell-shock or PTSD in soldiers (Guy, 2004; Rosenfeld and Ford, 2010).

Although the detected functional change was not matched by changes in tested cellular and molecular markers,

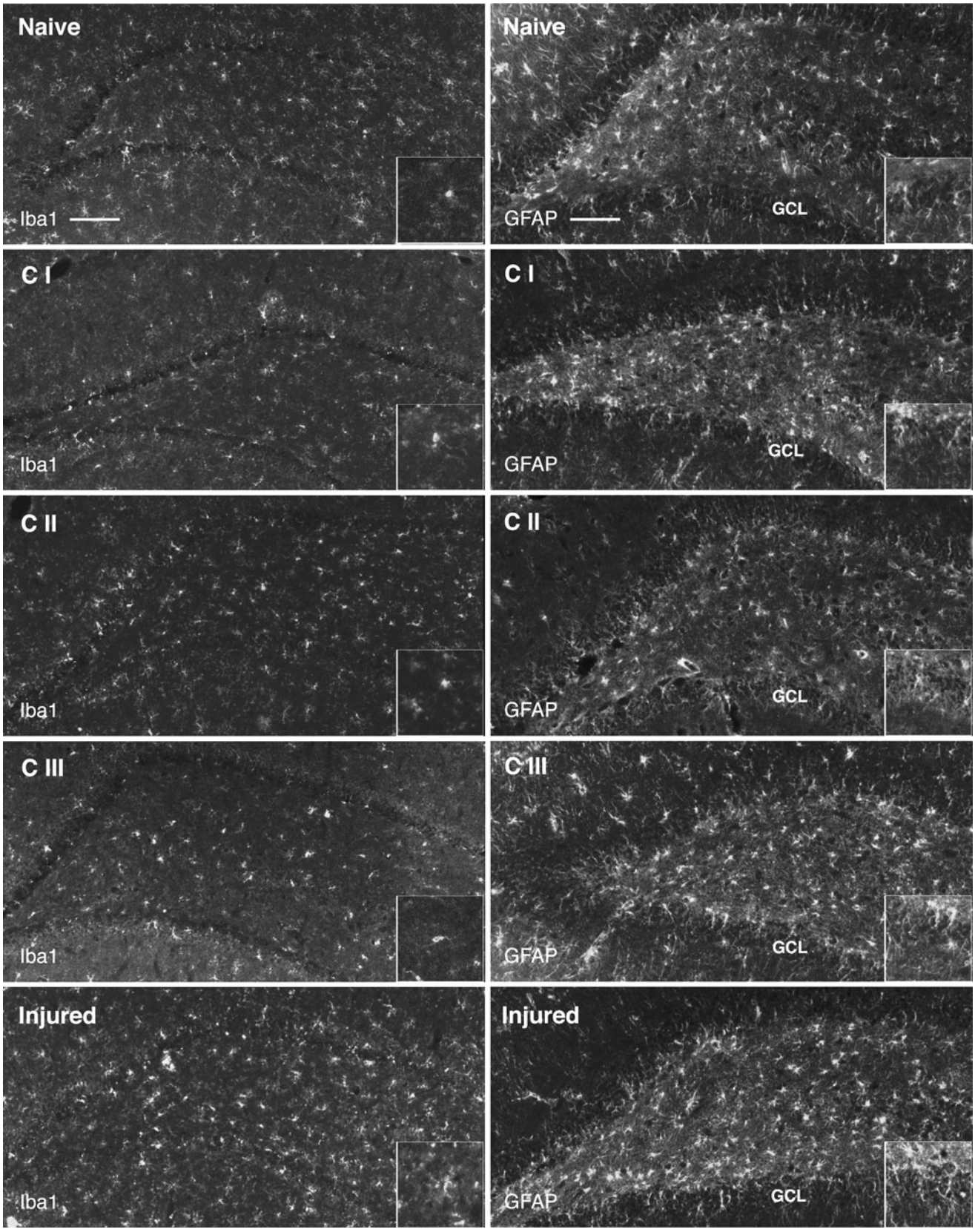

FIG. 3. (**A**) Ionized calcium-binding adapter molecule (Iba1-), and (**B**) glial fibrillary acidic protein (GFAP)-immunoreactive cells in the ventral hippocampus (VHC) of Naïve, C I, C II, C III, and Injured rats. Repeated mild blast-induced bTBI traumatic brain injury resulted in increased GFAP expression and branching in the granular cell layer (GCL), and Iba1 immunoreactivity in the VHC (scale bar = 100 μm).

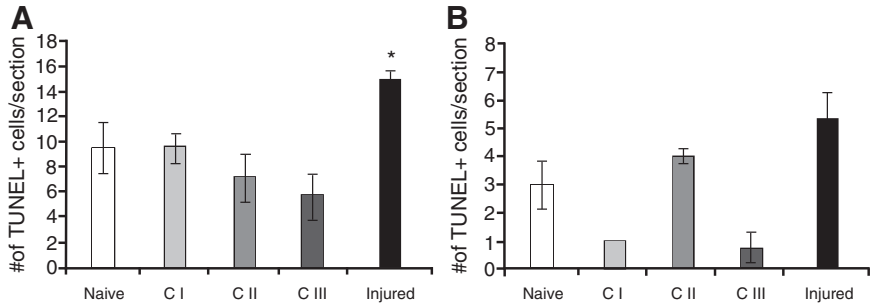

FIG. 4. TUNEL apoptotic cells in the GCL (**A**) and in the hilus (**B**) of the VHC. A significant increase in TUNEL-positive cells was only detected in the GCL of the VHC of Injured rats. C I and C III animals had lower numbers of TUNEL-positive cells in the hilus of the VHC. Data are presented as mean ± standard error of the mean (*$p < 0.05$ compared to Naïve rats; VHC, ventral hippocampus; GCL, granular cell layer; TUNEL, terminal-deoxy-transferase-mediated dUTP nick-end labeling).

transportation alone had a significant effect on anxiety in C I animals. In a military blast environment, travel in potentially dangerous areas adds a considerable amount of stress on soldiers. Experimentally, confounding factors (e.g., anesthesia) associated with animal studies make it more challenging to ascertain the exact pathological and symptomatic contribution of stress and injury.

Anesthetics like isoflurane can exert complex neuroprotective effects on the injured brain (Xiong et al., 2003). Moreover, repeated exposure to isoflurane can provide significant dose-dependent neuroprotection against the effects of ischemia, including reduced neuronal death (Zhang et al., 2010). However, in our current study, all animals except Naïve animals were exposed to the same duration, concentration, and frequency of anesthesia, thus ruling out anesthesia as a major confounding factor. Similarly, the relative contribution of the transportation stress is equal across all experimental groups.

In summary, we found that repeated exposure to standard experimental conditions, particularly the acoustics of blast, increases anxiety and triggers specific cellular and molecular changes. Importantly, it is the direct exposure to blast overpressure that triggers the gliotic response and cellular death. These findings need to be taken into account when designing, analyzing, and interpreting bTBI studies. When independently verified, our findings will help in the development of tools to distinguish between psychological and physical traumas and their overlapping pathologies as evidenced in bTBI and PTSD.

Acknowledgments

We thank the Neurotrauma Team (WRAIR) for their technical help during the exposures. This work was supported by Center for Neuroscience and Regenerative Medicine (CNRM) grant no. G1703F.

Author Disclosure Statement

The views, opinions, and/or findings contained herein are those of the authors and should not be construed as an official position, policy, or decision of the Department of the Army or the Department of Defense. The authors have no financial disclosures.

Animal handling and treatments were conducted in compliance with the Animal welfare Act and other Federal statutes and regulations related to animals and experiments involving animals, and adhered to principles stated in the Guide to the Care and Use of Laboratory Animals, National Research Council. The facilities are fully accredited by the Association for Assessment and Accreditation of Laboratory Animal Care International.

References

Agoston, D.V., Gyorgy A., Eidelman, O., and Pollard, H.B. (2009). Proteomic biomarkers for blast neurotrauma: targeting cerebral edema, inflammation, and neuronal death cascades. J. Neurotrauma 26, 901–911.

Bannerman, D.M., Rawlins, J.N., McHugh, S.B., Deacon, R.M., Yee, B.K., Bast, T., Zhang, W.N., Pothuizen, H.H., and Feldon, J. (2004). Regional dissociations within the hippocampus—memory and anxiety. Neurosci. Biobehav. Rev. 28, 273–283.

Belanger, H.G., Vanderploeg, R.D., Curtiss, G., and Warden, D.L. (2007). Recent neuroimaging techniques in mild traumatic brain injury. J. Neuropsychiatry Clin. Neurosci. 19, 5–20.

Blalock, J.E. (1989). A molecular basis for bidirectional communication between the immune and neuroendocrine systems. Physiol. Rev. 69, 1–32.

Brenner, L.A., Vanderploeg, R.D., and Terrio, H. (2009). Assessment and diagnosis of mild traumatic brain injury, posttraumatic stress disorder, and other polytrauma conditions: burden of adversity hypothesis. Rehabil. Psychol. 54, 239–246.

Breslau, N., and Kessler, R.C. (2001). The stressor criterion in DSM-IV posttraumatic stress disorder: an empirical investigation. Biol. Psychiatry 50, 699–704.

Cernak, I., Merkle, A.C., Koliatsos, V.E., Bilik, J.M., Luong, Q.T., Mahota, T.M., Xu, L., Slack, N., Windle, D., and Ahmed, F.A. (2011). The pathobiology of blast injuries and blast-induced neurotrauma as identified using a new experimental model of injury in mice. Neurobiol. Dis. 41, 538–551.

Cernak, I., Wang, Z., Jiang, J., Bian, X., and Savic, J. (2001a). Cognitive deficits following blast injury-induced neurotrauma: possible involvement of nitric oxide. Brain Inj. 15, 593–612.

Cernak, I., Wang, Z., Jiang, J., Bian, X., and Savic, J. (2001b). Ultrastructural and functional characteristics of blast injury-induced neurotrauma. J. Trauma 50, 695–706.

Chavko, M., Watanabe, T., Adeeb, S., Lankasky, J., Ahlers, S.T., and McCarron, R.M. (2011). Relationship between orientation to a blast and pressure wave propagation inside the rat brain. J. Neurosci. Methods 195, 61–66.

Dancer, A., Buck, K., Parmentier, G., and Hamery, P. (1998). The specific problems of noise in military life. Scand. Audiol. Suppl. 48, 123–130.

Elder, G.A., and Cristian, A. (2009). Blast-related mild traumatic brain injury: mechanisms of injury and impact on clinical care. Mt. Sinai J. Med. 76, 111–118.

Elder, G.A., Mitsis, E.M., Ahlers, S.T., and Cristian, A. (2010). Blast-induced mild traumatic brain injury. Psychiatr. Clin. North Am. 33, 757–781.

Eng, L.F., and Ghirnikar, R.S. (1994). GFAP and astrogliosis. Brain Pathol. 4, 229–237.

Fitch, M.T., and Silver, J. (2008). CNS injury, glial scars, and inflammation: Inhibitory extracellular matrices and regeneration failure. Exp. Neurol. 209, 294–301.

Garcia-Bueno, B., Caso, J.R., and Leza, J.C. (2008). Stress as a neuroinflammatory condition in brain: damaging and protective mechanisms. Neurosci. Biobehav. Rev. 32, 1136–1151.

Guy, R.J. (2004). Shell shock. J. R. Soc. Med. 97, 255–256.

Gyorgy, A.B., Walker, J., Wingo, D., Eidelman, O., Pollard, H.B., Molnar, A., and Agoston, D.V. (2010). Reverse phase protein microarray technology in traumatic brain injury. J. Neurosci. Methods.

Haddad, J.J., Saade, N.E., and Safieh-Garabedian, B. (2002). Cytokines and neuro-immune-endocrine interactions: a role for the hypothalamic-pituitary-adrenal revolving axis. J. Neuroimmunol. 133, 1–19.

Holscher, C. (2003). Time, space and hippocampal functions. Rev. Neurosci. 14, 253–284.

Jaffee, M.S., and Meyer, K.S. (2009). A brief overview of traumatic brain injury (TBI) and post-traumatic stress disorder (PTSD) within the Department of Defense. Clin. Neuropsychol. 23, 1291–1298.

Keane, T.M., Marshall, A.D., and Taft, C.T. (2006). Posttraumatic stress disorder: etiology, epidemiology, and treatment outcome. Annu. Rev. Clin. Psychol. 2, 161–197.

Kovesdi, E., Gyorgy, A.B., Kwon, S.K., Wingo, D.L., Kamnaksh, A., Long, J.B., Kasper, C.E., and Agoston, D.V. (2011). The effect of enriched environment on the outcome of traumatic brain injury; a behavioral, proteomics, and histological study. Front. Neurosci. 5, 42.

Kurz, A., Xiong, J., Sessler, D.I., Plattner, O., Christensen, R., Dechert, M., and Ikeda, T. (1997). Isoflurane produces marked and nonlinear decreases in the vasoconstriction and shivering thresholds. Ann. NY Acad. Sci. 813, 778–785.

Kwon, S.K., Kovesdi, E., Gyorgy, A.B., Wingo, D., Kamnaksh, A., Walker, J., Long, J.B., and Agoston, D.V. (2011). Stress and traumatic brain injury: a behavioral, proteomics, and histological study. Front. Neurol. 2, 12.

Lenzlinger, P.M., Morganti-Kossmann, M.C., Laurer, H.L., and McIntosh, T.K. (2001). The duality of the inflammatory response to traumatic brain injury. Mol. Neurobiol. 24, 169–181.

Long, J.B., Bentley, T.L., Wessner, K.A., Cerone, C., Sweeney, S., and Bauman, R.A. (2009). Blast overpressure in rats: recreating a battlefield injury in the laboratory. J. Neurotrauma 26, 827–840.

Miller, A.H., Maletic, V., and Raison, C.L. (2009). Inflammation and its discontents: the role of cytokines in the pathophysiology of major depression. Biol. Psychiatry 65, 732–741.

Okie, S. (2005). Traumatic brain injury in the war zone. N. Engl. J. Med. 352, 2043–2047.

Pun, P.B., Kan, E.M., Salim, A., Li, Z., Ng, K.C., Moochhala, S.M., Ling, E.A., Tan, M.H., and Lu, J. (2011). Low level primary blast injury in rodent brain. Front. Neurol. 2, 19.

Richardson, L.K., Frueh, B.C., and Acierno, R. (2010). Prevalence estimates of combat-related post-traumatic stress disorder: critical review. Aust. NZ J. Psychiatry 44, 4–19.

Risling, M., Plantman, S., Angeria, M., Rostami, E., Bellander, B.M., Kirkegaard, M., Arborelius, U., and Davidsson, J. (2010). Mechanisms of blast induced brain injuries, experimental studies in rats. Neuroimage.

Rosenfeld, J.V., and Ford, N.L. (2010). Bomb blast, mild traumatic brain injury and psychiatric morbidity: a review. Injury 41, 437–443.

Rosenstein, J.M., and Krum, J.M. (2004). New roles for VEGF in nervous tissue—beyond blood vessels. Exp. Neurol. 187, 246–253.

Ryan, L.M., and Warden, D.L. (2003). Post concussion syndrome. Int. Rev. Psychiatry 15, 310–316.

Säljö, A., Arrhen, F., Bolouri, H., Mayorga, M., and Hamberger, A. (2008). Neuropathology and pressure in the pig brain resulting from low-impulse noise exposure. J. Neurotrauma 25, 1397–1406.

Säljö, A., Bao, F., Hamberger, A., Haglid, K.G., and Hansson, H.A. (2001). Exposure to short-lasting impulse noise causes microglial and astroglial cell activation in the adult rat brain. Pathophysiology 8, 105–111.

Säljö, A., Bao, F., Jingshan, S., Hamberger, A., Hansson, H.A., and Haglid, K.G. (2002). Exposure to short-lasting impulse noise causes neuronal c-Jun expression and induction of apoptosis in the adult rat brain. J. Neurotrauma 19, 985–991.

Säljö, A., Huang, Y.L., and Hansson, H.A. (2003). Impulse noise transiently increased the permeability of nerve and glial cell membranes, an effect accentuated by a recent brain injury. J. Neurotrauma 20, 787–794.

Skold, M.K., von Gertten, C., Sandberg-Nordqvist, A.C., Mathiesen, T., and Holmin, S. (2005). VEGF and VEGF receptor expression after experimental brain contusion in rat. J. Neurotrauma 22, 353–367.

Sorrells, S.F., Caso, J.R., Munhoz, C.D., and Sapolsky, R.M. (2009). The stressed CNS: when glucocorticoids aggravate inflammation. Neuron 64, 33–39.

Stoll, G., Jander, S., and Schroeter, M. (2000). Cytokines in CNS disorders: neurotoxicity versus neuroprotection. J. Neural Transm. Suppl. 59, 81–89.

Van Boven, R.W., Harrington, G.S., Hackney, D.B., Ebel, A., Gauger, G., Bremner, J.D., D'Esposito, M., Detre, J.A., Haacke, E.M., Jack, C.R., Jr., Jagust, W.J., Le Bihan, D., Mathis, C.A., Mueller, S., Mukherjee, P., Schuff, N., Chen, A., and Weiner, M.W. (2009). Advances in neuroimaging of traumatic brain injury and posttraumatic stress disorder. J. Rehabil. Res. Dev. 46, 717–757.

Vasterling, J.J., Verfaellie, M., and Sullivan, K.D. (2009). Mild traumatic brain injury and posttraumatic stress disorder in returning veterans: perspectives from cognitive neuroscience. Clin. Psychol. Rev. 29, 674–684.

Xiong, L., Zheng, Y., Wu, M., Hou, L., Zhu, Z., Zhang, X., and Lu, Z. (2003). Preconditioning with isoflurane produces dose-dependent neuroprotection via activation of adenosine triphosphate-regulated potassium channels after focal cerebral ischemia in rats. Anesth. Analg. 96, 233–237, table of contents.

Zhang, H.P., Yuan, L.B., Zhao, R.N., Tong, L., Ma, R., Dong, H.L., and Xiong, L. (2010). Isoflurane preconditioning induces neuroprotection by attenuating ubiquitin-conjugated protein aggregation in a mouse model of transient global cerebral ischemia. Anesth. Analg. 111, 506–514.

Address correspondence to:
Denes V. Agoston, M.D.
Department of Anatomy, Physiology, and Genetics
School of Medicine
Uniformed Services University
4301 Jones Bridge Road
Bethesda, MD 20814

E-mail: vagoston@usuhs.edu

Alaa Kamnaksh[1,2]
Sook-Kyung Kwon[1,2]
Erzsebet Kovesdi[3]
Farid Ahmed[1,2]
Erin S. Barry[2,4]
Neil E. Grunberg[2,4]
Joseph Long[5]
Denes Agoston[1,2]

[1]Department of Anatomy, Physiology and Genetics
[2]Center for Neuroscience and Regenerative Medicine at the Uniformed Services University, Bethesda, MD, USA
[3]U.S. Department of Veterans Affairs, Veterans Affairs Central Office, Washington, DC, USA
[4]Department of Medical and Clinical Psychology
[5]Blast-Induced Neurotrauma Branch, Center for Military Psychiatry and Neuroscience, Walter Reed Army Institute of Research, Silver Spring, MD, USA

Received June 15, 2012
Revised September 11, 2012
Accepted September 18, 2012

Research Article

Neurobehavioral, cellular, and molecular consequences of single and multiple mild blast exposure

Mild traumatic brain injury, caused by the exposure to single or repeated blast overpressure, is a principal concern due to its pathological complexity and neurobehavioral similarities with posttraumatic stress disorder. In this study, we exposed rats to a single or multiple (five total; administered on consecutive days) mild blasts, assessed their behavior at 1 and 16 days postinjury) and performed histological and protein analyses of brains and plasma at an early (2 h) and a late (22 days) termination time point. One day postinjury, multiple-injured (MI) rats showed the least general locomotion and the most depression- and anxiety-related behaviors among the experimental groups; there were no such differences at 16 days. However, at the later time point, both injured groups displayed elevated levels of select protein biomarkers. Histology showed significantly increased numbers of TUNEL+ (terminal-deoxy-transferase-mediated dUTP nick-end labeling)-positive cells in the dorsal and ventral hippocampus (DHC and VHC) of both injured groups as early as 2 h after injury. At 22 days, the increase was limited to the VHC of MI animals. Our findings suggest that the exposure to mild blast overpressure triggers early hippocampal cell death as well as neuronal, glial, and vascular damage that likely contribute to significant, albeit transient increases in depression- and anxiety-related behaviors. However, the severity of the observed pathological changes in MI rats failed to support the hypothesized cumulative effect of repeated injury. We infer that at this blast frequency, a potential conditioning phenomenon counteracts with and reduces the extent of subsequent damage in MI rats.

Keywords:
Blast / Cumulative effect / Neurobehavior / Protein biomarkers / Traumatic brain injury
DOI 10.1002/elps.201200319

Additional supporting information may be found in the online version of this article at the publisher's web-site

1 Introduction

Mild traumatic brain injury (mTBI) is the most frequent form of neurotrauma among civilian and military populations [1–4]. While sports injuries, motor vehicle accidents, and assaults represent the bulk of mTBI incidence among civilians, improvised explosive devices account for the majority (~80%) of the casualties sustained during recent military conflicts. Most of these casualties (~60%) involved injuries to the head, resulting in various severities of blast-induced traumatic brain injury (bTBI). Of the bTBIs, mild blast-induced traumatic brain injury (mbTBI), caused by the exposure to low levels of explosive blast, is the most frequent and its true occurrence is probably underreported [2, 3, 5, 6]. mbTBI

Correspondence: Dr. Denes V. Agoston, Department of Anatomy, Physiology and Genetics, School of Medicine, Uniformed Services University, 4301 Jones Bridge Road, Bethesda, MD 20814, USA
E-mail: vagoston@usuhs.edu
Fax: +1-301-295-1786

Abbreviations: AD, amygdala; **BM**, Barnes maze; **BOP**, blast overpressure; **bTBI**, blast-induced traumatic brain injury; **DCX**, doublecortin; **DHC**, dorsal hippocampus; **FLK-1**, fetal liver kinase-1 or VEGF receptor-2; **GCL**, granular cell layer; **GFAP**, glial fibrillary acidic protein; **mbTBI**, mild blast-induced traumatic brain injury; **MI**, multiple-injured; **MS**, multiple sham; **mTBI**, mild traumatic brain injury; **NCad**, N-cadherin; **NF-H**, neurofilament-heavy chain; **NSE**, neuron-specific enolase; **OF**, open field; **PFC**, prefrontal cortex; **PTSD**, posttraumatic stress disorder; **SI**, single-injured; **SS**, single sham; **Tau**, tau protein; **TUNEL**, terminal-deoxy-transferase-mediated dUTP nick-end labeling; **USU**, Uniformed Services University; **VEGF**, vascular endothelial growth factor; **VHC**, ventral hippocampus; **vWF**, von Willebrand factor; ***Y*-cept**, *Y*-axis intercept

represents a major challenge for the military healthcare system due to its high incidence, partly overlapping symptoms with posttraumatic stress disorder (PTSD), and a lack of objective diagnostics and specific treatments [4, 7–10].

Soldiers exposed to low levels of blast typically do not lose consciousness or experience very brief periods of unconsciousness [10–13]. Consequently, most soldiers pass the Automated Neuropsychological Assessment Metrics or the Military Acute Concussion Evaluation as they exhibit transient and mild symptoms, and are sent back into the field where many of them may be re-exposed to one or more additional blasts. Some individuals develop various neurobehavioral problems following a single blast exposure while others do so after several exposures [2, 5, 12]. Importantly, practically no mbTBI occurs without psychological and physiological stress in a battlefield scenario.

The exposure to psychological stress, particularly chronic and repeated stress, can cause substantial neurobehavioral abnormalities and occasionally result in severe affective disorders such as anxiety and memory dysfunctions, even without physical injury. Therefore, stress as a cofactor in mbTBI can be significant, particularly in the case of repeated exposure [2, 3, 12, 14, 15]. Among the leading neurobehavioral abnormalities observed in mbTBI are increased anxiety and memory impairments, both of which have been observed as a part of PTSD's symptomatology [3, 7, 15–17]. While reports suggest that increased anxiety may be transient in nature and can disappear over time, memory deficits typically have a delayed onset and may last for an extended period of time (months and even years).

On a cellular and molecular level, these neurobehavioral changes imply damage to the hippocampus. The ventral hippocampus (VHC) and its afferent and efferent connections is predominantly involved in mediating depression- and anxiety-related behavior, while the dorsal hippocampus (DHC) and its afferent and efferent connections is predominantly involved in mediating spatial learning and memory [18, 19]. Previous works using various animal models of bTBI have shown that the pathobiology of bTBI includes inflammation, neuronal and glial cell loss, gliosis, as well as axonal and vascular damage [2, 14, 20–22]. It has been found that even a single exposure to mild blast can cause lasting increases in serum levels of neuron- and glia-specific markers, implicating neuronal and glial cell damage and/or loss in mbTBI [22, 23]. Interestingly, some of these pathological changes have shown distinct anatomical localization and corresponded with the observed functional deficits.

Studies have shown that exposing an organism to brief periods of various physiological stressors such as ischemia and hypoxia can lead to an increased tolerance to subsequent insults; a phenomenon known as conditioning [24–27]. Conversely, it has been well demonstrated that some patients who have suffered an mTBI, usually in sports accidents, have an elevated risk for sustaining severe damage if exposed to subsequent mTBIs [28–30]. This condition, known as secondary impact syndrome, suggests that the repeated exposure to mild blast can have a similar cumulative effect that increases the severity of the functional outcome. While epidemiological data indicate that repeated exposure to mild levels of blast can increase the severity of the neurobehavioral outcome in some cases [2, 3, 5, 6, 11, 13, 31, 32], the key factors responsible for the observed cumulative effect (e.g., predisposing genetics, preexisting and comorbid conditions, frequency of impacts) are currently unknown.

In order to assess the validity of a presumed damage accumulation hypothesis as it relates to functional outcome severity, we determined the effects of single and multiple mild blast overpressure (BOP) exposure in a rodent model of bTBI on basic neurobehavior, plasma and brain tissue levels of select protein biomarkers, and cellular changes at two differing postinjury time points.

2 Materials and methods

2.1 Animals and housing conditions

A total of 66 male Sprague Dawley rats [weight at arrival: 245–265 g] (Charles River Laboratories, Wilmington, MA, USA) were used in our study. For the duration of the experiments, all animals were housed in pairs in standard rat cages in a reverse 12–12 h light–dark cycle with food and water ad libitum. Animals were handled according to protocol, approved by the Institutional Animal Care and Use Committee at the Uniformed Services University (USU; Bethesda, MD, USA).

2.2 Experimental groups and manipulations

This study is composed of two separate experiments that vary with respect to the time animals were terminated after the completion of the blast exposure(s); all other experimental manipulations were otherwise identical (Fig. 1). Experiment One was terminated ~2 h after blast (or sham) injury, while Experiment Two was terminated following the completion of two sets of behavioral analyses at 22 days postinjury. Experiment One was carried out to completion before the commencement of Experiment Two.

All animals underwent an acclimation and handling period of 5 days and were then assigned to the following experimental groups: Naïve, single sham (SS), single-injured (SI), multiple sham (MS), and multiple-injured (MI). Animal group numbers in Experiments One and Two are: ($N = 30$; Naïve = 3, SS = 6, SI = 7, MS = 6, MI = 8) and ($N = 36$; Naïve = 6, SS = 6, SI = 10, MS = 6, MI = 8), respectively.

For the duration of the experiments, Naïve animals were kept in the animal facility at USU without any manipulation except on behavioral testing days. SS animals were transported once from USU to Walter Reed Army Institute of Research (Silver Spring, MD, USA) and anesthetized for 6 min in an induction chamber with 4% isoflurane (Forane; Baxter Healthcare Corporation, Deerfield, IL, USA) without being exposed to BOP. MS animals were similarly transported and anesthetized daily for five consecutive days. Sham rats were

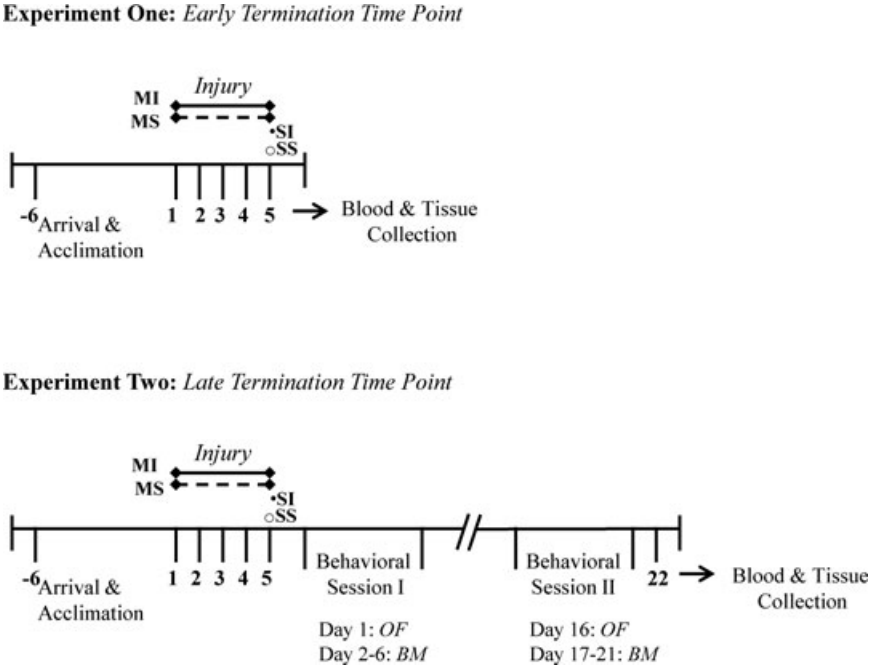

Figure 1. Outline of the experimental schedules. Blood and brain tissue were collected from animals in Experiment One approximately 2 h after the last blast on injury day 5; Experiment Two was terminated 22 days after. The timelines are not drawn to scale.

kept in the procedure room adjacent to the shock tube for the length of the injured animals' exposures.

2.3 Injury

SI and MI animals underwent the same procedures as their respective sham groups in addition to being exposed to a single or multiple (five total) mild blasts, respectively. Blast injury was administered to rats (weight at injury: 300–330 g) while wearing chest protection using a compressed air-driven shock tube as described earlier in detail [15, 22, 23, 33]. Briefly, rats were placed in the shock tube holder in a transverse prone position and exposed to mild BOP (average peak total pressure: ∼138 KPa at the animal level); the right side of the animal faced the direction of the membrane and the incidence of the blast waves. All animals were transported back to the USU animal facility at the conclusion of the daily exposures.

2.4 Behavioral tests

All animals in Experiment Two were tested for general locomotion as well as depression- and anxiety-related behaviors using the open field (OF) system, and for spatial learning and memory using the Barnes maze (BM). Behavioral assessments were performed on separate days starting at day 1 (Behavioral Session I) and day 16 (Behavioral Session II) after the last exposure (Fig. 1). Behavioral tests were conducted during animals' dark cycle.

2.4.1 Open field

Horizontal and vertical activity as well as time spent in the center of the OF were measured during the 60 min testing sessions as described earlier [15, 22, 23]. The Omnitech Electronics Digiscan infrared photocell system (Test box model RXYZCM; Omnitech Electronics, Columbus, OH, USA), consisting of a 40 × 40 × 30 cm clear Plexiglas arena equipped with infrared photocells to track the movement of the testing subject, was used. Each animal was placed on the floor of the testing arena, the perforated lid was secured, and the subject was left undisturbed for the duration of testing. Data were automatically recorded and transmitted to a computer via an Omnitech Model DCM-BBU analyzer. Cage mates were tested concurrently to avoid additional separation anxiety for any of the subjects, and the testing arenas were thoroughly cleaned with a 30% ethanol solution between animals.

2.4.2 Barnes maze

The latency to locate and enter the escape box was measured in the BM as described earlier [15, 22, 23]. Briefly, each rat was tested twice per day for five consecutive days except on the first day of BM (three trials). The first of the three trials was an untimed training trial for animals to locate and enter the escape chamber. During training, each animal was placed in the escape box and covered for 30 s, after which the rat was removed while in the escape box and placed in the center of the maze. The animal was then allowed to explore the maze for a few seconds before it was returned to its cage. During the testing trials, the same rat was placed under a start box in the center of the maze for 30 s. The start box was then removed and the animal was allowed to explore the maze freely to locate the escape chamber. The trial ended when the animal entered the escape box or when a predetermined time (240 s) elapsed without finding the escape box. In the case that the animal was unable to find the escape box within the allotted time, it

was placed in the escape box for 1 min and then returned to its cage. The second timed trial for the animal commenced after the remaining subjects in the same experimental group completed their first timed trial. The latency to locate and enter the escape box was measured with ANY-maze 4.2 Software (Stoelting Company, Wood Dale, IL, USA). Throughout the behavioral sessions, animals were tested in the same order each day, the position of the escape box (relative to the maze and the testing room) was kept constant. The escape chamber and the maze were thoroughly cleaned with a 30% ethanol solution between animals to eliminate any olfactory cues.

2.5 Blood and tissue collection

For protein measures, rats from Experiment One ($N = 17$; Naïve = 3, SS = 3, SI = 4, MS = 3, MI = 4) and Experiment Two ($N = 18$; Naïve = 3, SS = 4, SI = 4, MS = 4, MI = 3) were deeply anesthetized with Isoflurane inhalant; blood was collected and samples were promptly centrifuged at 10 000 revolutions per minute for 15 min at 4°C. The supernatants were aliquoted, flash-frozen, and stored at −80°C until processing. Animals were then decapitated using a guillotine (Harvard Apparatus Co.; Dover, MA, USA) and the brains were immediately removed. The prefrontal cortex (PFC), amygdala (AD), VHC, and DHC were dissected over wet ice and the dissected brain regions were then flash-frozen and stored at −80°C until processing.

For histology, rats from Experiment One ($N = 12$; SS = 3, SI = 3, MS = 3, MI = 3) and Experiment Two ($N = 12$; Naïve = 2, SS = 2, SI = 2, MS = 2, MI = 4) were similarly anesthetized and transcardially perfused with cold 1× PBS followed by a 4% paraformaldehyde in 1x PBS solution. Fixed brains were then cryoprotected, frozen, and sectioned coronally using a cryostat (Cryocut 1800; Leica Microsystems; Bannockburn, IL, USA) as described in detail [15, 22, 23].

2.6 Protein measures

Relative protein concentrations of the selected biomarkers were determined using reverse phase protein microarray. Sample preparation, printing, scanning, and data analysis were performed as described in detail [15, 22, 23]. Briefly, dissected brain regions were pulverized in liquid nitrogen and then sonicated in the presence of protease and phosphatase inhibitors. Protein concentrations were measured using a bicinchoninic acid assay (Thermo Scientific, PI-23250). Samples were diluted in print buffer to a final protein concentration of 1 mg/mL and printed on ONCYTE Avid (tissue samples) or ONCYTE Nova (serum samples) single-pad NC-coated glass slides using an Aushon 2470 Arrayer (Aushon Biosystems, Billerica, MA, USA). Primary antibodies were diluted to 10× the optimal Western analysis concentration in antibody incubation buffer as described [21–23, 34]. Primary antibodies were used in the following dilutions: vascular endothelial growth factor (VEGF; 1:50) (Abcam, ab53465), neurofilament-heavy chain (NF-H; 1:20) (Sigma-Aldrich, N4142), neuron-specific enolase (NSE; 1:50) (Abcam, ab53025), glial fibrillary acidic protein (GFAP; 1:500) (Abcam, ab7260), tau protein (Tau; 1:20) (Santa Cruz Biotechnology, sc-1995), N-Cadherin (NCad; 1:20) (Santa Cruz Biotechnology, sc-31031), von Willebrand factor (vWF; 1:20) (Santa Cruz Biotechnology, sc-8068), and VEGF receptor-2 or fetal liver kinase-1 (FLK-1) (1:50) (Santa Cruz Biotechnology, sc-315). Slides were incubated with the primary antibody solutions overnight at 4°C, then washed and incubated with the secondary antibodies Alexa Fluor® 635 goat antimouse (A-31574), goat antirabbit (A-31576), or Alexa Fluor® 633 rabbit antigoat Ig G (heavy + light chains) (A-21086) (Molecular Probes®, Invitrogen) at 1:6000 dilution in antibody incubation buffer for 1 h at room temperature. Fluorescent signals were measured in a Scan Array Express HT microarray scanner (Perkin Elmer, Waltham, MA, USA), and data were imported into a Microsoft Excel-based bioinformatics program developed in house for analysis [21–23, 34]. The linear regression of the log–log data was calculated after the removal of flagged data, which include S/N ratios of less than 2, spot intensities in the saturation or noise range, or high variability between duplicate spots (>10–15%). The total amount of antigen is determined by the *Y*-axis intercept or *Y*-cept [21–23, 34].

2.7 Histology

2.7.1 Immunohistochemistry

Every first and tenth coronal section containing the DHC or the VHC were mounted on positively charged glass slides two sections per slide. Three slides per animal, containing sections with identical *Z*-axes, were selected per brain region for each immunostaining. Immunohistochemical staining was performed as described in detail [22, 23]. Briefly, sections were incubated with the primary antibodies mouse anti-GFAP (Millipore, MAB360) at 1:400 dilution and rabbit antidoublecortin (DCX; Cell Signaling Technology, 4604) at 1:1000 overnight at 4°C. After washing with 1× PBS, the slides were incubated with the secondary antibodies Alexa Fluor® 555 goat antimouse (A-21422) or 488 goat antirabbit Ig G (heavy + light chains) (A-11008) at 1:100 for 1 h at room temperature; Hoechst 33342 was then applied for 2 min at 1 μg/mL (Molecular Probes®, Invitrogen). After a second wash, sections were coverslipped using antifading media (Vectashield; Vector Laboratories, Burlingame, CA, USA).

2.7.2 Histological data acquisition

Histological sections were visualized in an Olympus IX-71 microscope using the appropriate filters, and images were collected using a SPOT digital camera (Diagnostic Instruments, Sterling Heights, MI, USA).

2.7.3 TUNEL assay

DNA fragmentation as a result of apoptotic signaling cascades was determined using a terminal-deoxy-transferase-mediated

dUTP nick-end labeling (TUNEL) in situ cell death detection kit, POD (Roche, Indianapolis, IN, USA), according to the manufacturer's instructions and as described earlier [22]. TUNEL+ cells were then visualized by 3,3′-diaminobenzidine substrate and counted.

2.8 Statistical analyses and data comparison

2.8.1 Behavior

ANOVA, repeated measures ANOVA, and Dunnett's *t* tests were conducted for each of the behavioral variables using IBM SPSS Statistics 19. OF activity scores were separated into three subscales: horizontal activity, vertical activity, and center time. Latency to find the escape box was analyzed for BM. All animals in Experiment Two ($N = 30$; Naïve = 5, SS = 6, SI = 6, MS = 6, MI = 7) were used for the behavioral analyses. Data are presented as the mean ± S.E.M. All tests were two tailed using $\alpha = 0.05$.

2.8.2 Protein measures

Differences in the mean protein biomarker levels measured in plasma and in brain tissue were analyzed with ANOVA followed by the Tukey–Kramer Multiple Comparisons Test for all pairwise comparisons across the five experimental groups. The statistical analyses for Experiments One and Two were performed separately using Graph Pad Instat software. Statistical significance within each experiment was reported for blast injury (MS versus MI* and SS versus SI$^{\$}$) and frequency (SI versus MI$^{\#}$). A total of 17 animals from Experiment One (Naïve = 3, SS = 3, SI = 4, MS = 3, MI = 4) and 18 from Experiment Two (Naïve = 3, SS = 4, SI = 4, MS = 4, MI = 3) were used for the analyses. Data are presented as the mean ± S.E.M. A two-sided p value of <0.05 is depicted by one special character, $p < 0.01$ by two, and $p < 0.001$ by three.

2.8.3 Histology

TUNEL+ cells were counted from four brain sections per animal in the hilus and in the granular cell layer (GCL) of the DHC and the VHC. Data were analyzed with ANOVA followed by the Tukey–Kramer Multiple Comparisons Test as described above. A total of 12 animals from Experiment One (SS = 3, SI = 3, MS = 3, MI = 3) and 12 from Experiment Two (Naïve = 2, SS = 2, SI = 2, MS = 2, MI = 4) were used for the analyses. Data are presented as the mean ± S.E.M. A two-sided p value of <0.05 is depicted by one special character, $p < 0.01$ by two, and $p < 0.001$ by three. GFAP- and DCX-immunoreactive cells were not quantified for group comparison; the images are for illustrative purposes only.

3 Results

3.1 Behavioral changes

3.1.1 Open field

Figure 2A represents the horizontal activity, an index of general health and locomotion, of all animals at day 1 and 16 after the injury. Overall, animals had significantly lower horizontal activity at day 1 (18 222.93 ± 764.94) than at day 16 (23 054.80 ± 836.49), ($F(1, 25) = 27.03$, $p < 0.001$, $\eta^2 = 0.520$). There was also a significant group by time interaction on day 1, ($F(4, 25) = 4.35$, $p = 0.008$, $\eta^2 = 0.410$). Pairwise comparisons revealed that the MI group had significantly less horizontal activity than the Naïve, SS, and SI groups ($p < 0.05$). A Dunnett's *t* test was conducted to decrease type I error (four comparisons compared to ten with pairwise), revealing that MI animals were significantly different from Naïve ($p < 0.05$). No such differences were observed between the groups at day 16.

Figure 2B represents the vertical activity, an index of depression-related behaviors, of all animals at day 1 and 16 postinjury; decreased vertical activity indicates more depression-related behaviors. Overall, animals had lower vertical activity at day 1 (2279.22 ± 143.19) than at day 16 (3290.05 ± 188.02), ($F(1, 25) = 30.91$, $p < 0.001$, $\eta^2 = 0.553$). There was also a significant Group by Time interaction, ($F(4, 25) = 6.47$, $p = 0.001$, $\eta^2 = 0.509$). At day 1, there was a main effect for Group $F(4, 25) = 6.32$, $p = 0.001$, $\eta^2 = 0.50$), such that the Naïve group had significantly greater vertical activity than the SS, MS, and MI groups ($p < 0.05$). Similarly, SI animals had greater vertical activity than MI animals ($p < 0.05$). Dunnett's *t* test supported the finding that Naïve animals had significantly greater vertical activity than SS, MS, and MI animals ($p < 0.05$). At day 16, there were no differences in vertical activity between the groups.

Figure 2C represents the amount of time animals spent in the center of the OF chamber. Center time is an index of anxiety-related behaviors: a greater time spent in the center (as opposed to the margins and corners of the testing chamber) indicates less anxiety-related behaviors. Overall, animals spent less time in the center of the chamber at day 1 postinjury (718.03 ± 60.87) than at day 16 (1364.24 ± 63.53), ($F(1, 25) = 75.25$, $p < 0.001$, $\eta^2 = 0.751$). At day 1, pairwise comparisons revealed that the Naïve group spent significantly more time in the center than the SS, MS, and MI groups ($p < 0.05$). At this early time point, Dunnett's *t* test revealed that MS and MI animals were significantly different from Naïve ($p < 0.05$). No significant differences were observed in anxiety-related behaviors on day 16.

3.1.2 Barnes maze

Figure 3A and B represent the latency to find the escape box on days 2–6 (Test Session I) and 17–21 (Test Session II) after the injury. Data for Test Session I showed a significant effect

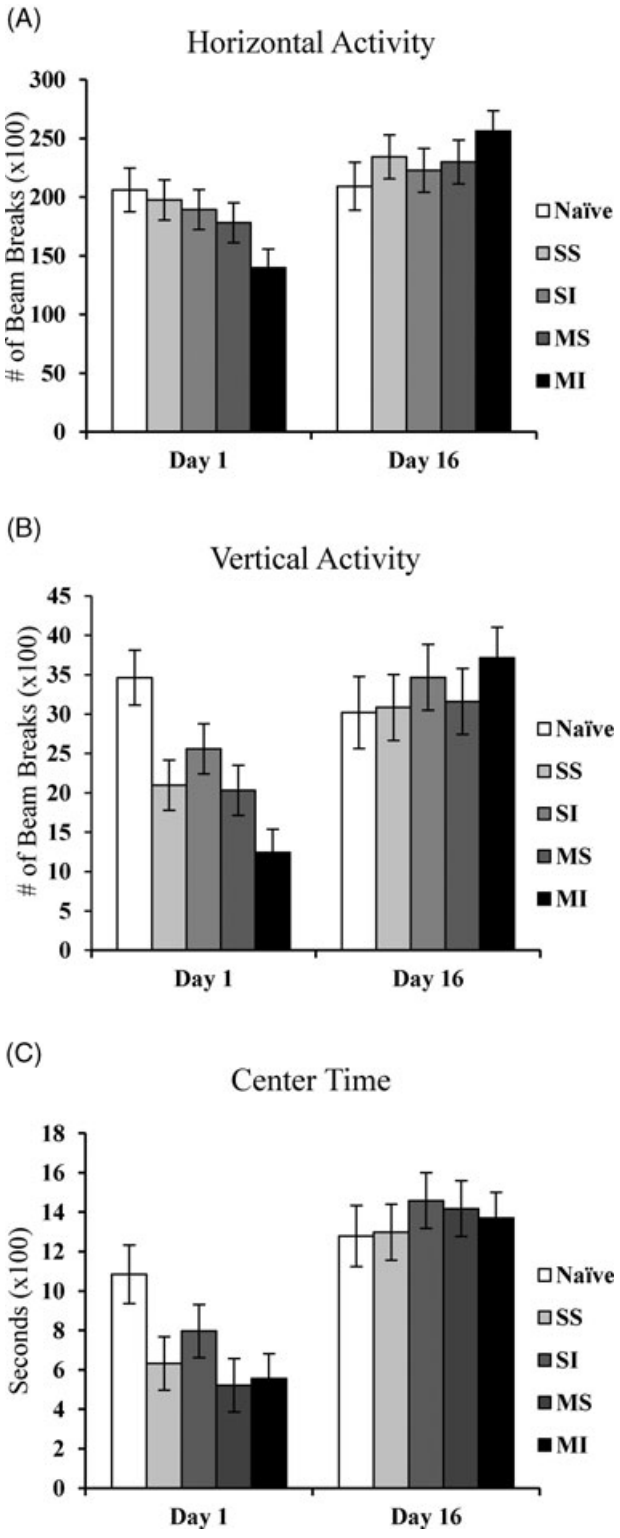

Figure 2. The general health and depression/anxiety-related behavior of animals in Experiment Two; an open field system was used to measure horizontal activity (number of beam breaks) (A), vertical activity (number of beam breaks) (B), and center time (seconds) (C) at day 1 and 16 postinjury. Data are presented as the mean ± S.E.M.

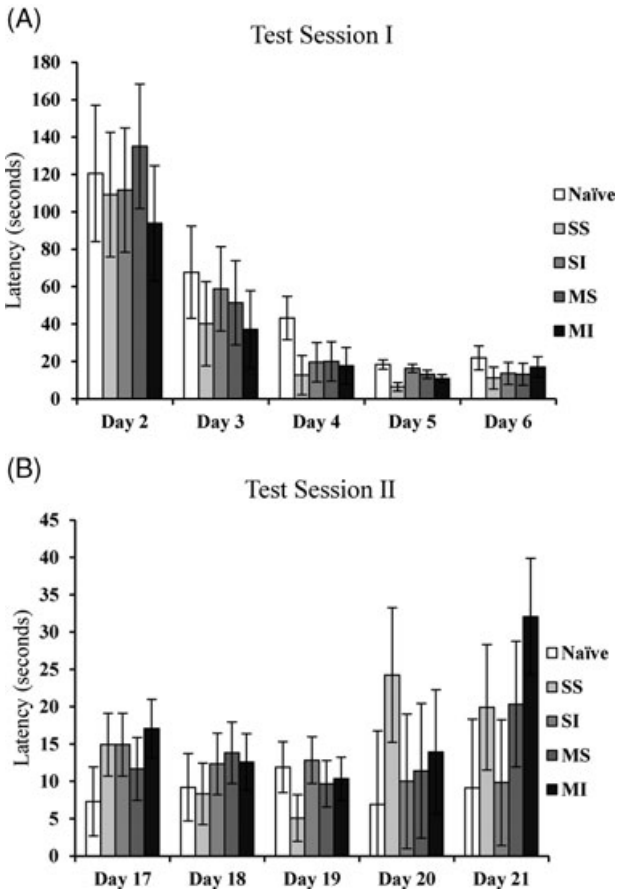

Figure 3. The spatial learning and memory of animals in Experiment Two; a Barnes maze was used to determine the latency (seconds) to find the escape box for five consecutive days starting at day 2 (A) and day 17 (B) postinjury. The depicted values represent the averages of two timed trials per animal in each experimental group. Data are presented as the mean ± S.E.M.

for time, such that the time to locate the escape box decreased over time ($F(4, 100) = 25.89$, $p < 0.001$, $\eta^2 = 0.509$). There was also a significant difference at day 5 of Test Session I ($F(1, 25) = 4.00$, $p = 0.012$, $\eta^2 = 0.390$), where Naïve animals spent a longer time to find the escape box than SS and MI animals but these differences were minimal.

The data for Test Session II showed no significant differences between the experimental groups on any of the testing days. It is noteworthy that on the final testing day, the MI group took substantially longer (32.07 ± 7.79) to located the escape box than the other groups, and that the difference between the MI and Naïve group (9.10 ± 9.22) approached significance (pairwise comparison, $p = 0.06$).

3.2 Molecular changes

3.2.1 Protein markers in plasma

We analyzed the effects of single and multiple mild blast exposure on the plasma levels of VEGF, NF-H, NSE, and

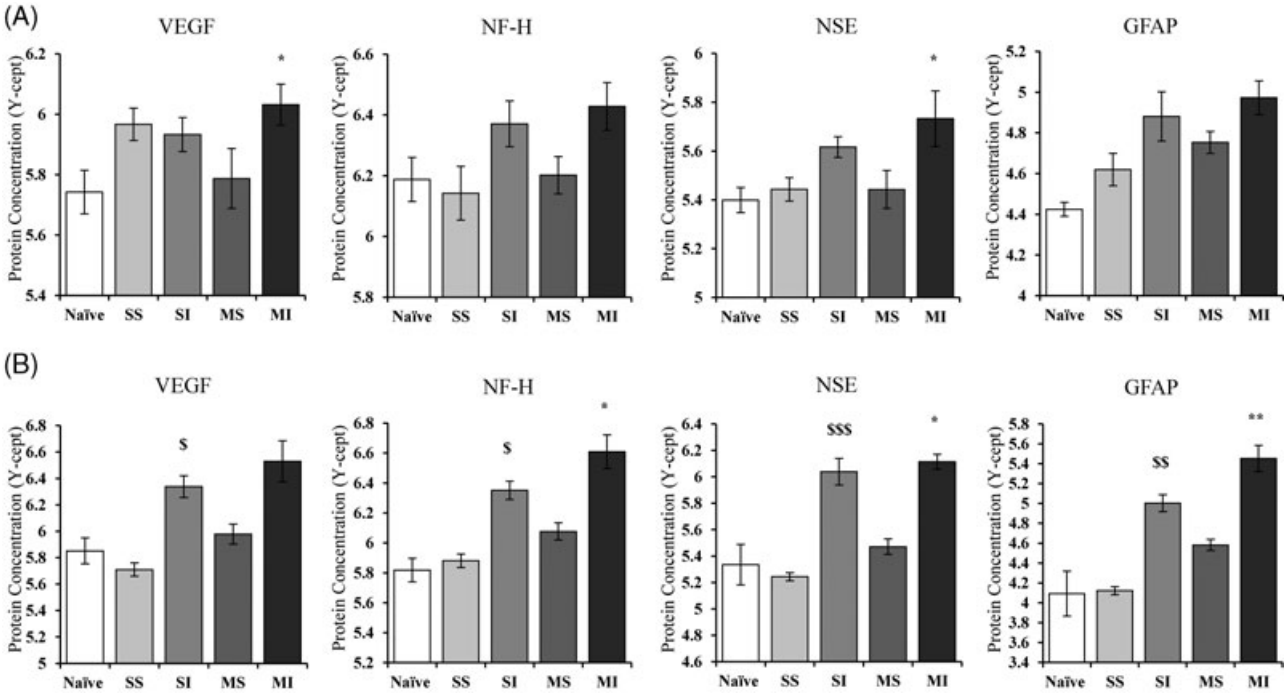

Figure 4. Plasma levels of select protein biomarkers at the early (A) and late (B) termination time points. Protein levels were assayed using reverse phase protein microarray; the reported *Y*-cept values (log10) indicate relative protein concentrations. Data are presented as the mean ± S.E.M. (SS versus SI $^{\$\$}p < 0.01$ and $^{\$\$\$}p < 0.001$; MS versus MI $^{*}p < 0.05$ and $^{**}p < 0.01$).

GFAP at the two described termination time points following injury (or sham). At the early time point (Experiment One; ~2 h after the last exposure), VEGF and NSE plasma levels were significantly increased in MI animals compared to their sham controls (MS) (Fig. 4A). The plasma levels of the other two markers, NF-H and GFAP, were not statistically different in either one of the injured groups (SI and MI) compared to their respective sham groups (SS and MS). At this time point, there were no statistically significant differences between the protein values measured in SI and SS animals for any of the four markers.

At the late termination time point (Experiment Two; 22 days after the last exposure), the plasma levels of all four markers were significantly elevated in both injured animal groups compared to their sham controls, except for VEGF protein levels in MI animals (Fig. 4B). Importantly, there were no significant differences between the plasma levels of any of the markers between SI and MI animals.

3.2.2 Protein markers in select brain regions

To identify some of the molecular consequences of single and multiple mild BOP exposure, we analyzed Tau, NCad, vWF, and FLK-1 concentrations in the AD, PFC, DHC, and VHC. At the early time point, Tau levels were only significantly elevated in the VHC of SI animals compared to their sham group. At the late time point, Tau levels were significant in the DHC as well as in the AD of SI animals. Interestingly, Tau levels were significantly decreased in the AD of MI rats compared to SI rats. Contrary to Tau, tissue levels of NCad were significantly increased in the PFC of MI animals at the early time point. Similarly significant increases were measured in the DHC of MI rats as well as SI rats at the late time point; MI animals also had significant NCad increases in the VHC compared to MS animals (Supporting Information Table 1).

No significant changes were observed in vWF or FLK-1 at the early time point; tissue levels of both markers were relatively similar in each brain region for injured animals and their corresponding sham groups. At the late time point, significantly increased vWF tissue levels were measured in the PFC and in the VHC of SI animals. Similarly, MI rats had significant vWF increases in the PFC in addition to the DHC. FLK-1 was only significantly elevated in the AD of SI rats as well as in the VHC of both, SI and MI rats. There were no significant differences in tissue levels for any of the measured markers between SI and MI animals (Supporting Information Table 1).

3.3 Cellular changes

3.3.1 GFAP and DCX immunoreactivities

To determine the effects of single and multiple mild blast exposure on astroglial response and hippocampal de novo

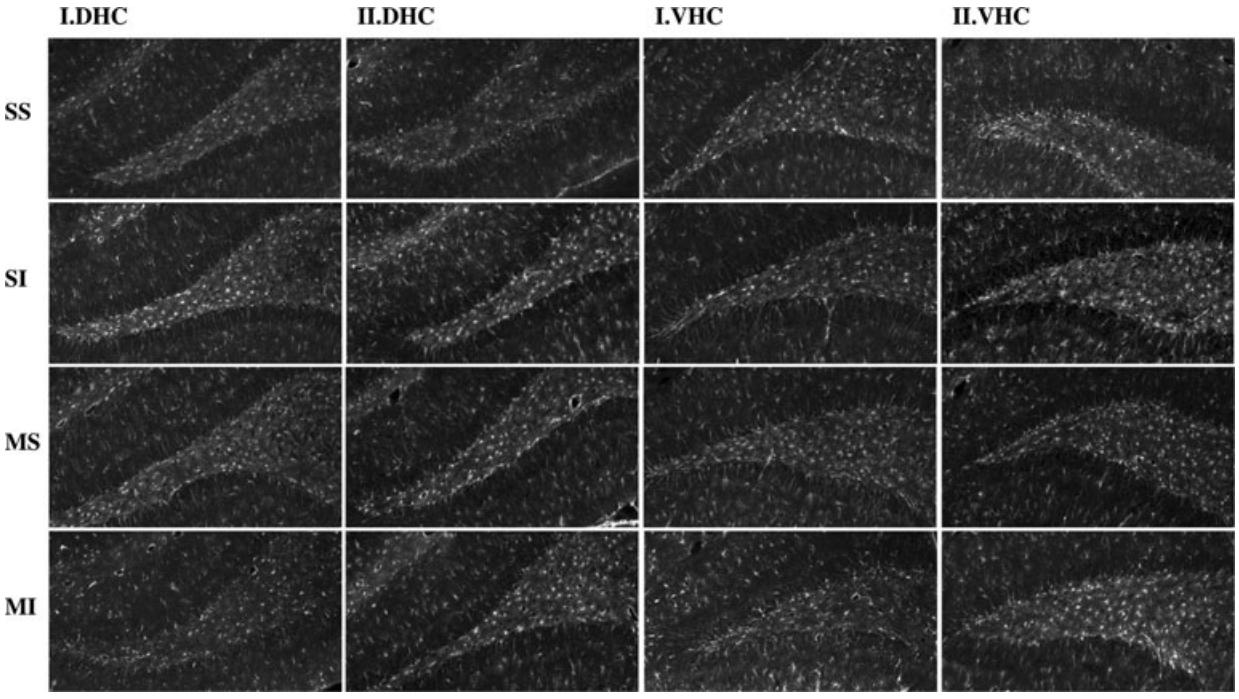

Figure 5. GFAP immunoreactivity in the dorsal and ventral hippocampus of SS, SI, MS, and MI animals at the early (I.DHC and I.VHC) and the late (II.DHC and II.VHC) termination time point, respectively.

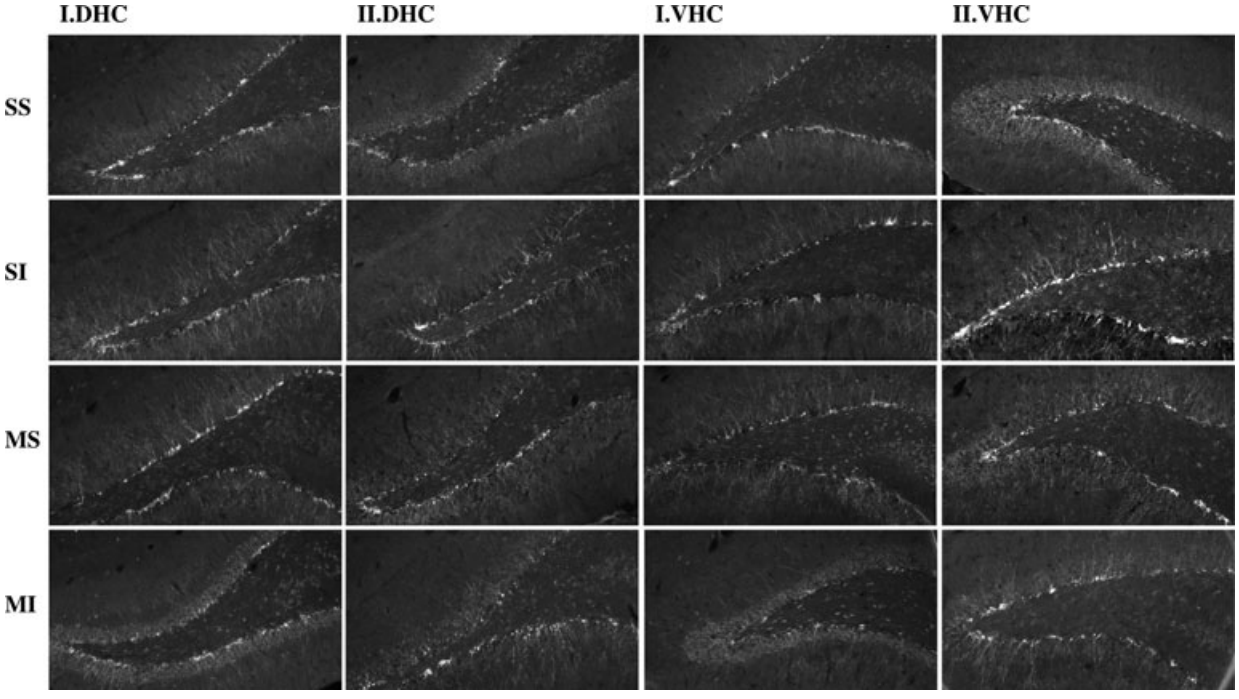

Figure 6. DCX immunoreactivity in the dorsal and ventral hippocampus of SS, SI, MS, and MI animals at the early (I.DHC and I.VHC) and the late (II.DHC and II.VHC) termination time point, respectively.

neurogenesis, we analyzed the DHC and the VHC by GFAP (Fig. 5) and DCX (Fig. 6) immunohistochemistry, respectively. At the early time point, we observed an apparent increase in GFAP immunoreactivity in the DHC (Fig. 5 I.DHC) as well as the VHC of SI animals (Fig. 5 I.VHC). Interestingly, no such increase was seen in MI animals at the early termination time point (Fig. 5 I.DHC and I.VHC). However, there was an apparent increase in GFAP immunoreactive cells at the late time point in both, the DHC and the VHC of MI rats (Fig. 5 II.DHC and II.VHC).

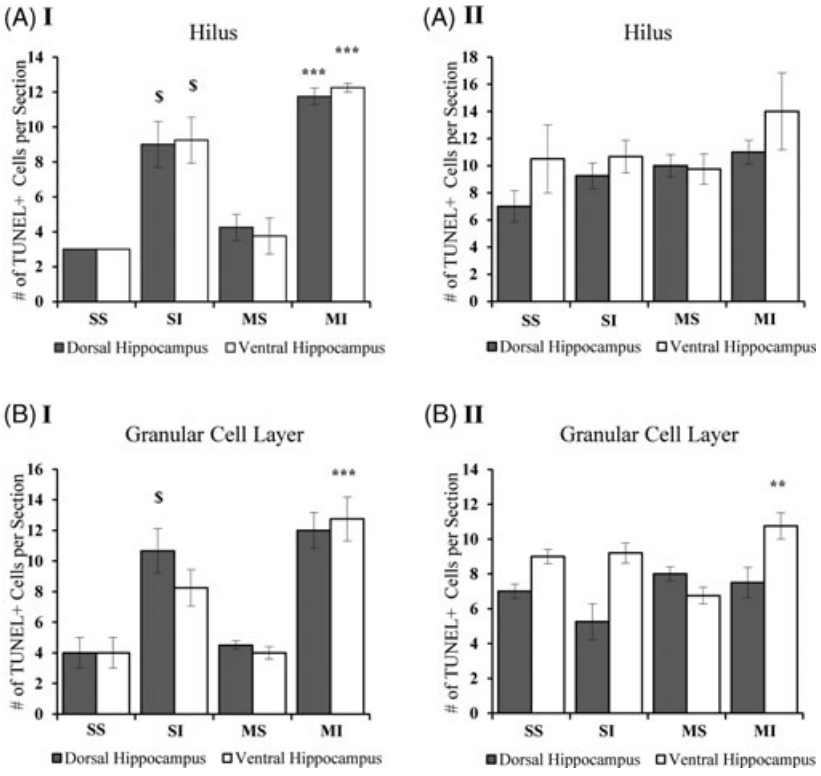

Figure 7. Presumed apoptotic cells marked by DNA fragmentation in the dorsal and ventral hippocampus. TUNEL+ cells per brain section in the hilus (A) and in the granular cell layer (B) of SS, SI, MS, and MI animals at the early (A.I and B.I) and the late (A.II and B.II) termination time point. Data are presented as the mean ± S.E.M. ($^{\$}p < 0.05$ SS versus SI; $^{**}p < 0.01$ and $^{***}p < 0.001$ MS versus MI; $^{\#}p < 0.05$ SI versus MI).

We detected an apparent increase in DCX immunoreactivity in the DHC of SI animals at the late but not at the early time point compared to SS animals (Fig. 6 I. and II.DHC). No such effect was observed in the DHC or the VHC of MI animals compared to their sham group at either termination time point (Fig. 6 I. and II. DHC; I. and II.VHC).

3.3.2 TUNEL histology

We used TUNEL histology to assess the extent of DNA fragmentation, and in turn the number of presumed apoptotic cells in the DHC and the VHC, following single and multiple mild blasts. At the early time point, the number of TUNEL+ cells was significantly increased in the hilus of the DHC and the VHC of SI and MI animals compared to their sham groups (Fig. 7 A.I). At the same time point, differences were only significant in the GCL of the DHC in SI animals and in the VHC of MI animals (Fig. 7 B.I). At the late time point, we detected no significant differences in the number of TUNEL+ cells in the hilus of injured and sham animals (Fig. 7 A.II). However, significant numbers of TUNEL+ cells were present in the GCL of the VHC in MI rats (Fig. 7 B.II).

4 Discussion

The goal of our study was threefold: (i) to compare the effects of single and multiple exposures to mild BOP on select neurobehavioral, cellular, and molecular (protein) outcomes; (ii) to assess the extent of the cellular and molecular damage immediately following injury and at a later time point; (iii) to determine whether a presumed cumulative effect of repeated blast exposure increases the severity of the observed neurobehavioral abnormalities. We found that the exposure to mild BOP results in specific time-dependent functional, cellular, and molecular changes. However, we failed to detect the anticipated cumulative effect of repeated mild blast exposure. We hypothesize that at this particular frequency of blast exposure (i.e., once per day for five consecutive days), a conditioning phenomenon among other factors reduces the extent of the cumulative damage.

4.1 Behavioral changes

At the functional level, clinical observations have indicated mood disorders including depression, increased aggression, anxiety, and memory impairments as hallmarks of mbTBI [11, 13, 32]. Some of these neurobehavioral abnormalities, particularly memory impairment, develop over time while other affective symptoms, such as anxiety, can be transient in nature. In our current study, we found that anxiety- and depression-related behaviors were greatest in MI rats 1 day following the injury. The only other study comparing the effects of single and repeated (3×) exposure to moderate levels of BOP used a basic locomotor test (Rotarod) to evaluate the functional outcome in a mouse model [35]. Interestingly, the Rotarod test failed to show any cumulative effect on basic motor function following repeated blast exposure [35].

Consistent with our previous reports, the observed locomotor differences (including anxiety- and depression-related activities) were transient [22, 23]. In a long-term study (69 day survival following a single mild blast injury), we also found that while anxiety was significantly increased in injured animals 1 day after the exposure, at 1 and 2 months after the injury, animals displayed no signs of increased anxiety [22, 23]. Importantly, stress alone without any injury triggered a similar temporal increase in anxiety levels at the early testing point. Stress alone and as a cofactor in mbTBI is extremely important because at the clinical level, mbTBI and PTSD exhibit partly overlapping neurobehavioral symptoms [12, 17, 36, 37].

Consistent with our previous observations [22, 23], spatial learning and memory were not affected immediately following the injury; all experimental groups learned and performed the task of locating the escape box in the BM at about the same rate (Test Session I). On the other hand, on day 21 after the injury MI rats displayed signs of memory impairment. This finding is consistent with the chronic nature of mbTBI and the delayed functional deficits that develop in humans [12, 17, 38].

4.2 Molecular changes

Clinical as well as experimental findings indicate that the exposure to BOP causes a specific form of TBI (i.e., bTBI). The highly complex environment caused by explosive blast consists of (supersonic) pressure waves, kinetic energy, heat, and toxic gases among others. All of these components likely contribute to the complex pathology of bTBI. In fact, evidence suggests that the various severities of blast induce distinct biological responses that are reflected in different temporal profiles of protein biomarkers, which may be used to develop blood-based diagnostics. At the biological interface of each of these components, specific molecular and cellular responses can be initiated as a part of the secondary injury mechanism. In the case of mbTBI, these biological responses include neuronal and glial loss, neuroinflammation, and gliosis [2, 14, 20–22].

In our assessment of the temporal profile of four commonly used blood-based biomarkers, we found that plasma VEGF and NSE levels were significantly increased within 2 h of the injury. The rapid increase in plasma VEGF levels is consistent with the observation of a rapid and transient increase in brain water content following repeated injury in the mouse model [39]. VEGF is involved in the regulation of various endothelial functions including vascular permeability. The increase in plasma VEGF concentrations after repeated (but not a single) BOP exposure suggests that multiple exposures may cause early and sufficient damage to the vasculature that can contribute to the elevated brain water content [40–43]. Neuronal damage and loss, reflected in the elevated plasma levels of neuron-specific proteins, has been documented after various types of brain insults [44]. NSE is a soluble neuron-specific enzyme that is frequently used as a blood-based marker in various TBI studies. The detected rapid and early rise in NSE's plasma concentrations in response to multiple but not to a single blast injury indicates significant neuronal cell damage incurred by repeated mild blast, which causes the release of NSE from injured neuronal cell bodies. This protein should be further investigated as a potential early blood-based marker of repeated mbTBI.

At the later time point, that is, 22 days after injury, the plasma concentrations of all four markers were significantly increased indicating axonal and glial damage (NF-H and GFAP, respectively), in addition to the vascular and neuronal damage that was detected previously at the early termination time point. The increase in NF-H plasma concentrations in both SI and MI rats is indicative not only of axonal damage, but also of a compromised blood brain barrier and/or increased permeability [34, 45–47]. The significant increases in GFAP levels at this time point may reflect a gliotic response to injury that can be associated with repair processes in the central nervous system. Importantly, at both time points, we found no correlation between biomarker plasma levels and the number of blast exposures. Although protein levels for each marker were slightly higher in the MI group compared to the SI group, the expected cumulative effect of repeated injury as indicated by substantially increased vascular, neuronal, axonal, and glial damage was not observed in MI rats compared to SI rats.

In addition to the biomarkers measured in plasma, we analyzed changes in protein markers in select brain regions with direct neurobehavioral implications; these include the AD, PFC, DHC, and VHC. Our measurements revealed brain region- and time-dependent changes in some of the markers. While there were practically no changes in the tissue concentrations of markers 2 h after the injury, we found significant increases in the tissue levels of Tau in the VHC of SI rats and NCad in the PFC of MI rats at this early time point. Tau is a marker of axonal function while NCad is involved in cell adhesion [23, 48–50]. The other two markers, vWF and FLK-1, are involved in mediating inflammation and the neuron-specific effects of VEGF, respectively [51, 52].

At the later time point, changes in tissue protein levels were induced by both types of injury, single and repeated, with the VHC and the DHC being more affected than the other two brain regions. The hippocampus is involved in mediating anxiety as well as spatial learning and memory [18, 19]. Increased tissue levels of the selected markers in the DHC and the VHC may be a part of the injury-related response and/or the compensatory mechanism. Consistent with our measurements in sera, we found no indication of the hypothesized cumulative effect on the tissue levels of the measured markers. The preliminary characterization of the mouse model of repeated blast also found no cumulative effect of repeated blast on cortical levels of reactive oxygen species [39].

4.3 Cellular changes

The hippocampus has been long implicated in various neuropsychiatric conditions due to its central role in mediating learning and memory, as well as anxiety [19,53]. In bTBI, damage to hippocampal structures can occur due to the primary injury (i.e., the physical forces of the BOP), as well as various secondary injury processes such as metabolic changes or inflammation. Considering the nature of the neurobehavioral abnormalities associated with mbTBI, our histological analyses focused on different subregions within the hippocampus. While the VHC is implicated in anxiety-related behaviors, the DHC is involved in cognitive functions such as learning and memory [18, 53, 54]. The pathological changes we observed hereinafter are consistent with our previous findings showing distinct anatomical localizations in mbTBI [22, 23]. However, it is important to note that due to the exploratory nature of this study and the absence of stereological analyses, our immunohistochemistry data are nonquantitative and are for illustrative purposes only.

Our immunohistochemical analysis showed an apparent increase in GFAP immunoreactivity, especially in the hilus of both parts of the hippocampus (the DHC and the VHC), within 2 h after a single exposure. However, multiple blast injuries failed to produce the anticipated (i.e., greater) increase in GFAP immunoreactivity in MI rats compared to their MS controls in both of the tested brain regions. Interestingly, at the later time point, GFAP immunoreactivity is comparable in both injured groups as well as the MS group, particularly in the DHC. The apparent increase in GFAP immunoreactive astrocytes in MS animals is consistent with our previous finding that the repeated exposure to environmental and psychological stressors alone (without injury) is capable of inducing pathological changes and altering functional outcome [15]. Increased GFAP expression by astrocytes has been observed after various neuronal insults and is generally considered to be a part of the gliotic response to injury [55–58]. This gliotic response has been viewed as both, beneficial and detrimental. Astroglia have been shown to be involved in eliminating toxic molecules and in providing trophic factors in support of recovery after injury. De novo hippocampal neurogenesis, partly supported by astroglia, has been implicated as a part of the recovery/regenerative process following neuronal insults including TBI.

Unlike the apparent early onset of the GFAP response, the increase in DCX immunoreactivity was more apparent at the later termination time point. The apparent increase in DCX immunoreactivity would be consistent with the known temporal pattern of hippocampal de novo neurogenesis following TBI. New neurons marked by DCX expression typically become detectable 2–3 wk after injury [59–62]. Importantly, the largest increase in DCX immunoreactivity was observed in the subgranular zone of the dentate gyrus in the VHC of SI animals. It should be noted that the VHC is predominantly involved in mediating anxiety, and that at this late time point injured animals' anxiety levels were similar to those of their respective shams. While it is intriguing to think about de novo neurogenesis playing a role in the normalization of anxiety levels, testing this hypothesis would require highly complex experiments. The lack of increase in DCX immunoreactivity in MI rats (in either hippocampal region) compared to their sham controls can be potentially explained by the presence of negative growth signals generated by the repeated exposure to blast, which interfere with the injury-induced neurogenesis apparent after a single exposure; this, too, warrants further investigation.

Our TUNEL histology provided evidence for a very early onset of DNA fragmentation indicating an increased rate of apoptotic cell death [41, 62–64]. It was at the early time point (2 h after injury) that we detected the most significant increase in the number of TUNEL+ cells in the hilus as well as in the GCL of the DHC and the VHC of injured animals. The detected increases may reflect the damage caused by the primary injury process, which results in an acute cellular injury that can lead to programmed cell death. Interestingly, the number of TUNEL+ cells was significant only in the GCL of the VHC of MI animals at the late time point. Again, there were no significant differences in the number of TUNEL positive cells following single or multiple exposures.

4.4 Conclusions

This exploratory study is the first to compare single and multiple BOP exposure on select functional, cellular, and molecular outcomes in an effort to assess the extent of the damage in repeated mbTBI. Although the apparent damage was not substantially higher following five blast exposures as opposed to one, a slight cumulative effect was observed in MI rats. We believe that several factors can account for this potentially important finding. These include obvious species differences, the frequency of BOP exposures, and a conditioning phenomenon, which may all be interconnected.

Species differences have been a significant issue in experimental biomedical research, especially in TBI. In addition to the anatomical, biomechanical, and physiological differences that exist across species, there are significant differences in metabolism, life expectancy, and the dynamics of disease progression. A "human year" is calculated to be between 10 and 12 "rat days" [65]. Consequently, the daily blast exposures administered to MI rats in this preliminary study can be roughly equivalent to monthly exposures in humans. Although there are currently no publicly available epidemiological data that correlate between the frequency of blast exposures and the observed cumulative effect, it is safe to assume that this blast frequency (coupled with rodent physiology) provides too long of a recovery period between exposures.

Another possible and intriguing explanation is that this rate of exposure triggers a conditioning effect in rats. It has been known that brief periods of physiological stress provide temporary protection or an increased tolerance to subsequent stressors. It should be noted that the conditioning effect we postulate in this study is related to the injury process itself, and not to the neuroprotective effect of repeated anesthesia.

In our experimental design, we deliberately compare injured animals to their respective sham groups (as opposed to Naïve animals) to account for all variables (i.e., handling, transportation, and anesthesia) not related to the BOP. Therefore, significant differences between injured animals and their respective shams can be attributed to the blast injury alone.

Conditioning has been particularly well studied in various models of ischemia affecting the heart as well as the brain. Ischemic conditioning can significantly improve the outcome of an otherwise fatal ischemic attack. In a rodent model of conditioning, repeated mild focal TBI delivered once a day for 3 days resulted in a significantly improved functional outcome after a severe focal TBI was delivered 3–5 days after the last mild (conditioning) injury targeting the same site [24–26]. In this model, the (focal) injury activated the local astroglia population, which upregulated their Hsp27 expression. Even though there are differences between the pathologies of focal and global types of TBI (e.g., bTBI), our group as well as others have observed astroglial activation in various models of bTBI. Future testing of the effects of repeated BOP exposures on astroglial expression of Hsp27 can serve as a useful marker, which can potentially identify the extent of vulnerability and/or conditioning after injury.

A limitation of this study (and more generally the rodent model for studying bTBI) is that under controlled experimental conditions, animals are positioned to receive the blast unilaterally, at the same anatomical location, and at consistent BOP peak ranges each time. Although it is standard procedure to use identical experimental conditions, this is rarely, if ever, the case in real life. Considering that BOP exposure in our blast model is unilateral, it is noteworthy to mention that there is evidence of brain hemisphere specialization in rodents [66, 67]. The right hemisphere controls emotional expression and behavioral responses to novel events and threats as supported by the significant increases in anxiety- and depression-related behaviors in MI rats following the injury. Learning, a left hemisphere specialization, is not affected as seen in Test Session I of the BM. Animals, irrespective of their experimental manipulations, learned the task of locating the escape box at a similar rate. Therefore, the functional outcome of injury as it relates to the incidence of blast can be a substantial confounding factor in behavioral analyses. Given the nonfocal, global nature of bTBI, a more randomly targeted delivery of blast waves (with varying peak pressures) can more closely mimic operationally relevant scenarios of repeated mbTBI; an issue that will be investigated at length in future studies.

We thank the Neurotrauma Team at the Walter Reed Army Institute of Research for their technical help during the exposures. This work was supported by the Center for Neuroscience and Regenerative Medicine grant number G1703F. The views, opinions, and/or findings contained herein are those of the authors and should not be construed as an official position, policy, or decision of the Department of the Army or the Department of Defense. Animal handling and treatments were conducted in compliance with the Animal Welfare Act and other Federal statutes and regulations related to animals and experiments involving animals, and adhered to principles stated in the Guide to the Care and Use of Laboratory Animals, National Research Council. The facilities are fully accredited by the Association for Assessment and Accreditation of Laboratory Animal Care International.

The authors have declared no conflict of interest.

5 References

[1] Bay, E. H., Liberzon, I., *Res. Theory Nurs. Pract.* 2009, *23*, 42–61.

[2] Elder, G. A., Cristian, A., *Mt. Sinai. J. Med.* 2009, *76*, 111–118.

[3] Rosenfeld, J. V., Ford, N. L., *Injury* 2010, *41*, 437–443.

[4] Vanderploeg, R. D., Belanger, H. G., Curtiss, G., *Arch. Phys. Med. Rehabil.* 2009, *90*, 1084–1093.

[5] Elder, G. A., Mitsis, E. M., Ahlers, S. T., Cristian, A., *Psychiatr. Clin. North. Am.* 2010, *33*, 757–781.

[6] Levin, H. S., Wilde, E., Troyanskaya, M., Petersen, N. J., Scheibel, R., Newsome, M., Radaideh, M., Wu, T., Yallampalli, R., Chu, Z., Li, X., *J. Neurotrauma* 2010, *27*, 683–694.

[7] Brenner, L. A., Vanderploeg, R. D., Terrio, H., *Rehabil. Psychol.* 2009, *54*, 239–246.

[8] Otis, J. D., McGlinchey, R., Vasterling, J. J., Kerns, R. D., *J. Clin. Psychol. Med. Settings* 2011, *18*, 145–154.

[9] Pietrzak, R. H., Johnson, D. C., Goldstein, M. B., Malley, J. C., Southwick, S. M., *J. Nerv. Ment. Dis.* 2009, *197*, 748–753.

[10] Vasterling, J. J., Verfaellie, M., Sullivan, K. D., *Clin. Psychol. Rev.* 2009, *29*, 674–684.

[11] Thompson, J. M., Scott, K. C., Dubinsky, L., *Can. Fam. Physician* 2008, *54*, 1549–1551.

[12] Trudeau, D. L., Anderson, J., Hansen, L. M., Shagalov, D. N., Schmoller, J., Nugent, S., Barton, S., *J. Neuropsychiatry Clin. Neurosci.* 1998, *10*, 308–313.

[13] Wilk, J. E., Thomas, J. L., McGurk, D. M., Riviere, L. A., Castro, C. A., Hoge, C. W., *J. Head Trauma. Rehabil.* 2010, *25*, 9–14.

[14] DeWitt, D. S., Prough, D. S., *J. Neurotrauma* 2009, *26*, 877–887.

[15] Kamnaksh, A., Kovesdi, E., Kwon, S. K., Wingo, D., Ahmed, F., Grunberg, N. E., Long, J., Agoston, D. V., *J. Neurotrauma* 2011, *28*, 2145–2153.

[16] Brenner, L. A., Ivins, B. J., Schwab, K., Warden, D., Nelson, L. A., Jaffee, M., Terrio, H., *J. Head Trauma. Rehabil.* 2010, *25*, 307–312.

[17] Jaffee, M. S., Meyer, K. S., *Clin. Neuropsychol.* 2009, *23*, 1291–1298.

[18] Bannerman, D. M., Rawlins, J. N., McHugh, S. B., Deacon, R. M., Yee, B. K., Bast, T., Zhang, W. N., Pothuizen, H. H., Feldon, J., *Neurosci. Biobehav. Rev.* 2004, *28*, 273–283.

[19] Engin, E., Treit, D., *Behav. Pharmacol.* 2007, *18*, 365–374.

[20] Cernak, I., Noble-Haeusslein, L. J., *J. Cereb. Blood Flow Metab.* 2010, *30*, 255–266.

[21] Gyorgy, A. B., Walker, J., Wingo, D., Eidelman, O., Pollard, H. B., Molnar, A., Agoston, D. V., *J. Neurosci. Methods* 2010, *192*, 96–101.

[22] Kwon, S. K., Kovesdi, E., Gyorgy, A. B., Wingo, D., Kamnaksh, A., Walker, J., Long, J. B., Agoston, D. V., *Front Neurol.* 2011, *2*, 1–14.

[23] Kovesdi, E., Gyorgy, A. B., Kwon, S. K., Wingo, D. L., Kamnaksh, A., Long, J. B., Kasper, C. E., Agoston, D. V., *Front Neurosci.* 2011, *5*, 1–12.

[24] Allen, G. V., Gerami, D., Esser, M. J., *Neuroscience* 2000, *99*, 93–105.

[25] Mota, B. C., Pereira, L., Souza, M. A., Silva, L. F., Magni, D. V., Ferreira, A. P., Oliveira, M. S., Furian, A. F., Mazzardo-Martins, L., Silva, M. D., Santos, A. R., Ferreira, J., Fighera, M. R., Royes, L. F., *Neurotox. Res.* 2012, *21*, 175–184.

[26] Ren, C., Gao, M., Dornbos, D., 3rd, Ding, Y., Zeng, X., Luo, Y., Ji, X., *Neurol. Res.* 2011, *33*, 514–519.

[27] Zhao, H., *J. Cereb. Blood Flow Metab.* 2009, *29*, 873–885.

[28] Aarabi, B., Simard, J. M., *Curr. Opin. Crit. Care* 2009, *15*, 548–553.

[29] Bazarian, J. J., Cernak, I., Noble-Haeusslein, L., Potolicchio, S., Temkin, N., *J. Head Trauma. Rehabil.* 2009, *24*, 439–451.

[30] Maas, A. I., Menon, D. K., Lingsma, H. F., Pineda, J. A., Sandel, M. E., Manley, G. T., *J. Neurotrauma* 2012, *29*, 32–46.

[31] Belanger, H. G., Proctor-Weber, Z., Kretzmer, T., Kim, M., French, L. M., Vanderploeg, R. D., *Clin. Neuropsychol.* 2011, *25*, 702–715.

[32] Luethcke, C. A., Bryan, C. J., Morrow, C. E., Isler, W. C., *J. Int. Neuropsychol. Soc.* 2011, *17*, 36–45.

[33] Long, J. B., Bentley, T. L., Wessner, K. A., Cerone, C., Sweeney, S., Bauman, R. A., *J. Neurotrauma* 2009, *26*, 827–840.

[34] Gyorgy, A. B., Ling, G. S., Wingo, D. L., Walker, J., Tong, L. C., Parks, S., Januszkiewicz, A., Baumann, R., Agoston, D. V., *J. Neurotrauma* 2011, *28*, 1121–1126.

[35] Ahlers, S. T., Vasserman-Stokes, E., Shaughness, M. C., Hall, A. A., Shear, D. A., Chavko, M., McCarron, R. M., Stone, J. R., *Front Neurol.* 2012, *3*, 32.

[36] Karl, A., Schaefer, M., Malta, L. S., Dorfel, D., Rohleder, N., Werner, A., *Neurosci. Biobehav. Rev.* 2006, *30*, 1004–1031.

[37] Tan, G., Fink, B., Dao, T. K., Hebert, R., Farmer, L. S., Sanders, A., Pastorek, N., Gevirtz, R., *Pain Med.* 2009, *10*, 1237–1245.

[38] Tischler, L., Brand, S. R., Stavitsky, K., Labinsky, E., Newmark, R., Grossman, R., Buchsbaum, M. S., Yehuda, R., *Ann. N Y Acad. Sci.* 2006, *1071*, 405–409.

[39] Koliatsos, V. E., Cernak, I., Xu, L., Song, Y., Savonenko, A., Crain, B. J., Eberhart, C. G., Frangakis, C. E., Melnikova, T., Kim, H., Lee, D., *J. Neuropathol. Exp. Neurol.* 2011, *70*, 399–416.

[40] Lee, C., Agoston, D. V., *J. Neurotrauma* 2010, *27*, 541–553.

[41] Lee, C., Agoston, D. V., *Exp. Neurol.* 2009, *220*, 400–403.

[42] Nag, S., Eskandarian, M. R., Davis, J., Eubanks, J. H., *J. Neuropathol. Exp. Neurol.* 2002, *61*, 778–788.

[43] van Bruggen, N., Thibodeaux, H., Palmer, J. T., Lee, W. P., Fu, L., Cairns, B., Tumas, D., Gerlai, R., Williams, S. P., van Lookeren Campagne, M., Ferrara, N., *J. Clin. Invest.* 1999, *104*, 1613–1620.

[44] Pleines, U. E., Morganti-Kossmann, M. C., Rancan, M., Joller, H., Trentz, O., Kossmann, T., *J. Neurotrauma* 2001, *18*, 491–498.

[45] Eng, L. F., Ghirnikar, R. S., *Brain Pathol.* 1994, *4*, 229–237.

[46] Garcia, A. D., Doan, N. B., Imura, T., Bush, T. G., Sofroniew, M. V., *Nat. Neurosci.* 2004, *7*, 1233–1241.

[47] Larsson, A., Wilhelmsson, U., Pekna, M., Pekny, M., *Neurochem. Res.* 2004, *29*, 2069–2073.

[48] Barr, T. L., Alexander, S., Conley, Y., *Biol. Res. Nurs.* 2011, *13*, 140–153.

[49] Begaz, T., Kyriacou, D. N., Segal, J., Bazarian, J. J., *J. Neurotrauma* 2006, *23*, 1201–1210.

[50] Warden, D. L., Labbate, L. A., Salazar, A. M., Nelson, R., Sheley, E., Staudenmeier, J., Martin, E., *J. Neuropsychiatry Clin. Neurosci.* 1997, *9*, 18–22.

[51] Gu, X., Zhang, J., Brann, D. W., Yu, F. S., *Invest. Ophthalmol. Vis. Sci.* 2003, *44*, 3219–3225.

[52] Sun, Y., Jin, K., Xie, L., Childs, J., Mao, X. O., Logvinova, A., Greenberg, D. A., *J. Clin. Invest.* 2003, *111*, 1843–1851.

[53] Moser, M. B., Moser, E. I., *Hippocampus* 1998, *8*, 608–619.

[54] Fanselow, M. S., Dong, H. W., *Neuron* 2010, *65*, 7–19.

[55] Bellander, B. M., Bendel, O., Von Euler, G., Ohlsson, M., Svensson, M., *J. Neurotrauma* 2004, *21*, 605–615.

[56] Hailer, N. P., Wirjatijasa, F., Roser, N., Hischebeth, G. T., Korf, H. W., Dehghani, F., *Eur. J. Neurosci.* 2001, *14*, 315–326.

[57] Hatten, M. E., Liem, R. K., Shelanski, M. L., Mason, C. A., *Glia* 1991, *4*, 233–243.

[58] Kaur, C., Singh, J., Lim, M. K., Ng, B. L., Yap, E. P., Ling, E. A., *Neuropathol. Appl. Neurobiol.* 1995, *21*, 369–377.

[59] Kempermann, G., *Ernst. Schering Res. Found Workshop* 2002, *35*, 17–28.

[60] Kempermann, G., Gage, F. H., *Novartis Found Symp.* 2000, *231*, 220–235; discussion 235–241, 302–226.

[61] Kempermann, G., Jessberger, S., Steiner, B., Kronenberg, G., *Trends Neurosci.* 2004, *27*, 447–452.

[62] Lee, C., Agoston, D. V., *J. Neurotrauma* 2010, *27*, 541–553.

[63] Cernak, I., Chapman, S. M., Hamlin, G. P., Vink, R., *J. Clin. Neurosci.* 2002, *9*, 565–572.

[64] Pun, P. B., Kan, E. M., Salim, A., Li, Z., Ng, K. C., Moochhala, S. M., Ling, E. A., Tan, M. H., Lu, J., *Front Neurol.* 2011, *2*, 1–15.

[65] Quinn, R., *Nutrition* 2005, *21*, 775–777.

[66] Andrew, R. J., in: Rogers, L. J., Andrew, R. J. (Eds.), *Comparative Vertebrate Lateralization*, Cambridge University Press, Cambridge, UK 2002, pp. 157–205.

[67] Robinson, R. D., in: Glick, S. D. (Ed.), *Cerebral Lateralization in Nonhuman Species*, Academic Press, Philadelphia, PA 1985, pp. 135–156.

Farid A. Ahmed[1,2]
Alaa Kamnaksh[1,2]
Erzsebet Kovesdi[3]
Joseph B. Long[4]
Denes V. Agoston[1,2]

[1]Department of Anatomy, Physiology and Genetics, Uniformed Services University, Bethesda, MD, USA
[2]Center for Neuroscience and Regenerative Medicine, Uniformed Services University, Bethesda, MD, USA
[3]U.S. Department of Veterans Affairs, Veterans Affairs Central Office, Washington, DC, USA
[4]Blast-Induced Neurotrauma Branch, Center for Military Psychiatry and Neuroscience, Walter Reed Army Institute of Research, Silver Spring, MD, USA

Received February 6, 2013
Revised March 15, 2013
Accepted April 3, 2013

Short Communication

Long-term consequences of single and multiple mild blast exposure on select physiological parameters and blood-based biomarkers

Mild traumatic brain injury (mTBI), especially when it is repeated (rmTBI), can lead to progressive degenerative diseases and lasting neuropsychiatric abnormalities. To better understand the long-term pathobiological changes in mTBI and rmTBI, we exposed rats to single or repeated (5 total; administered on consecutive days) mild blast overpressure, monitored changes in physiological parameters, and determined the plasma levels of select biomarkers at 42 days post injury by proteomics. We unexpectedly found comparable changes in arterial oxygen saturation levels and heart rates of single-injured (SI) and multiple-injured (MI) rats throughout the observation period. Our analyses indicated lasting oxidative stress, vascular abnormalities, and neuronal and glial cell loss in both injured groups. However, MI rats exhibited a relatively more pronounced increase in the plasma levels of most of the tested markers—particularly those associated with inflammation—albeit the differences between the two injured groups were not statistically significant. Our findings indicate that the frequency of blast exposures is an important determinant of the resulting cumulative damage in rmTBI.

Keywords:
Animal models / Brain trauma / Experimental / Physiology / Proteomics
DOI 10.1002/elps.201300077

Mild traumatic brain injury (mTBI) accounts for the majority of civilian and military traumatic brain injury (TBI) cases [1, 2]. In both civilian and military environments, affected individuals (e.g. football players) often sustain additional mild injuries. mTBI symptoms are typically mild and transient, however, repeated mild TBIs (rmTBI) can result in disproportionately severe acute symptoms suggesting some sort of cumulative effect of repeated injuries [3]. rmTBIs also increase the risk of developing late onset, progressive degenerative conditions such as chronic traumatic encephalopathy [4]. Despite their high prevalence, the pathobiology and consequently the diagnosis and treatment of mTBI and rmTBI have not been adequately addressed.

In a previous study assessing some of the neurobehavioral, cellular, and molecular consequences of single and multiple mild blast exposure at an early (~2 h) and a later post injury time point (22 days), we unexpectedly found a mild cumulative effect following repeated injury [5]. Based on these findings, we hypothesized that the cumulative effect in rmTBI requires a longer post injury time period to manifest. To test this hypothesis, we extended our experimental timeline to 42 days post injury and utilized noninvasive, clinically relevant tools to follow long-term changes in basic physiological parameters and blood-based biomarkers.

A total of 30 Sprague Dawley male rats, weighing 245–265 g at arrival (Charles River Laboratories, Wilmington, MA, USA), were used in our study. Housing, handling, and experimental manipulations of animals have been described earlier [5]. After an acclimation and handling period of five days, animals were randomly assigned to the following groups: naïve ($N = 3$), single sham (SS; $N = 6$), single-injured (SI; $N = 7$), multiple sham (MS; $N = 6$), and multiple-injured (MI; $N = 8$). Naïve rats were kept in the Uniformed Services University (USU) animal facility for the duration of the study without any manipulation. SS rats were transported once from USU to Walter Reed Army Institute of Research (Silver Spring, MD, USA) and anesthetized in an induction chamber for

Correspondence: Dr. Denes V. Agoston, Department of Anatomy, Physiology and Genetics, School of Medicine, Uniformed Services University, 4301 Jones Bridge Road, Bethesda, MD 20814, USA
E-mail: vagoston@usuhs.edu
Fax: +1-301-295-1786

Abbreviations: CCR5, chemokine (C-C motif) receptor 5; **FPR1**, formyl peptide receptor 1; **GFAP**, glial fibrillary acidic protein; **HIF-1α**, hypoxia-inducible factor-1α; **HNE**, 4-hydroxynonenal; **MBP**, myelin basic protein; **MI**, multiple-injured; **MMP8**, matrix metalloproteinase 8; **MS**, multiple sham; **mTBI**, mild TBI; **NF-H**, neurofilament-heavy chain; **p38**, p38 mitogen-activated protein kinase; **rmTBI**, repeated mild TBI; **SI**, single-injured; **SS**, single sham; **TBI**, traumatic brain injury; **TLR9**, Toll-like receptor 9; **USU**, Uniformed Services University; **VEGF**, vascular endothelial growth factor; **vWF**, von Willebrand factor

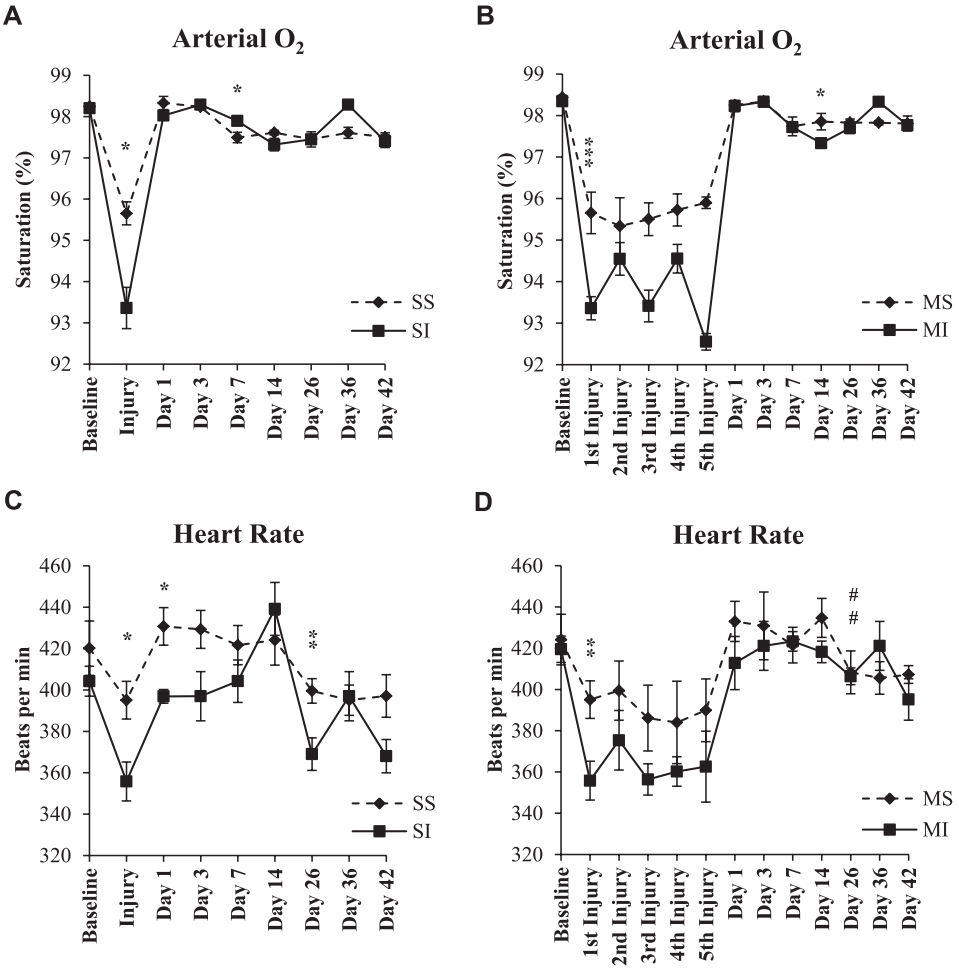

Figure 1. Arterial oxygen saturation levels (%) (A and B) and heart rates (beats per min) (C and D) of SS, SI, MS and MI rats. Measurements were obtained under isoflurane anesthesia at baseline, immediately following injury (5× for MI rats), and at days 1, 3, 7, 14, 26, 36, and 42 post injury. Data are presented as the mean ± SEM (*$p < 0.05$, **$p < 0.01$, and ***$p < 0.001$ sham versus injured; ##$p < 0.01$ SI versus MI).

6 min with 4% isoflurane (Forane; Baxter Healthcare Corporation, Deerfield, IL, USA). MS rats were similarly transported and anesthetized once per day for 5 consecutive days. SI and MI rats, weighing 300–330 g on injury day, underwent the same pre-injury procedures as their respective sham groups. SI and MI rats were then transferred to a compressed air-driven shock tube and exposed to a single or repeated (5 total administered on consecutive days) mild blast overpressure (average peak total pressure: ∼138 kPa) as described in detail [6, 7]. Mortality was: SI = 3 and MI = 4. Following the exposure(s), animals were transported back to the USU animal facility.

Arterial blood oxygen saturation (%), heart rate (beats per min), pulse distention (μm), and breath rate (breaths per min) were noninvasively monitored under light isoflurane anesthesia prior to injury (baseline), immediately after blast (or sham) exposure, and at days 1, 3, 7, 14, 26, 36, and 42 post injury using the MouseOx® Pulse Oximeter adopted for rats (Starr Life Sciences, Oakmont, PA, USA) [8]. At the termination of the experiment (day 42 post injury), rats (Naïve = 3, SS = 6, SI = 4, MS = 6, MI = 4) were deeply anesthetized in a bell jar with isoflurane inhalant until a tail or toe pinch produced no reflex movement. Blood was obtained by cardiac puncture, and samples were promptly centrifuged at 10 000 rpm for 15 min at 4°C; the supernatants (plasma) were then transferred into tubes, flash-frozen, and stored at −80°C until processing for reverse phase protein microarray [5].

Sample preparation, printing, scanning, and data analysis for reverse phase protein microarray were performed as described earlier in detail [9]. Primary antibodies were diluted to 10× the optimal Western analysis concentration in antibody incubation buffer and used in the following dilutions: 4-hydroxynonenal (HNE; 1:100) (Calbiochem, 393207), hypoxia-inducible factor-1α (HIF-1α; 1:20) (Santa Cruz, sc-53546), ceruloplasmin (1:20) (GeneTex, GTX28813), vascular endothelial growth factor (VEGF; 1:50) (Abcam, ab53465), von Willebrand factor (vWF; 1:20) (Santa Cruz, sc-8068), neurofilament-heavy chain (NF-H; 1:20) (Sigma–Aldrich, N4142), glial fibrillary acidic protein (GFAP; 1:500) (Abcam, ab7260), myelin basic protein (MBP; 1:20) (Santa Cruz, sc-13914), matrix metalloproteinase 8 (MMP8; 1:20) (Santa Cruz, sc-50384), formyl peptide receptor 1 (FPR1; 1:20) (Santa Cruz, sc-13198), p38 mitogen-activated protein kinase (p38; 1:20) (Cell Signaling Technology, 9212), chemokine (C-C motif) receptor 5 (CCR5; 1:20) (GeneTex, GTX61751), and toll-like receptor 9 (TLR9; 1:100) (Santa Cruz, sc-13218).

Table 1. Oxidative stress and vascular biomarker levels in the plasma at 42 days post injury

Marker	Group	Mean ± SEM	ANOVA		Comparison of means		
			F-value	*p*-value	2–3 (*p*)	4–5 (*p*)	3–5 (*p*)
4-Hydroxynonenal (HNE)	Naïve (1)	4.95 ± 0.17	7.89	0.000	− 0.39	− 0.48	− 0.03
	SS (2)	4.97 ± 0.04			**0.016**	**0.001**	0.999
	SI (3)	**5.37 ± 0.12**					
	MS (4)	4.91 ± 0.07					
	MI (5)	**5.40 ± 0.05**					
Hypoxia-inducible factor-1α (HIF-1α)	Naïve (1)	4.10 ± 0.59	4.53	0.005	− 0.56	− 1.09	− 0.91
	SS (2)	4.11 ± 0.17			0.474	**0.023**	0.137
	SI (3)	4.67 ± 0.18					
	MS (4)	4.48 ± 0.18					
	MI (5)	**5.58 ± 0.41**					
Ceruloplasmin	Naïve (1)	6.29 ± 0.08	10.87	0.000	− 0.41	− 0.51	− 0.06
	SS (2)	6.23 ± 0.05			**0.003**	**0.000**	0.980
	SI (3)	**6.64 ± 0.08**					
	MS (4)	6.20 ± 0.05					
	MI (5)	**6.71 ± 0.12**					
Vascular endothelial growth factor (VEGF)	Naïve (1)	4.29 ± 0.05	6.27	0.001	− 0.32	− 0.59	− 0.21
	SS (2)	4.36 ± 0.07			0.209	**0.001**	0.663
	SI (3)	4.68 ± 0.04					
	MS (4)	4.30 ± 0.06					
	MI (5)	**4.89 ± 0.19**					
von Willebrand Factor (vWF)	Naïve (1)	4.80 ± 0.09	22.74	0.000	− 0.60	− 0.63	− 0.07
	SS (2)	4.74 ± 0.04			**0.000**	**0.000**	0.951
	SI (3)	**5.34 ± 0.06**					
	MS (4)	4.78 ± 0.04					
	MI (5)	**5.41 ± 0.13**					

Mean protein values of naïve, SS, SI, MS and MI rats are log10. Tabulated results include the comparisons for blast injury, SS versus SI (2–3) and MS versus MI (4–5), and for the number of blast events, SI versus MI (3–5). Significant differences in biomarker levels are indicated in boldface.

Slides were incubated with the primary antibody solutions overnight at 4°C, then washed and incubated with the secondary antibodies Alexa Fluor® 633 donkey antisheep (A-21100), Alexa Fluor® 635 goat antimouse (A-31574), Alexa Fluor® 647 goat antirabbit (A-21245), or rabbit antigoat Immunoglobulin G (A-21446) (Molecular Probes®, Invitrogen) at 1:6000 dilution in antibody incubation buffer for 1 h at room temperature. Spot intensity data were imported into a Microsoft Excel-based bioinformatics program for analysis. The total amount of antigen is determined by the *Y*-axis intercept, that is by extrapolating the regression line to zero; reported protein values are log10 [9].

A total of 23 animals (Naïve = 3, SS = 6, SI = 4, MS = 6, MI = 4) were used for the statistical analyses. Student's *t*-test followed by a one-way ANOVA was used to analyze differences in the measured physiological parameters between injured groups and their respective sham groups at baseline, immediately after injury (5 consecutive days for MI rats), and days 1, 3, 7, 14, 26, 36, and 42 post injury. The SI and MI groups were compared on injury day (first injury for MI rats to correspond with SI rats) and each subsequent post injury time point. Statistical significance was reported for blast injury (SS versus SI and MS versys MI*) and for the number of blast events (SI versus MI#). A p value of < 0.05 is depicted by one special character, $p < 0.01$ by two, and $p < 0.001$ by three. Differences in the mean protein biomarker levels measured in plasma were analyzed with ANOVA followed by Tukey's HSD Test. All statistical analyses were performed using IBM SPSS Statistics 20 software. Tests were two tailed using $\alpha = 0.05$; data are presented as the mean ± SEM.

Consistent with our previous findings, the exposure to experimental manipulations alone (i.e. handling, transportation, and anesthesia) can elicit physiological changes as seen in sham animals on the injury day(s) (Fig. 1A–D) [6]. For logistical reasons we were not able to measure the immediate pre and post injury values of the selected physiological parameters, thus the extent and temporal pattern of acute changes remain unknown. However, the restoration of O_2 saturation levels to pre-injury values within a day after a single blast exposure (Fig. 1A) suggests that MI rats similarly recover after each daily exposure (Fig. 1B).

Of the four physiological parameters, only arterial O_2 saturation levels and heart rate changed significantly in response to either type of injury; the detected changes were transient over the length of the experiment (Fig. 1A–D). No significant injury-induced changes (i.e. sham versus injured) were measured in pulse distension and breath rate at any of the time points (data not shown). Importantly, we did not

Table 2. Neuronal, glial, and inflammatory biomarker levels in the plasma at 42 days post injury

Marker	Group	Mean ± SEM	ANOVA		Comparison of means		
			F-value	*p*-value	2–3 (*p*)	4–5 (*p*)	3–5 (*p*)
Neurofilament-heavy chain (NF-H)	Naïve (1)	5.94 ± 0.06	6.29	0.001	−0.37	−0.24	0.06
	SS (2)	5.83 ± 0.05			**0.002**	**0.049**	0.975
	SI (3)	**6.21 ± 0.13**					
	MS (4)	5.90 ± 0.03					
	MI (5)	**6.15 ± 0.04**					
Glial fibrillary acidic protein (GFAP)	Naïve (1)	2.55 ± 0.23	8.87	0.000	−0.98	−1.25	−0.09
	SS (2)	2.94 ± 0.16			**0.038**	**0.000**	0.999
	SI (3)	**3.92 ± 0.39**					
	MS (4)	2.75 ± 0.14					
	MI (5)	**4.01 ± 0.21**					
Myelin basic protein (MBP)	Naïve (1)	4.59 ± 0.14	6.45	0.001	−0.63	−0.7	−0.12
	SS (2)	4.64 ± 0.06			**0.013**	**0.012**	0.984
	SI (3)	**5.28 ± 0.24**					
	MS (4)	4.70 ± 0.07					
	MI (5)	**5.40 ± 0.15**					
Matrix metalloproteinase 8 (MMP8)	Naïve (1)	5.27 ± 0.10	3.24	0.022	−0.12	−0.27	−0.12
	SS (2)	5.25 ± 0.07			0.659	**0.016**	0.720
	SI (3)	5.37 ± 0.04					
	MS (4)	5.21 ± 0.04					
	MI (5)	**5.49 ± 0.07**					
Formyl peptide receptor 1 (FPR1)	Naïve (1)	4.96 ± 0.07	4.02	0.009	−0.33	−0.44	−0.06
	SS (2)	5.00 ± 0.06			0.175	**0.034**	0.996
	SI (3)	5.34 ± 0.04					
	MS (4)	4.95 ± 0.05					
	MI (5)	**5.39 ± 0.09**					
P38 mitogen-activated protein kinase (p38)	Naïve (1)	3.10 ± 0.22	5.26	0.002	−0.56	−0.73	−0.02
	SS (2)	2.97 ± 0.05			0.091	**0.008**	0.999
	SI (3)	3.52 ± 0.15					
	MS (4)	2.80 ± 0.13					
	MI (5)	**3.53 ± 0.12**					
Chemokine (C-C motif) receptor 5 (CCR5)	Naïve (1)	2.56 ± 0.12	5.08	0.003	−0.85	−0.48	0.41
	SS (2)	3.05 ± 0.10			**0.041**	0.33	0.697
	SI (3)	**3.90 ± 0.11**					
	MS (4)	3.01 ± 0.12					
	MI (5)	3.50 ± 0.07					
Toll-like receptor 9 (TLR9)	Naïve (1)	4.00 ± 0.06	0.82	0.523	−0.29	0.53	−0.08
	SS (2)	4.01 ± 0.39			0.987	0.876	0.999
	SI (3)	4.30 ± 0.17					
	MS (4)	3.95 ± 0.74					
	MI (5)	4.38 ± 0.48					

Mean protein values of naïve, SS, SI, MS and MI rats are log10. Tabulated results include the comparisons for blast injury, SS versus SI (2–3) and MS versus MI (4–5), and for the number of blast events, SI versus MI (3–5). Significant differences in biomarker levels are indicated in boldface.

detect any lasting changes between SI and MI animals in any of the measured vitals.

Forty-two days post injury, it appears that repeated exposure to mild blast overpressure resulted in hypoxia and oxidative stress as reflected in significantly increased plasma levels of oxidative stress markers HNE, HIF-1α, and ceruloplasmin (Table 1). At this late time point, HNE and ceruloplasmin levels were also increased in SI animals albeit to a lesser degree than in MI animals. These changes indicate a potential role for hypoxia and oxidative stress in the pathobiology of blast-induced TBI [10]. An increase in HNE levels during periods of oxidative stress is due to an increase in the lipid peroxidation chain reaction that affects a variety of biological pathways, including the cell cycle and cellular adhesion. Elevated ceruloplasmin levels are another indication of oxidative stress triggered by hypoxia [11]. As well demonstrated in stroke models, hypoxia can cause lasting increases in HIF-1α levels [12]. HIF-1α plays a crucial role in the adaptive and restorative response of organisms following neuronal insults (e.g. stroke and TBI) as it coordinates the expression of numerous genes to cope with noxious conditions thus mitigating the effects of ischemic conditions.

TBI also adversely affects several vascular functions including blood brain barrier permeability [13]. VEGF along with vWF is a key regulator of vascular permeability and other endothelial functions [14, 15]. The more robust increase in VEGF levels in MI rats suggests that VEGF may be involved in mediating the cumulative, more severe outcomes of rmTBI (Table 1). While VEGF levels were only significantly elevated at 42 days post injury in MI rats, vWF plasma levels remained significantly elevated in response to both types of injury. These findings implicate long-term alterations in endothelial functions after TBI including increased blood brain barrier permeability, which enables large molecules such as neuron- and glia-specific proteins to cross into the systemic circulation.

Consistent with our previous findings, even a single mild blast exposure significantly increased NF-H, GFAP, and MBP levels in the plasma (Table 2). Unlike the neuronal marker NF-H, GFAP, and MBP concentrations were relatively higher in MI animals than in SI animals as observed in the majority of the tested protein markers. Increased NF-H and MBP concentrations reflect damage to axons and their myelin sheaths as a result of the physical forces of the blast. Damage to axons and white matter tracts have been identified both clinically and experimentally as hallmarks of blast TBI along with damage to astroglia reflected in increased GFAP levels [16, 17].

Of the markers associated with various aspects of inflammation, MMP8, FPR1, and p38 were only elevated in MI animals suggesting greater damage accumulation and/or a more severe outcome in rmTBI. Given the role of these markers in the mediation of the neuroinflammatory process in several central nervous system disorders [18], it is not surprising that rmTBIs increase the risk for debilitating conditions like chronic traumatic encephalopathy. At this late time point, CCR5 levels were significantly elevated in SI animals alone while TLR9 was relatively unchanged in both injured groups. A potential explanation for the insignificant CCR5 response in MI rats is the late sampling time after injury. This can also account for the insignificant TLR9 levels in both injured groups due to the protein's rapid elevation and decline after injury.

In conclusion, the exposure to single and repeated mild blast at this frequency of insults triggers lasting changes in the form of oxidative stress, vascular abnormalities, and neuronal and glial cell damage/death. The chronic nature of these changes is particularly important considering that a rat week is the equivalent of 6–8 human months. However, we found no increase in the magnitude of the cumulative effect at this late time point suggesting that the frequency of the repetitive insults plays a critical role in determining the extent of the damage accumulation in rmTBI.

We thank the Neurotrauma Team at the Walter Reed Army Institute of Research for their technical help during the exposures. This work was supported by the Center for Neuroscience and Regenerative Medicine grant number G1703F. The views, opinions, and/or findings contained herein are those of the authors and should not be construed as an official position, policy, or decision of the Department of the Army or the Department of Defense. The authors have no financial disclosures. Animal handling and treatments were conducted in compliance with the Animal Welfare Act and other Federal statutes and regulations related to animals and experiments involving animals, and adhered to principles stated in the Guide to the Care and Use of Laboratory Animals, National Research Council. The facilities are fully accredited by the Association for Assessment and Accreditation of Laboratory Animal Care International.

The authors have declared no conflict of interest.

References

[1] Elder, G. A., Mitsis, E. M., Ahlers, S. T., Cristian, A., *Psychiatr. Clin. North Am.* 2010, *33*, 757–781.

[2] Laker, S. R., *PM R* 2011, *3*, S354–358.

[3] Hayes, J. P., Morey, R. A., Tupler, L. A., *Neurocase* 2012, *18*, 258–269.

[4] Stern, R. A., Riley, D. O., Daneshvar, D. H., Nowinski, C. J., Cantu, R. C., McKee, A. C., *PM R* 2011, *3*, S460–467.

[5] Kamnaksh, A., Kwon, S. K., Kovesdi, E., Ahmed, F., Barry, E. S., Grunberg, N. E., Long, J., Agoston, D., *Electrophoresis* 2012, *24*, 3680–3690.

[6] Kamnaksh, A., Kovesdi, E., Kwon, S. K., Wingo, D., Ahmed, F., Grunberg, N. E., Long, J., Agoston, D. V., *J. Neurotrauma* 2011, *28*, 2145–2153.

[7] Long, J. B., Bentley, T. L., Wessner, K. A., Cerone, C., Sweeney, S., Bauman, R. A., *J. Neurotrauma* 2009, *26*, 827–840.

[8] Cernak, I., Merkle, A. C., Koliatsos, V. E., Bilik, J. M., Luong, Q. T., Mahota, T. M., Xu, L., Slack, N., Windle, D., Ahmed, F. A., *Neurobiol. Dis.* 2011, *41*, 538–551.

[9] Gyorgy, A. B., Walker, J., Wingo, D., Eidelman, O., Pollard, H. B., Molnar, A., Agoston, D. V., *J. Neurosci. Methods* 2010, *192*, 96–101.

[10] Readnower, R. D., Chavko, M., Adeeb, S., Conroy, M. D., Pauly, J. R., McCarron, R. M., Sullivan, P. G., *J. Neurosci. Res.* 2010, *88*, 3530–3539.

[11] Dash, P. K., Redell, J. B., Hergenroeder, G., Zhao, J., Clifton, G. L., Moore, A., *J. Neurosci. Res.* 2010, *88*, 1719–1726.

[12] Yeh, S. H., Ou, L. C., Gean, P. W., Hung, J. J., Chang, W. C., *Brain Pathol.* 2011, *21*, 249–262.

[13] Schoknecht, K., Shalev, H., *Epilepsia* 2012, *53*(Suppl 6), 7–13.

[14] De Oliveira, C. O., Reimer, A. G., Da Rocha, A. B., Grivicich, I., Schneider, R. F., Roisenberg, I., Regner, A., Simon, D., *J. Neurotrauma* 2007, *24*, 1331–1338.

[15] Ferrara, N., *Curr. Opin. Biotechnol.* 2000, *11*, 617–624.

[16] Agoston, D. V., Elsayed, M., *Front Neurol.* 2012, *3*, 107.

[17] Matthews, S. C., Strigo, I. A., Simmons, A. N., O'Connell, R. M., Reinhardt, L. E., Moseley, S. A., *Neuroimage* 2011, *54(Suppl 1)*, S69–75.

[18] Barone, F. C., Parsons, A. A., *Expert Opin. Investig. Drugs* 2000, *9*, 2281–2306.

Journal of Neurotrauma

Journal of Neurotrauma: http://mc.manuscriptcentral.com/neurotrauma

Cerebrospinal fluid CCL2 is an early-response biomarker for blast overpressure wave- induced neurotrauma in rats

Journal:	*Journal of Neurotrauma*
Manuscript ID	NEU-2016-4465.R1
Manuscript Type:	Regular Manuscript
Date Submitted by the Author:	n/a
Complete List of Authors:	Wang, Ying; Walter Reed Army Institution of Research, Center for Military Psychiatry and Neuroscience Wei, Yanling; Walter Reed Army Institution of Research, Center for Military Psychiatry and Neuroscience Oguntaya, Samuel; Walter Reed Army Institution of Research, Center for Military Psychiatry and Neuroscience Wilder, Donna; Walter Reed Army Institution of Research, Center for Military Psychiatry and Neuroscience, Tong, Lawrence; Walter Reed Army Institution of Research, Center for Military Psychiatry and Neuroscience Su, Yan; Walter Reed Army Institution of Research, Center for Military Psychiatry and Neuroscience Gist, Irene; Walter Reed Army Institution of Research, Center for Military Psychiatry and Neuroscience Arun, Peethambaran; Walter Reed Army Institute of Research, Center for Military Psychiatry and Neuroscience Long, Joseph; Walter Reed Army Institute of Research, Center for Military Psychiatry and Neuroscience
Keywords:	TRAUMATIC BRAIN INJURY, CEREBROSPINAL FLUID, AXONAL INJURY, BIOMARKERS, Rat

Cerebrospinal fluid CCL2 is an early-response biomarker for blast overpressure wave- induced neurotrauma in rats

Ying Wang*, Yanling Wei, Samuel Oguntayo, Donna Wilder, Lawrence Tong, Yan Su, Irene Gist, Peethambaran Arun and Joseph B. Long*

Blast-Induced Neurotrauma Branch, Center for Military Psychiatry and Neuroscience, Walter Reed Army Institute of Research, Silver Spring, MD 20910

Running Head: Blast exposure alters CCL2 levels

Ying Wang, 301-319-9853, ying.wang5.ctr@mail.mil, Co-corresponding author
Yanling Wei, 301-319-9652, yanling.wei.ctr@mail.mil
Samuel A. Oguntayo, 301-319-7665, samuel.a.oguntaya.ctr@mail.mil
Donna M. Wilder, 301-319-7685, donna.m.wilder2.ctr@mail.mil
Lawrence C. Tong, 301-319-9547, lawrence.c.tong.ctr@mail.mil
Yan Su, 301-319-9853, yan.su.ctr@mail.mil
Irene D. Gist, 301-319-9108, irene.d.gist.civ@mail.mil
Peethambaran Arun, 301-319-2009, peethambaran.arun.ctr@mail.mil
Joseph B. Long, 301-319-9853, joseph.b.long.civ@mail.mil, Corresponding author

For all authors' fax and mail address,
Fax: 301-319-9839
Mail address: 503 Robert Grant Avenue, Silver Spring, MD 20910

Abstract

Chemokines and their receptors are of great interest within the milieu of immune responses elicited in CNS in response to trauma. Chemokine ligand 2 (CCL2), which is also known as monocyte chemotactic protein-1 (MCP-1), has been implicated in the pathogenesis of traumatic brain injury, brain ischemia, Alzheimer's disease and other neurodegenerative diseases. In this study, we investigated the time-course of CCL2 accumulation in cerebrospinal fluid (CSF) following exposures to single and repeated blast overpressures of varied intensities along with the neuropathological changes and motor deficits resulting from these blast conditions. Significantly increased concentrations of CCL2 in CSF were evident by one hour of blast exposure and persisted over 24 hrs with peak levels measured at 6 hrs post-injury. The increased levels of CCL2 in CSF corresponded with both the number and the intensities of blast overpressure and were also commensurate with the extent of neuro-motor impairment and neuropathological abnormalities resulting from these exposures. CCL2 levels in CSF and in plasma were tightly correlated with the levels of CCL2 mRNA in cerebellum, the brain region most consistently neuropathologically disrupted by blast. In view of the roles of CCL2 that have been implicated in multiple neurodegenerative disorders, it is likely that the sustained high levels of CCL2 and the increased expression of its main receptor CCR2 in the brain after blast may similarly contribute to neurodegenerative processes after blast exposure. In addition, the markedly elevated concentration of CCL2 in CSF might be a candidate early-response biomarker for diagnosis and prognosis of blast-induced traumatic brain injury.

Key words: Blast-induced neurotrauma; cerebrospinal fluid; biomarker; chemokines; CCL2

Introduction

Blast-induced traumatic brain injury (bTBI) can occur over a wide range of severities as a result of both combat operations and terrorist bombings. The clinical presentation and pathophysiological sequelae are varied and multifaceted[1], and classification criteria[2, 3], particularly for mild TBI, presently lack consensus definition. In the absence of clear and widely accepted objective criteria for assessments of mild TBI, current diagnoses often rely on self-reported symptoms. To date, mild TBI is difficult to diagnose early by clinical examination and standard neuroimaging techniques. Moreover, no effective treatment strategies have been developed for bTBI even though brain injury resulting from blast exposure has been postulated to predispose victims to post-concussive symptoms, post-traumatic stress disorders and/or chronic traumatic encephalopathy (CTE)[4-8] . Identification of reliable biomarker(s) and pathophysiological mediators has been widely pursued as a means to achieve more precise diagnosis and therapeutic countermeasures for bTBI[9-11] .

Induction of inflammatory processes has long been recognized to be among the first responses of the body to a localized injury. Neuroinflammation is prominently involved in acute and chronic neuropathological conditions[12], and TBI-induced neuroinflammatory responses are now recognized as critical steps in the development of a variety of brain diseases[13, 14]. Inflammation is mediated by cytokines and eicosanoids which are released predominantly from injured tissue and from accumulated macrophages and contribute to both secondary tissue damage and repair[15]. Chemokines are a family of small cytokines that are chemoattractants for leukocytes and guide the directional migration of monocytes, neutrophils and other effector cells to the site of tissue damage. In particular, the chemokine ligand 2 (CCL2), also known as monocyte chemotactic

protein-1 (MCP-1), is secreted by leukocytes in the blood and is also produced by astrocytes, microglia and neurons in the brain. It is involved in cellular migration and intercellular communication through interactions with glycol-protein receptors coupled to a G protein signaling pathway. Its pattern of neuroanatomical localization and co-distribution with neurotransmitters and neuroregulatory peptides has prompted speculation that CCL2 might act as a modulator of neuronal activity and neuroendocrine function[16]. CCL2 has also been shown to act as a key factor in both the initiation and maintenance of neuroinflammation in the spinal cord after peripheral nerve injury[17], and has been strongly implicated in the pathogenesis of brain ischemia[18], autoimmune encephalomyelitis [19], epilepsy[20], traumatic brain injury[21-29], and neurodegenerative diseases[30-32]. Notably, Semple *et al.*[22] detected > 20-fold immediate elevations in CCL2 in the CSF of severe TBI patients which although diminished, persisted for 10 days post-trauma[22]. They additionally found transiently increased levels of CCL2 in the cortices of mice subjected to closed head injury (with peak levels by 4 to 12 hrs) and established that the absence of CCL2 in CCL2-/- mice was associated with improved neurological recovery and a delayed reduction in lesion volume, macrophage accumulation, and astrogliosis, pointing to a potentially important role of CCL2 as both a biomarker and a mediator of acute secondary brain degeneration after trauma.

In addition to its role as a mediator of acute neurotrauma, CCL2 has also been implicated in chronic neurodegenerative disorders[31-35], and may potentially serve as a link between the former and the latter with CSF CCL2 levels providing diagnostic insights. For example, Westin et al. found that in patients with prodromal Alzheimer's disease (AD), CCL2 levels in CSF correlate with a faster cognitive decline observed during follow-up,[35] suggesting that CCL2 in CSF may have predictive diagnostic utility of AD-related pathology, and that CCL2-related signaling

pathways might provide therapeutic targets to counter progression of this and perhaps other neurodegenerative disorders. In the present study, we used a well-defined bTBI model in rats to determine the acute changes in CCL2 levels in the brain, CSF and plasma following blast exposure(s) and assessed its association with the acute functional disruptions and pathological changes resulting from these traumatic insults.

Material and methods

Animal and blast injury

All animal experiments were conducted in an AAALACi accredited facility in compliance with the Animal Welfare Act and other federal statutes and regulations relating to animals and experiments involving animals and adheres to principles stated in the *Guide for the Care and Use of Laboratory Animals*, NRC Publication, 2011 edition. Male Sprague Dawley rats, weighing 325-350 g at 8-10 weeks of age (Charles River Laboratories, Inc, MD), were housed at 20 - 22°C (12 h light/dark cycle) with free access to food and water ad libitum. After 4% isoflurane gas anesthesia in an induction chamber for 8 min (O_2 flow rate 1.5L/min), rats were immediately tautly secured in a transverse prone position 2.5 ft within the mouth of a 1 ft diameter compressed air-driven shock tube with the right side of the animal facing the oncoming shockwave. Animals were exposed to a single blast at a peak total pressure of 12 psi (83 KPa, single low-level blast, SLB) or 19 psi (131 KPa, single high-level blast, SHB) or were exposed to closely coupled repeated 19 psi blasts separated by a 1 min interval (double high-level blast, DHB). All BOPs had an 8 - 9 msec. positive phase duration. Sham control animals were

included in all individual experiments and were treated in the same fashion without exposure to blast waves.

Biosamples preparation

Blood, CSF and brain tissue samples were collected at different times (1 hr, 6 hrs, 24 hrs, and 7 days) post-blast. Blood was collected under isoflurane anesthesia by cardiac puncture and plasma was separated immediately by centrifugation at 1000 rpm for 10 min. For cerebrospinal fluid (CSF) collection, isoflurane-anesthetized rats were secured in a stereotaxic frame (Stoelting Inc) and after a midline incision; the cervico-spinal muscle was separated to expose the atlanto-ocipital membrane. CSF was removed using a needle puncture of the atlanto-occipital membrane. Tissue protein extraction was carried out by homogenizing brains in tissue protein extraction reagent (T-PER, Thermo Fisher Scientific, Rockford, IL) containing protease and phosphatase inhibitors (Sigma-Aldrich, St. Louis, MO) using an ultrasonic homogenizer. The homogenate was centrifuged at 17700 ×g for 15 min at 4°C and the supernatant was collected and stored at -80°C.

Enzyme-Linked Immunosorbent Assay (ELISA)

CCL2 concentrations in plasma, CSF and homogenate supernatant of brain tissue were determined using ELISA kits (Thermo Scientic Inc. Rockford, IL) in accordance with the manufacturer's instructions. All samples were assayed in duplicates. Standards and control samples were run simultaneously for validation.

RNA extraction and PCR analyses

Total RNA from brain tissue was isolated using QUAzol reagent and purified using RNeasy kit after being treated with DNase according to the manufacturer's instructions (QIAGEN, Valencia, CA). Equal amount (1 μg) of RNA from each sample was reverse transcribed using the RT² first-strand kit (QIAGEN, Valencia, CA). The custom RT² profiler PCR array was employed and the cDNA was amplified with the RT² SYBR Green ROX qPCR Mastermix on ABI 7500 Fast real-time PCR system (Thermofisher scientific, Carlsbad, CA). The RT² qPCR primer assay was used for verification of relative gene expression.

Histopathology

Rats were anesthetized with isoflurane and perfused transcardially with saline followed by 4% paraformaldehyde (PFA). After 6 hrs of further immersion fixation in PFA, the brain was cryoprotected with 20% sucrose for 72 hours and rapidly frozen in isopentane pre-cooled to −70°C with dry ice. Serial coronal sections (50 μm) were cut from the cerebrum and brain stem/cerebellum (Bregma 2.68 mm to -4.84 mm and Bregma -5.68 mm to -6.40 mm, respectively), immersed in 4% PFA for 5 days, and then processed using the FD Neurosilver™ kit II (FD NeuroTechologies, Ellicott City, MD). Brain sectioning and silver staining were performed by FD NeuroTechnologies. Silver stained sections were scored based on relative visible intensity of silver precipitates by an experienced, blinded neuropathologist using a bright field microscope. Scores were assigned from 1 to 4 on a rank scale to indicate an increasing severity of axonal degeneration.

Rotarod testing

The Rotamex-5 rotarod apparatus (Columbus Instruments, Columbus, OH) was used to assess motor coordination and balance. A fixed-speed training regimen was conducted at10 and 20 rpm with 120 sec/trial and 3 trials per day for each fixed-speed. Rats were trained for 4 consecutive days followed by a 2-day break and then received 1 additional day of training. The baseline testing was recorded on the day of blast exposure, and the testing paradigm was the same as that used for training. Rats failing to establish a ≥ 60 sec baseline runtime were excluded.

Statistical analysis

Statistical analyses were performed using GraphPad Prism 6 software (GraphPad Software Inc., San Diego, CA). Data were analyzed using Student's *t*-test or repeated measures ANOVA. For multiple comparisons, following ANOVA significant differences among treatment groups were identified using Tukey's multiple comparison tests. Differences were considered to be significant at the level *p* less than 0.05 and values are expressed as the mean ± standard error.

Results:

Blast exposure impaired motor coordination

Rats with baseline performances over 60 seconds with both 10 and 20 rpm fixed speeds on the rotarod were randomly assigned to the DHB, SHB and sham treatment groups. Runtimes (latencies to fall) and % change in runtimes relative to baseline performance for each rat were

analyzed by one-way ANOVA with Tukey's multiple comparison. At 10 rpm (FIG. 1A and 1B), DHB rats' runtimes and % changes in runtimes were significantly different from those of sham controls at 1 and 2 days post-injury. Compared to SHB, DHB rats presented a significant decrease in % changes in runtimes at 1 day post-injury. At 20 rpm (FIG. 1C and 1D), DHB rats displayed significantly reduced runtimes (e.g. 31.7 ± 11.3 sec at 24 hrs post-injury) and greater % changes in runtime from baseline (e.g. – 71.1 ± 9.1% at 24 hrs post-injury) compared to the values recorded for both SHB (71.3 ± 10.9 sec., - 27.9 ± 8.3%) and sham controls (87.2 ± 5.4 sec., - 8.7 ± 4.6%). The changes persisted through 7 days post-injury. The % changes in runtimes in SHB rats were also significantly different from shams on each test date through 7 days post-injury.

Blast exposure induced axonal degeneration

The extent of axonal degeneration after blast exposure was determined by silver staining and scored by a blinded neuropathologist, with higher scores reflecting increasing severities of axonal degeneration. Our previous studies consistently showed that blast-induced axonal degeneration was particularly pronounced in cerebellum compared to other brain regions[36, 37]. In the present study, the greatest axonal degeneration was again observed in the cerebellar white matter at 7 days post-BOP (FIG. 2A). Double blast exposures resulted in a significant increase in axonal degeneration relative to that seen after a single blast exposure ($p < 0.01$, FIG. 2B).

CCL2 levels in CSF increased following blast injury

Figure 3A illustrates the CSF concentrations of CCL2 at 1 hr, 6 hrs, 24 hrs and 7 days after blast exposure(s). These data show that CCL2 levels in CSF were significantly elevated by 1 hr and remained increased up to 24 hrs after double blast exposures, with the greatest CCL2 concentrations measured at 6 hrs post-injury. At 6 hrs after DHB exposure, the levels of CCL2 were significantly higher than at 1 h post exposure. In order to address whether the magnitude of the CSF CCL2 changes is injury severity-dependent, we exposed rats to a single blast with 12 psi (SLB) or 19 psi (SHB) peak total pressure or a double blast (DHB) with 19 psi peak total pressures and measured CCL2 levels at 6 hrs post-insult. Compared to sham controls, CCL2 levels in the CSF were significantly increased after SLB, SHB, and DHB (FIG. 3B). The CCL2 concentrations in CSF following SHB were significantly greater than following SLB, and the elevated CCL2 concentrations elicited by DHB were significantly greater than measured in all other treatment groups.

CCL2 levels in the plasma increased after blast exposure

Plasma CCL2 were unchanged following exposure to a single 12 psi blast overpressure (SLB). In contrast, plasma CCL2 levels increased dramatically at 6 hrs post-insult in the 19 psi single blast (SHB) and double (DHB) exposed groups and were significantly different from CCL2 levels measured in both sham and SLB rats (FIG. 4A). The time-course of changes in plasma CCL2 after SHB and DHB reveals a peak elevation around 6 hrs post-exposure (FIG. 4B). There was no difference between the plasma CCL2 levels measured in the DHB and SHB treatment groups at any time point studied.

The increase in CCL2 in the CSF after blast exposure was greater than that in plasma

Comparison of the relative increases in CCL2 in the CSF and plasma after DHB reveal that the changes in CCL2 after repeated blasts persisted longer and were considerably greater in CSF than in plasma (FIG. 5A). Specifically, the fold changes of CCL2 in the CSF at 1 hr, 6 hrs and 24 hrs post-double exposures were 8.70 ± 1.32, 16.49 ± 2.27 and 11.35 ± 2.89, respectively, while in the plasma at these times the fold changes were 1.73 ± 0.23, 2.00 ± 0.17 and 1.24 ± 0.23, respectively. The data also showed a positive correlation between CCL2 levels in CSF and plasma (FIG. 5B, Pearson's $r = 0.76$, $p < 0.0002$). When compared to sham, the ratio of CSF/plasma CCL2 showed no significant change in rats exposed to 12 psi single blast. In contrast, after exposure to a 19 psi single blast (FIG. 5C) the ratio increased significantly at 6 hrs and 24 hrs. Furthermore, rats exposed to double 19 psi BOP had significantly greater CSF/plasma CCL2 ratios at both 6 hrs and 24 hrs post-injury compared to the other experimental groups.

Up-regulation of CCL2 in the cerebellum after blast exposure

Compared to the sham controls (FIG. 6), CCL2 protein levels increased significantly at 6 hrs and 24 hrs after SHB. DHB elicited significantly higher levels of CCL2 in the cerebellum than SHB at 6 hrs post-injury, and these increases persisted at 24 hrs and 3 day after DHB.

Expressions of CCL2 and CCR2 genes increased after blast exposure

We further examined the changes in mRNA levels of CCL2 and its main receptor CCR2 in the cerebellum after DHB. Total RNA isolated from the cerebellum was subjected to RT² qPCR primer assay. Compared to sham controls, exposure to DHB resulted in higher levels of CCL2

mRNA in the cerebellum at 6 hrs and 7 d post-injury (FIG.7). The blast-induced increase in CCL2 gene expression was greater at 6 hrs than at 7 d post-injury. Compared to sham controls, the expression of CCR2 mRNA also increased significantly at 6 hr after DHB.

To determine an association between CCL2 protein in CSF or plasma and CCL2 gene expression in the brain tissue, we performed a statistical analysis on paired data from 20 animals. The ΔCt-method, calculating a difference in threshold cycle between the target and house keep genes was used to quantify gene expression[38]. The results revealed a strong negative correlation (inverse relationship) between the ΔCt value of CCL2 mRNA in the cerebellum and CCL2 protein in CSF (FIG. 8A, Pearson $r = -0.86$, $p < 0.0001$) or in plasma (FIG. 8B, Pearson $r = -0.76$, $p < 0.001$), respectively. These data indicate that blast-induced elevations in CCL2 gene expression in brain cells may contribute to the increased CCL2 protein in CSF.

Discussion

The primary clinical indicators of TBI and its severity are the Glasgow Coma Scale (GCS), pupil reactivity, and conventional neuroimaging including head computed axial tomography (CAT) and magnetic resonance imaging (MRI)[39, 40]. Unfortunately, these outcome measures are typically insensitive to diffuse axonal injury and mild TBI. Although advanced structural neuroimaging techniques have been explored as more sensitive quantitative measures of abnormalities in the brain related to TBI, they are still under investigation to substantiate the clinical relevance in individual patients[41, 42]. Over the past decade, molecular biomarkers derived from acute neuronal, axonal, glial and endothelial injuries that can be measured in bio-fluids (e.g. CSF and blood) have received considerable attention as promising candidates for diagnosis and

prognosis of traumatic brain injury. Although numerous candidate biomarkers of structural damage such as NF-L, MAP2, UCHL1, GFAP and S100B have been identified and investigated, most are hampered by low specificity and/or sensitivity when used individually[42-46]. Biomarkers of secondary and reparative processes such as IL-6, IL-1β, IL-8 and TNFα have also been evaluated in animal studies[47] and in clinical trials[48], but verification and validation of their utility, particularly for mild TBI, remains a sizeable obstacle.

The major challenges confronted in the exploration of biomarkers for blast-induced TBI include the development of fidelic, reliable, and predictive mild TBI animal models and the establishment of 'high throughput' biomarker detection methods. In previous studies, we have characterized neuropathological, neurobehavioral, and neurochemical features of mouse and rat models of bTBI using single and tightly coupled repetitive blast overpressure wave exposures within a compressed air driven shock tube[36, 37, 49]. Along with others[50, 51], we have observed neuropathological features that closely correspond to neuroimaging findings described in patients with blast-related mTBIs[50, 52]. In particular, cerebellar white matter abnormalities and cerebellar dysfunction described in combat veterans parallel the consistent fiber degeneration and Purkinje cell loss observed in these rodent preclinical models[50, 51]. Using voxelwise analysis of diffusion tensor imaging to quantify white matter injury, we further observed a pronounced increase in microstructural damage with a closely coupled second blast exposure. This was particularly prominent in the cerebellum and suggests that primary bTBI may sensitize the brain to subsequent insult from either blast or impact acceleration[37]. In the present study, we have further evaluated the effects of single and closely coupled repeated blast exposures on the levels of CCL2 in the CSF, plasma, and brain and determined their association with neurobehavioral and neuroanatomical outcomes. These blast-induced disruptions were preceded by significant acute

increases in levels of CCL2 in CSF and brain tissue extracts which corresponded with the number and intensities of blast overpressure exposures and were also commensurate with the eventual extent of neuro-motor impairment and neuropathological abnormalities resulting from these exposures. Tightly coupled repeated blast exposures, which caused appreciably greater functional deficits and neuropathological and biochemical changes than a single blast of identical intensity, caused similarly significantly greater elevations of CCL2 in both CSF and brain tissue. The changes in CCL2 in CSF and in plasma correlated with the levels of CCL2 mRNA in cerebellum, which as noted above is the brain region most consistently and severely neuropathologically disrupted by repeated blast. Although clearly these findings do not reveal a causal involvement of CCL2 in the injury mechanisms triggered by BOP, they nevertheless point to this possibility as well as the utility of further consideration of CCL2 as a biomarker for these events.

Chemokines and their receptors are essential for brain development and the maintenance of homeostasis in the CNS. In the MCP family, CCL2 is the most potent at activating signal transduction leading to monocyte transmigration[53]. CCL2 has been suggested to be a biomarker for acute kidney damage and other autoimmune diseases[54, 55] and also has been identified as an important mediator of the initiation and maintenance of pain hypersensitivity[56-58]. The sustained elevation of CCL2 levels in the CSF of patients with severe TBI for 10 days post-injury further points to the potential utility of CSF levels of CCL2 as a diagnostic and prognostic marker of brain injury[22]. In the present study, we have demonstrated that changes in CSF CCL2 levels corresponded with the relative severity of the blast overpressure injuries. Since CCL2 mRNA and protein expression increased substantially in the brain acutely after blast injury, the concomitant sizeable acute spikes in CCL2 concentrations in the CSF likely originated in the

brain, even though possible minor contributions from the circulation due to leakage across the blast-damaged blood-brain barrier (BBB) cannot be completely ruled out.

In a recent series of studies, a brain-wide network of of paravascular channels, known as the glymphatic system, has been shown to be responsible for the clearance of interstitial solutes from the brain and is principally responsible for the transport of biomarkers to the blood via the cervical lymphatics[59, 60]. Glymphatic activity is impaired after TBI[59], which potentially confounds biomarker appearance in the circulation and consequently compromises the clinical utility of blood-based biomarkers to objectively and consistently predict the severity of injury. In addition, TBI-induced impairment of glymphatic function has also been shown to be a key factor contributing to the aberrant accumulation of phosphorylated tau after TBI, promoting tau aggregation and the onset of neurodegeneration[59]. Since elevated CCL2 levels were significantly greater at 6 hrs than at 1 hr post-injury, it would appear that CCL2 production and release in the brain increased subsequent to the primary blast insult. The elevated CSF CCL2 levels, which corresponded with the magnitude of motor coordination impairment, persisted longer than did the CCL2 elevations in plasma and might thus have greater utility as an early-response biomarker for diagnosis and prognosis of blast-induced brain injuries than measurements taken from the circulation.

CCL2 is one of a number of brain chemokines that have been extensively evaluated after various forms of experimental TBI, including FPI[27, 28], CCI[25, 29], blast and head-only blast exposure[21, 23], and weight drop[22]. Semple et al. reported that CCL2 levels increased rapidly in the cerebral cortices of mice subjected to weight drop closed head injury, with a maximum 40-fold increase at 4 to 12 hr and a return to near normal levels by 24 hr post-trauma[22]. A similar temporal pattern of CCL2 change was recorded in the cerebellum after a single blast exposure in

the current study and in the CSF after single and double blast exposures. In contrast, significantly greater increases in CCL2 in the cerebellum after double blast exposure persisted through 3 days postinjury. It is noteworthy that head-only exposure of rats to blast overpressure transiently altered the expression of several brain cytokines and chemokines which, with the exception of macrophage inflammatory protein-1α, returned to baseline levels by 24 hrs postinjury, confirming that these changes in the CNS can occur independently of systemic injury responses[21].

In addition to measuring CCL2, we investigated the stability of CCL2 protein and sensitivity of the ELISA kit. We did not find a significant difference in measurements among the samples which were stored in -20 °C, 4 °C and room temperature (data are not shown), indicating a high stability of CCL2 protein. ELISA detection of CCL2 requires only 4 µl of CSF or 2 µl of plasma and is reliable and reproducible.

Recent studies on glia-neuron cross talk show that astrocyte-derived CCL2 is an important immediate mediator of neuroprotection against excitotoxicity[61]. Although this immediate inflammatory response following primary injury to the brain initially provides a restorative/reparative function, it can persist beyond its beneficial effect and potentially lead to secondary injuries involving alterations in neuronal excitability, axonal integrity, central processing, and other changes stemming from a cytokine storm. These protracted biochemical changes following the insult reflect progressive and potentially reversible molecular and cellular pathophysiological mechanisms, including chemokine-mediated accumulation of inflammatory cells in the brain parenchyma, which appears to play a crucial role in the pathogenesis of traumatic injuries[15] and in the evolution of neuroinflammatory diseases[22, 34, 35]. For decades, TBI has been linked to Alzheimer's disease and new data suggest important additional links between

neurotrauma and other neurodegenerative diseases including Parkinson's disease, amyotrophic lateral sclerosis, multiple sclerosis, and Huntington's disease[62-64]. As these studies expand to explore neurodegeneration and/or neurorestoration after blast TBI, CCL2 warrants consideration as part of the neurobiological linkage.

Conclusion

Cytokines have both beneficial and detrimental effects in the injured brain, contributing to the facilitation of neural regeneration and also to secondary brain damage through neuroinflammatory processes. Chemokines and their receptors are of particular interest in the CNS in response to brain injuries. Acute increase in CCL2 expression in the brain and associated elevation in the CSF suggested that the CCL2 levels in the CSF can be used as a biomarker of bTBI. Since the whole body is exposed to blast, plasma CCL2 levels can be more appropriately considered alone as an indicator for blast-induced polytrauma. Paralleling its proposed roles in other neurodegenerative disorders, sustained high levels of CCL2 and increases in its receptor expression in the CNS after blast may contribute to neurodegenerative processes including chronic traumatic encephalopathy, and therefore should be recognized as a potentially important target for therapeutic drug intervention.Thus chemokine ligands and receptors may be targets for immunomodulatory therapy against bTBI.

Acknowledgments

We thank Dr. James DeMar for useful manuscript corrections and comments and Dr. Yuanzhang Li for valuable suggestions regarding data analysis. Technical guidance and assistance from Stephen VanAlbert and Andrea Edwards are also gratefully acknowledged. This work was supported by Congressionally Directed Medical Research Program awards W81XWH-11-2-0127, W81-XWH-08-2-0018, and W81XWH-08-2-0017.

Author Disclosure Statement

The authors have no financial or personal conflicts of interests.

Disclaimer: The contents, opinions and assertions contained herein are private views of the authors and are not to be construed as official or reflecting the views of the Department of the Army or the Department of Defense.

References

1. Sayer, N.A., Rettmann, N.A., Carlson, K.F., Bernardy, N., Sigford, B.J., Hamblen, J.L. and Friedman, M.J. (2009). Veterans with history of mild traumatic brain injury and posttraumatic stress disorder: challenges from provider perspective. Journal of rehabilitation research and development 46, 703-716.

2. (2009). VA/DoD Clinical Practice Guideline for Management of Concussion/Mild Traumatic Brain Injury. Journal of rehabilitation research and development 46, Cp1-68.

3. Marshall, S., Bayley, M., McCullagh, S., Velikonja, D., Berrigan, L., Ouchterlony, D. and Weegar, K. (2015). Updated clinical practice guidelines for concussion/mild traumatic brain injury and persistent symptoms. Brain injury : [BI] 29, 688-700.

4. Goldstein, L.E., Fisher, A.M., Tagge, C.A., Zhang, X.L., Velisek, L., Sullivan, J.A., Upreti, C., Kracht, J.M., Ericsson, M., Wojnarowicz, M.W., Goletiani, C.J., Maglakelidze, G.M., Casey,

N., Moncaster, J.A., Minaeva, O., Moir, R.D., Nowinski, C.J., Stern, R.A., Cantu, R.C., Geiling, J., Blusztajn, J.K., Wolozin, B.L., Ikezu, T., Stein, T.D., Budson, A.E., Kowall, N.W., Chargin, D., Sharon, A., Saman, S., Hall, G.F., Moss, W.C., Cleveland, R.O., Tanzi, R.E., Stanton, P.K. and McKee, A.C. (2012). Chronic traumatic encephalopathy in blast-exposed military veterans and a blast neurotrauma mouse model. Science translational medicine 4, 134ra160.

5. Hoge, C.W., McGurk, D., Thomas, J.L., Cox, A.L., Engel, C.C. and Castro, C.A. (2008). Mild traumatic brain injury in U.S. Soldiers returning from Iraq. N.Engl.J.Med. 358, 453-463.

6. Stratton, K.J., Clark, S.L., Hawn, S.E., Amstadter, A.B., Cifu, D.X. and Walker, W.C. (2014). Longitudinal interactions of pain and posttraumatic stress disorder symptoms in U.S. Military service members following blast exposure. The journal of pain : official journal of the American Pain Society 15, 1023-1032.

7. Boyle, E., Cancelliere, C., Hartvigsen, J., Carroll, L.J., Holm, L.W. and Cassidy, J.D. (2014). Systematic review of prognosis after mild traumatic brain injury in the military: results of the International Collaboration on Mild Traumatic Brain Injury Prognosis. Archives of physical medicine and rehabilitation 95, S230-237.

8. Troyanskaya, M., Pastorek, N.J., Scheibel, R.S., Petersen, N.J., McCulloch, K., Wilde, E.A., Henson, H.K. and Levin, H.S. (2015). Combat exposure, PTSD symptoms, and cognition following blast-related traumatic brain injury in OEF/OIF/OND service members and Veterans. Military medicine 180, 285-289.

9. Patterson, Z.R. and Holahan, M.R. (2012). Understanding the neuroinflammatory response following concussion to develop treatment strategies. Frontiers in cellular neuroscience 6, 58.

10. Agoston, D.V. and Elsayed, M. (2012). Serum-based protein biomarkers in blast-induced traumatic brain injury spectrum disorder. Frontiers in neurology 3, 107.

11. Agoston, D.V. and Kamnaksh, A. (2015). Modeling the Neurobehavioral Consequences of Blast-Induced Traumatic Brain Injury Spectrum Disorder and Identifying Related Biomarkers. In: *Brain Neurotrauma: Molecular, Neuropsychological, and Rehabilitation Aspects*. Kobeissy, F.H. (ed): Boca Raton (FL).

12. Lucas, S.M., Rothwell, N.J. and Gibson, R.M. (2006). The role of inflammation in CNS injury and disease. British journal of pharmacology 147 Suppl 1, S232-240.

13. Amor, S., Puentes, F., Baker, D. and van der Valk, P. (2010). Inflammation in neurodegenerative diseases. Immunology 129, 154-169.

14. Johnson, V.E., Stewart, J.E., Begbie, F.D., Trojanowski, J.Q., Smith, D.H. and Stewart, W. (2013). Inflammation and white matter degeneration persist for years after a single traumatic brain injury. Brain : a journal of neurology 136, 28-42.

15. Ziebell, J.M. and Morganti-Kossmann, M.C. (2010). Involvement of pro- and anti-inflammatory cytokines and chemokines in the pathophysiology of traumatic brain injury.

Neurotherapeutics : the journal of the American Society for Experimental NeuroTherapeutics 7, 22-30.

16. Conductier, G., Blondeau, N., Guyon, A., Nahon, J.L. and Rovere, C. (2010). The role of monocyte chemoattractant protein MCP1/CCL2 in neuroinflammatory diseases. J.Neuroimmunol. 224, 93-100.

17. Van Steenwinckel, J., Reaux-Le Goazigo, A., Pommier, B., Mauborgne, A., Dansereau, M.A., Kitabgi, P., Sarret, P., Pohl, M. and Melik Parsadaniantz, S. (2011). CCL2 released from neuronal synaptic vesicles in the spinal cord is a major mediator of local inflammation and pain after peripheral nerve injury. The Journal of neuroscience : the official journal of the Society for Neuroscience 31, 5865-5875.

18. Amantea, D., Nappi, G., Bernardi, G., Bagetta, G. and Corasaniti, M.T. (2009). Post-ischemic brain damage: pathophysiology and role of inflammatory mediators. The FEBS journal 276, 13-26.

19. Proudfoot, A.E., de Souza, A.L. and Muzio, V. (2008). The use of chemokine antagonists in EAE models. Journal of neuroimmunology 198, 27-30.

20. Fabene, P.F., Bramanti, P. and Constantin, G. (2010). The emerging role for chemokines in epilepsy. Journal of neuroimmunology 224, 22-27.

21. Kochanek, P.M., Dixon, C.E., Shellington, D.K., Shin, S.S., Bayir, H., Jackson, E.K., Kagan, V.E., Yan, H.Q., Swauger, P.V., Parks, S.A., Ritzel, D.V., Bauman, R., Clark, R.S., Garman, R.H., Bandak, F., Ling, G. and Jenkins, L.W. (2013). Screening of biochemical and molecular mechanisms of secondary injury and repair in the brain after experimental blast-induced traumatic brain injury in rats. Journal of neurotrauma 30, 920-937.

22. Semple, B.D., Bye, N., Rancan, M., Ziebell, J.M. and Morganti-Kossmann, M.C. (2010). Role of CCL2 (MCP-1) in traumatic brain injury (TBI): evidence from severe TBI patients and CCL2-/- mice. Journal of cerebral blood flow and metabolism : official journal of the International Society of Cerebral Blood Flow and Metabolism 30, 769-782.

23. Cho, H.J., Sajja, V.S., Vandevord, P.J. and Lee, Y.W. (2013). Blast induces oxidative stress, inflammation, neuronal loss and subsequent short-term memory impairment in rats. Neuroscience 253, 9-20.

24. Ho, L., Zhao, W., Dams-O'Connor, K., Tang, C.Y., Gordon, W., Peskind, E.R., Yemul, S., Haroutunian, V. and Pasinetti, G.M. (2012). Elevated plasma MCP-1 concentration following traumatic brain injury as a potential "predisposition" factor associated with an increased risk for subsequent development of Alzheimer's disease. Journal of Alzheimer's disease : JAD 31, 301-313.

25. Graber, D.J., Costine, B.A. and Hickey, W.F. (2015). Early inflammatory mediator gene expression in two models of traumatic brain injury: ex vivo cortical slice in mice and in vivo cortical impact in piglets. Journal of neuroinflammation 12, 76.

26. Lozano, D., Gonzales-Portillo, G.S., Acosta, S., de la Pena, I., Tajiri, N., Kaneko, Y. and Borlongan, C.V. (2015). Neuroinflammatory responses to traumatic brain injury: etiology, clinical consequences, and therapeutic opportunities. Neuropsychiatric disease and treatment 11, 97-106.

27. Muccigrosso, M.M., Ford, J., Benner, B., Moussa, D., Burnsides, C., Fenn, A.M., Popovich, P.G., Lifshitz, J., Walker, F.R., Eiferman, D.S. and Godbout, J.P. (2016). Cognitive deficits develop 1month after diffuse brain injury and are exaggerated by microglia-associated reactivity to peripheral immune challenge. Brain, behavior, and immunity 54, 95-109.

28. Rhodes, J.K., Sharkey, J. and Andrews, P.J. (2009). The temporal expression, cellular localization, and inhibition of the chemokines MIP-2 and MCP-1 after traumatic brain injury in the rat. Journal of neurotrauma 26, 507-525.

29. Shein, S.L., Shellington, D.K., Exo, J.L., Jackson, T.C., Wisniewski, S.R., Jackson, E.K., Vagni, V.A., Bayir, H., Clark, R.S., Dixon, C.E., Janesko-Feldman, K.L. and Kochanek, P.M. (2014). Hemorrhagic shock shifts the serum cytokine profile from pro- to anti-inflammatory after experimental traumatic brain injury in mice. Journal of neurotrauma 31, 1386-1395.

30. Madrigal, J.L. and Caso, J.R. (2014). The chemokine (C-C motif) ligand 2 in neuroinflammation and neurodegeneration. Advances in experimental medicine and biology 824, 209-219.

31. Tanuma, N., Sakuma, H., Sasaki, A. and Matsumoto, Y. (2006). Chemokine expression by astrocytes plays a role in microglia/macrophage activation and subsequent neurodegeneration in secondary progressive multiple sclerosis. Acta neuropathologica 112, 195-204.

32. Kiyota, T., Gendelman, H.E., Weir, R.A., Higgins, E.E., Zhang, G. and Jain, M. (2013). CCL2 affects beta-amyloidosis and progressive neurocognitive dysfunction in a mouse model of Alzheimer's disease. Neurobiology of aging 34, 1060-1068.

33. Yamamoto, M., Horiba, M., Buescher, J.L., Huang, D., Gendelman, H.E., Ransohoff, R.M. and Ikezu, T. (2005). Overexpression of monocyte chemotactic protein-1/CCL2 in beta-amyloid precursor protein transgenic mice show accelerated diffuse beta-amyloid deposition. The American journal of pathology 166, 1475-1485.

34. Kiyota, T., Yamamoto, M., Xiong, H., Lambert, M.P., Klein, W.L., Gendelman, H.E., Ransohoff, R.M. and Ikezu, T. (2009). CCL2 accelerates microglia-mediated Abeta oligomer formation and progression of neurocognitive dysfunction. PloS one 4, e6197.

35. Westin, K., Buchhave, P., Nielsen, H., Minthon, L., Janciauskiene, S. and Hansson, O. (2012). CCL2 is associated with a faster rate of cognitive decline during early stages of Alzheimer's disease. PloS one 7, e30525.

36. Wang, Y., Wei, Y., Oguntayo, S., Wilkins, W., Arun, P., Valiyaveettil, M., Song, J., Long, J.B. and Nambiar, M.P. (2011). Tightly coupled repetitive blast-induced traumatic brain injury: development and characterization in mice. J.Neurotrauma 28, 2171-2183.

37. Calabrese, E., Du, F., Garman, R.H., Johnson, G.A., Riccio, C., Tong, L.C. and Long, J.B. (2014). Diffusion tensor imaging reveals white matter injury in a rat model of repetitive blast-induced traumatic brain injury. Journal of neurotrauma 31, 938-950.

38. Schefe, J.H., Lehmann, K.E., Buschmann, I.R., Unger, T. and Funke-Kaiser, H. (2006). Quantitative real-time RT-PCR data analysis: current concepts and the novel "gene expression's CT difference" formula. Journal of molecular medicine 84, 901-910.

39. Toyama, Y., Kobayashi, T., Nishiyama, Y., Satoh, K., Ohkawa, M. and Seki, K. (2005). CT for acute stage of closed head injury. Radiation medicine 23, 309-316.

40. Hergenroeder, G.W., Redell, J.B., Moore, A.N. and Dash, P.K. (2008). Biomarkers in the clinical diagnosis and management of traumatic brain injury. Molecular diagnosis & therapy 12, 345-358.

41. Wintermark, M., Sanelli, P.C., Anzai, Y., Tsiouris, A.J. and Whitlow, C.T. (2015). Imaging evidence and recommendations for traumatic brain injury: advanced neuro- and neurovascular imaging techniques. AJNR. American journal of neuroradiology 36, E1-e11.

42. Mechtler, L.L., Shastri, K.K. and Crutchfield, K.E. (2014). Advanced neuroimaging of mild traumatic brain injury. Neurologic clinics 32, 31-58.

43. Huang, X.J., Glushakova, O., Mondello, S., Van, K., Hayes, R.L. and Lyeth, B.G. (2015). Acute Temporal Profiles of Serum Levels of UCH-L1 and GFAP and Relationships to Neuronal and Astroglial Pathology following Traumatic Brain Injury in Rats. Journal of neurotrauma.

44. Czeiter, E., Mondello, S., Kovacs, N., Sandor, J., Gabrielli, A., Schmid, K., Tortella, F., Wang, K.K., Hayes, R.L., Barzo, P., Ezer, E., Doczi, T. and Buki, A. (2012). Brain injury biomarkers may improve the predictive power of the IMPACT outcome calculator. Journal of neurotrauma 29, 1770-1778.

45. Chabok, S.Y., Moghadam, A.D., Saneei, Z., Amlashi, F.G., Leili, E.K. and Amiri, Z.M. (2012). Neuron-specific enolase and S100BB as outcome predictors in severe diffuse axonal injury. The journal of trauma and acute care surgery 72, 1654-1657.

46. Di Pietro, V., Amorini, A.M., Lazzarino, G., Yakoub, K.M., D'Urso, S., Lazzarino, G. and Belli, A. (2015). S100B and Glial Fibrillary Acidic Protein as Indexes to Monitor Damage Severity in an In Vitro Model of Traumatic Brain Injury. Neurochemical research 40, 991-999.

47. Dalgard, C.L., Cole, J.T., Kean, W.S., Lucky, J.J., Sukumar, G., McMullen, D.C., Pollard, H.B. and Watson, W.D. (2012). The cytokine temporal profile in rat cortex after controlled cortical impact. Frontiers in molecular neuroscience 5, 6.

48. Hinson, H.E., Rowell, S. and Schreiber, M. (2015). Clinical evidence of inflammation driving secondary brain injury: a systematic review. The journal of trauma and acute care surgery 78, 184-191.

49. Wang, Y., Arun, P., Wei, Y., Oguntayo, S., Gharavi, R., Valiyaveettil, M., Nambiar, M.P. and Long, J.B. (2014). Repeated blast exposures cause brain DNA fragmentation in mice. Journal of neurotrauma 31, 498-504.

50. Meabon, J.S., Huber, B.R., Cross, D.J., Richards, T.L., Minoshima, S., Pagulayan, K.F., Li, G., Meeker, K.D., Kraemer, B.C., Petrie, E.C., Raskind, M.A., Peskind, E.R. and Cook, D.G. (2016). Repetitive blast exposure in mice and combat veterans causes persistent cerebellar dysfunction. Science translational medicine 8, 321ra326.

51. Garman, R.H., Jenkins, L.W., Switzer, R.C., 3rd, Bauman, R.A., Tong, L.C., Swauger, P.V., Parks, S.A., Ritzel, D.V., Dixon, C.E., Clark, R.S., Bayir, H., Kagan, V., Jackson, E.K. and Kochanek, P.M. (2011). Blast exposure in rats with body shielding is characterized primarily by diffuse axonal injury. Journal of neurotrauma 28, 947-959.

52. Mac Donald, C., Johnson, A., Cooper, D., Malone, T., Sorrell, J., Shimony, J., Parsons, M., Snyder, A., Raichle, M., Fang, R., Flaherty, S., Russell, M. and Brody, D.L. (2013). Cerebellar white matter abnormalities following primary blast injury in US military personnel. PloS one 8, e55823.

53. Sozzani, S., Zhou, D., Locati, M., Rieppi, M., Proost, P., Magazin, M., Vita, N., van Damme, J. and Mantovani, A. (1994). Receptors and transduction pathways for monocyte chemotactic protein-2 and monocyte chemotactic protein-3. Similarities and differences with MCP-1. Journal of immunology 152, 3615-3622.

54. Obermuller, N., Geiger, H., Weipert, C. and Urbschat, A. (2014). Current developments in early diagnosis of acute kidney injury. International urology and nephrology 46, 1-7.

55. Czaja, A.J. (2014). Review article: chemokines as orchestrators of autoimmune hepatitis and potential therapeutic targets. Alimentary pharmacology & therapeutics 40, 261-279.

56. Quick, M.L., Mukherjee, S., Rudick, C.N., Done, J.D., Schaeffer, A.J. and Thumbikat, P. (2012). CCL2 and CCL3 are essential mediators of pelvic pain in experimental autoimmune prostatitis. American Journal of Physiology - Regulatory, Integrative and Comparative Physiology 303, R580-589.

57. Locatelli, D., Terao, M., Fratelli, M., Zanetti, A., Kurosaki, M., Lupi, M., Barzago, M.M., Uggetti, A., Capra, S., D'Errico, P., Battaglia, G.S. and Garattini, E. (2012). Human Axonal Survival of Motor Neuron (a-SMN) Protein Stimulates Axon Growth, Cell Motility, C-C Motif Ligand 2 (CCL2), and Insulin-like Growth Factor-1 (IGF1) Production*. The Journal of Biological Chemistry 287, 25782-25794.

58. Hackel, D., Pflücke, D., Neumann, A., Viebahn, J., Mousa, S., Wischmeyer, E., Roewer, N., Brack, A. and Rittner, H.L. (2013). The Connection of Monocytes and Reactive Oxygen Species in Pain. PloS one 8.

59. Iliff, J.J., Chen, M.J., Plog, B.A., Zeppenfeld, D.M., Soltero, M., Yang, L., Singh, I., Deane, R. and Nedergaard, M. (2014). Impairment of glymphatic pathway function promotes tau

pathology after traumatic brain injury. The Journal of neuroscience : the official journal of the Society for Neuroscience 34, 16180-16193.

60. Plog, B.A., Dashnaw, M.L., Hitomi, E., Peng, W., Liao, Y., Lou, N., Deane, R. and Nedergaard, M. (2015). Biomarkers of traumatic injury are transported from brain to blood via the glymphatic system. The Journal of neuroscience : the official journal of the Society for Neuroscience 35, 518-526.

61. Rosito, M., Deflorio, C., Limatola, C. and Trettel, F. (2012). CXCL16 orchestrates adenosine A3 receptor and MCP-1/CCL2 activity to protect neurons from excitotoxic cell death in the CNS. The Journal of neuroscience : the official journal of the Society for Neuroscience 32, 3154-3163.

62. Shively, S.B. and Perl, D.P. (2012). Traumatic brain injury, shell shock, and posttraumatic stress disorder in the military--past, present, and future. The Journal of head trauma rehabilitation 27, 234-239.

63. Schmidt, M.L., Zhukareva, V., Newell, K.L., Lee, V.M. and Trojanowski, J.Q. (2001). Tau isoform profile and phosphorylation state in dementia pugilistica recapitulate Alzheimer's disease. Acta neuropathologica 101, 518-524.

64. Chauhan, N.B. (2014). Chronic neurodegenerative consequences of traumatic brain injury. Restorative neurology and neuroscience 32, 337-365.

Figure Legends:

FIG. 1. Rat's performance on the rotarod. (A) Latency to fall on the fixed-speed of 10 rpm testing, (B) Change in latency to fall on the fixed-speed of 10 rpm testing, (C) Latency to fall on the fixed-speed of 20 rpm testing, (D) Change in latency to fall on the fixed-speed of 20 rpm testing. Data are shown as mean ± SEM. One-way ANOVA with Tukey's multiple comparison was used (n = 10 for each group). DHB or SHB vs. Sham *p < 0.05, **$p < 0.01$, ***$p < 0.005$, ****$p < 0.001$; DHB vs. SHB $^{\#}p < 0.05$ and $^{\#\#}p < 0.01$.

FIG. 2. Silver staining showing axonal degeneration induced by blast exposure. At 7 - 9 days after single blast (b, e and h), double blast (c, f and i) exposures and sham controls (a, d and g), rat's brain sections (50 µm) were stained with Neurosilver kit and the images were taken using Ax-80 microscope. (A) Compared to the sham controls, blast injured rats showed dense precipitation in the white matter of cerebellum (a, b and c), brainstem (d, e and f) and optic tract (g, h and i), scale bar = 100 µm. (B) Brain injury scores were determined as a mean from 5 different fields of each section and 5 serial brain sections for each animal. Values are expressed as mean ± SEM. n = 6 - 11, * $p < 0.05$, ** $p < 0.01$, ***$p < 0.005$ and ****$p < 0.001$.

FIG. 3. Effect of blast exposure on CCL2 levels in the CSF. (A) time-course of increase in CCL2 levels in DHB and sham controls, (B) at 6 hrs post insult, CSF CCL2 concentrations among three experimental groups and sham controls. Data are shown as mean ± SEM. data were analyzed by One-way ANOVA with Tukey's multiple comparisons. Sham n = 12 and other experimental groups n = 8, *$p < 0.05$, **$p < 0.01$, ***$p < 0.005$, ****$p < 0.0001$.

FIG. 4. Effect of blast exposure on CCL2 plasma levels. (A) At 6 hrs post-injury, correlation of plasma CCL2 to blast overpressure, (B) time-course of plasma CCL2 levels in DHB, SHB and sham controls. Data are shown as mean ± SEM. One-way ANOVA with Tukey's multiple comparison were used. Sham n = 12 and other experimental groups n = 8, *$p < 0.05$, **$p < 0.01$, ***$p < 0.005$, ****$p < 0.0001$.

FIG. 5 Comparison of CCL2 concentration in CSF and plasma. (A) Double blast-induced time-course change in CCL2 expression in CSF and plasma, (B) Correlation between CSF CCL2 and plasma CCL2, (C) The change in ratio of CCL2 in CSF/plasma at 6 hrs and 24 hrs after overpressure exposure; Sham n = 12 and other experimental groups n = 8. Data were analyzed by one-way ANOVA with Tukey's multiple comparisons. *$p < 0.05$, **$p < 0.01$, ***$p < 0.005$, ****$p < 0.0001$.

FIG. 6. Blast-induced up-regulation of CCL2 protein in the cerebellum. Values are expressed as mean ± sem for each group. The student's *t* test and one-way ANOVA with Tukey's multiple comparisons test were carried out for statistical analysis (n = 8); *$p < 0.05$, **$p < 0.01$ and ***$p < 0.005$, **** $p < 0.001$.

FIG. 7. RT-qPCR analysis showing the effect of blast exposure on the expressions of CCL2 and CCR2 genes in cerebellum. The mRNA levels are presented as a fold change relative to sham control. Statistical analysis was carried out by one-way ANOVA followed by Tukey's multiple comparisons, n = 8, *$p < 0.05$ and **$p < 0.01$.

FIG 8. Association between CCL2 level in CSF or plasma and CCL2 gene expression in the cerebellum. ΔCt is the difference after subtracting Ct of actin mRNA from the Ct of CCL2 mRNA in the same sample to normalize for variation in the amount. (A) Correlation between CSF CCL2 and cerebellum CCL2 mRNA, n = 20, Pearson r = -0.86, $p < 0.0001$; (B) Correlation between plasma CCL2 and cerebellum CCL2 mRNA, n = 20, Pearson r = -0.76, $p < 0.001$.

Fig. 1

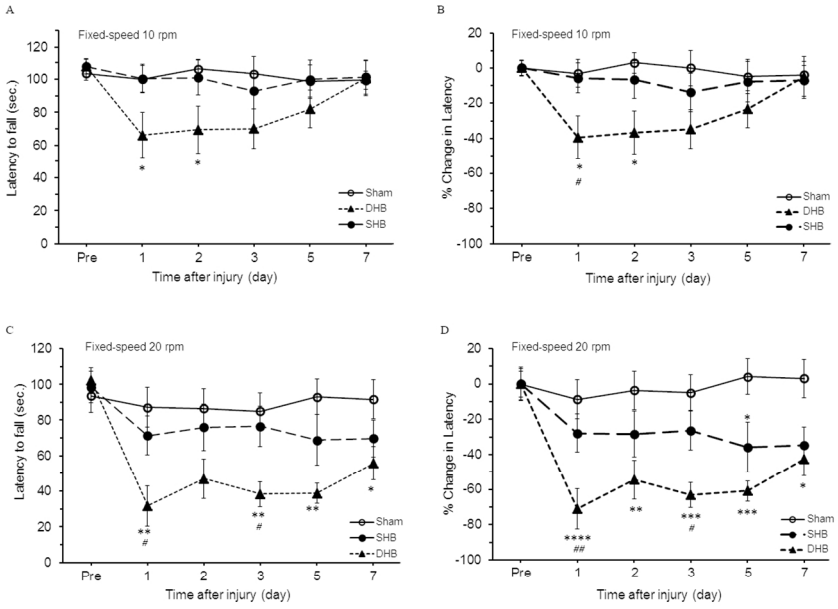

FIG. 1. Rat's performance on the rotarod. (A) Latency to fall on the fixed-speed of 10 rpm testing, (B) Change in latency to fall on the fixed-speed of 10 rpm testing, (C) Latency to fall on the fixed-speed of 20 rpm testing, (D) Change in latency to fall on the fixed-speed of 20 rpm testing. Data are shown as mean ± SEM. One-way ANOVA with Tukey's multiple comparison was used (n = 10 for each group). DHB or SHB vs. Sham *p < 0.05, **p < 0.01, ***p < 0.005, ****p < 0.001; DHB vs. SHB #p <0.05 and ##p < 0.01.
121x88mm (300 x 300 DPI)

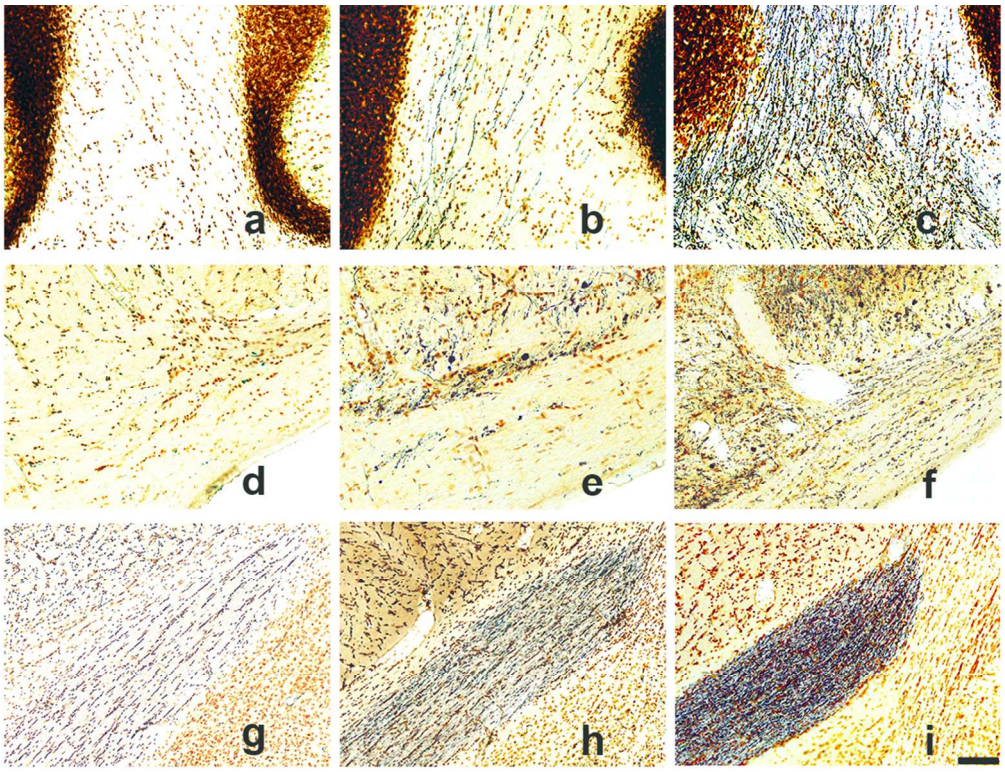

FIG. 2. Silver staining showing axonal degeneration induced by blast exposure. At 7 - 9 days after single blast (b, e and h), double blast (c, f and i) exposures and sham controls (a, d and g), rat's brain sections (50 µm) were stained with Neurosilver kit and the images were taken using Ax-80 microscope. (A) Compared to the sham controls, blast injured rats showed dense precipitation in the white matter of cerebellum (a, b and c), brainstem (d, e and f) and optic tract (g, h and i), scale bar = 100 µm.
101x77mm (300 x 300 DPI)

Fig. 2

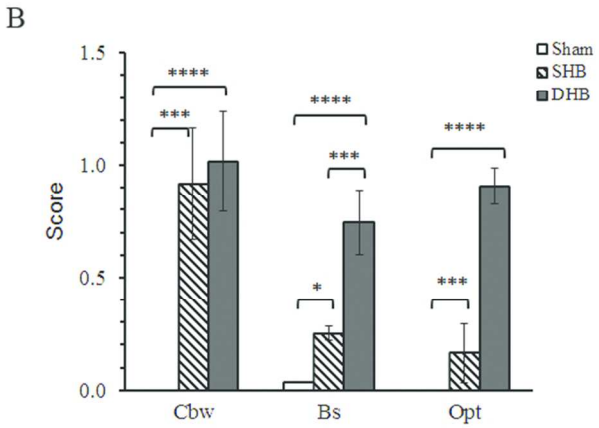

FIG. 2. Silver staining showing axonal degeneration induced by blast exposure. (B) Brain injury scores were determined as a mean from 5 different fields of each section and 5 serial brain sections for each animal. Values are expressed as mean ± SEM. n = 6 - 11, * $p < 0.05$, ** $p < 0.01$, ***$p < 0.005$ and ****$p < 0.001$.
72x59mm (300 x 300 DPI)

FIG 3

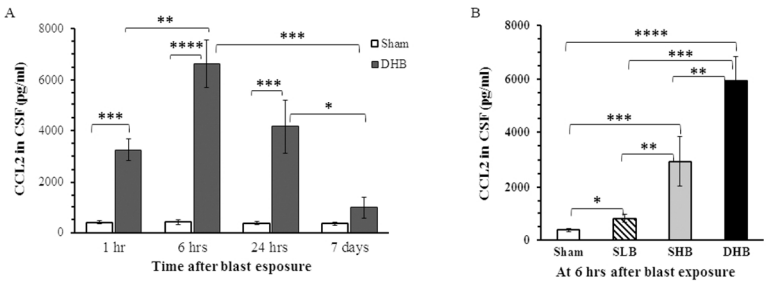

FIG. 3. Effect of blast exposure on CCL2 levels in the CSF. (A) time-course of increase in CCL2 levels in DHB and sham controls, (B) at 6 hrs post insult, CSF CCL2 concentrations among three experimental groups and sham controls. Data are shown as mean ± SEM. data were analyzed by One-way ANOVA with Tukey's multiple comparisons. Sham n = 12 and other experimental groups n = 8, *p < 0.05, **p < 0.01, ***p < 0.005, ****p < 0.0001.
107x54mm (300 x 300 DPI)

Fig. 4

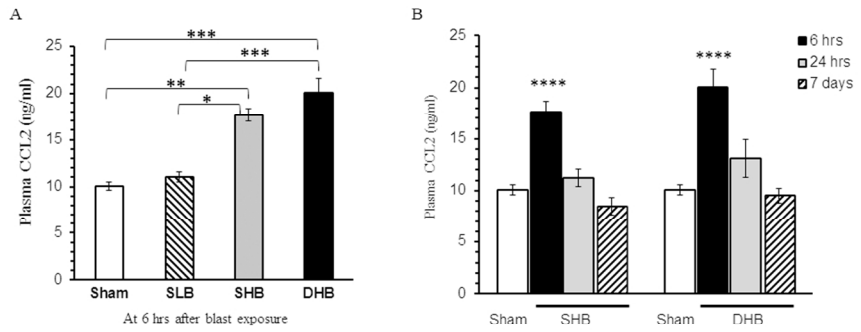

FIG. 4. Effect of blast exposure on CCL2 expression in plasma. (A) At 6 hrs post-injury, correlation of plasma CCL2 to blast overpressure, (B) time-course of plasma CCL2 levels in DHB, SHB and sham controls. Data are shown as mean ± SEM. One-way ANOVA with Tukey's multiple comparison were used. Sham n = 12 and other experimental groups n = 8, *p < 0.05, **p < 0.01, ***p < 0.005, ****p < 0.0001.
91x48mm (300 x 300 DPI)

Fig. 5

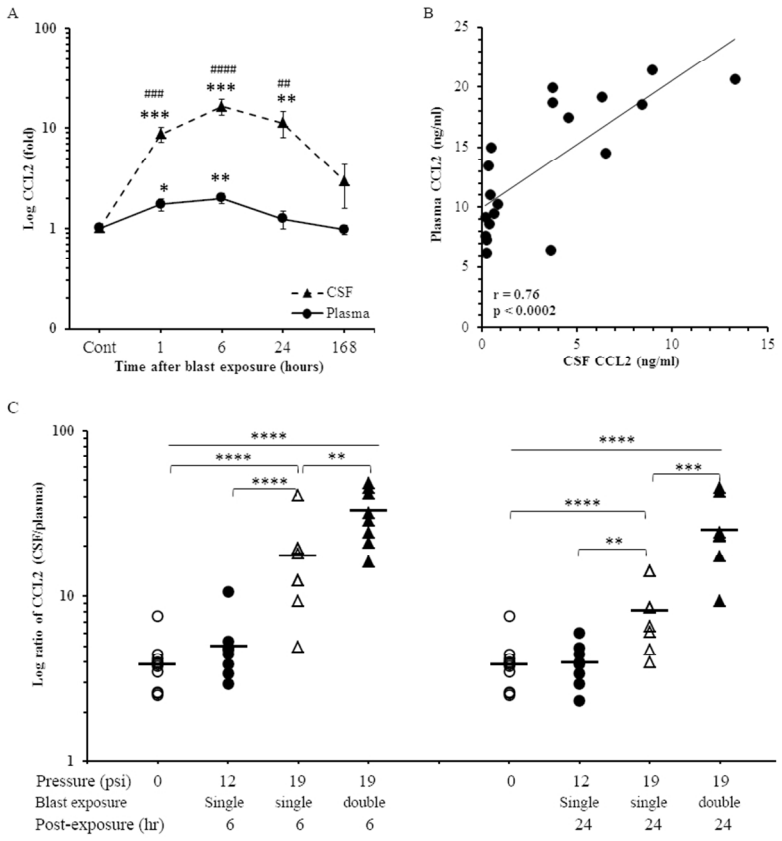

FIG. 5 Comparison of CCL2 concentration in CSF and plasma. (A) Double blast-induced time-course change in CCL2 expression in CSF and plasma, (B) Correlation between CSF CCL2 and plasma CCL2, (C) The change in ratio of CCL2 in CSF/plasma at 6 hrs and 24 hrs after overpressure exposure; Sham n = 12 and other experimental groups n = 8. Data were analyzed by one-way ANOVA with Tukey's multiple comparisons. *p < 0.05, **p < 0.01, ***p < 0.005, ****p < 0.0001.
91x98mm (300 x 300 DPI)

Fig. 6

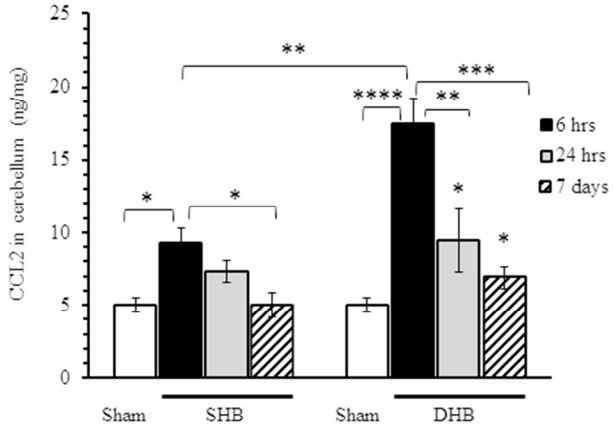

FIG. 6. Blast-induced up-regulation of CCL2 protein in the cerebellum. Values are expressed as mean ± sem for each group. The student's t test and one-way ANOVA with Tukey's multiple comparisons test were carried out for statistical analysis (n = 8); *p < 0.05, **p < 0.01 and ***p < 0.005, **** p < 0.001.
65x55mm (300 x 300 DPI)

Fig. 7

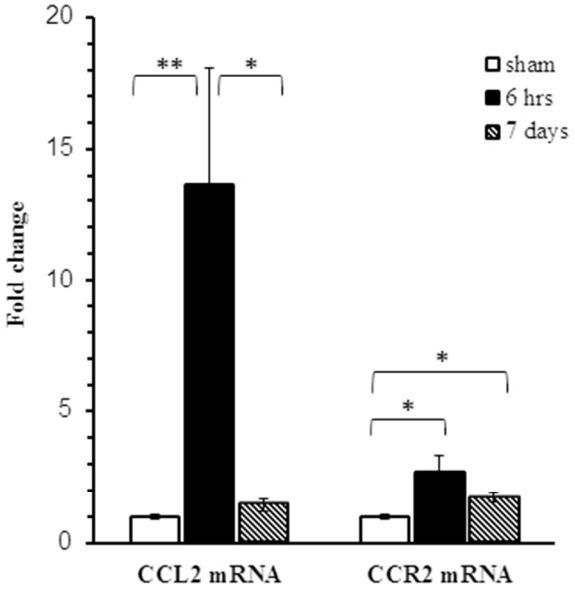

FIG. 7. RT-qPCR analysis showing the effect of blast exposure on the expressions of CCL2 and CCR2 genes in cerebellum. The mRNA levels are presented as a fold change relative to sham control. Statistical analysis was carried out by one-way ANOVA followed by Tukey's multiple comparisons, n = 8, *p < 0.05 and **p < 0.01.
54x56mm (300 x 300 DPI)

Fig. 8

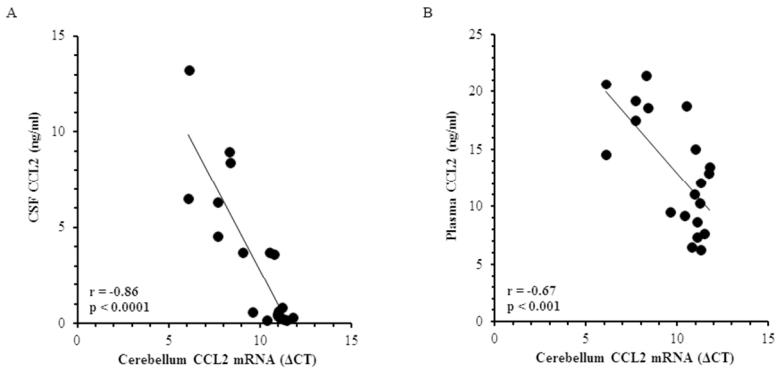

FIG 8. Association between CCL2 level in CSF or plasma and CCL2 gene expression in cerebellum. ΔCt is the difference after subtracting Ct of actin mRNA from the Ct of CCL2 mRNA in the same sample to normalize for variation in the amount. (A) Correlation between CSF CCL2 and cerebellum CCL2 mRNA, n = 20, Pearson r = -0.86, p < 0.0001; (B) Correlation between plasma CCL2 and cerebellum CCL2 mRNA, n = 20, Pearson r = -0.76, p < 0.001.
94x55mm (300 x 300 DPI)

frontiers in NEUROLOGY

ORIGINAL RESEARCH ARTICLE
published: 07 March 2011
doi: 10.3389/fneur.2011.00012

Stress and traumatic brain injury: a behavioral, proteomics, and histological study

Sook-Kyung C. Kwon[1†], Erzsebet Kovesdi[1†], Andrea B. Gyorgy[1], Daniel Wingo[1], Alaa Kamnaksh[1], John Walker[1], Joseph B. Long[2] and Denes V. Agoston[1]*

[1] *Department of Anatomy, Physiology and Genetics, School of Medicine, Uniformed Services University, Bethesda, MD, USA*
[2] *Division of Military Casualty Research, Walter Reed Army Institute of Research, Silver Spring, MD, USA*

Edited by:
Marten Risling, Karolinska Institutet, Sweden

Reviewed by:
Linda Noble, University of California at San Francisco, USA
Robert Vink, University of Adelaide, Australia

****Correspondence:***
Denes V. Agoston, Department of Anatomy, Physiology and Genetics, School of Medicine, Uniformed Services University, 4301 Jones Bridge Road, Bethesda, MD 20814, USA.
e-mail: vagoston@usuhs.edu

[†]Sook-Kyung C. Kwon and Erzsebet Kovesdi have contributed equally.

Psychological stress and traumatic brain injury (TBI) can both result in lasting neurobehavioral abnormalities. Post-traumatic stress disorder and blast induced TBI (bTBI) have become the most significant health issues in current military conflicts. Importantly, military bTBI virtually never occurs without stress. In this experiment, we assessed anxiety and spatial memory of rats at different time points after repeated exposure to stress alone or in combination with a single mild blast. At 2 months after injury or sham we analyzed the serum, prefrontal cortex (PFC), and hippocampus (HC) of all animals by proteomics and immunohistochemistry. Stressed sham animals showed an early increase in anxiety but no memory impairment at any measured time point. They had elevated levels of serum corticosterone (CORT) and hippocampal IL-6 but no other cellular or protein changes. Stressed injured animals had increased anxiety that returned to normal at 2 months and significant spatial memory impairment that lasted up to 2 months. They had elevated serum levels of CORT, CK-BB, NF-H, NSE, GFAP, and VEGF. Moreover, all of the measured protein markers were elevated in the HC and the PFC; rats had an increased number of TUNEL-positive cells in the HC and elevated GFAP and Iba1 immunoreactivity in the HC and the PFC. Our findings suggest that exposure to repeated stress alone causes a transient increase in anxiety and no significant memory impairment or cellular and molecular changes. In contrast, repeated stress and blast results in lasting behavioral, molecular, and cellular abnormalities characterized by memory impairment, neuronal and glial cell loss, inflammation, and gliosis. These findings may have implications in the development of diagnostic and therapeutic measures for conditions caused by stress or a combination of stress and bTBI.

Keywords: stress, blast traumatic brain injury, anxiety, memory, gliosis, inflammation, neurogenesis

INTRODUCTION

Traumatic brain injury (TBI) is one of the leading causes of death and chronic disability worldwide (Bruns and Hauser, 2003; Tagliaferri et al., 2006). Blast induced TBI (bTBI) caused by explosive devices is especially frequent in recent conflicts in Iraq and in Afghanistan (Warden and French, 2005; Taber et al., 2006; Warden, 2006). Epidemiological studies have shown that mild bTBI (mbTBI) can result in chronic neurobehavioral changes such as increased anxiety and memory impairment (Ryan and Warden, 2003; Okie, 2005). Importantly, virtually no bTBI occurs on the battlefield without the exposure to psychological stress. Exposure to stress alone (i.e., traumatic and/or life-threatening events) without physical injury can lead to a chronic condition called post-traumatic stress disorder (PTSD) in some but not all affected individuals (Breslau and Kessler, 2001). PTSD is especially frequent among soldiers; about 14% of soldiers suffer from PTSD-like symptoms compared to 4% of the US adult population (Keane et al., 2006; Richardson et al., 2010).

Although bTBI shares some of the clinical features of the closed head and the penetrating TBIs, bTBI appears to be a fundamentally different form of neurotrauma (Ling et al., 2009). Several factors are responsible for the uniqueness of bTBI; explosive blast rapidly dissipates very high levels of energy in the form of supersonic pressure waves (Mayorga, 1997; Okie, 2005). Within the brain parenchyma, the high-energy high-velocity blast waves can cause substantial damage to blood vessels, neuronal and glial cell bodies and their processes (Kaur et al., 1997; Cernak et al., 2001). Clinical hallmarks of severe bTBI include an unusually early onset (hours after injury) and rapid development of diffuse malignant cerebral edema, and delayed (10–14 days post-injury) vasoconstriction (Armonda et al., 2006; Ling et al., 2009; Ling and Ecklund, 2011). Given that blast almost always affects the whole body, subclinical thoracic or abdominal injuries can also contribute to the pathophysiology of bTBI (Cernak et al., 2010). It has been thought that the secondary injury process in bTBI includes vascular changes, neuroinflammation, and gliosis (Kaur et al., 1997; Mayorga, 1997; Cernak et al., 2001; Taber et al., 2006).

Exposure to mild blast poses especially difficult challenges. Even though there are no life-threatening injuries in mbTBI and soldiers do not lose consciousness, 6–9 months later many soldiers develop neurobehavioral abnormalities that include memory impairment, anxiety, and mood disorders (Belanger et al., 2007; Brenner et al., 2009). These symptoms indicate damage to the hippocampus (HC) and the prefrontal cortex (PFC), brain structures that are also indicated as the neuroanatomical substrates of PTSD (Jaffee and Meyer, 2009). Stress is a constant factor on the battlefield

(Warden et al., 1997; Brenner et al., 2009); soldiers are repeatedly exposed to various life-threatening situations and to the visual and audible cues of blasts without necessarily suffering from any visible physical injury.

In order to better understand the long-term consequences of stress with and without the exposure to blast, we used a rodent model of stress and mbTBI and assessed the behavior of animals at various time points after sham or injury and analyzed their sera and brains for cellular and molecular changes. Due to our experimental setup, we were unable to determine the effect of blast injury alone. During our pilot studies we learned that handling and transporting animals (associated with the exposure to blast) resulted in a significant amount of stress as indicated by substantially elevated serum CORT levels of animals.

MATERIALS AND METHODS

ANIMALS, HOUSING CONDITIONS, AND EXPERIMENTAL SCHEDULE

Sprague-Dawley male rats (245–265 g; Charles River Laboratories, Wilmington, MA, USA) were housed in cages with free access to food and water in a reverse 12/12 h light/dark cycle. The experimental schedule is depicted in **Figure 1**. After 7 days of acclimation and handling in our animal facility, control animals (C) were housed two per cage; stressed sham injured (SS) and stressed injured animals (SI) were housed individually. All animals were handled according to protocol approved by the Institutional Animal Care and Use Committee (IACUC) at the Uniformed Services University of the Health Sciences. All behavioral tests were conducted during animals' dark cycle.

INJURY

On the day of the exposure, animals in the SS and SI groups were transported from USU (Bethesda, MD, USA) to Walter Reed Army Institute of Research (Silver Spring, MD, USA) for injury. Blast TBI was generated using a compression-driven shock tube as described earlier (Long et al., 2009). Before injury, rats in the SI group were anesthetized with 4% isoflurane (Forane, Baxter Healthcare Corporation, Deerfield, IL, USA), placed in an animal holder in a transverse prone position and then transferred to the shock tube where they were exposed to whole body blast overpressure (20.6 ± 3 psi). Immediately after exposure, the duration of apnea was measured and rats were moved back to their home cages. Animals in the SS group received the same amount of anesthesia and underwent the same procedure but were not exposed to blast overpressure. However, SS as well as SI animals were exposed to the sounds of the blast, which is likely an additional stressor. Following exposures (or sham), animals were transported back to USU.

CHRONIC STRESS

Rats in the SI and SS groups were exposed to a combination of predator and unpredictable stressors for 1 week prior to and 1 week after the first behavioral testing session (**Figure 1**). Unpredictable stress is a face-valid model of human stress that has been shown to reliably elevate stress hormone levels in rodents (Fride et al., 1986; Weinstock et al., 1992).

A combination of fox urine and unpredictable stress (Campbell et al., 2003) was performed with modifications (Berger and Grunberg, in preparation). Rats were exposed to fox urine for 10 min/day (Red fox urine, Buck Stop Lure Company, Stanton, MI, USA) as a predator stress, and loud noises and sudden cage movements at irregular times as an unpredictable stressor. During the stress routine, rats were moved to the animal facility's procedure room. Each rat was transferred to a clean empty cage with a cotton ball containing 15 ml of fox urine; each day the position of the cotton ball was changed. Within the 10 min stress period, rats were exposed to loud noises and irregular cage movement. After stress, the rats were immediately moved back to their home cages and transferred back to the animal housing room. Control rats were neither transferred to the procedure room nor exposed to any of the stressors.

SCHEDULE OF BEHAVIORAL TESTS

Before chronic stress and injury all animals underwent a baseline open field (OF) measurement (**Figure 1**). Horizontal activity results were used to create three groups with no statistical significance among them. After the first stress phase and blast (or sham) injury, rats underwent a series of behavioral evaluations. In each behavioral session OF was conducted first to ascertain whether animals had any motor problems, which can confound other behavioral tests. One day after OF, elevated plus maze (EPM) was performed to measure anxiety levels. Barnes maze (BM) was performed last to measure spatial learning and memory. The three behavioral assessments were performed on separate days starting at 24 h, 1, and 2 months after injury (**Figure 1**).

Open field

The OF test is an indicator of potential motor deficits but can also reflect fluctuations in anxiety levels based on changes in exploratory behavior (Heath and Vink, 1999). Several studies have shown this test to reliably measure anxiety and depression in rodents (von Horsten et al., 1998) including after TBI (Vink et al., 2003). OF tests were performed using Omnitech Electronics' Digiscan infrared photocell system (test box model RXYZCM, Omnitech Electronics, Columbus, OH; Elliott and Grunberg, 2005). The OF system is a

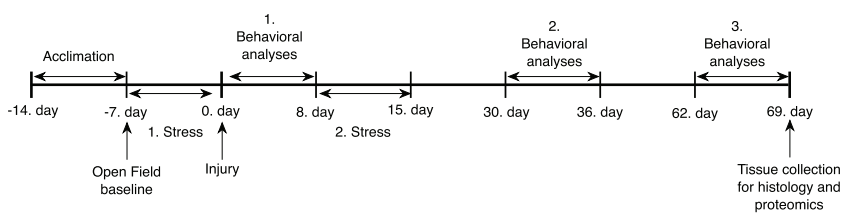

FIGURE 1 | Outline of the experimental schedule.

40 × 40 × 30 (*L* × *W* × *H*) cm clear Plexiglas arena with a perforated lid. During the 60 min testing period, we measured horizontal activity (locomotor activity), time spent in the margins (anxiety), and in the center. Data were automatically gathered and transmitted to a computer via an Omnitech Model DCM-BBU analyzer.

Elevated plus maze

The EPM is a widely used, ethologically relevant test that assesses anxiety states in rodents (Carobrez and Bertoglio, 2005; Salzberg et al., 2007; Walf and Frye, 2007). The maze is an elevated structure (1 m above ground) consisting of four intersecting arms. The arms of the maze are 50 cm long and 10 cm wide; the closed arms have walls on three sides that are 40 cm high while the open arms have none. The lighting in the middle of the maze was set at 90 lux. On testing days rats were placed one by one in the center of the maze facing one of the open arms; each animal was allowed to explore freely for 5 min while its movement was video-tracked. Total distance traveled, number of entries made, and time spent (duration) in each arm was recorded using ANY-maze 4.2 Software (Stoelting Company, Wood Dale, IL, USA).

Barnes maze

Barnes maze was used to assess spatial learning and memory (Barnes, 1979; Maegele et al., 2005; Doll et al., 2009). BM represents a widely used, validated, and less stressful alternative to the commonly used water maze test (Harrison et al., 2009). The maze is a circular platform (1.2 m in diameter) with 18 evenly spaced holes around the periphery. One of the holes is the entrance to a darkened escape box that is not visible from the surface of the board. Each rat was tested twice per day for six consecutive days to find the escape box (only day 1 of the first BM session had three trials). In each trial, latency to locate and enter the escape box was measured (ANY-maze 4.2 Software, Stoelting Company, Wood Dale, IL, USA).

During the first (teaching) trial of the first BM session, all animals were trained to locate the escape chamber. Each animal was placed in the escape box and covered for 30 s. The escape box was then removed with the animal inside and moved to the center of the maze. The rat was removed from the box and allowed to explore the maze for a few seconds, after which the rat was returned to its home cage. No latency times were recorded for the teaching trials. The escape box and the maze were cleaned with 30% ethanol solution between each trial. In the second trial the same rat was placed under a start box in the center of the maze for 30 s; the start box was then removed and the rat was allowed to explore freely to find the escape chamber. Training sessions ended after the animal had entered the escape box or when a pre-determined time (240 s) had elapsed. If the animal had not found the escape box during the given time period, it was placed in the escape box for 1 min at the end of the trial.

TISSUE COLLECTION AND PROCESSING

On day 67 post-injury (or sham; **Figure 1**) all animals were deeply anesthetized with isoflurane until a tail pinch produced no reflex movement. Anesthesia was maintained using a mask/nose cone attached to the anesthetic vaporizer, and blood was collected (1.5 ml) from a tail vein. For proteomics and ELISA assays, rats were decapitated under deep anesthesia. Brains were immediately removed and placed on ice. The PFC and HC were dissected, frozen, and stored at −80°C. For histology, rats were transcardially perfused with cold phosphate-buffered saline (PBS) followed by 4% buffered paraformaldehyde solution under deep isoflurane anesthesia. Following overnight post-fixation in 4% buffered paraformaldehyde solution brains were consecutively immersed in cold 15 and 30% sucrose solutions in 1× PBS for cryoprotection and then frozen on dry ice. Frozen brains were sectioned coronally at a 20-μm thickness using a cryostat (Cryocut 1800; Leica Microsystems, Bannockburn, IL, USA) and sections were kept at −80°C until use.

PROTEOMICS

Preparation of samples

Sample preparation, printing, scanning, and data analysis were performed as described later in detail (Gyorgy et al., 2010). Flash-frozen tissues were briefly pulverized in liquid nitrogen; 200 mg of the frozen powder was transferred into 1 ml of T-per lysis buffer (Thermo Fisher, Waltham, MA, USA) with protease and phosphatase inhibitors (Thermo Fisher) and then sonicated. Samples were centrifuged for 15 min at 4°C; the supernatants were aliquoted and stored at −80°C. Protein concentrations were measured by using a BCA assay (Thermo Fisher). Blood samples were promptly centrifuged after removal at 10,000×*g* for 15 min at 4°C; the supernatants were aliquoted, flash-frozen, and stored at −80°C. Tissue samples were diluted in print buffer (10% glycerol, 0.05% SDS, 50 mM DTT in 1× TBS) to a final protein concentration of 1 mg/ml, while serum samples were diluted 1:10. Samples were then subjected to an 11-point serial 1:2 dilution and transferred into Genetix 384-well plates (X7022, Fisher Scientific, Pittsburgh, PA, USA) as described (Gyorgy et al., 2010). Plates were transferred into an Aushon 2470 Arrayer (Aushon Biosystems, Billerica, MA, USA) and samples were printed on ONCYTE Avid (tissue samples) or ONCYTE Nova (serum samples) single-pad nitrocellulose coated glass slides (Grace Bio-Labs, Bend, OR, USA).

Printing parameters

The Aushon Arrayer was programmed to use 16 pins (4 × 4 pattern). Each sample was printed in 12 dilutions (12 rows) and in triplicate (3 columns), resulting in a block of 3 × 12 dots per sample. The Spot Diameter was set to 250 nm with a spacing of 500 nm between dots on the *x*-axis and 375 nm on the *y*-axis. Wash time was set at 2 s without delays. The printer was programmed for a single deposition per dot for printing serum and tissue extracts.

Immunochemical detection

Primary antibodies were diluted to 10× the optimal Western analysis concentration in antibody incubation buffer (0.1% bovine serum albumin (BSA), protease inhibitors (EDTA-free Halt protease and phosphatase inhibitor cocktail, Thermo Fisher, Waltham, MA, USA; 1× TBS, 0.5% Tween 20) as described (Gyorgy et al., 2010). Primary antibodies were used in the following dilutions: VEGF 1:100 (Abcam ab-53465), s100b 1:50 (Abcam ab-41548), GFAP 1:500 (Abcam ab-7260), Tau-protein 1:20 (Santa Cruz sc-1995), CK-BB 1:20 (Santa Cruz sc-15157), NSE 1: 100 (Abcam, Cat# ab53025), NF-H 1:20 (Sigma N4142). Slides were incubated with the primary antibody solution overnight at 4°C covered by a cover slip (Nunc* mSeries LifterSlips, Fisher Scientific, Pittsburg, PA).

The following day slides were washed and then incubated with an Alexa Fluor® 635 goat anti-mouse (Cat# A-31574), goat anti-rabbit (Cat# A-31576), or rabbit anti-goat IgG (H + L; Cat# A-21086) secondary antibodies from Invitrogen at 1:6000 dilution in antibody incubation buffer for 1 h at room temperature (RT). After washing and drying, the fluorescent signals were measured in a Scan Array Express HT microarray scanner (Perkin Elmer, Waltham, MA, USA) using a 633 nm wavelength laser and a 647 nm filter. Data from the scanned images were imported into a Microsoft Excel-based bioinformatics program developed in house for analysis (Gyorgy et al., 2010).

Data analysis and bioinformatics

The program calculates total net intensity after local background subtraction for each spot. The intensity data from the dilution series of each sample are then plotted against dilution on a log–log graph. The linear regression of the log–log data was calculated after the removal of flagged data, which include signal to noise ratios of less than 2, spot intensities in the saturation range or noise range, or high variability between duplicate spots (>10–15%). The total amount of antigen is determined by the *y*-axis intercept (Gyorgy et al., 2010).

CORTICOSTERONE ASSAY

Serum corticosterone (CORT) levels were measured using Cayman's Corticosterone EIA Kit according to the manufacturer's instructions (Cayman Chemical, Ann Arbor, MI, USA). Each sample was diluted 1:500 and measured in triplicate.

IL-6 AND INFγ ASSAYS

INFγ and IL-6 levels were measured from brain tissues using the rat Interferon gamma ELISA and the Rat IL-6 ELISA kits (both are from Thermo Fisher, Waltham, MA, USA). The IL-6 ELISA kit required a 1:5 dilution using the supplied dilution buffer in order to avoid saturation in the wells. After the dilution of brain samples, the assay was performed according to the manufacturer's instructions.

HISTOLOGY

Immunohistochemistry

Every first and tenth coronal section containing either the PFC, the dorsal HC (DHC), or the ventral HC (VHC) were mounted on positively charged glass slides with two sections per slide. Three slides per animal, containing sections with identical *z*-axes, were selected per brain region for each immunostaining. Slides containing the frozen sections were equilibrated at RT and hydrated with 1× PBS for 30 min. Antigen retrieval was performed by incubating the sections in 10 mM citrate buffer (pH 6.0) at 80°C for 30 min followed by cooling down to RT. After rehydration with 1× PBS, sections were permeabilized with 0.5% Triton X-100 in PBS for 1 h and blocked in 1× PBS containing 5% normal goat serum (NGS), 5% BSA, 0.1% sodium azide, and 0.5% Triton X-100 for 1 h. The same solution minus NGS was used to dilute primary antibodies. The following primary antibodies were used: mouse anti-GFAP (Millipore, Temecula, CA, USA; 1:400) rabbit anti-doublecortin (DCX; Cell Signaling Technology, Beverly, MA, USA; 1:1000), and goat anti-Iba1 (Abcam, Cambridge, MA, USA; 1:1000). Sections were incubated with the primary antibodies overnight at 4°C. After washing with 1× PBS, they were incubated with appropriate secondary antibodies (Alexa Fluor 555 goat anti-mouse IgG, 488 goat anti-rabbit IgG, or 488 donkey anti-goat IgG (Invitrogen, Carlsbad, CA) was applied for 1 h at RT 1:100), Hoechst 33342 (Molecular Probes, Eugene, OR, USA) at 1 μg/ml was applied for 2 min, sections washed and coverslipped using anti-fading media (Vectashield, Vector Laboratories, Burlingame, CA, USA).

TUNEL assay

Apoptotic cell death marked by DNA fragmentation was determined using a TUNEL *in situ* cell death detection kit, POD (Roche, Indianapolis, IN, USA) according to the manufacturer's instructions. Sections were hydrated with PBS and endogenous peroxidase activity was quenched by 3% H_2O_2 in methanol for 10 min at RT. Sections were permeabilized by 0.1 M sodium citrate buffer (pH 6.0) at 70°C for 30 min followed by PBST for 30 min at RT. TUNEL reaction was performed for 1 h at 37°C and the signal was converted using converter-POD. TUNEL-positive cells were visualized by DAB substrate. Dark brown TUNEL-positive cells were counted from four sections per animal.

Histological data acquisition

Histological sections were visualized in an Olympus IX-71 microscope using the appropriate filters and images were collected using a SPOT digital camera (Diagnostic Instruments Inc., Sterling Heights, MI, USA). The collected images were colored using TIFFany Caffeine Software.

STATISTICAL ANALYSIS AND COMPARISON OF DATA

Behavioral test results were analyzed with ANOVA and Tukey *post hoc* tests. Differences with a p-value of <0.05 were considered significant. Statistical analyses were performed using GraphPad InStat software. Proteomics and ELISA results were analyzed with Student's t-test. Data are reported as the average ± standard error of the mean. Proteomics data results were followed up with a one-way ANOVA. For each of our numerical measurements, we determined statistical significance among experimental groups by ($p < 0.05$ depicted by one star; $p < 0.01$ by two and $p < 0.001$ by three).

RESULTS

BEHAVIORAL EFFECTS

Locomotor activity

Twenty-four hours after exposure to blast (or sham), rats in the SI group showed a decrease in horizontal activity compared to rats in the SS and C groups (**Figure 2A**) but the difference was statistically insignificant. Animals in the SI group spent significantly more time in the periphery and significantly less time in the center (**Figures 2B,C**) compared to C and SS animals. SS animals showed no significant difference compared to C animals.

At 1 and 2 months after injury (or sham), we found no significant differences in any of the measured parameters between animals in all experimental groups (**Figures 2A–C**).

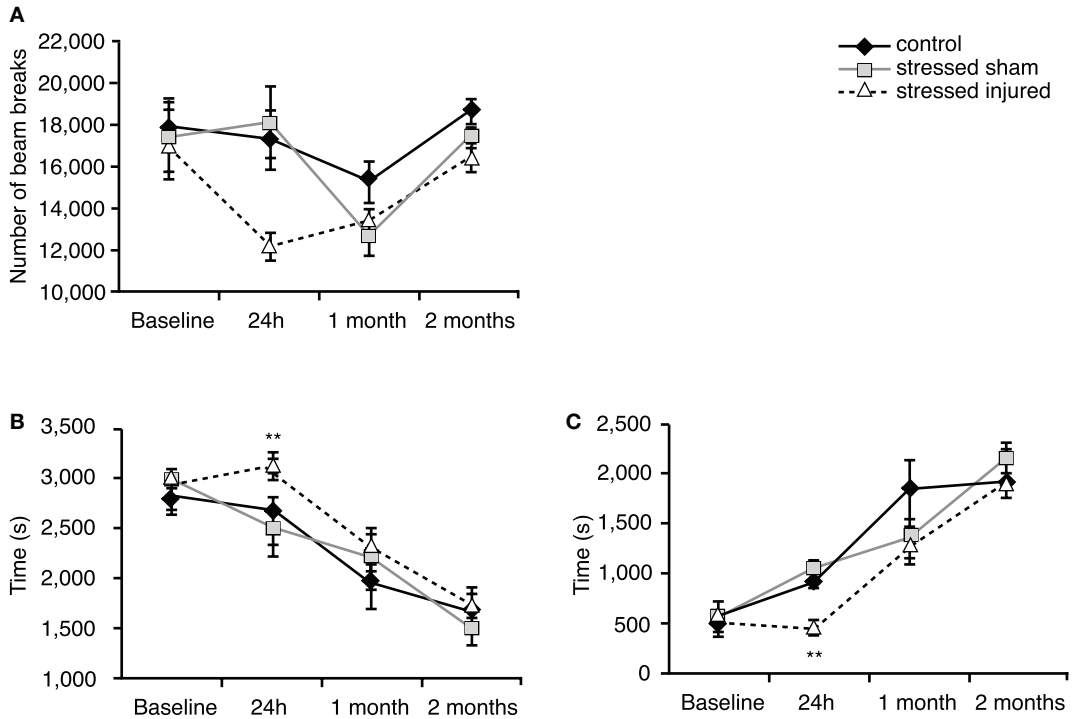

FIGURE 2 | Locomotor activity of animals in the various experimental groups. Open field was used to assess **(A)** horizontal activity (number of beam breaks), **(B)** time spent in the peripheral zone (seconds) and **(C)** time spent in the central zone (seconds). $^{**}p < 0.01$ SI compared to C rats. Data are presented in mean ± SEM. (C: $n = 4$; SS: $n = 6$; and SI: $n = 6$).

Anxiety

Forty-eight hours after blast (or sham) injury, we found that SI rats traveled significantly shorter distances than C animals (**Figure 3A**). Animals in the SS group also traveled shorter distances but the differences were not statistically significant. Animals in both SS and SI groups spent significantly less time in the open arms and more time in the closed arms (**Figures 3B,C**).

At 1 month both SS and SI groups traveled shorter distances compared to C animals (**Figure 3A**). Among the stressed groups only SI animals exhibited raised anxiety by spending less time in the open arms and more time in the closed arms (**Figures 3B,C**). Animals in the SS group did not show significant differences in the time spent in the open arms vs. closed arms compared to the controls.

Two months after blast or sham injury, all animals performed similarly with no significant differences in total distance traveled or time spent in the open and the closed arms.

Spatial learning and memory

During the first BM session, performed between days 3 and 8 post-blast (or sham; see **Figure 1** for schedule) we observed significant differences in the performance of animals on the last testing day only (day 8). SS rats needed significantly more time to find the escape box compared to C rats. SI rats spent less time finding the escape box than SS rats, but more time compared to C rats; the difference was not statistically significant (**Figure 4A**).

During the second BM session, performed between days 32 and 36 post-blast (or sham), we found no difference in the latency times of animals in the SS and the C groups. However, SI animals required significantly longer times to find the escape box on day 33 through 36 (**Figure 4B**).

The last BM session was performed between days 64 and 69 post-injury (or sham). Again, the performance of SS animals was not statistically different from animal in the control group (**Figure 4C**). In contrast, SI rats performed very poorly in the BM on day 64. These animals had increased latency times similar to those measured during the first BM session (**Figures 4C,D**) showing significant memory problems on days 65 and 68, indicating lasting memory impairment caused by blast.

EFFECTS ON PROTEIN MARKERS

Serum changes

At the end of the last behavioral session (69 days post-injury or sham), we obtained serum from each animal and compared NF-H, CK-BB, GFAP, VEGF, and NSE levels across all experimental groups. We found that serum levels of all protein markers listed above were significantly elevated at this late time point in SI animals (**Figure 5**). As expected, serum CORT levels were significantly elevated in both SS and SI groups. However, the difference in serum CORT levels between the two groups was statistically insignificant.

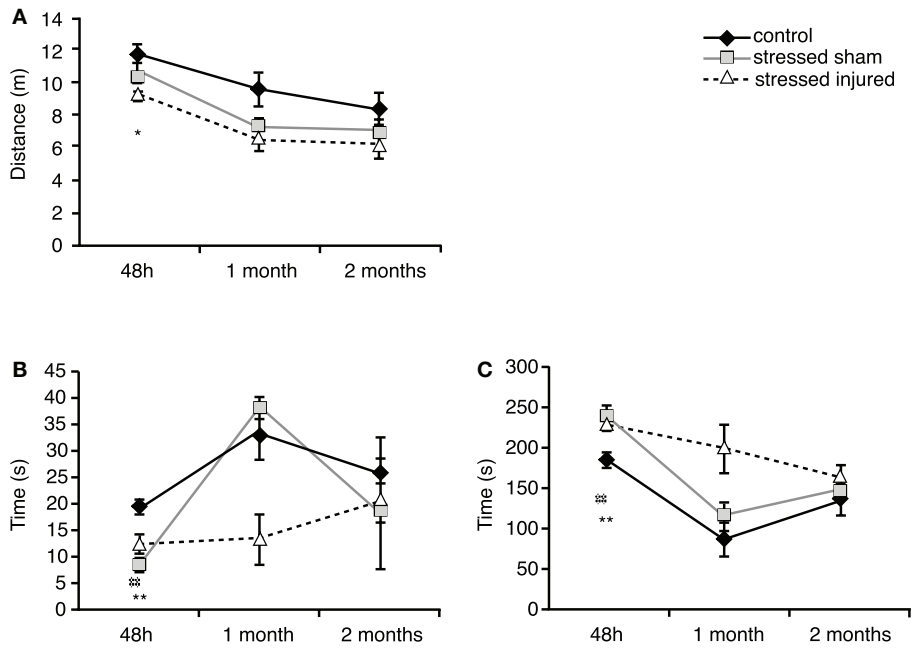

FIGURE 3 | Anxiety of animals in the various experimental groups. Elevated plus maze was used to assess **(A)** total distance traveled (meter), **(B)** time spent in the open arms (seconds) and **(C)** time spent in the closed arms (seconds). $*p < 0.05$ and $**p < 0.01$ SI compared to C rats, $^{\#\#}p < 0.01$ SS to C rats. Data are presented in mean ± SEM. (C: $n = 4$; SS: $n = 6$; and SI: $n = 6$).

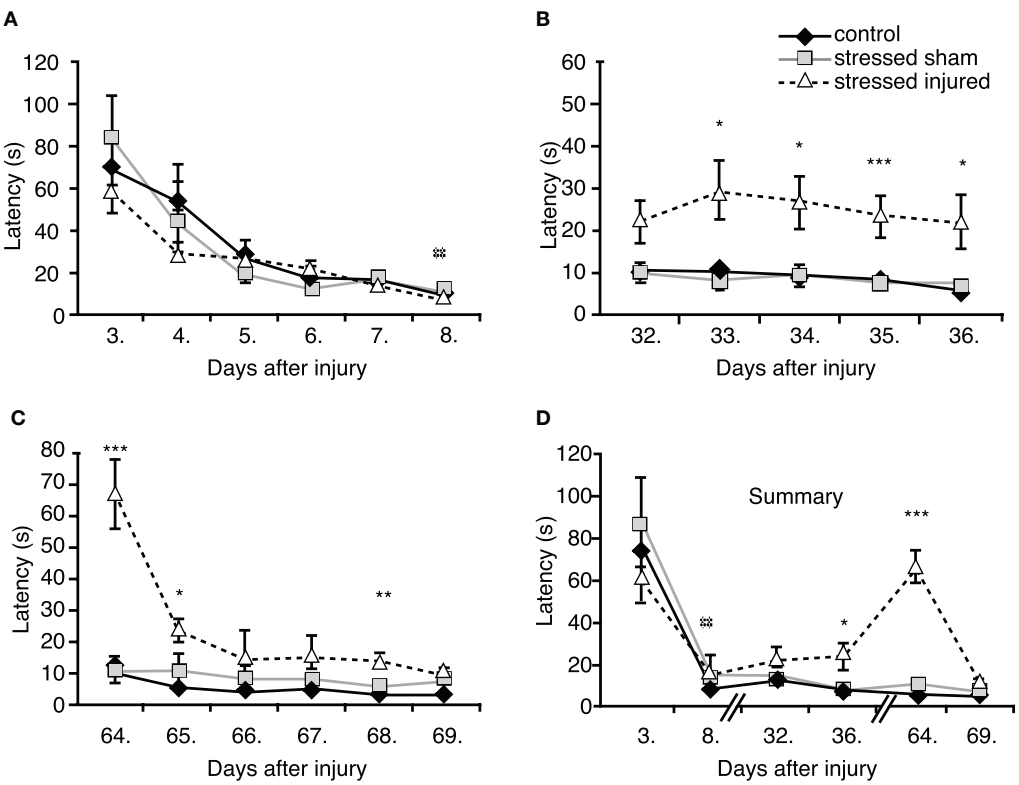

FIGURE 4 | Spatial learning and memory of animals in the various experimental groups. Barnes maze was used to determine latencies to find the escape box **(A)** 3–8 days post-injury, **(B)** 32–36 days post-injury, **(C)** 64–69 days post-injury. **(D)** Summarized time-line of latencies of the three sets of Barnes maze test. $*p < 0.05$, $**p < 0.01$, and $***p < 0.01$ SI compared to C rats, $^{\#\#}p < 0.01$ SS to C rats. Data are presented in mean ± SEM (C: $n = 4$; SS: $n = 6$; and SI: $n = 6$).

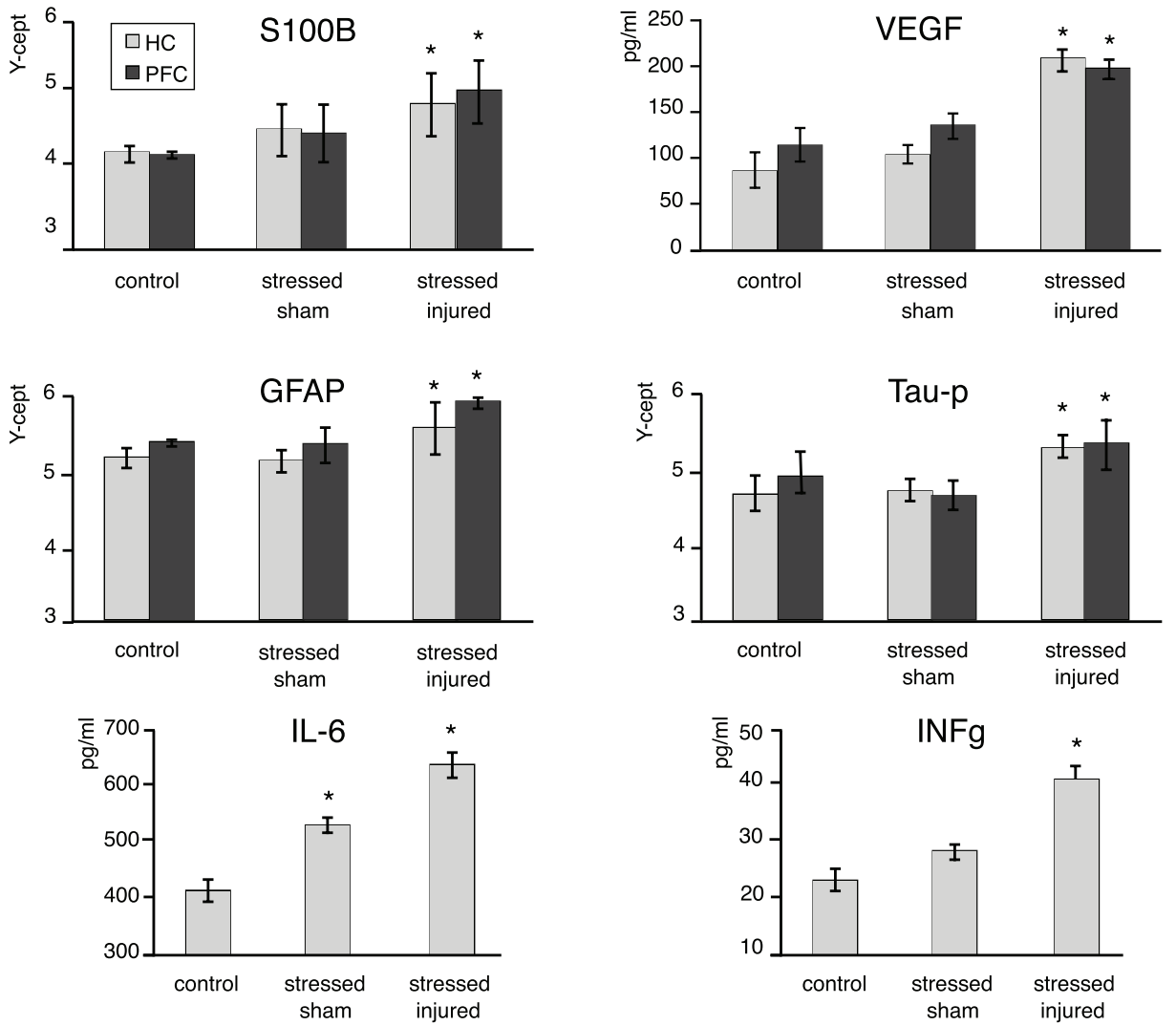

FIGURE 5 | Protein markers in the PFC and the HC of animals in the various experimental groups. Tissue extracts were prepared from dissected PFC and HC regions of C, SS, and SI rat brains. The tissue levels of the selected marker proteins were assayed using either RPPM or ELISA. The *y*-axis intercept (Y-cept) and pg/ml (IL-6 and IFNg) indicate the measured protein levels. $*p < 0.05$, $**p < 0.01$ compared to C rats, error bars are ± SEM. (C: $n = 2$; SS: $n = 3$; and SI: $n = 3$).

Changes in the brain

At the end of the last behavioral session we analyzed changes in the expression of S100β, VEGF, GFAP, Tau-protein, IL-6, and INFγ in the PFC and the HC of all animals. We found significantly elevated levels of all markers (except IL-6) in the PFC and the HC of SI animals only (**Figure 6**). Interestingly, we found that IL-6 levels were significantly increased in the HC of SS animals while no such effect of stress alone was seen on hippocampal INFγ levels.

CELLULAR CHANGES

Astrogliosis

To identify the cellular changes underlying the observed behavioral abnormalities, we analyzed the HC and the PFC for GFAP expression at 2 months post-blast (or sham). Consistent with our proteomics data, we found that exposure to stress alone (SS) had no observable effect on GFAP expression in the PFC or the HC (**Figure 7**). However, in SI animals we detected a noticeable increase in GFAP immunoreactivity in the PFC and the VHC.

Importantly, an increase in GFAP+ cells displaying a stellar morphology characteristic of reactive astrocytes was observed in the PFC and the VHC of SI animals (**Figure 7C**, and insert).

Inflammation

Similar to the gliotic response above, exposure to stress alone had no significant effect on Iba1 immunoreactivity in the PFC or the HC (**Figure 8**). While increased Iba1 immunoreactivity was observed in the SI group, there was a noticeable increase in Iba1 immunoreactivity (albeit to a lesser degree) in the PFC of SS animals. No significant differences were observed in Iba1 immunoreactivity in the DHC of any of the experimental groups.

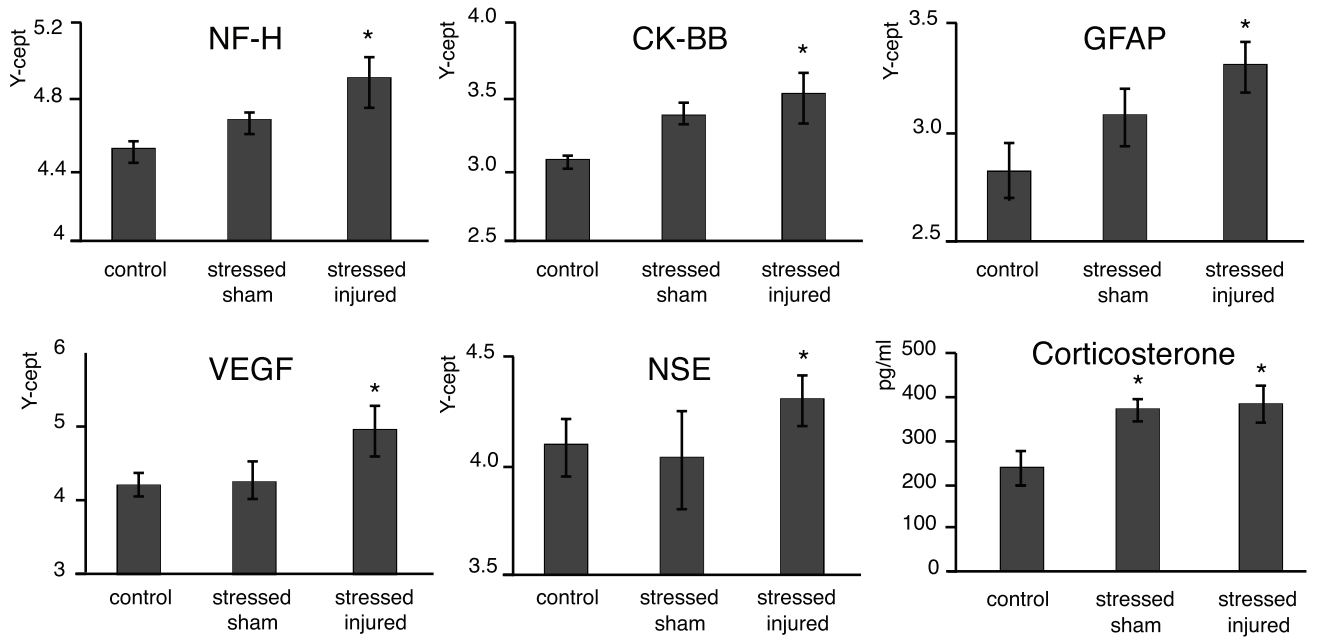

FIGURE 6 | Serum markers of animals in the various experimental groups. Blood was drawn and sera were prepared from the C, SS, and SI rats. The levels of the selected marker proteins were assayed using either RPPM or ELISA, and corticosterone levels were assayed using ELISA. The *y*-axis intercept (Y-cept) and pg/ml (corticosterone) indicate the measured protein levels. $*p < 0.05$, $**p < 0.01$ compared to C rats, error bars are ± SEM (C: $n = 4$; SS: $n = 6$; and SI: $n = 6$).

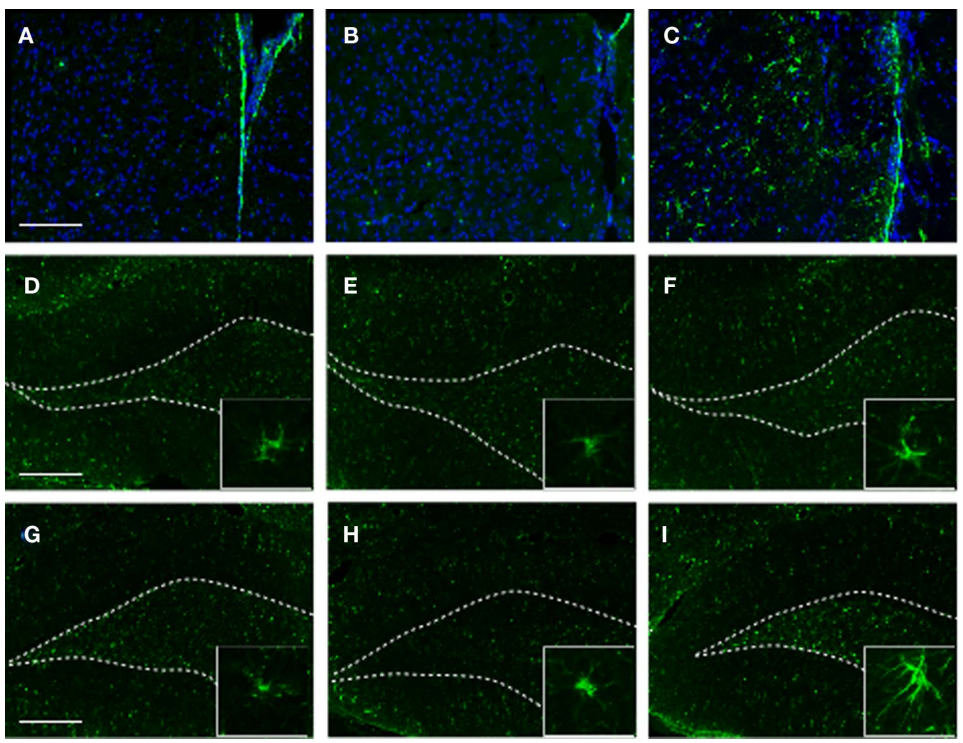

FIGURE 7 | GFAP immunoreactivity in selected brain regions of animals in the various experimental groups. Frozen coronal sections containing the PFC, DHC, and VHC were cut and processed for immunohistochemistry using a GFAP antibody. Sections were stained with Hoechst 33342 to mark cellular nuclei. PFC of **(A)** C, **(B)** SS, and **(C)** SI rats; DHC of **(D)** C, **(E)** SS, and **(F)** SI rats; VHC of **(G)** C, **(H)** SS, and **(I)** SI rats. Inlays display morphological extension of stellar-like processes in VHC of SI rats. White-dotted line outlines DG layer of hippocampus.

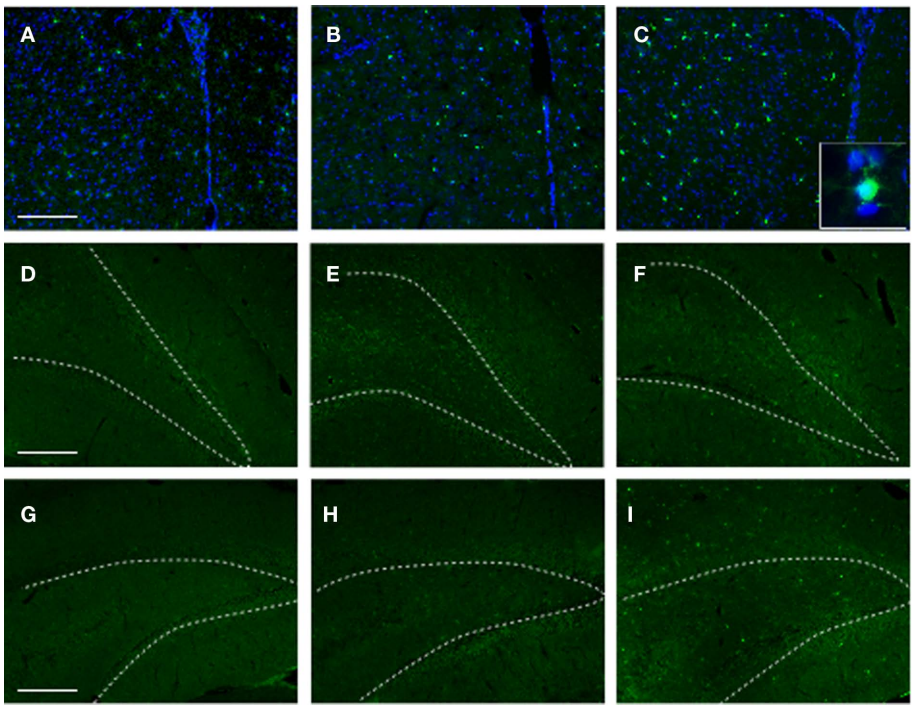

FIGURE 8 | Iba1 immunoreactivity in selected brain regions of animals in the various experimental groups. Frozen coronal sections containing the PFC, DHC, and VHC were cut and processed for immunohistochemistry using an Iba1 antibody. Sections were stained with Hoechst 33342 to mark cellular nuclei. PFC of **(A)** C, **(B)** SS, and **(C)** SI rats; DHC of **(D)** C, **(E)** SS, and **(F)** SI rats; VHC of **(G)** C, **(H)** SS, and **(I)** SI rats. White-dotted line outlines DG layer of hippocampus.

Apoptotic cell death

TUNEL histology was used to determine the extent of apoptotic cell death in the PFC, VHC, and DHC across all experimental groups. The number of TUNEL-positive cells was significantly increased in the hilus of the VHC and the DHC of the SI group (**Figure 9**). Interestingly, there was no increase in the number of TUNEL-positive cells in the PFC of animals in any of the experimental groups (**Figure A1** in Appendix). The exposure to stress alone resulted in no increase in the number of TUNEL-positive cells in any of the SS brain regions investigated.

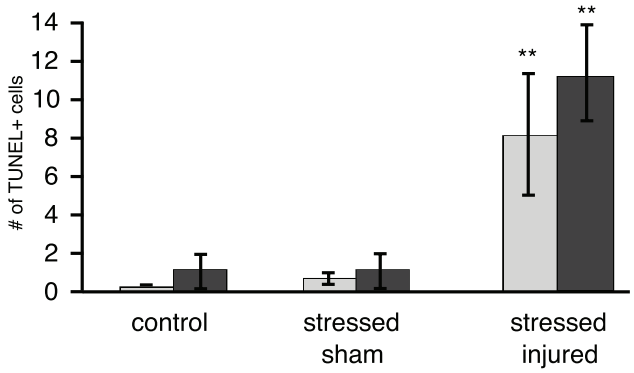

FIGURE 9 | TUNEL-positive cells in selected brain regions of animals in the various experimental groups. Frozen coronal sections containing the hilus of the DHC and VHC of C, SS, and SI rats were cut and processed for TUNEL histology. The number of TUNEL-positive cells were counted and expressed as positive cells per unit area ± SEM. $*p < 0.05$ and $**p < 0.01$ compared to C rats.

Neurogenesis

To gain insight into the potential effects of stress (with or without injury) on hippocampal *de novo* neurogenesis, we performed DCX immunohistochemistry. We observed a noticeable increase in DCX expression in the VHC of SI animals; DCX immunoreactive cells displayed specific morphologies with elaborate processes reaching well into the DG (**Figure 10F** and insert). Stress alone caused an apparent increase in DCX positive cells in the VHC compared to the controls (**Figure 10**). However, the DCX+ cells in SS animals lacked the elaborate processes seen in SI animals.

DISCUSSION

The main finding of this study is that repeated stress alone caused a transient increase in anxiety and no major cellular and molecular abnormalities, while the exposure to stress and a single mild blast resulted in a transient (but longer lasting) increase in anxiety and chronic memory impairment. These behavioral changes are associated with neuroinflammation, vascular changes, and neuronal and glial cell loss.

Repetitive stress alone resulted in an early (48 h) increase in anxiety that dissipated at later time points. Our finding is consistent with previous studies where the exposure of rats to a fear-provoking environment resulted in a short-term increase in anxiety

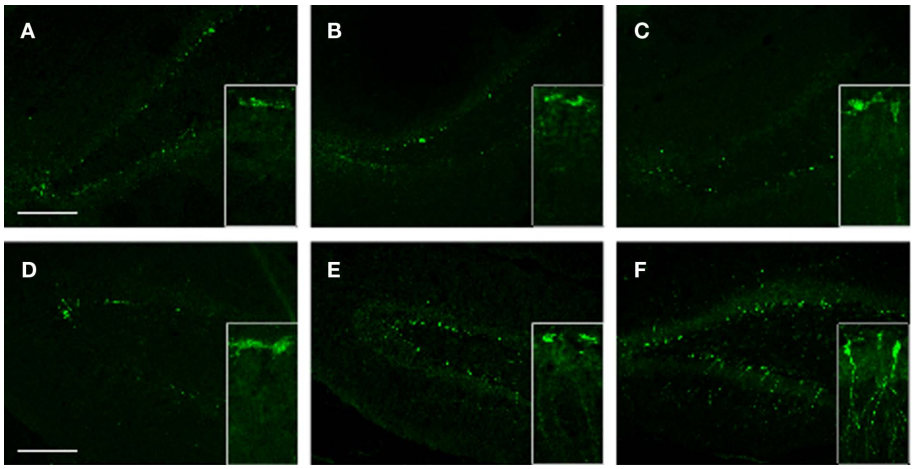

FIGURE 10 | DCX immunoreactivity in selected brain regions of animals in the various experimental groups. Frozen coronal sections containing the PFC, DHC, and VHC were cut. Immunohistochemistry was performed using a DCX antibody. Sections were stained with Hoechst 33342 to mark cellular nuclei. DHC of **(A)** C, **(B)** SS, and **(C)** SI rats; VHC of **(D)** C, **(E)** SS, and **(F)** SI rats. Inlays show the finer details of the cell bodies and processes of DCX cells within the DG of the VHC.

(Pynoos et al., 1996). Other studies also reported increased anxiety that lasted up to 7 days after daily exposure to predator odor (Adamec and Shallow, 1993; Cohen et al., 1996, 2000, 2003; Adamec et al., 1997, 1999). On the other hand, exposure of stressed animals to blast appears to prolong the period of increased anxiety, as these animals had elevated anxiety levels up to 1 month after injury. Importantly, anxiety levels of even these animals returned to normal at 2 months post-injury (or sham).

These findings suggest that the long-term effects of stress and injury can dissipate. However, epidemiological studies show that traumatic event(s) or repeated stress can result in PTSD, a chronic condition (Woon et al., 2010), although not all individuals exposed to traumatic events develop PTSD (Gross and Hen, 2004; Yehuda and LeDoux, 2007). The neuroanatomical substrates mediating symptom formation in PTSD include the medial PFC, amygdala, and HC (Bremner, 2007; Liberzon and Sripada, 2008). Within the HC, the VHC is predominantly involved in mediating anxiety-related functions while the DHC is involved in learning and memory-associated functions (Henke, 1990; Moser et al., 1995). *In vivo* imaging studies have found correlation between hippocampal volume and susceptibility to PTSD development (Karl et al., 2006). A recent meta-analytic study concluded that hippocampal volume reduction is associated with the exposure to trauma independent of PTSD diagnosis, but additional hippocampal reduction is associated with the development of PTSD compared to the trauma-exposed group without PTSD (Woon et al., 2010). A recent comprehensive *in vivo* imaging study showed that the volume of CA3/DG fields of the HC was significantly reduced in veterans with combat-related PTSD (Wang et al., 2010).

Both genetic and epigenetic factors are suspected in individuals' susceptibility to developing PTSD. These include an abnormal serotonin system and an altered response to CORT (Gross and Hen, 2004). Stress can alter the function of the hypothalamus–pituitary–adrenal axis (HPA), which in turn leads to abnormally elevated levels of CORT (Yehuda, 2006). Chronically elevated levels of CORT, as we observed, can adversely affect the architecture of the HC. However, a recent study found that chronically elevated CORT levels did not reduce cell number but caused a pronounced loss of synapses, suggesting that volume measures can substantially underestimate the effects of CORT on hippocampal structure and importantly on function (Tata et al., 2006; Tata and Anderson, 2010).

The HC, specifically the DHC, is also a critical neuroanatomical substrate of learning and memory (Henke, 1990; Moser and Humpel, 2005); elevated CORT levels can adversely affect memory (Bannerman et al., 2004). Although we found that CORT levels remained elevated even after 2 months in both SS and SI groups, we found that SS animals did not display memory deficits. Previous studies showed that following daily (foot-shock) stress for 14 days, CORT levels were elevated during the first 7 days post-stress, but returned to control levels by day 14 (Kant et al., 1987). However, there have been no studies to our knowledge that measure the long-term (e.g., 2 months) effects of stress on CORT levels.

In contrast to the transient increase in anxiety, we found that memory impairment was both specific to blast injury and also appeared to be a "chronic" condition. In BM, the performance of SS animals was not significantly different from C animals at any given time point, except on day 8 post-injury. Previous behavioral paradigms, in which rats were exposed to another form of predator stress (Diamond et al., 2006) have indicated that stress can have different effects on memory formation and consolidation depending on the time of exposure. Importantly, our data showed that memory impairment was at its highest at 2 months post-injury. These findings suggest that blast injury predominantly affects the DHC as evidenced by impaired spatial memory.

We found an increased number of TUNEL-positive cells in the hilus of the HC but not in the PFC of animals in the SI group at 2 months post-injury. This apparent lasting apoptotic processes after TBI is quite unusual. The limited information available indicates that in other models of TBI apoptotic activity returned to control levels 2 months after injury (Luo et al., 2002). There were no significant differences in the number of TUNEL-positive cells

of animals that were exposed to chronic stress only. As discussed above, SS animals had elevated serum CORT levels but showed no increase in the number of TUNEL-positive cells in their HC or PFC. These findings suggest that in addition to elevated CORT levels, other factors like inflammation may be required to sustain the increase in apoptotic cell death.

Our immunohistochemical data showed an increase in Iba1 immunoreactivity in the PFC as well as the HC of SI animals. Within the HC of SI animals, Iba1 immunoreactivity appeared to be higher in the VHC than in the DHC. However, we also found that exposure to stress alone resulted in an increase in hippocampal IL-6 (but not INFγ) levels 2 month after injury (or sham). IL-6 and INFγ are inflammatory cytokines produced by activated microglia and astroglia and are involved in mediating various responses to injury (Morganti-Kossmann et al., 2001, 2002; Nimmo et al., 2004). Depending on the cellular and molecular context, IL-6 can be neurotoxic or can act as a neuroprotectant (Toulmond et al., 1992).

IL-6 can act as a potent inhibitor of *de novo* hippocampal neurogenesis; one of several innate regenerative processes triggered by TBI (Vallieres et al., 2002). After a latency period following TBI, the rate of *de novo* hippocampal neurogenesis increases (Dash et al., 2001; Chirumamilla et al., 2002; Lee and Agoston, 2010). Newborn neurons, marked by DCX expression, migrate from the SGL to the granule cell layer (GCL) where many of the surviving neurons differentiate into granule cells (Altman and Das, 1965; Cameron et al., 1993). We found an apparent increase in DCX positive cells at 2 months after injury in the VHC but not in the DHC of SI rats. Additionally, these cells showed elaborate processes extending well into the DG. Animals in the SS group also showed an increase in DCX immunoreactivity in the VHC but the cells lacked the elaborate processes observed in SI rats. These findings suggest an increase in *de novo* neurogenesis in the VHC in response to stress, but particularly to the combination of stress and blast. This may indicate that increased *de novo* neurogenesis in the VHC is partly responsible for the normalization of anxiety observed at 2 months.

The apparent increase in DCX+ cells in the VHC of SI animals contradict what the Iba1 immunohistochemistry and the IL-6 ELISA data would imply. In addition to chronically elevated CORT levels, elevated hippocampal IL-6 levels and the presence of Iba1+ cells in the HC would imply a decrease or repression in neurogenetic activity as neuroinflammation and elevated CORT levels are known inhibitors of hippocampal *de novo* neurogenesis (Cameron and Gould, 1994; Yu et al., 2004; Montaron et al., 2006); with males showing a greater vulnerability to elevated CORT (Brummelte and Galea, 2010). However, the regulation of *de novo* hippocampal neurogenesis is rather complex; large numbers of molecules are involved and the exact nature of the regulatory process is currently not fully understood (Kempermann and Gage, 2000; Kempermann, 2002). Even though it has been accepted that an increase in DCX+ cells indicates increased *de novo* neurogenesis, DCX is only transiently expressed by *de novo* neurons. Thus, a more detailed BrdU/Prox1 double immunohistochemical and stereological quantification of the histology results is required to determine changes in *de novo* neurogenesis after stress and blast.

One of the positive regulators of *de novo* neurogenesis is VEGF; we and others have found that VEGF is significantly upregulated in various forms of TBI (Jin et al., 2002; Lee and Agoston, 2010) increased VEGF level promotes survival of *de novo* hippocampal neurons by blocking apoptotic cell death (Lee and Agoston, 2010). Consistent with the previous observation, we found that injury and stress, but not stress alone, increases VEGF levels in the HC and also in the PFC. Consistent with the previous observation, we found that injury and stress, but not stress alone, increases VEGF levels in the HC and also in the PFC. Previous studies have demonstrated that an increase in VEGF concentration can also increase vascular permeability as indicated by the breach of the BBB (Dvorak et al., 1995). Interestingly, a recent clinical study has shown that increased serum level of VEGF is indicative of good outcome after ischemic stroke (Sobrino et al., 2009).

We found increased serum levels of several neuronal and glia-specific proteins including NF-H, NSE, CK-BB, and GFAP 2 months post-injury. These molecules have previously been used to assess the extent and the outcome of TBI (Berger, 2006; Korfias et al., 2009). For example, NF-H has been used as a biomarker of neuronal loss and BBB damage and predicting outcome (Anderson et al., 2008). That serum levels of these proteins remain elevated at 2 month after injury suggest ongoing neuronal and glial cell loss as well as a chronically increased BBB permeability in which elevated levels of VEGF may play a role (Ay et al., 2008; Gerstner et al., 2009).

We also found significantly elevated levels of S100β and GFAP in the HC and in the PFC of SI animals. Elevated tissue levels of S100β may indicate astroglial proliferation and overall glial response to injury (Kleindienst et al., 2005). Elevated expression of GFAP by astrocytes, combined with morphological changes (reactive astrogliosis), is a hallmark of CNS neurotrauma (Eng and Ghirnikar, 1994; Fitch and Silver, 2008). We found that the VHC and the DHC appear to have differential expression of stellar GFAP astroglia following exposure to stress only and to the combination stress and injury. The role of increased GFAP immunoreactivity and stellar astroglia in CNS injury is complex. Astrocytic responses can lead to either reparative or detrimental outcomes depending on the type and time after injury (Eng and Ghirnikar, 1994; Fitch and Silver, 2008). However, increasing evidence also indicates a protective role of astrogliosis in reducing the toxic effects of extracellular glutamate and enabling barrier reconstruction after TBI (Buffo et al., 2010). In light of our behavioral findings, showing normalized anxiety levels of SI animals at 2 months post-injury, we speculate that the apparent increase in GFAP positive cells in the VHC may contribute to reparative pathomechanisms and the restoration of normal anxiety levels. Chronic stress has been shown to significantly reduce both the number and somal volume of astroglia in the HC (Czeh et al., 2006). Interestingly, we did see a differential effect of stress alone and stress and injury in the DHC and VHC. While the VHC displayed an apparent increase in GFAP+ cells with stellar processes, the same was not observed in the DHC and memory impairment remained significant 2 months post-injury. A possible explanation for the lasting memory deficits occurring in SI animals is that stress may selectively impair the restorative and/or regenerative action of reactive astrocytes in the DHC. While compelling, the results obtained require further exploration.

In summary, we found that when stressed animals are exposed to a single mild blast overpressure, there are lasting behavioral, molecular, and cellular abnormalities characterized by memory

impairment, neuronal and glial cell losses, inflammation, and gliosis. In contrast, stress alone resulted only in a transient increase in anxiety, no memory deficit and no detectable tissue damage. If our findings are independently verified, the potential ramifications can be significant in developing tools to assess the severity and to predict the outcome of psychological and physical traumas.

ACKNOWLEDGMENTS

We thank the Neurotrauma Team (WRAIR) for their technical help during the exposures; Ms. Cara Olsen (USU) for her help in statistical analysis; Drs. Grunberg and Wu (USU) for their input in designing and interpreting the behavioral experiments. The work was supported by CDMRP, grant# W81XWH-08-2-0176.

REFERENCES

Adamec, R. E., Burton, P., Shallow, T., and Budgell, J. (1999). NMDA receptors mediate lasting increases in anxiety-like behavior produced by the stress of predator exposure – implications for anxiety associated with posttraumatic stress disorder. *Physiol. Behav.* 65, 723–737.

Adamec, R. E., and Shallow, T. (1993). Lasting effects on rodent anxiety of a single exposure to a cat. *Physiol. Behav.* 54, 101–109.

Adamec, R. E., Shallow, T., and Budgell, J. (1997). Blockade of CCK(B) but not CCK(A) receptors before and after the stress of predator exposure prevents lasting increases in anxiety-like behavior: implications for anxiety associated with posttraumatic stress disorder. *Behav. Neurosci.* 111, 435–449.

Altman, J., and Das, G. D. (1965). Autoradiographic and histological evidence of postnatal hippocampal neurogenesis in rats. *J. Comp. Neurol.* 124, 319–335.

Anderson, K. J., Scheff, S. W., Miller, K. M., Roberts, K. N., Gilmer, L. K., Yang, C., and Shaw, G. (2008). The phosphorylated axonal form of the neurofilament subunit NF-H (pNF-H) as a blood biomarker of traumatic brain injury. *J. Neurotrauma* 25, 1079–1085.

Armonda, R. A., Bell, R. S., Vo, A. H., Ling, G., Degraba, T. J., Crandall, B., Ecklund, J., and Campbell, W. W. (2006). Wartime traumatic cerebral vasospasm: recent review of combat casualties. *Neurosurgery* 59, 1215–1225; discussion 1225.

Ay, I., Francis, J. W., and Brown, R. H. Jr. (2008). VEGF increases blood–brain barrier permeability to Evans blue dye and tetanus toxin fragment C but not adeno-associated virus in ALS mice. *Brain Res.* 1234, 198–205.

Bannerman, D. M., Rawlins, J. N., Mchugh, S. B., Deacon, R. M., Yee, B. K., Bast, T., Zhang, W. N., Pothuizen, H. H., and Feldon, J. (2004). Regional dissociations within the hippocampus – memory and anxiety. *Neurosci. Biobehav. Rev.* 28, 273–283.

Barnes, C. A. (1979). Memory deficits associated with senescence: a neurophysiological and behavioral study in the rat. *J. Comp. Physiol. Psychol.* 93, 74–104.

Belanger, H. G., Vanderploeg, R. D., Curtiss, G., and Warden, D. L. (2007). Recent neuroimaging techniques in mild traumatic brain injury. *J. Neuropsychiatry Clin. Neurosci.* 19, 5–20.

Berger, R. P. (2006). The use of serum biomarkers to predict outcome after traumatic brain injury in adults and children. *J. Head Trauma Rehabil.* 21, 315–333.

Bremner, J. D. (2007). Functional neuroimaging in post-traumatic stress disorder. *Expert Rev. Neurother.* 7, 393–405.

Brenner, L. A., Vanderploeg, R. D., and Terrio, H. (2009). Assessment and diagnosis of mild traumatic brain injury, posttraumatic stress disorder, and other polytrauma conditions: burden of adversity hypothesis. *Rehabil. Psychol.* 54, 239–246.

Breslau, N., and Kessler, R. C. (2001). The stressor criterion in DSM-IV posttraumatic stress disorder: an empirical investigation. *Biol. Psychiatry* 50, 699–704.

Brummelte, S., and Galea, L. A. (2010). Chronic high corticosterone reduces neurogenesis in the dentate gyrus of adult male and female rats. *Neuroscience* 168, 680–690.

Bruns, J., and Hauser, W. A. (2003). The epidemiology of traumatic brain injury: a review. *Epilepsia* 44(Suppl.), 2.

Buffo, A., Rolando, C., and Ceruti, S. (2010). Astrocytes in the damaged brain: molecular and cellular insights into their reactive response and healing potential. *Biochem. Pharmacol.* 79, 77–89.

Cameron, H. A., and Gould, E. (1994). Adult neurogenesis is regulated by adrenal steroids in the dentate gyrus. *Neuroscience* 61, 203–209.

Cameron, H. A., Woolley, C. S., Mcewen, B. S., and Gould, E. (1993). Differentiation of newly born neurons and glia in the dentate gyrus of the adult rat. *Neuroscience* 56, 337–344.

Campbell, T., Lin, S., Devries, C., and Lambert, K. (2003). Coping strategies in male and female rats exposed to multiple stressors. *Physiol. Behav.* 78, 495–504.

Carobrez, A. P., and Bertoglio, L. J. (2005). Ethological and temporal analyses of anxiety-like behavior: the elevated plus-maze model 20 years on. *Neurosci. Biobehav. Rev.* 29, 1193–1205.

Cernak, I., Merkle, A. C., Koliatsos, V. E., Bilik, J. M., Luong, Q. T., Mahota, T. M., Xu, L., Slack, N., Windle, D., and Ahmed, F. A. (2010). The pathobiology of blast injuries and blast-induced neurotrauma as identified using a new experimental model of injury in mice. *Neurobiol. Dis.* 41, 538–551.

Cernak, I., Wang, Z., Jiang, J., Bian, X., and Savic, J. (2001). Ultrastructural and functional characteristics of blast injury-induced neurotrauma. *J. Trauma.* 50, 695–706.

Chirumamilla, S., Sun, D., Bullock, M. R., and Colello, R. J. (2002). Traumatic brain injury induced cell proliferation in the adult mammalian central nervous system. *J. Neurotrauma* 19, 693–703.

Cohen, H., Benjamin, J., Kaplan, Z., and Kotler, M. (2000). Administration of high-dose ketoconazole, an inhibitor of steroid synthesis, prevents posttraumatic anxiety in an animal model. *Eur. Neuropsychopharmacol.* 10, 429–435.

Cohen, H., Friedberg, S., Michael, M., Kotler, M., and Zeev, K. (1996). Interaction of CCK-4 induced anxiety and post-cat exposure anxiety in rats. *Depress. Anxiety* 4, 144–145.

Cohen, H., Zohar, J., and Matar, M. (2003). The relevance of differential response to trauma in an animal model of posttraumatic stress disorder. *Biol. Psychiatry* 53, 463–473.

Czeh, B., Simon, M., Schmelting, B., Hiemke, C., and Fuchs, E. (2006). Astroglial plasticity in the hippocampus is affected by chronic psychosocial stress and concomitant fluoxetine treatment. *Neuropsychopharmacology* 31, 1616–1626.

Dash, P. K., Mach, S. A., and Moore, A. N. (2001). Enhanced neurogenesis in the rodent hippocampus following traumatic brain injury. *J. Neurosci. Res.* 63, 313–319.

Diamond, D. M., Campbell, A. M., Park, C. R., Woodson, J. C., Conrad, C. D., Bachstetter, A. D., and Mervis, R. F. (2006). Influence of predator stress on the consolidation versus retrieval of long-term spatial memory and hippocampal spinogenesis. *Hippocampus* 16, 571–576.

Doll, H., Truebel, H., Kipfmueller, F., Schaefer, U., Neugebauer, E. A., Wirth, S., and Maegele, M. (2009). Pharyngeal selective brain cooling improves neurofunctional and neurocognitive outcome after fluid percussion brain injury in rats. *J. Neurotrauma* 26, 235–242.

Dvorak, H. F., Brown, L. F., Detmar, M., and Dvorak, A. M. (1995). Vascular permeability factor/vascular endothelial growth factor, microvascular hyperpermeability, and angiogenesis. *Am. J. Pathol.* 146, 1029–1039.

Elliott, B. M., and Grunberg, N. E. (2005). Effects of social and physical enrichment on open field activity differ in male and female Sprague-Dawley rats. *Behav. Brain Res.* 165, 187–196.

Eng, L. F., and Ghirnikar, R. S. (1994). GFAP and astrogliosis. *Brain Pathol.* 4, 229–237.

Fitch, M. T., and Silver, J. (2008). CNS injury, glial scars, and inflammation: inhibitory extracellular matrices and regeneration failure. *Exp. Neurol.* 209, 294–301.

Fride, E., Dan, Y., Feldon, J., Halevy, G., and Weinstock, M. (1986). Effects of prenatal stress on vulnerability to stress in prepubertal and adult rats. *Physiol. Behav.* 37, 681–687.

Gerstner, E. R., Duda, D. G., Di Tomaso, E., Ryg, P. A., Loeffler, J. S., Sorensen, A. G., Ivy, P., Jain, R. K., and Batchelor, T. T. (2009). VEGF inhibitors in the treatment of cerebral edema in patients with brain cancer. *Nat. Rev. Clin. Oncol.* 6, 229–236.

Gross, C., and Hen, R. (2004). Genetic and environmental factors interact to influence anxiety. *Neurotox. Res.* 6, 493–501.

Gyorgy, A. B., Walker, J., Wingo, D., Eidelman, O., Pollard, H. B., Molnar, A., and Agoston, D. V. (2010). Reverse phase protein microarray technology in traumatic brain injury. *J. Neurosci. Methods.* 192, 96–101.

Harrison, F. E., Hosseini, A. H., and Mcdonald, M. P. (2009). Endogenous anxiety and stress responses in water maze and Barnes maze spatial memory tasks. *Behav. Brain Res.* 198, 247–251.

Heath, D. L., and Vink, R. (1999). Optimization of magnesium therapy after severe diffuse axonal brain injury in rats. *J. Pharmacol. Exp. Ther.* 288, 1311–1316.

Henke, P. G. (1990). Hippocampal pathway to the amygdala and stress ulcer development. *Brain Res. Bull.* 25, 691–695.

Jaffee, M. S., and Meyer, K. S. (2009). A brief overview of traumatic brain injury (TBI) and post-traumatic stress disorder (PTSD) within the Department of Defense. *Clin. Neuropsychol.* 23, 1291–1298.

Jin, K., Zhu, Y., Sun, Y., Mao, X. O., Xie, L., and Greenberg, D. A. (2002). Vascular endothelial growth factor (VEGF) stimulates neurogenesis in vitro and in vivo. *Proc. Natl. Acad. Sci. U.S.A.* 99, 11946–11950.

Kant, G. J., Leu, J. R., Anderson, S. M., and Mougey, E. H. (1987). Effects of chronic stress on plasma corticosterone, ACTH and prolactin. *Physiol. Behav.* 40, 775–779.

Karl, A., Schaefer, M., Malta, L. S., Dorfel, D., Rohleder, N., and Werner, A. (2006). A meta-analysis of structural brain abnormalities in PTSD. *Neurosci. Biobehav. Rev.* 30, 1004–1031.

Kaur, C., Singh, J., Lim, M. K., Ng, B. L., Yap, E. P., and Ling, E. A. (1997). Ultrastructural changes of macroglial cells in the rat brain following an exposure to a non-penetrative blast. *Ann. Acad. Med. Singap.* 26, 27–29.

Keane, T. M., Marshall, A. D., and Taft, C. T. (2006). Posttraumatic stress disorder: etiology, epidemiology, and treatment outcome. *Annu. Rev. Clin. Psychol.* 2, 161–197.

Kempermann, G. (2002). Regulation of adult hippocampal neurogenesis – implications for novel theories of major depression. *Bipolar Disord.* 4, 17–33.

Kempermann, G., and Gage, F. H. (2000). Neurogenesis in the adult hippocampus. *Novartis Found. Symp.* 231, 220–235; discussion 235–241, 302–226.

Kleindienst, A., Mcginn, M. J., Harvey, H. B., Colello, R. J., Hamm, R. J., and Bullock, M. R. (2005). Enhanced hippocampal neurogenesis by intraventricular S100B infusion is associated with improved cognitive recovery after traumatic brain injury. *J. Neurotrauma* 22, 645–655.

Korfias, S., Papadimitriou, A., Stranjalis, G., Bakoula, C., Daskalakis, G., Antsaklis, A., and Sakas, D. E. (2009). Serum biochemical markers of brain injury. *Mini Rev. Med. Chem.* 9, 227–234.

Lee, C., and Agoston, D. V. (2010). Vascular endothelial growth factor is involved in mediating increased de novo hippocampal neurogenesis in response to traumatic brain injury. *J. Neurotrauma* 27, 541–553.

Liberzon, I., and Sripada, C. S. (2008). The functional neuroanatomy of PTSD: a critical review. *Prog. Brain Res.* 167, 151–169.

Ling, G., Bandak, F., Armonda, R., Grant, G., and Ecklund, J. (2009). Explosive blast neurotrauma. *J. Neurotrauma* 26, 815–825.

Ling, G. S., and Ecklund, J. M. (2011). Traumatic brain injury in modern war. *Curr. Opin. Anaesthesiol.* doi: 10.1097/ACO.0b013e32834458da. [Epub ahead of print].

Long, J. B., Bentley, T. L., Wessner, K. A., Cerone, C., Sweeney, S., and Bauman, R. A. (2009). Blast overpressure in rats: recreating a battlefield injury in the laboratory. *J. Neurotrauma* 26, 827–840.

Luo, C., Jiang, J., Lu, Y., and Zhu, C. (2002). Spatial and temporal profile of apoptosis following lateral fluid percussion brain injury. *Chin. J. Traumatol.* 5, 24–27.

Maegele, M., Lippert-Gruener, M., Ester-Bode, T., Sauerland, S., Schafer, U., Molcany, M., Lefering, R., Bouillon, B., Neiss, W. F., Angelov, D. N., Klug, N., Mcintosh, T. K., and Neugebauer, E. A. (2005). Reversal of neuromotor and cognitive dysfunction in an enriched environment combined with multimodal early onset stimulation after traumatic brain injury in rats. *J. Neurotrauma* 22, 772–782.

Mayorga, M. A. (1997). The pathology of primary blast overpressure injury. *Toxicology* 121, 17–28.

Montaron, M. F., Drapeau, E., Dupret, D., Kitchener, P., Aurousseau, C., Le Moal, M., Piazza, P. V., and Abrous, D. N. (2006). Lifelong corticosterone level determines age-related decline in neurogenesis and memory. *Neurobiol. Aging* 27, 645–654.

Morganti-Kossmann, M. C., Rancan, M., Otto, V. I., Stahel, P. F., and Kossmann, T. (2001). Role of cerebral inflammation after traumatic brain injury: a revisited concept. *Shock* 16, 165–177.

Morganti-Kossmann, M. C., Rancan, M., Stahel, P. F., and Kossmann, T. (2002). Inflammatory response in acute traumatic brain injury: a double-edged sword. *Curr. Opin. Crit. Care* 8, 101–105.

Moser, K. V., and Humpel, C. (2005). Vascular endothelial growth factor counteracts NMDA-induced cell death of adult cholinergic neurons in rat basal nucleus of Meynert. *Brain Res. Bull.* 65, 125–131.

Moser, M. B., Moser, E. I., Forrest, E., Andersen, P., and Morris, R. G. (1995). Spatial learning with a minislab in the dorsal hippocampus. *Proc. Natl. Acad. Sci. U.S.A.* 92, 9697–9701.

Nimmo, A. J., Cernak, I., Heath, D. L., Hu, X., Bennett, C. J., and Vink, R. (2004). Neurogenic inflammation is associated with development of edema and functional deficits following traumatic brain injury in rats. *Neuropeptides* 38, 40–47.

Okie, S. (2005). Traumatic brain injury in the war zone. *N. Engl. J. Med.* 352, 2043–2047.

Pynoos, R. S., Ritzmann, R. F., Steinberg, A. M., Goenjian, A., and Prisecaru, I. (1996). A behavioral animal model of posttraumatic stress disorder featuring repeated exposure to situational reminders. *Biol. Psychiatry* 39, 129–134.

Richardson, L. K., Frueh, B. C., and Acierno, R. (2010). Prevalence estimates of combat-related post-traumatic stress disorder: critical review. *Aust. N. Z. J. Psychiatry* 44, 4–19.

Ryan, L. M., and Warden, D. L. (2003). Post concussion syndrome. *Int. Rev. Psychiatry* 15, 310–316.

Salzberg, M., Kumar, G., Supit, L., Jones, N. C., Morris, M. J., Rees, S., and O'brien, T. J. (2007). Early postnatal stress confers enduring vulnerability to limbic epileptogenesis. *Epilepsia* 48, 2079–2085.

Sobrino, T., Arias, S., Rodriguez-Gonzalez, R., Brea, D., Silva, Y., De La Ossa, N. P., Agulla, J., Blanco, M., Pumar, J. M., Serena, J., Davalos, A., and Castillo, J. (2009). High serum levels of growth factors are associated with good outcome in intracerebral hemorrhage. *J. Cereb. Blood Flow Metab.* 29, 1968–1974.

Taber, K. H., Warden, D. L., and Hurley, R. A. (2006). Blast-related traumatic brain injury: what is known? *J. Neuropsychiatry Clin. Neurosci.* 18, 141–145.

Tagliaferri, F., Compagnone, C., Korsic, M., Servadei, F., and Kraus, J. (2006). A systematic review of brain injury epidemiology in Europe. *Acta Neurochir. (Wien)* 148, 255–268.

Tata, D. A., and Anderson, B. J. (2010). The effects of chronic glucocorticoid exposure on dendritic length, synapse numbers and glial volume in animal models: implications for hippocampal volume reductions in depression. *Physiol. Behav.* 99, 186–193.

Tata, D. A., Marciano, V. A., and Anderson, B. J. (2006). Synapse loss from chronically elevated glucocorticoids: relationship to neuropil volume and cell number in hippocampal area CA3. *J. Comp. Neurol.* 498, 363–374.

Toulmond, S., Vige, X., Fage, D., and Benavides, J. (1992). Local infusion of interleukin-6 attenuates the neurotoxic effects of NMDA on rat striatal cholinergic neurons. *Neurosci. Lett.* 144, 49–52.

Vallieres, L., Campbell, I. L., Gage, F. H., and Sawchenko, P. E. (2002). Reduced hippocampal neurogenesis in adult transgenic mice with chronic astrocytic production of interleukin-6. *J. Neurosci.* 22, 486–492.

Vink, R., O'Connor, C. A., Nimmo, A. J., and Heath, D. L. (2003). Magnesium attenuates persistent functional deficits following diffuse traumatic brain injury in rats. *Neurosci. Lett.* 336, 41–44.

von Horsten, S., Exton, M. S., Voge, J., Schult, M., Nagel, E., Schmidt, R. E., Westermann, J., and Schedlowski, M. (1998). Cyclosporine A affects open field behavior in DA rats. *Pharmacol. Biochem. Behav.* 60, 71–76.

Walf, A. A., and Frye, C. A. (2007). The use of the elevated plus maze as an assay of anxiety-related behavior in rodents. *Nat. Protoc.* 2, 322–328.

Wang, Z., Neylan, T. C., Mueller, S. G., Lenoci, M., Truran, D., Marmar, C. R., Weiner, M. W., and Schuff, N. (2010). Magnetic resonance imaging of hippocampal subfields in posttraumatic stress disorder. *Arch. Gen. Psychiatry* 67, 296–303.

Warden, D. (2006). Military TBI during the Iraq and Afghanistan wars. *J. Head Trauma Rehabil.* 21, 398–402.

Warden, D. L., and French, L. (2005). Traumatic brain injury in the war zone. *N. Engl. J. Med.* 353, 633–634.

Warden, D. L., Labbate, L. A., Salazar, A. M., Nelson, R., Sheley, E., Staudenmeier, J., and Martin, E. (1997). Posttraumatic stress disorder in patients with traumatic brain injury and amnesia for the event? *J. Neuropsychiatry Clin. Neurosci.* 9, 18–22.

Weinstock, M., Matlina, E., Maor, G. I., Rosen, H., and Mcewen, B. S. (1992). Prenatal stress selectively alters the reactivity of the hypothalamic-pituitary adrenal system in the female rat. *Brain Res.* 595, 195–200.

Woon, F. L., Sood, S., and Hedges, D. W. (2010). Hippocampal volume deficits associated with exposure to psychological trauma and posttraumatic stress disorder in adults: a meta-analysis. *Prog. Neuropsychopharmacol. Biol. Psychiatry* 34, 1181–1188.

Yehuda, R. (2006). Advances in understanding neuroendocrine alterations in PTSD and their therapeutic implications. *Ann. N. Y. Acad. Sci.* 1071, 137–166.

Yehuda, R., and LeDoux, J. (2007). Response variation following trauma: a translational neuroscience approach to understanding PTSD. *Neuron* 56, 19–32.

Yu, I. T., Lee, S. H., Lee, Y. S., and Son, H. (2004). Differential effects of corticosterone and dexamethasone on hippocampal neurogenesis in vitro. *Biochem. Biophys. Res. Commun.* 317, 484–490.

Conflict of Interest Statement: The authors declare that the research was conducted in the absence of any commercial or financial relationships that could be construed as a potential conflict of interest.

Received: 11 December 2010; accepted: 19 February 2011; published online: 07 March 2011.

Citation: Kwon S-KC, Kovesdi E, Gyorgy AB, Wingo D, Kamnaksh A, Walker J, Long JB and Agoston DV (2011) Stress and traumatic brain injury: a behavioral, proteomics, and histological study. Front. Neur. ***2****:12. doi: 10.3389/fneur.2011.00012*

This article was submitted to Frontiers in Neurotrauma, a specialty of Frontiers in Neurology.

APPENDIX

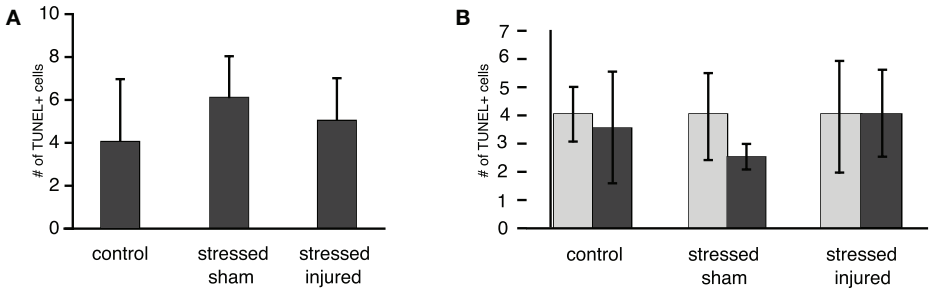

FIGURE A1 | TUNEL-positive cells in selected brain regions of animals in the various experimental groups. Frozen coronal sections containing the **(A)** PFC and **(B)** DG of the DHC and VHC of C, SS, and SI rats were counted and expressed as positive cells per unit area ± SEM. $*p < 0.05$ and $**p < 0.01$ compared to C rats.

frontiers in
NEUROSCIENCE

ORIGINAL RESEARCH ARTICLE
published: 01 April 2011
doi: 10.3389/fnins.2011.00042

The effect of enriched environment on the outcome of traumatic brain injury; a behavioral, proteomics, and histological study

Erzsebet Kovesdi[1], Andrea B. Gyorgy[2], Sook-Kyung C. Kwon[2], Daniel L. Wingo[2], Alaa Kamnaksh[2], Joseph B. Long[3], Christine E. Kasper[1] and Denes V. Agoston[2]*

[1] *U.S. Department of Veterans Affairs, Veterans Affairs Central Office, Washington, DC, USA*
[2] *Department of Anatomy, Physiology and Genetics, School of Medicine, Uniformed Services University, Bethesda, MD, USA*
[3] *Division of Military Casualty Research, Walter Reed Army Institute of Research, Silver Spring, MD, USA*

Edited by:
Gerd Kempermann, Center for Regenerative Therapies, Germany

Reviewed by:
Brian R. Christie, University of British Columbia, Canada
Dong Sun, Virginia Commonwealth University, USA

****Correspondence:***
Denes V. Agoston, Department of Anatomy, Physiology and Genetics, School of Medicine, Uniformed Services University, 4301 Jones Bridge Road, Bethesda, MD 20814, USA.
e-mail: vagoston@usuhs.edu

De novo hippocampal neurogenesis contributes to functional recovery following traumatic brain injury (TBI). Enriched environment (EEN) can improve the outcome of TBI by positively affecting neurogenesis. Blast induced traumatic brain injury (bTBI) characterized by memory impairment and increased anxiety levels, is a leading cause of chronic disability among soldiers. Using a rodent model of bTBI we asked: (a) whether long-term exposure to EEN after injury can ameliorate behavioral abnormalities and (b) what the effects of EEN are at the molecular and cellular levels and on *de novo* neurogenesis. We found that housing injured animals in EEN resulted in significantly improved spatial memory while animals in normal housing (NH) showed persistent memory impairment. VEGF and Tau protein but not Interleukin-6 (IL-6) levels were normalized in the dorsal hippocampus (DHC) of EEN rats while all three markers remained elevated in NH rats. Interestingly, after peaking at 6 weeks post-injury, anxiety returned to normal levels at 2 months independent of housing conditions. Housing animals in EEN had no significant effect on VEGF and Tau protein levels in the ventral hippocampus (VHC) and the amygdala (AD). We also found that EEN reduced IL-6 and IFNγ levels in the VHC; these markers remained elevated following NH. We observed an increase in GFAP and DCX immunoreactivities in the VHC of NH animals at 2 months post-injury. Conversely, injured animals housed in EEN showed no increase in GFAP or DCX immunoreactivity in their VHC. In summary, long-term exposure of injured animals to EEN appears to play a positive role in the restoration of memory functions but not on anxiety, which returned to normal levels after a significant period of time. Cellular and molecular changes in response to EEN appear to be a part of neurogenesis-independent as well as dependent recovery processes triggered by bTBI.

Keywords: neurogenesis, enriched environment, traumatic brain injury, memory, anxiety, hippocampus, histology, proteomics

INTRODUCTION

Traumatic brain injury (TBI) is one of the leading causes of chronic disability worldwide (Bruns and Hauser, 2003; Tagliaferri et al., 2006). The main neurobehavioral symptoms of survivable TBI include memory problems, increased anxiety, and depression (Gentilini et al., 1985; Schoenhuber and Gentilini, 1988; Ponsford et al., 1995). Blast induced traumatic brain injury (bTBI) caused by explosive devices has become a signature injury of the recent conflicts in Iraq and in Afghanistan (Warden and French, 2005; Taber et al., 2006; Warden, 2006). Although bTBI shares some of the clinical features of the closed head and the penetrating TBI models, bTBI appears to be a different form of neurotrauma (Ling et al., 2009). The secondary injury process after either form of TBI includes metabolic changes, hypoxia, edema, neuroinflammation, and gliosis (Kaur et al., 1997; Mayorga, 1997; Cernak et al., 2001; Taber et al., 2006). As epidemiological and experimental data show, even moderate and mild forms of bTBI can cause long-term behavioral changes (Ryan and Warden, 2003; Okie, 2005; Cernak et al., 2010). The observed changes include impaired memory and increased anxiety, implicating damage to the hippocampus (HC) and the prefrontal cortex (PFC).

Exposure to severe blast causes vascular, neuronal, and glial damage that results in cerebral edema, vasospasm, and the loss of fiber tracts (Kaur et al., 1997; Mayorga, 1997; Cernak et al., 2001; Taber et al., 2006). Moderate and mild blast result in gliosis and neuroinflammation characterized by elevated levels of proinflammatory molecules like Interleukin-6 (IL-6; Vallieres et al., 2002; Kwon et al., 2011). Inflammation can cause neuronal cell death as well as increase vulnerability to noxious factors like neurotoxins (Cacci et al., 2005; Agoston et al., 2009). IL-6 is also a potent inhibitor of hippocampal *de novo* neurogenesis (Vallieres et al., 2002; Barkho et al., 2006).

Intact *de novo* hippocampal neurogenesis in the adult brain has been shown to play an important role in maintaining normal neurobehavioral functions (Kempermann, 2002b; Kempermann and Kronenberg, 2003; Kempermann et al., 2004; Sahay and Hen, 2007; Aimone et al., 2010; Deng et al., 2010). Neurogenesis is

a part of the innate regenerative processes triggered by various insults to the brain including TBI (Dash et al., 2001; Hallbergson et al., 2003; Parent, 2003). Following TBI, the rate of *de novo* neurogenesis is substantially upregulated (Dash et al., 2001; Chirumamilla et al., 2002; Lee and Agoston, 2009), which contributes to the amelioration of the neurobehavioral consequences of TBI (Sun et al., 2007). Neurogenesis is a complex process that is not restricted to the proliferation of neural stem (progenitor) cells; it includes neuronal fate determination, differentiation of immature neurons, migration, survival, and functional integration into neuronal circuits (Kempermann, 2002a; Kozorovitskiy and Gould, 2003; Abrous et al., 2005; Hagg, 2005; Ming and Song, 2005; Zhao et al., 2008).

Previous studies indicated that socially and physically enriched environments (EEN) can significantly improve working memory, especially spatial learning along with other beneficial neurobehavioral effects (Kempermann et al., 1997; Pham et al., 1999; Van Praag et al., 2000; Dhanushkodi et al., 2007). The positive effects of EEN have been described in young intact animals (Tees et al., 1990) after various forms of brain lesions (Einon et al., 1980; Whishaw et al., 1984) like TBI, spinal cord injury (Berrocal et al., 2007; Fischer and Peduzzi, 2007; Kline et al., 2007; Hoffman et al., 2008), and ischemia (Johansson and Ohlsson, 1996; Dahlqvist et al., 2004; Buchhold et al., 2007; Briones et al., 2009). Kempermann et al. (1997) found that mice housed in EEN had more new granule cells in the dentate gyrus than control mice. The combination of physical and social interactions in EEN enhances hippocampal neurogenesis, synaptic efficacy, learning, and memory functions (Van Praag et al., 2000; Cao et al., 2004; Tashiro et al., 2007; Wright and Conrad, 2008). Therefore, the demonstrated benefits of EEN may offer an easily implementable "treatment" option to improve neurobehavior following brain insults.

In this study, we aimed to identify the effect of EEN on behavioral outcome as well as cellular and molecular alterations ensuing bTBI. The observed cellular and molecular changes suggest that recovery after bTBI involves complex processes like *de novo* neurogenesis and that EEN may modulate the temporal characteristics of these processes.

MATERIALS AND METHODS

ANIMALS AND HOUSING CONDITIONS

Sprague-Dawley male rats (245–265 g, n = 23; Charles River Laboratories, Wilmington, MA, USA) were housed in cages with free access to food and water in a reverse 12–12 h light-dark cycle. After 7 days of acclimation and handling, animals were exposed to a single blast (or sham) injury and then placed into the separate housing conditions until the end of the study. The experimental schedule is depicted in **Figure 1**. All animals were handled according to protocol approved by the Institutional Animal Care and Use Committee (IACUC) at the Uniformed Services University of the Health Sciences (USUHS). All behavioral tests were performed during animals' dark cycle.

INJURY

On the day of the injury all rats (injury weight: ~300 g) were transferred to Walter Reed Army Institute of Research (Silver Spring, MD, USA) where blast was generated using a compression-driven shock tube (Long et al., 2009). Before the induction of injury, rats were anesthetized in a bell jar for 6 min with 4% isoflurane (Forane, Baxter Healthcare Corporation, Deerfield, IL, USA). Anesthetized rats in chest protection were then placed in a holder in a transverse prone position and exposed to whole body blast injury at 20.63 psi pressure. Immediately after injury rats were moved back to their home cages and transported back to the USUHS animal facility. Sham-injured animals underwent the same procedure without being exposed to blast overpressure.

HOUSING CONDITIONS AFTER INJURY

Following bTBI (n = 15) or sham injury (n = 8), rats were assigned to the following groups: normal housed-injured (NH-I; n = 8), normal housed-sham (NH-S; n = 8), and enriched environment-injured (EEN-I; n = 7). Rats under NH conditions were housed on hardwood chip bedding without any toys, two rats/standard rat cage. Rats under EEN conditions were housed in a four level metal cage (dimensions: 36″L × 25″W × 62 1/2″H; MIDWEST Ferret Nation Double Unit Home with Stand, PetSmart) that contained different kinds of toys like activity wheels, tunnels, balls, and rodent igloos (**Figure A1** in Appendix). Toys (PetSmart) were replaced with new ones weekly.

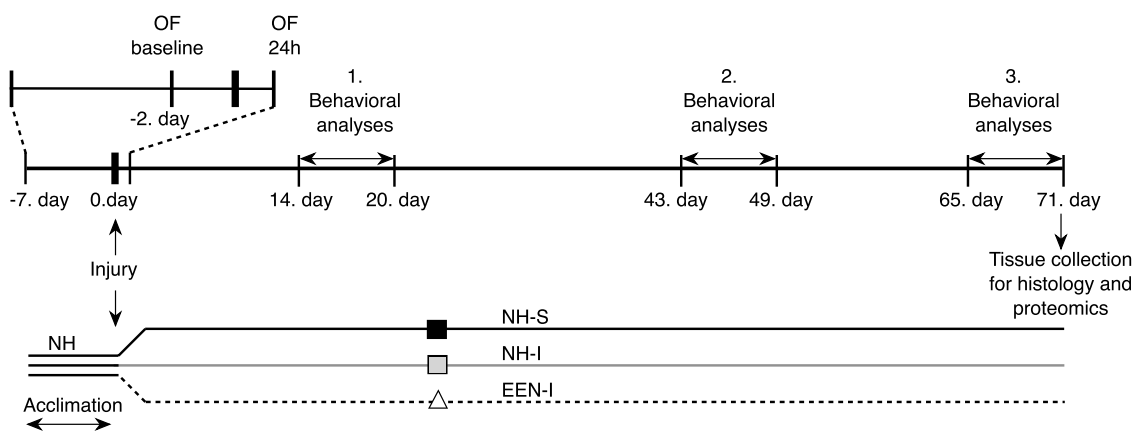

FIGURE 1 | Outline of the experimental schedule.

BEHAVIORAL TESTS

All rats underwent a series of behavioral evaluations; basic motor function and anxiety were measured by elevated plus maze (EPM), and spatial learning and memory by Barnes maze (BM). Behavioral assessments were performed on separate days starting at 15, 44, and 66 days after injury (**Figure 1**).

Elevated plus maze

The EPM is a widely used, ethologically relevant test that assesses anxiety states in rodents (Carobrez and Bertoglio, 2005; Salzberg et al., 2007; Walf and Frye, 2007). The maze is an elevated structure (1 m above ground) consisting of four intersecting arms. The arms of the maze are 50 cm long and 10 cm wide; the closed arms have walls on three sides that are 40 cm high while the open arms have none. The lighting in the middle of the maze was set at 90 lux. On testing days rats were placed one by one in the center of the maze facing one of the open arms; each animal was allowed to explore freely for 5 min while its movement was video-tracked. Total distance traveled (meters) was used to measure changes in basic motor function. Time spent in the closed and open arms (seconds) was used to measure anxiety levels. All data from the maze were recorded using ANY-maze 4.2 Software (Stoelting Company, Wood Dale, IL, USA). The maze was cleaned with a 30% ethanol solution between each rat.

Barnes maze

Barnes maze represents an approved and less stressful alternative to the commonly used water maze test (Barnes, 1979; Maegele et al., 2005; Doll et al., 2009; Harrison et al., 2009). The maze is a circular platform (1.2 m in diameter) with 18 evenly spaced holes around the periphery. One of the holes is the entrance to a darkened escape box that is not visible from the surface of the board. Each rat was tested twice per day for five consecutive days to find the escape box (only day 1 of the first BM session had three trials). In each trial latency to locate and enter the escape box was measured (ANY-maze 4.2 Software, Stoelting Company, Wood Dale, IL, USA). During the first (teaching) trial of the first BM session, animals were trained to locate the escape chamber. Each animal was placed in the escape box and covered for 30 s; the escape box was then removed with the animal inside and moved to the center of the maze. The rat was removed from the box and allowed to explore the maze for a few seconds, after which the rat was returned to its home cage. No latency times were recorded for the teaching trials. The escape box and the maze were cleaned with a 30% ethanol solution between each trial. In the second trial the same rat was placed under a start box in the center of the maze for 30 s; the start box was then removed and the rat was allowed to explore freely to find the escape chamber. Training sessions ended after the animal had entered the escape box or when a pre-determined time (240 s) had elapsed. If the animal had not found the escape box during the given time period, it was placed in the escape box for 1 min at the end of the trial.

TISSUE COLLECTION AND PROCESSING

At the conclusion of the last behavioral testing session (day 71 post-blast or sham injury), animals were placed inside an induction chamber saturated with isoflurane and deeply anesthetized. For proteomics and ELISA assays (NH-S: $n = 5$; NH-I: $n = 5$; and EEN-I: $n = 4$), rats were decapitated and brains were immediately removed and placed on ice. The amygdala (AD), PFC, dorsal (DHC), and ventral hippocampus (VHC) were dissected, frozen, and stored at −80°C. For histology (NH-S: $n = 3$; NH-I: $n = 3$; and EEN-I: $n = 3$), rats were placed under deep isoflurane anesthesia and transcardially perfused with cold phosphate-buffered saline (PBS) followed by 4% paraformaldehyde solution. Fixed brains were then immersed in cold 15 and 30% sucrose in 1 × PBS (consecutively) for cryoprotection. Frozen brains were sectioned coronally at a 40-μm thickness using a cryostat (Cryocut 1800; Leica Microsystems, Bannockburn, IL, USA) and sections containing the DHC and the VHC were kept at −80°C until use.

PROTEOMICS

Preparation of samples

Sample preparation, printing, scanning, and data analysis were performed as described in detail (Gyorgy et al., 2010). Briefly, flash frozen brain samples were pulverized in liquid nitrogen; 200 mg of the powder was transferred into 1 ml of T-per lysis buffer (Thermo Fisher, Waltham, MA, USA) with protease and phosphatase inhibitors (Thermo Fisher) and then sonicated. Samples were centrifuged for 15 min at 4°C and the supernatants were aliquoted and stored at −80°C. Tissue samples were diluted in print buffer (10% glycerol, 0.05% SDS, 50 mM DTT in 1 × TBS) to a final protein concentration of 1 mg/ml. Samples were then subjected to an 11-point serial 1:2 dilution and transferred into Genetix 384-well plates (X7022, Fisher Scientific, Pittsburg, PA, USA) using a JANUS Varispan Integrator and Expanded Platform Workstation (PerkinElmer, Waltham, MA, USA). Plates were transferred into an Aushon 2470 Arrayer (Aushon Biosytems, Billerica, MA, USA) to be printed on ONCYTE Avid (tissue samples) or ONCYTE Nova (serum samples) single-pad nitrocellulose coated glass slides (Grace Bio-Labs, Bend, OR, USA).

Printing parameters

The Aushon Arrayer was programmed to use 16 pins (4 × 4 pattern). Each sample was printed in 12 dilutions (12 rows) and in triplicate (3 columns), resulting in a block of 3 × 12 dots per sample. The Spot Diameter was set to 250 nm with a spacing of 500 nm between dots on the *x*-axis and 375 nm on the *y*-axis. Wash time was set at 2 s without delays. The printer was programmed for a single deposition per dot for printing serum and tissue extracts.

Immunochemical detection

Primary antibodies were diluted to 10× the optimal Western analysis concentration in antibody incubation buffer [0.1% bovine serum albumin (BSA), protease inhibitors (EDTA-free Halt protease and phosphatase inhibitor cocktail, Thermo Fisher, Waltham, MA, USA), 1 × TBS, 0.5%Tween 20]. Primary antibodies were used in the following dilutions for reverse phase protein microarray (RPPA): VEGF 1:100 (Abcam ab-53465) and Tau protein 1:20 (Santa Cruz sc-1995). The primary antibody solution was incubated overnight at 4°C with a cover slip (Nunc® mSeries LifterSlips, Fisher Scientific, Pittsburg, PA, USA). The following day slides were washed and then incubated with an Alexa Fluor® 635 goat anti-mouse (Cat# A-31574), goat anti-rabbit (Cat# A-31576), or rabbit anti-goat IgG (H + L; Cat# A-21086) secondary antibodies from Invitrogen at 1:6000 dilution

in antibody incubation buffer for 1 h at room temperature (RT). After washing and drying, the fluorescent signals were measured by a Scan Array Express HT microarray scanner (Perkin Elmer, Waltham, MA, USA) using a 633-nm wavelength laser and a 647-nm filter; data were imported into a bioinformatics program.

Data analysis and bioinformatics

Data from the scanned images were imported into a Microsoft Excel-based bioinformatics program developed in house for analysis (Gyorgy et al., 2010). The tool calculates total net intensity after local background subtraction for each spot. The intensity data from the dilution series of each sample were then plotted against dilution on a log–log graph. The linear regression of the log–log data was calculated after the removal of flagged data, which include signal to noise ratios of less than 2, spot intensities in the saturation range or noise range, or high variability between duplicate spots (>10–15%). The total amount of antigen is determined by the *Y*-axis intercept (Gyorgy et al., 2010).

INTERLEUKIN-6 AND INTERFERON GAMMA ELISA

Interferon gamma (IFNγ) and IL-6 levels were measured from brain tissues using the Rat IFNγ ELISA and the Rat IL-6 ELISA kits (both are from Thermo Fisher, Waltham, MA, USA). The IL-6 ELISA kit required a 1:5 dilution using the supplied dilution buffer in order to avoid saturation in the wells. After the dilution of brain samples, the assay was performed according to the manufacturer's instructions.

HISTOLOGY

Immunohistochemistry

Sections from the PFC, DHC, and VHC were identified based on *z*-axis and morphology as described in the Chemoerchitectonic Atlas of The Rat Forebrain (Paxinos et al., 1999). The 1st and 10th sections were mounted on positively charged glass slides two sections per slide. Three slides per animal were selected per brain region for each immunostaining. Sections were equilibrated at RT and hydrated with 1 × PBS for 30 min. Antigen retrieval was performed by incubating in 10 mM citrate buffer (pH 6.0) at 80°C for 30 min followed by cooling down to RT. After rehydration with 1 × PBS, sections were permeabilized with 0.5% Triton X-100 in PBS for 1 h and blocked in 1 × PBS containing 5% normal goat serum (NGS), 5% BSA, 0.1% Sodium Azide, and 0.5% Triton X-100 for 1 h. The same solution used for blocking, with the exception of NGS, was used to dilute the primary antibodies. Primary antibodies include mouse anti-GFAP (Millipore, Temecula, CA, USA) and rabbit anti-Doublecortin (DCX; Cell Signaling Technology, Beverly, MA, USA). Sections were incubated with the primary antibodies overnight at 4°C. After washing with 1 × PBS, secondary antibody (Alexa Fluor 555 goat anti-mouse IgG or 488 goat anti-rabbit IgG was applied for 1 h at RT; 1 μg/ml of Hoechst 33342 (Molecular Probes, Eugene, OR, USA) was applied for 2 min for nuclear counterstaining and sections were coverslipped with anti-fading media (Vectashield, Vector Laboratories, Burlingame, CA, USA). Histological sections were visualized in an Olympus IX-71 microscope and images were collected using a SPOT digital camera (Diagnostic Instruments Inc., Sterling Heights, MI, USA). Immunofluorescent staining was acquired using the appropriate filters. The collected images were colored using TIFFany3rr Software.

STATISTICAL ANALYSIS

Statistical analysis was performed using Graph Pad Instat software. Behavioral test results were analyzed with ANOVA and Tukey *post hoc* tests. Differences were considered significant with a p value of 0.05. Proteomics data results were followed up with a one-way ANOVA (Gyorgy et al., 2010; Kwon et al., 2011) a significance level of 0.05 was used throughout. No adjustment was made for multiple comparisons, thus, significant findings should be considered exploratory and in need of confirmation by further studies. IL-6 and IFNγ ELISA results were analyzed with Student t-test. Data are reported as the average ± SE of the mean. For each of our numerical measurements, we determined statistical significance among experimental groups by ($p < 0.05$ depicted by one star; and $p < 0.01$ by two).

RESULTS

BEHAVIORAL CHANGES

Anxiety

We found that general locomotion decreased over the period of 2 months in all experimental groups. Animals traveled less distances on day 66 post-injury (or sham) than day 15 at the beginning of the behavioral tests (**Figure 2A**). Among all experimental groups, NH-I animals traveled the least at all time points measured, however the values were only statistically significant at day 44 post-injury. EEN-I rats traveled greater distances than NH-I animals but the difference was not statistically significant.

At 15 days post-injury, injured animals (regardless of housing) spent less time in the open arms and more time in the closed arms of the EPM compared to NH-S animals; the differences were statistically insignificant (**Figures 2B,C**). The difference in anxiety levels of NH-S and injured animals was the greatest at 44 days post-injury; animals in both EEN-I and NH-I groups spent substantially more time in the open arms and less time in the closed arms compared to the non-injured controls (**Figures 2B,C**).

At 66 days post-injury there were no significant differences among the experimental groups. All animals spent roughly the same amount of time in the closed arms as well as in the open arms of the maze independent of housing conditions or injury (**Figures 2A–C**).

Spatial learning and memory

The first testing session was performed between days 16 and 20 post-injury or sham. We found that NH-I animals had significant difficulty in learning the task on the first day of BM compared to animals in the NH-S or EEN-I groups (**Figure 3A**). Rats in the EEN-I and NH-S groups performed similarly and significantly better than NH-I rats.

The second BM session was performed between days 45 and 49 post-injury (or sham). Again, EEN-I rats performed similar to NH-S rats on every day of the testing period (**Figure 3B**). In contrast, rats in the NH-I group required more time to find the escape box every day of the testing session, however the difference was statistically insignificant.

The last BM testing session was performed between days 67 and 71 post-injury. The performance of EEN-I animals was practically identical to NH-S animals (**Figure 3C**). NH-I animals required significantly longer times to locate the escape box on days 67, 68,

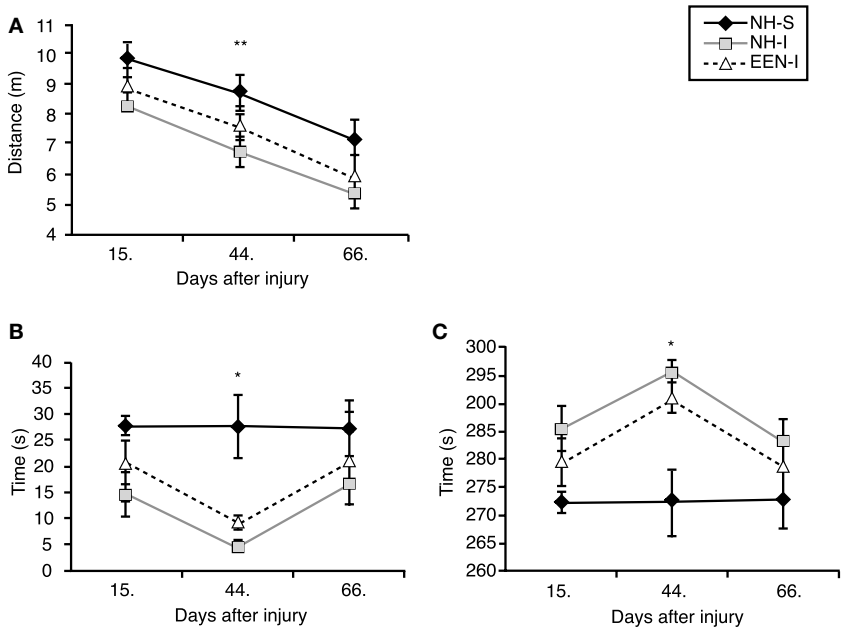

FIGURE 2 | Anxiety and basic motor function of animals in the various experimental groups. Elevated plus maze was used to measure changes in basic motor function and anxiety levels. Total distance traveled (meter) **(A)**, duration of time spent (seconds) in open arms **(B)** and duration of time spent (second) in closed arms **(C)** were measured at 15, 44, and 66 days after mbTBI. Housing rats in EEN after mbTBI mildly improved motor function and reduced anxiety. $*p < 0.05$ and $**p < 0.01$ for NH-I versus NH-S. Data are presented as mean ± SEM. (NH-I, normal housed-injured; NH-S, normal housed-sham; EEN-I, enriched environment-injured).

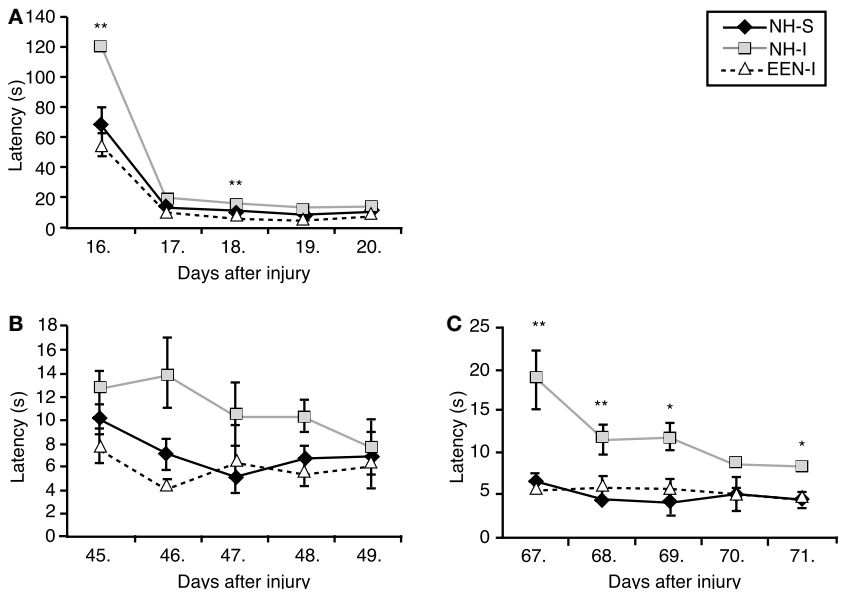

FIGURE 3 | Spatial learning and memory of animals in the various experimental groups. Barnes maze was used to determine spatial learning and memory performance. Latency times (second) to find the escape box were measured on days 16–20 **(A)**, days 45–49 **(B)**, and days 67–71 **(C)** after mbTBI. Housing rats in EEN after mbTBI significantly improved spatial memory. $*p < 0.05$ and $**p < 0.01$ for NH-I versus NH-S. Data are presented as mean ± SEM. (NH-I, normal housed-injured; NH-S, normal housed-sham; EEN-I, enriched environment-injured).

69, and 71 post-injury. Interestingly, the behavior of NH-I animals in the last BM session was similar to the one measured during the first testing session. On the first day of BM, NH-I animals required the longest period of time to find the escape box.

PROTEIN CHANGES

At the end of the last behavioral session, we analyzed changes in the expression of selected proteins in the AD, PFC, DHC, and VHC of animals in the various experimental groups using RPPA. NH-I

animals had significantly elevated levels of Tau protein, a marker of axonal degeneration, in all brain regions compared to levels detected in the NH-S group (**Figure 4**). Importantly, housing injured animals in EEN resulted in a significant decrease in Tau levels in the DHC compared to those measured in the DHC of NH-S animals; no such decrease was detected in the DHC of NH-I animals. A similar decrease in Tau levels was observed in the PFC of EEN-I animals; no such effect of EEN was seen in the VHC or the AD.

Housing animals in EEN after injury had a similar effect on VEGF levels. EEN-I animals had decreased VEGF levels in the DHC but not in the VHC. In NH-I animals, VEGF levels increased in both the DHC and the VHC, but not in the AD or the PFC (**Figure 4**). Importantly, neither injury nor housing conditions had any significant effect on VEGF levels in the AD or the PFC (**Figure 4**).

To assess the potential inflammatory response to injury and housing conditions, we measured IL-6 and IFNγ, molecules associated with neuroinflammation in the same brain regions. Injury increased IL-6 concentrations in all brain regions except in the PFC of NH-I animals (**Figure 4**). Interestingly, housing injured animals in EEN restored IL-6 levels to NH-S levels in the VHC but not in the DHC. A similar trend was seen in the AD but the differences between EEN-I and NH-S animals were not statistically significant. Importantly, housing conditions had no effect on IL-6 values in the DHC; IL-6 remained elevated regardless of post-injury housing conditions compared to values measured in NH-S animals.

Injury had a similar effect on IFNγ levels; we measured elevated values in all brain regions except in the PFC (**Figure 4**). Interestingly, housing animals in EEN after injury restored IFNγ to control levels not only in the VHC and the AD, but also in the DHC.

CELLULAR CHANGES

Astrogliosis

We analyzed the DHC and the VHC at 71 days post-injury for GFAP expression to identify some of the cellular responses to injury and the effects of EEN. We found increased GFAP immunoreactivity in the VHC of NH-I animals compared to NH-S (**Figures 5A–F**). GFAP immunoreactive cells were located in the hilus of the VHC but many GFAP positive cells were also present in the dentate gyrus; these cells resembled reactive astrocytes with a stellar appearance and elaborate processes. Importantly, housing animals in EEN resulted in GFAP immunoreactivity similar to that of the DHC of NH-S animals, suggesting that EEN may mitigate the effect of injury on GFAP immunoreactivity.

Neurogenesis

To identify the potential effects of injury and EEN on *de novo* neurogenesis, we analyzed the DHC and the VHC for DCX immunoreactivity. We found similar DCX immunoreactivity in the DHC and the VHC of NH-S animals (**Figures 6A,D**). We also found an apparent increase in DCX immunoreactivity in the VHC of NH-I animals (**Figure 6F**). Many of these DCX immunoreactive cells displayed elaborate, branching processes (**Figure 6C**, insert). Interestingly, we observed the lowest DCX immunoreactivity in the DHC and the VHC of EEN-I animals. Conversely, the highest DCX immunoreactivity was in the DHC and the VHC of NH-I animals (compare **Figures 6A–F**).

DISCUSSION

Our study shows that the normalization of anxiety in a rodent model of bTBI can take more than 2 months after the insult, the process is independent of housing conditions and most likely

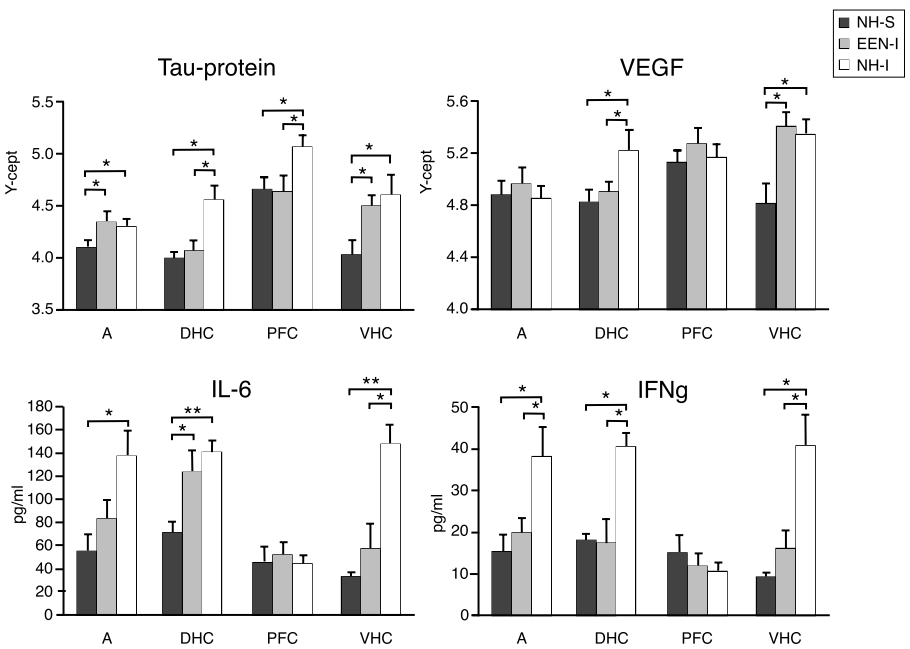

FIGURE 4 | Protein markers in the AD, PFC, DHC, and the VHC of animals in the various experimental groups. Tissue extracts were prepared from dissected brain regions of NH-S, NH-I, and EEN-I rats. Tissue levels of selected protein markers were assayed using either RPPM or ELISA. The *Y*-axis intercept (*Y*-cept) and pg/ml (IL-6 and IFNγ) indicate measured protein levels. $*p < 0.05$ and $**p < 0.01$; data are presented as mean ± SEM. (NH-I, normal housed-injured; NH-S, normal housed-sham; EEN-I, enriched environment-injured).

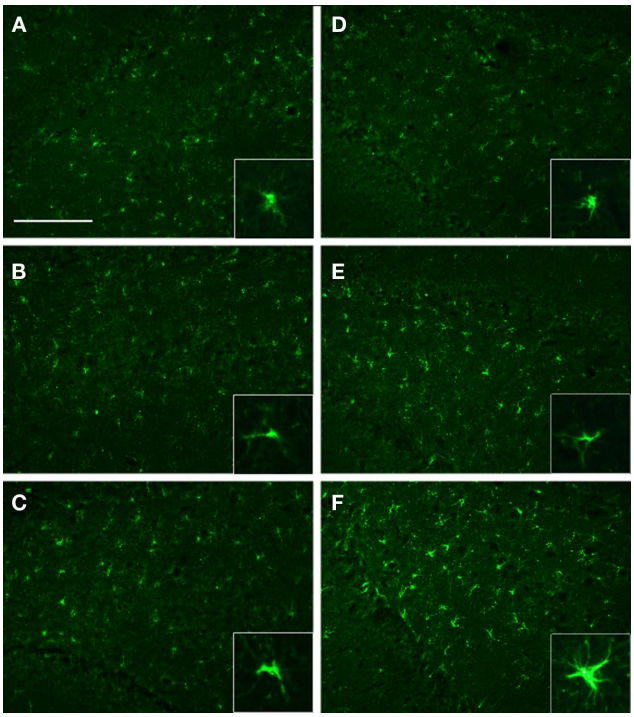

FIGURE 5 | GFAP immunoreactivity in selected brain regions of animals in the various experimental groups. Frozen coronal sections containing the DHC and the VHC were cut and processed for immunohistochemistry using a GFAP antibody. DHC of NH-S **(A)**, NH-I **(B)**, and EEN-I **(C)** rats; VHC of NH-S **(D)**, NH-I **(E)**, and EEN-I **(F)** rats. Inlays magnify GFAP morphology. Scale bar **(A–F)** = 100 μm.

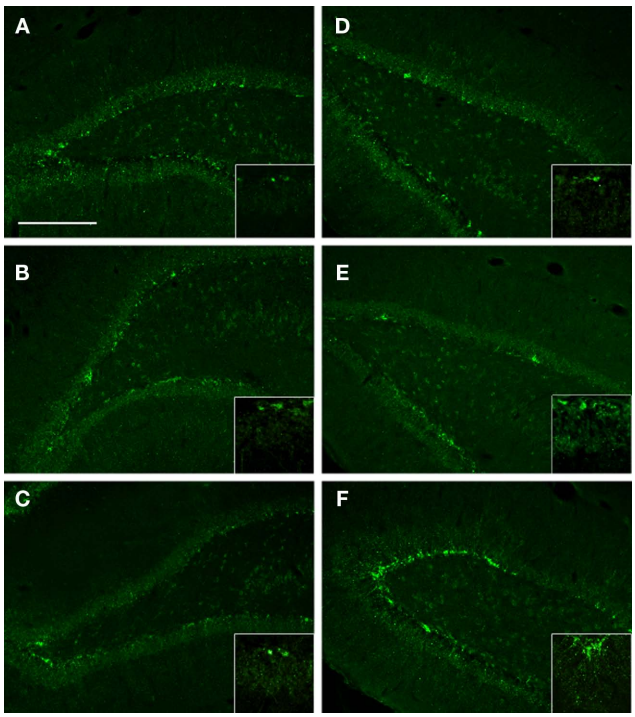

FIGURE 6 |The DCX immunoreactivity in selected brain regions of animals in the various experimental groups. Frozen coronal sections containing the DHC and the VHC were cut and processed for immunohistochemistry using a DCX antibody. DHC of **(A)** NH-S, **(B)** NH-I, and **(C)** EEN-I rats; VHC of **(D)** NH-S, **(E)** NH-I, and **(F)** EEN-I rats. Inlays magnify DCX cell body and process. Scale bar (A–F) = 200 μm.

involves *de novo* neurogenesis. We found that anxiety was high at 15 days and further increased at 44 days post-injury. Importantly, at 66 days the anxiety of animals was rather similar irrespective of housing conditions or injury. To our knowledge, our study is one of the very few that conducted behavioral assessments at various time points after injury over a 2-month period of time. Two months in rodent life roughly translates into a multi-year period of time for humans (Quinn, 2005). Thus, our findings may have implications for conducting longitudinal human clinical studies.

Our work also implicates studies that only measure the short-term effects of TBI in that they may not be able to provide insight into the full effect of the insult and/or the various treatments tested. Therefore, our findings underline the importance of monitoring behavior at several time points post-injury in the same sets of animals. There are very few studies that examine neurobehavior following TBI for longer than 2 weeks and even less that assess behavior at several time points post-injury. A recent study (Liu et al., 2010b) using the lateral fluid percussion injury model in rats monitored behavior and performed *in vivo* imaging at 1, 3, and 6 months after injury. The study showed that a single insult is capable of triggering behavioral and morphological changes that evolve over several months. Using the same blast overpressure TBI model in an independent study, we found that anxiety increased within the first 2 days after injury, reached a maximum at 1 month, and returned to normal levels at 2 months after bTBI (Kwon et al., 2011). This illustrates that the pathophysiology as well as the recovery process after bTBI changes significantly over a longer period of time than previously thought.

Our findings indicate that increased anxiety resulting from bTBI should dissipate over time. However, epidemiological studies demonstrate that some individuals develop a chronic condition (Woon et al., 2010) with symptoms similar to post-traumatic stress disorder (PTSD; Gross and Hen, 2004; Yehuda and Ledoux, 2007). Previous studies have shown that hippocampal abnormalities can play a role in individuals' vulnerability to the long-term effects of stress. According to human imaging studies, reduced hippocampal volume increases pathologic vulnerability to psychological trauma and the development of PTSD (Tischler et al., 2006). An *in vivo* imaging study indicates that CA3/DG volume is significantly reduced in veterans with combat-related PTSD (Wang et al., 2010). The abovementioned long-term animal study also showed significant morphological changes in the HC 6 months after injury (Liu et al., 2010a). Neuroanatomical substrates mediating anxiety include the HC in addition to the medial PFC and the AD (Bremner, 2007; Liberzon and Sripada, 2008); anxiety possesses neurogenesis dependent and independent components (Sahay and Hen, 2007).

While the VHC is predominantly involved in mediating anxiety-related functions, the DHC mediates learning and memory (Henke, 1990; Moser et al., 1995). As opposed to the housing-independent normalization of anxiety levels, the recovery of

spatial memory after bTBI was clearly EEN dependent. The conception of EEN comes from Hebb's (1947, 1949) research ; EEN is an experimental model that provides multiple possibilities for physical and social interactions (Rosenzweig and Bennett, 1996; Van Praag et al., 2000; Puurunen and Sivenius, 2002; Mora et al., 2007). In EEN, rats are usually housed in big multi-level cages containing a variety of toys, which are changed daily to provide opportunities for sensory and physical interaction (Van Praag et al., 2000). The average rat number in EEN is 8–12 rats per cage for social interaction purposes. EENs impart various learning experiences to animals such as motor learning through the exploration of new toys or objects in the cage, and spatial learning as they learn the place of water bottles, food, and toys. In addition to other social learning mechanisms as the rats interact with each other. EEN improved motor performance on a beam-walk task in adult rats after sensorimotor cortex lesions (Held et al., 1985; Gentile et al., 1987; Rose et al., 1987). Rats housed in larger EEN cages demonstrated better recovery of motor function than standard housed rats (Johansson, 1996), largely due to the space available for exploration and other activities. EEN improved spatial learning in a water maze task after moderate (Hamm et al., 1996) and severe fluid percussion brain injury (Passineau et al., 2001). EEN housing also enhanced cell genesis and microglia proliferation in adult murine neocortices (Ehninger and Kempermann, 2003).

Interestingly, the learning ability of EEN-I rats was significantly better than NH-I rats after 2 weeks only; day 16 was the first day of BM and rats had no pre-training before bTBI. Moreover, the performance of EEN-I rats was slightly better than that of control rats (NH-S). The positive effect of EEN was observed throughout the entire length of the study. This early improvement in spatial memory performance suggests that the positive effect of EEN did not involve *de novo* neurogenesis but rather the mitigation of the pathological processes induced by bTBI. Housing animals in EEN results in other complex molecular, morphological, and functional changes in the brain; these include increased synaptic plasticity and neuronal survival (Will et al., 2004). EEN can also induce the expression of various trophic factors and mitigate neuroinflammation (Shum et al., 2007) in addition to increasing the number of synapses per neuron and dendritic branching in the HC (Juraska et al., 1985; Juraska and Kopcik, 1988).

Some of our proteomics and immunohistochemical findings are consistent with the conclusion that EEN can exert its positive effects in a neurogenesis-independent manner. In our experiment, EEN normalized tau protein levels in the DHC but not in the VHC. Tau protein is a microtubule-associated protein that is involved in microtubule assembly and stabilization and is predominantly present in neurons and axons (Wilhelmsen, 1999); damaged axons may be an important source of amyloid-beta (Aβ) and Tau proteins following TBI (Marklund et al., 2009). Tau can become toxic and in turn lead to neuronal cell death. Therefore, increased Tau is a pathological hallmark of many neurodegenerative disorders (Lasagna-Reeves et al., 2010). The normalization of Tau levels by EEN suggests that EEN has a positive effect on axonal damage, a hallmark of bTBI (Buki and Povlishock, 2006; Farkas and Povlishock, 2007). Axonal damage can then result in neuronal malfunction and increased neuronal cell death.

Enriched environment specifically normalized VEGF levels in the DHC but not in the VHC. VEGF is a signaling protein that promotes the development of new blood vessels (Neufeld et al., 1999), regulates vascular permeability (Kaur and Ling, 2008), is associated with areas of growth or healing (Krum and Khaibullina, 2003), and acts as a positive regulator of adult *de novo* hippocampal neurogenesis (Rosenstein and Krum, 2004; Yasuhara et al., 2004). VEGF is significantly upregulated by TBI (Jin et al., 2002; Lee and Agoston, 2009, 2010). We previously found that VEGF promotes survival in the injured brain by blocking apoptotic cell death of *de novo* hippocampal neurons rather than a proliferative factor (Lee and Agoston, 2009). Due to its complex role in *de novo* neurogenesis and in other aspects of the post-injury process, changes in VEGF levels in the DHC compared to the VHC are difficult to interpret without additional studies.

Independent of housing conditions, IL-6 levels remained elevated after injury in the DHC, but were significantly lowered in the VHC of EEN animals. We found that IFNγ was elevated in the NH-I group, but decreased to control levels in the EEN-I group. These inflammatory molecules can have direct or indirect effects like increased neurotoxicity (Minagar et al., 2002). IL-6 is also a potent inhibitor of hippocampal *de novo* neurogenesis (Vallieres et al., 2002). The role of inflammation, including the role of microglia in the post-injury recovery process is rather complex (Barron, 1995; Kempermann and Neumann, 2003). Thus, whether elevated IL-6 levels contribute to the suppression of *de novo* neurogenesis in the DHC after bTBI remains to be established.

Our histological data showed brain region specific changes in GFAP immunoreactivity. Interestingly, housing conditions had no effect on GFAP immunoreactivity in the DHC, the VHC, or the AD at 71 days post-injury. However, housing injured animals in EEN resulted in an apparent decrease of GFAP positive cells in the VHC. Increased numbers of reactive astrocytes and elevated GFAP expression are hallmarks of CNS neurotrauma (Ridet et al., 1997; Dihne et al., 2001; Kernie et al., 2001). The role of elevated GFAP immunoreactivity and the presence of stellar astroglia in CNS injury is rather complex. Astrocytic response can either reflect reparative or pathological processes depending on the time elapsed after injury (Eng and Ghirnikar, 1994; Mueller et al., 2005). There is evidence indicating a protective role of astrogliosis in reducing the toxic effects of extracellular glutamate and enabling barrier reconstruction (Buffo et al., 2010). Elevated GFAP immunoreactivity in the VHC of injured animals may reflect reparative mechanisms that may involve *de novo* neurogenesis for the restoration of anxiety levels (Alvarez-Buylla and Garcia-Verdugo, 2002).

The full maturation and functional integration of *de novo* granule cells requires ~6–8 weeks in the adult rodent brain (Kempermann et al., 2004). Newborn neurons, marked by DCX expression, migrate from the subgranular layer (SGL) to the granular cell layer (GCL) where many of the surviving neurons differentiate into granule cells (Altman and Das, 1965; Cameron et al., 1993). Some of the differentiated granule cells are then integrated into the existing hippocampal circuitry where they contribute to hippocampal function in the normal adult brain (Shors et al., 2001; Saxe et al., 2006). The rate of *de novo* hippocampal neurogenesis can be significantly upregulated by environmental conditions like EEN (Kempermann et al., 1997).

The DCX has been shown to be a specific, reliable marker that reflects adult neurogenesis levels and its modulation (Couillard-Despres et al., 2005). Importantly, the analysis of neurogenesis through the detection of DCX does not require *in vivo* labeling of proliferating cells. Even though it has been accepted that an increase in DCX+ cells indicate increased *de novo* hippocampal neurogenesis, DCX is only transiently expressed by *de novo* neurons (Kempermann and Gage, 2000; Kempermann, 2002a). Our finding that DCX immunoreactivity was elevated in the VHC of NH-I animals can be interpreted as increased *de novo* neurogenesis in NH-I animals compared to EEN-I animals. However, an alternative interpretation can be that in EEN animals the neurogenetic process already passed the DCX positive phase. Thus, a more detailed BrdU/Prox1 double immunohistochemical and stereological quantification of the histology results is required to determine changes in *de novo* neurogenesis after EEN and blast.

In summary, our data suggests that complex neurogenesis dependent and independent processes are involved in functional recovery after bTBI. EEN appears to have a positive and relatively fast-acting effect on the restoration of spatial memory after bTBI probably through a neurogenesis-independent process. In contrast, post-injury normalization of anxiety levels seems to be independent of EEN but likely involves *de novo* neurogenesis. The latter being much longer than previously thought and investigated. Additional histological and proteomics analyses at multiple post-injury time points as well as the use of additional markers (e.g., quantitative BrdU/Prox1 double label immunohistochemistry) would clarify the precise involvement of *de novo* neurogenesis in the various aspects of the regenerative process following bTBI.

ACKNOWLEDGMENTS

We thank the Neurotrauma Team (WRAIR) for their technical help during the blast exposures; Dr. David Jacobowitz (USU) for his help in brain micropunch dissections; Ms. Cara Olsen (USU) for her help in statistical analysis; Drs. Neil Grunberg and John Wu (USU) for their input in designing and interpreting the behavioral experiments. The work was supported by VA grant # B5044R.

REFERENCES

Abrous, D. N., Koehl, M., and Le Moal, M. (2005). Adult neurogenesis: from precursors to network and physiology. *Physiol. Rev.* 85, 523–569.

Agoston, D. V., Gyorgy, A., Eidelman, O., and Pollard, H. B. (2009). Proteomic biomarkers for blast neurotrauma: targeting cerebral edema, inflammation, and neuronal death cascades. *J. Neurotrauma* 26, 901–911.

Aimone, J. B., Deng, W., and Gage, F. H. (2010). Adult neurogenesis: integrating theories and separating functions. *Trends Cogn. Sci.* 14, 325–337.

Altman, J., and Das, G. D. (1965). Autoradiographic and histological evidence of postnatal hippocampal neurogenesis in rats. *J. Comp. Neurol.* 124, 319–335.

Alvarez-Buylla, A., and Garcia-Verdugo, J. M. (2002). Neurogenesis in adult subventricular zone. *J. Neurosci.* 22, 629–634.

Barkho, B. Z., Song, H., Aimone, J. B., Smrt, R. D., Kuwabara, T., Nakashima, K., Gage, F. H., and Zhao, X. (2006). Identification of astrocyte-expressed factors that modulate neural stem/progenitor cell differentiation. *Stem Cells Dev.* 15, 407–421.

Barnes, C. A. (1979). Memory deficits associated with senescence: a neurophysiological and behavioral study in the rat. *J. Comp. Physiol. Psychol.* 93, 74–104.

Barron, K. D. (1995). The microglial cell. A historical review. *J. Neurol. Sci.* 134(Suppl.), 57–68.

Berrocal, Y., Pearse, D. D., Singh, A., Andrade, C. M., Mcbroom, J. S., Puentes, R., and Eaton, M. J. (2007). Social and environmental enrichment improves sensory and motor recovery after severe contusive spinal cord injury in the rat. *J. Neurotrauma* 24, 1761–1772.

Bremner, J. D. (2007). Functional neuroimaging in post-traumatic stress disorder. *Expert Rev. Neurother.* 7, 393–405.

Briones, T. L., Rogozinska, M., and Woods, J. (2009). Environmental experience modulates ischemia-induced amyloidogenesis and enhances functional recovery. *J. Neurotrauma* 26, 613–625.

Bruns, J. Jr., and Hauser, W. A. (2003). The epidemiology of traumatic brain injury: a review. *Epilepsia* 44(Suppl.), 2.

Buchhold, B., Mogoanta, L., Suofu, Y., Hamm, A., Walker, L., Kessler, C., and Popa-Wagner, A. (2007). Environmental enrichment improves functional and neuropathological indices following stroke in young and aged rats. *Restor. Neurol. Neurosci.* 25, 467–484.

Buffo, A., Rolando, C., and Ceruti, S. (2010). Astrocytes in the damaged brain: molecular and cellular insights into their reactive response and healing potential. *Biochem. Pharmacol.* 79, 77–89.

Buki, A., and Povlishock, J. T. (2006). All roads lead to disconnection? – Traumatic axonal injury revisited. *Acta Neurochir. (Wien)* 148, 181–193. [Discussion 193–184].

Cacci, E., Claasen, J. H., and Kokaia, Z. (2005). Microglia-derived tumor necrosis factor-alpha exaggerates death of newborn hippocampal progenitor cells in vitro. *J. Neurosci. Res.* 80, 789–797.

Cameron, H. A., Woolley, C. S., Mcewen, B. S., and Gould, E. (1993). Differentiation of newly born neurons and glia in the dentate gyrus of the adult rat. *Neuroscience* 56, 337–344.

Cao, L., Jiao, X., Zuzga, D. S., Liu, Y., Fong, D. M., Young, D., and During, M. J. (2004). VEGF links hippocampal activity with neurogenesis, learning and memory. *Nat. Genet.* 36, 827–835.

Carobrez, A. P., and Bertoglio, L. J. (2005). Ethological and temporal analyses of anxiety-like behavior: the elevated plus-maze model 20 years on. *Neurosci. Biobehav. Rev.* 29, 1193–1205.

Cernak, I., Merkle, A. C., Koliatsos, V. E., Bilik, J. M., Luong, Q. T., Mahota, T. M., Xu, L., Slack, N., Windle, D., and Ahmed, F. A. (2010). The pathobiology of blast injuries and blast-induced neurotrauma as identified using a new experimental model of injury in mice. *Neurobiol. Dis.* 41, 538–551.

Cernak, I., Wang, Z., Jiang, J., Bian, X., and Savic, J. (2001). Ultrastructural and functional characteristics of blast injury-induced neurotrauma. *J. Trauma.* 50, 695–706.

Chirumamilla, S., Sun, D., Bullock, M. R., and Colello, R. J. (2002). Traumatic brain injury induced cell proliferation in the adult mammalian central nervous system. *J. Neurotrauma* 19, 693–703.

Couillard-Despres, S., Winner, B., Schaubeck, S., Aigner, R., Vroemen, M., Weidner, N., Bogdahn, U., Winkler, J., Kuhn, H. G., and Aigner, L. (2005). Doublecortin expression levels in adult brain reflect neurogenesis. *Eur. J. Neurosci.* 21, 1–14.

Dahlqvist, P., Ronnback, A., Bergstrom, S. A., Soderstrom, I., and Olsson, T. (2004). Environmental enrichment reverses learning impairment in the Morris water maze after focal cerebral ischemia in rats. *Eur. J. Neurosci.* 19, 2288–2298.

Dash, P. K., Mach, S. A., and Moore, A. N. (2001). Enhanced neurogenesis in the rodent hippocampus following traumatic brain injury. *J. Neurosci. Res.* 63, 313–319.

Deng, W., Aimone, J. B., and Gage, F. H. (2010). New neurons and new memories: how does adult hippocampal neurogenesis affect learning and memory? *Nat. Rev. Neurosci.* 11, 339–350.

Dhanushkodi, A., Bindu, B., Raju, T. R., and Kutty, B. M. (2007). Exposure to enriched environment improves spatial learning performances and enhances cell density but not choline acetyltransferase activity in the hippocampus of ventral subicular-lesioned rats. *Behav. Neurosci.* 121, 491–500.

Dihne, M., Block, F., Korr, H., and Topper, R. (2001). Time course of glial proliferation and glial apoptosis following excitotoxic CNS injury. *Brain Res.* 902, 178–189.

Doll, H., Truebel, H., Kipfmueller, F., Schaefer, U., Neugebauer, E. A., Wirth, S., and Maegele, M. (2009). Pharyngeal selective brain cooling improves neurofunctional and neurocognitive outcome after fluid percussion brain injury in rats. *J. Neurotrauma* 26, 235–242.

Ehninger, D., and Kempermann, G. (2003). Regional effects of wheel running and environmental enrichment on cell genesis and microglia proliferation in the adult murine neocortex. *Cereb. Cortex* 13, 845–851.

Einon, D. F., Morgan, M. J., and Will, B. E. (1980). Effects of post-operative environment on recovery from dorsal hippocampal lesions in young rats: tests of

spatial memory and motor transfer. *Q. J. Exp. Psychol.* 32, 137–148.
Eng, L. F., and Ghirnikar, R. S. (1994). GFAP and astrogliosis. *Brain Pathol.* 4, 229–237.
Farkas, O., and Povlishock, J. T. (2007). Cellular and subcellular change evoked by diffuse traumatic brain injury: a complex web of change extending far beyond focal damage. *Prog. Brain Res.* 161, 43–59.
Fischer, F. R., and Peduzzi, J. D. (2007). Functional recovery in rats with chronic spinal cord injuries after exposure to an enriched environment. *J. Spinal. Cord Med.* 30, 147–155.
Gentile, A. M., Beheshti, Z., and Held, J. M. (1987). Enrichment versus exercise effects on motor impairments following cortical removals in rats. *Behav. Neural Biol.* 47, 321–332.
Gentilini, M., Nichelli, P., Schoenhuber, R., Bortolotti, P., Tonelli, L., Falasca, A., and Merli, G. A. (1985). Neuropsychological evaluation of mild head injury. *J. Neurol. Neurosurg. Psychiatr.* 48, 137–140.
Gross, C., and Hen, R. (2004). Genetic and environmental factors interact to influence anxiety. *Neurotox. Res.* 6, 493–501.
Gyorgy, A. B., Walker, J., Wingo, D., Eidelman, O., Pollard, H. B., Molnar, A., and Agoston, D. V. (2010). Reverse phase protein microarray technology in traumatic brain injury. *J. Neurosci. Methods.* 192, 96–101.
Hagg, T. (2005). Molecular regulation of adult CNS neurogenesis: an integrated view. *Trends Neurosci.* 28, 589–595.
Hallbergson, A. F., Gnatenco, C., and Peterson, D. A. (2003). Neurogenesis and brain injury: managing a renewable resource for repair. *J. Clin. Invest.* 112, 1128–1133.
Hamm, R. J., Temple, M. D., O'dell, D. M., Pike, B. R., and Lyeth, B. G. (1996). Exposure to environmental complexity promotes recovery of cognitive function after traumatic brain injury. *J. Neurotrauma* 13, 41–47.
Harrison, F. E., Hosseini, A. H., and Mcdonald, M. P. (2009). Endogenous anxiety and stress responses in water maze and Barnes maze spatial memory tasks. *Behav. Brain Res.* 198, 247–251.
Hebb, D. O. (1947). The effects of early experience on problem-solving at maturity. *Am. Psychol.* 2, 306–307.
Hebb, D. O. (1949). *The Organization of Behavior: A Neuropsychological Theory.* London: Wiley.
Held, J. M., Gordon, J., and Gentile, A. M. (1985). Environmental influences on locomotor recovery following cortical lesions in rats. *Behav. Neurosci.* 99, 678–690.
Henke, P. G. (1990). Hippocampal pathway to the amygdala and stress ulcer development. *Brain Res. Bull.* 25, 691–695.
Hoffman, A. N., Malena, R. R., Westergom, B. P., Luthra, P., Cheng, J. P., Aslam, H. A., Zafonte, R. D., and Kline, A. E. (2008). Environmental enrichment-mediated functional improvement after experimental traumatic brain injury is contingent on task-specific neurobehavioral experience. *Neurosci. Lett.* 431, 226–230.
Jin, K., Zhu, Y., Sun, Y., Mao, X. O., Xie, L., and Greenberg, D. A. (2002). Vascular endothelial growth factor (VEGF) stimulates neurogenesis in vitro and in vivo. *Proc. Natl. Acad. Sci. U.S.A.* 99, 11946–11950.
Johansson, B. B. (1996). Functional outcome in rats transferred to an enriched environment 15 days after focal brain ischemia. *Stroke* 27, 324–326.
Johansson, B. B., and Ohlsson, A. L. (1996). Environment, social interaction, and physical activity as determinants of functional outcome after cerebral infarction in the rat. *Exp. Neurol.* 139, 322–327.
Juraska, J. M., Fitch, J. M., Henderson, C., and Rivers, N. (1985). Sex differences in the dendritic branching of dentate granule cells following differential experience. *Brain Res.* 333, 73–80.
Juraska, J. M., and Kopcik, J. R. (1988). Sex and environmental influences on the size and ultrastructure of the rat corpus callosum. *Brain Res.* 450, 1–8.
Kaur, C., and Ling, E. A. (2008). Blood brain barrier in hypoxic-ischemic conditions. *Curr. Neurovasc. Res.* 5, 71–81.
Kaur, C., Singh, J., Lim, M. K., Ng, B. L., Yap, E. P., and Ling, E. A. (1997). Ultrastructural changes of macroglial cells in the rat brain following an exposure to a non-penetrative blast. *Ann. Acad. Med. Singapore* 26, 27–29.
Kempermann, G. (2002a). Regulation of adult hippocampal neurogenesis – implications for novel theories of major depression. *Bipolar Disord.* 4, 17–33.
Kempermann, G. (2002b). Why new neurons? Possible functions for adult hippocampal neurogenesis. *J. Neurosci.* 22, 635–638.
Kempermann, G., and Gage, F. H. (2000). Neurogenesis in the adult hippocampus. *Novartis Found. Symp.* 231, 220–235. [discussion 235–241, 302–226].
Kempermann, G., and Kronenberg, G. (2003). Depressed new neurons – adult hippocampal neurogenesis and a cellular plasticity hypothesis of major depression. *Biol. Psychiatry* 54, 499–503.
Kempermann, G., Kuhn, H. G., and Gage, F. H. (1997). More hippocampal neurons in adult mice living in an enriched environment. *Nature* 386, 493–495.
Kempermann, G., and Neumann, H. (2003). Neuroscience. Microglia: the enemy within? *Science* 302, 1689–1690.
Kempermann, G., Wiskott, L., and Gage, F. H. (2004). Functional significance of adult neurogenesis. *Curr. Opin. Neurobiol.* 14, 186–191.
Kernie, S. G., Erwin, T. M., and Parada, L. F. (2001). Brain remodeling due to neuronal and astrocytic proliferation after controlled cortical injury in mice. *J. Neurosci. Res.* 66, 317–326.
Kline, A. E., Wagner, A. K., Westergom, B. P., Malena, R. R., Zafonte, R. D., Olsen, A. S., Sozda, C. N., Luthra, P., Panda, M., Cheng, J. P., and Aslam, H. A. (2007). Acute treatment with the 5-HT(1A) receptor agonist 8-OH-DPAT and chronic environmental enrichment confer neurobehavioral benefit after experimental brain trauma. *Behav. Brain Res.* 177, 186–194.
Kozorovitskiy, Y., and Gould, E. (2003). Adult neurogenesis: a mechanism for brain repair? *J. Clin. Exp. Neuropsychol.* 25, 721–732.
Krum, J. M., and Khaibullina, A. (2003). Inhibition of endogenous VEGF impedes revascularization and astroglial proliferation: roles for VEGF in brain repair. *Exp. Neurol.* 181, 241–257.
Kwon, S.-K. C., Kovesdi, E., Gyorgy, A. B., Wingo, D., Kamnaksh, A., Walker, J., Long, J. B., and Agoston, D. V. (2011). Stress and traumatic brain injury; a behavioral, proteomics and histological study. *Front. Neurol.* 2:12. doi: 10.3389/fneur.2011.00012
Lasagna-Reeves, C. A., Castillo-Carranza, D. L., Guerrero-Muoz, M. J., Jackson, G. R., and Kayed, R. (2010). Preparation and characterization of neurotoxic tau oligomers. *Biochemistry* 49, 10039–10041.
Lee, C., and Agoston, D. V. (2009). Inhibition of VEGF receptor 2 increased cell death of dentate hilar neurons after traumatic brain injury. *Exp. Neurol.* 220, 400–403.
Lee, C., and Agoston, D. V. (2010). Vascular endothelial growth factor is involved in mediating increased de novo hippocampal neurogenesis in response to traumatic brain injury. *J. Neurotrauma* 27, 541–553.
Liberzon, I., and Sripada, C. S. (2008). The functional neuroanatomy of PTSD: a critical review. *Prog. Brain Res.* 167, 151–169.
Ling, G., Bandak, F., Armonda, R., Grant, G., and Ecklund, J. (2009). Explosive blast neurotrauma. *J. Neurotrauma* 26, 815–825.
Liu, Q., Li, B., Zhu, H. Y., Wang, Y. Q., Yu, J., and Wu, G. C. (2010a). Glia atrophy in the hippocampus of chronic unpredictable stress-induced depression model rats is reversed by electroacupuncture treatment. *J. Affect. Disord.* 128, 309–313.
Liu, Y. R., Cardamone, L., Hogan, R. E., Gregoire, M. C., Williams, J. P., Hicks, R. J., Binns, D., Koe, A., Jones, N. C., Myers, D. E., O'brien, T. J., and Bouilleret, V. (2010b). Progressive metabolic and structural cerebral perturbations after traumatic brain injury: an in vivo imaging study in the rat. *J. Nucl. Med.* 51, 1788–1795.
Long, J. B., Bentley, T. L., Wessner, K. A., Cerone, C., Sweeney, S., and Bauman, R. A. (2009). Blast overpressure in rats: recreating a battlefield injury in the laboratory. *J. Neurotrauma* 26, 827–840.
Maegele, M., Lippert-Gruener, M., Ester-Bode, T., Sauerland, S., Schafer, U., Molcany, M., Lefering, R., Bouillon, B., Neiss, W. F., Angelov, D. N., Klug, N., Mcintosh, T. K., and Neugebauer, E. A. (2005). Reversal of neuromotor and cognitive dysfunction in an enriched environment combined with multimodal early onset stimulation after traumatic brain injury in rats. *J. Neurotrauma* 22, 772–782.
Marklund, N., Blennow, K., Zetterberg, H., Ronne-Engstrom, E., Enblad, P., and Hillered, L. (2009). Monitoring of brain interstitial total tau and beta amyloid proteins by microdialysis in patients with traumatic brain injury. *J. Neurosurg.* 110, 1227–1237.
Mayorga, M. A. (1997). The pathology of primary blast overpressure injury. *Toxicology* 121, 17–28.
Minagar, A., Shapshak, P., Fujimura, R., Ownby, R., Heyes, M., and Eisdorfer, C. (2002). The role of macrophage/microglia and astrocytes in the pathogenesis of three neurologic disorders: HIV-associated dementia, Alzheimer disease, and multiple sclerosis. *J. Neurol. Sci.* 202, 13–23.
Ming, G. L., and Song, H. (2005). Adult neurogenesis in the mammalian central nervous system. *Annu. Rev. Neurosci.* 28, 223–250.
Mora, F., Segovia, G., and Del Arco, A. (2007). Aging, plasticity and environmental enrichment: structural changes and neurotransmitter dynamics in several areas of the brain. *Brain Res. Rev.* 55, 78–88.
Moser, M. B., Moser, E. I., Forrest, E., Andersen, P., and Morris, R. G. (1995). Spatial learning with a minislab in the dorsal hippocampus. *Proc. Natl. Acad. Sci. U.S.A.* 92, 9697–9701.
Mueller, F. J., Mckercher, S. R., Imitola, J., Loring, J. F., Yip, S., Khoury, S. J., and Snyder, E. Y. (2005). At the interface of the immune system and the nervous

system: how neuroinflammation modulates the fate of neural progenitors in vivo. *Ernst Schering Res. Found. Workshop* 53, 83–114.

Neufeld, G., Cohen, T., Gengrinovitch, S., and Poltorak, Z. (1999). Vascular endothelial growth factor (VEGF) and its receptors. *FASEB J.* 13, 9–22.

Okie, S. (2005). Traumatic brain injury in the war zone. *N. Engl. J. Med.* 352, 2043–2047.

Parent, J. M. (2003). Injury-induced neurogenesis in the adult mammalian brain. *Neuroscientist* 9, 261–272.

Passineau, M. J., Green, E. J., and Dietrich, W. D. (2001). Therapeutic effects of environmental enrichment on cognitive function and tissue integrity following severe traumatic brain injury in rats. *Exp. Neurol.* 168, 373–384.

Paxinos, G., Kus, L., Ashwell, K. W. S., and Watson, C. (1999). *Chemoarchitectonic Atlas of the Rat Forebrain*. San Diego: Academic Press.

Pham, T. M., Soderstrom, S., Winblad, B., and Mohammed, A. H. (1999). Effects of environmental enrichment on cognitive function and hippocampal NGF in the non-handled rats. *Behav. Brain Res.* 103, 63–70.

Ponsford, J. L., Olver, J. H., and Curran, C. (1995). A profile of outcome: 2 years after traumatic brain injury. *Brain Inj.* 9, 1–10.

Puurunen, K., and Sivenius, J. (2002). Influence of enriched environment on spatial learning following cerebral insult. *Rev. Neurosci.* 13, 347–364.

Quinn, R. (2005). Comparing rat's to human's age: how old is my rat in people years? *Nutrition* 21, 775–777.

Ridet, J. L., Malhotra, S. K., Privat, A., and Gage, F. H. (1997). Reactive astrocytes: cellular and molecular cues to biological function. *Trends Neurosci.* 20, 570–577.

Rose, F. D., Davey, M. J., Love, S., and Dell, P. A. (1987). Environmental enrichment and recovery from contralateral sensory neglect in rats with large unilateral neocortical lesions. *Behav. Brain Res.* 24, 195–202.

Rosenstein, J. M., and Krum, J. M. (2004). New roles for VEGF in nervous tissue – beyond blood vessels. *Exp. Neurol.* 187, 246–253.

Rosenzweig, M. R., and Bennett, E. L. (1996). Psychobiology of plasticity: effects of training and experience on brain and behavior. *Behav. Brain Res.* 78, 57–65.

Ryan, L. M., and Warden, D. L. (2003). Post concussion syndrome. *Int. Rev. Psychiatry* 15, 310–316.

Sahay, A., and Hen, R. (2007). Adult hippocampal neurogenesis in depression. *Nat. Neurosci.* 10, 1110–1115.

Salzberg, M., Kumar, G., Supit, L., Jones, N. C., Morris, M. J., Rees, S., and O'Brien, T. J. (2007). Early postnatal stress confers enduring vulnerability to limbic epileptogenesis. *Epilepsia* 48, 2079–2085.

Saxe, M. D., Battaglia, F., Wang, J. W., Malleret, G., David, D. J., Monckton, J. E., Garcia, A. D., Sofroniew, M. V., Kandel, E. R., Santarelli, L., Hen, R., and Drew, M. R. (2006). Ablation of hippocampal neurogenesis impairs contextual fear conditioning and synaptic plasticity in the dentate gyrus. *Proc. Natl. Acad. Sci. U.S.A.* 103, 17501–17506.

Schoenhuber, R., and Gentilini, M. (1988). Anxiety and depression after mild head injury: a case control study. *J. Neurol. Neurosurg. Psychiatr.* 51, 722–724.

Shors, T. J., Miesegaes, G., Beylin, A., Zhao, M., Rydel, T., and Gould, E. (2001). Neurogenesis in the adult is involved in the formation of trace memories. *Nature* 410, 372–376.

Shum, F. W., Wu, L. J., Zhao, M. G., Toyoda, H., Xu, H., Ren, M., Pinaud, R., Ko, S. W., Lee, Y. S., Kaang, B. K., and Zhuo, M. (2007). Alteration of cingulate long-term plasticity and behavioral sensitization to inflammation by environmental enrichment. *Learn. Mem.* 14, 304–312.

Sun, D., Mcginn, M. J., Zhou, Z., Harvey, H. B., Bullock, M. R., and Colello, R. J. (2007). Anatomical integration of newly generated dentate granule neurons following traumatic brain injury in adult rats and its association to cognitive recovery. *Exp. Neurol.* 204, 264–272.

Taber, K. H., Warden, D. L., and Hurley, R. A. (2006). Blast-related traumatic brain injury: what is known? *J. Neuropsychiatry Clin. Neurosci.* 18, 141–145.

Tagliaferri, F., Compagnone, C., Korsic, M., Servadei, F., and Kraus, J. (2006). A systematic review of brain injury epidemiology in Europe. *Acta Neurochir. (Wien)* 148, 255–256.

Tashiro, A., Makino, H., and Gage, F. H. (2007). Experience-specific functional modification of the dentate gyrus through adult neurogenesis: a critical period during an immature stage. *J. Neurosci.* 27, 3252–3259.

Tees, R. C., Buhrmann, K., and Hanley, J. (1990). The effect of early experience on water maze spatial learning and memory in rats. *Dev. Psychobiol.* 23, 427–439.

Tischler, L., Brand, S. R., Stavitsky, K., Labinsky, E., Newmark, R., Grossman, R., Buchsbaum, M. S., and Yehuda, R. (2006). The relationship between hippocampal volume and declarative memory in a population of combat veterans with and without PTSD. *Ann. N. Y. Acad. Sci.* 1071, 405–409.

Vallieres, L., Campbell, I. L., Gage, F. H., and Sawchenko, P. E. (2002). Reduced hippocampal neurogenesis in adult transgenic mice with chronic astrocytic production of interleukin-6. *J. Neurosci.* 22, 486–492.

Van Praag, H., Kempermann, G., and Gage, F. H. (2000). Neural consequences of environmental enrichment. *Nat. Rev. Neurosci.* 1, 191–198.

Walf, A. A., and Frye, C. A. (2007). The use of the elevated plus maze as an assay of anxiety-related behavior in rodents. *Nat. Protoc.* 2, 322–328.

Wang, Z., Neylan, T. C., Mueller, S. G., Lenoci, M., Truran, D., Marmar, C. R., Weiner, M. W., and Schuff, N. (2010). Magnetic resonance imaging of hippocampal subfields in posttraumatic stress disorder. *Arch. Gen. Psychiatry* 67, 296–303.

Warden, D. (2006). Military TBI during the Iraq and Afghanistan wars. *J. Head Trauma Rehabil.* 21, 398–402.

Warden, D. L., and French, L. (2005). Traumatic brain injury in the war zone. *N. Engl. J. Med.* 353, 633–634.

Whishaw, I. Q., Zaborowski, J. A., and Kolb, B. (1984). Postsurgical enrichment aids adult hemidecorticate rats on a spatial navigation task. *Behav. Neural Biol.* 42, 183–190.

Wilhelmsen, K. C. (1999). The tangled biology of tau. *Proc. Natl. Acad. Sci. U.S.A.* 96, 7120–7121.

Will, B., Galani, R., Kelche, C., and Rosenzweig, M. R. (2004). Recovery from brain injury in animals: relative efficacy of environmental enrichment, physical exercise or formal training (1990–2002). *Prog. Neurobiol.* 72, 167–182.

Woon, F. L., Sood, S., and Hedges, D. W. (2010). Hippocampal volume deficits associated with exposure to psychological trauma and posttraumatic stress disorder in adults: a meta-analysis. *Prog. Neuropsychopharmacol. Biol. Psychiatry* 34, 1181–1188.

Wright, R. L., and Conrad, C. D. (2008). Enriched environment prevents chronic stress-induced spatial learning and memory deficits. *Behav. Brain Res.* 187, 41–47.

Yasuhara, T., Shingo, T., Kobayashi, K., Takeuchi, A., Yano, A., Muraoka, K., Matsui, T., Miyoshi, Y., Hamada, H., and Date, I. (2004). Neuroprotective effects of vascular endothelial growth factor (VEGF) upon dopaminergic neurons in a rat model of Parkinson's disease. *Eur. J. Neurosci.* 19, 1494–1504.

Yehuda, R., and Ledoux, J. (2007). Response variation following trauma: a translational neuroscience approach to understanding PTSD. *Neuron* 56, 19–32.

Zhao, C., Deng, W., and Gage, F. H. (2008). Mechanisms and functional implications of adult neurogenesis. *Cell* 132, 645–660.

Conflict of Interest Statement: The authors declare that the research was conducted in the absence of any commercial or financial relationships that could be construed as a potential conflict of interest.

Received: 31 December 2010; accepted: 15 March 2011; published online: 01 April 2011.

Citation: Kovesdi E, Gyorgy AB, Kwon S-KC, Wingo DL, Kamnaksh A, Long JB, Kasper CE and Agoston DV (2011) The effect of enriched environment on the outcome of traumatic brain injury; a behavioral, proteomics, and histological study. Front. Neurosci. ***5****:42. doi:10.3389/fnins.2011.00042*

This article was submitted to Frontiers in Neurogenesis, a specialty of Frontiers in Neuroscience.

APPENDIX

FIGURE A1 | Photograph of enriched environment housing condition.